

# Molecular Mechanisms Underlying Associative Learning

Moleculaire mechanismen die ten grondslag liggen aan associatief leren

Proefschrift

ter verkrijging van de graad van doctor  
aan de Erasmus Universiteit Rotterdam  
op gezag van de Rector Magnificus

Prof.dr. S.W.J. Lamberts

en volgens besluit van het College voor Promoties

De openbare verdediging zal plaats vinden op  
woensdag 24 maart 2004 om 15:45 uur

door

Sebastiaan Karel Emile Koekkoek

geboren te Eindhoven

## **Promotiecommissie**

**Promotor:** Prof.dr. C.I. de Zeeuw

**Overige leden:** Prof.dr. B.A. Oostra  
Prof.dr. F.G. Grosveld  
Prof.dr. A. Hofman

# Table of Contents

<b>Chapter 1</b>	7
General introduction	
1.1 Classical conditioning	9
1.2 Eyeblink conditioning	10
1.2a - The search for the engram	11
1.2b - The cerebellum	13
1.2c - Long Term Depression (LTD)	15
1.2d - Pathways	17
- The unconditioned response pathway	17
- The conditioned response pathway	20
1.3 Fear conditioning	22
1.3a - Behavioral freezing	23
1.3b - The acoustic startle response	23
1.3c - Contextual and cued fear conditioning	25
1.3d - CS pathways	26
1.3e - US pathways	27
1.3f - Plasticity related to fear conditioning	28
1.4 Scope of this thesis	30
1.5 References	33
<b>Chapter 2</b>	43
Monitoring Kinetic and Frequency-Domain Properties of Eyelid Responses in Mice With Magnetic Distance Measurement Technique	
Koekkoek et al. <i>J Neurophysiol</i> 88: 2124–2133, 2002	
<b>Chapter 3</b>	63
Expression of a Protein Kinase C Inhibitor in Purkinje Cells Blocks Cerebellar LTD and Adaptation of the Vestibulo -Ocular Reflex.	
De Zeeuw et al. <i>Neuron</i> 20: 495–508, 1998	

<b>Chapter 4</b>	93
Cerebellar LTD and Learning-Dependent Timing of Conditioned Eye-lid Responses	
Koekkoek et al. <i>Science</i> 301: 1736-1739, 2003	
<b>Chapter 5</b>	101
Enhanced LTD at enlarged Purkinje cell spines causes motor learning deficits in fragile X syndrome	
Koekkoek et al. Submitted	
<b>Chapter 6</b>	121
Targeted mutation of <i>Cyln2</i> in the Williams syndrome critical region links CLIP-115 haploinsufficiency to neurodevelopmental abnormalities in mice	
Hoogenraad et al. <i>Nature Genetics</i> 32: 116-127, 2002	
<b>Chapter 7</b>	147
General discussion	
7.1 Technical considerations	148
7.2 Cellular mechanisms and molecular components underlying classical conditioning	150
7.3 Possible origins of the remnant CR's after anterior interposed lesions	153
7.4 references	158
<b>Summary</b>	163
<b>Nederlandse samenvatting</b>	167
<b>Dankwoord</b>	171



<b>Curriculum Vitae</b>	175
<b>List of publications</b>	177



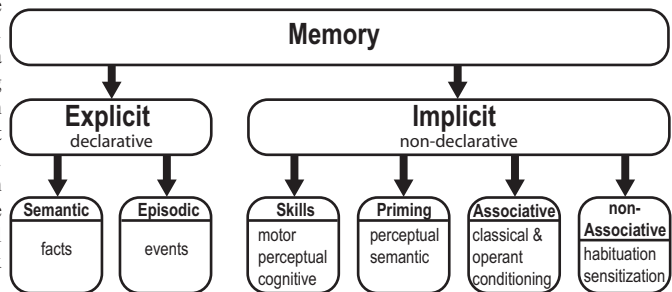
# Chapter 1

General introduction

Learning and memory are the most important mechanisms by which the environment alters our behavior. Learning is the acquisition of knowledge itself, while memory is the encoding, storage and retrieval of the learned knowledge. Throughout development we learn for example the motor skills necessary to master our environment and in addition we learn to adapt them when the environment changes. We learn how to interact with other human beings by complex forms of communication and we learn how to avoid objects or situations that are harmful. Learning and memory is displayed throughout the whole animal kingdom down to the simplest forms of life such as that of *C. elegans*. These nematodes with a nerve system of a few hundred cells are already capable of adjusting their behavior based on previous experiences (Rankin et al. 1990). When the process of learning and memory itself is studied, several questions come up: What are the different types of learning? Do different types of learning result in different memory processes? How and where is memory stored? How is it retrieved?

From the neurobiological point of view memory can be categorized as implicit or explicit. Implicit memory is a memory that is recalled unconsciously and is mostly involved with training of motor and perceptual skills. This type of memory is rather rigid and directly related to the stimulus conditions during the learning period. Implicit knowledge is also called non-declarative memory, procedural memory or know-how memory; you know how to do a particular task, but you do not have the explicit knowledge that would allow you to explain it to a young child trying to learn the task. Explicit memory is involved with factual knowledge of the individual's surrounding (e.g. people, things or places) and can be recalled consciously and deliberately. In contrast to implicit memory, explicit memory is much more flexible and is usually a result of a combination of bits and pieces of information. In analogy with know-how memory, explicit memory (or declarative memory) can be called know-that memory, because you can put the phrase "I know that" in front of it. Many tasks involve both types of memory but they do seem fundamentally different and often display different time courses of acquisition (proceduralization of a complex skill takes much longer than learning of a complex piece of knowledge). Further subdivisions of both forms of memory can be made (see figure 1.1).

**Figure 1.1 Memory taxonomy.** Explicit memory includes memory for facts and events; This type of memory requires awareness. Implicit memory refers to a heterogeneous group of learning and memory abilities, which can change performance but without awareness of what has been learned. The types of memory addressed in this thesis are adaptation of the vestibulo-ocular reflex, classical conditioning of the eyelid reflex and classical conditioning of fear. These types of learning are all dependent of associative processes. (Adapted from Squire 1992)



Explicit memory can be either semantic or episodic. Semantic memory is merely a memory for facts (e.g. Matlab is cool). Episodic memory, also called ‘personal’ memory is memory for experienced events and episodes such as a bike ride this morning or a trip to Africa a few years ago. These personal memories can be memories of more or less extended periods in time.

Implicit memory comes in different forms and is actually more a group of heterogeneous learning phenomena than an actual memory type. The forms are each mediated by different brain regions and acquired through different forms of learning. Four types of implicit learning have been observed; priming, learning of skills and habits, non-associative learning and associative learning. Priming refers to an increased facility for detecting or identifying words or other stimuli as a result of their prior presentation. Skills are typically acquired gradually without noticeable conscious memory of what information has been acquired. Non-associative learning occurs when a single stimulus is presented to a subject once or repetitively. Two forms can be distinguished: habituation and sensitization. With habituation a response to a particular stimulus decreases after repetitive exposure, and with sensitization a subject responds more heavily to a wide variety of stimuli after exposure to an intense or noxious stimulus. Associative learning also comes in two forms: operant conditioning; where the subject learns about relations between behavior and the results of that behavior and classical conditioning where the relationship between two stimuli is learned.

In this thesis I will focus on the associative memory types. Classical conditioning will receive the main focus, divided over classical conditioning of the eyelid reflex and classically conditioned fear. In addition, adaptation of the vestibulo-ocular reflex will be addressed.

## 1.1 Classical conditioning

Everybody who has a dog knows that you do not have to show food to your dog for it to start slobbering. Just the hint that food might be a possible event in the near future makes your dog run into the kitchen with a wagging tail, leaving a trail of anticipatory dribble. Dogs salivate when they think they are going to eat. During the early 1900’s, a Russian physiologist by the name of Ivan Pavlov was studying the digestive tracks of dogs. Pavlov was interested in the role of saliva in the digestive process, and dogs proved to be quite effective subjects for the study of this topic. To get his dogs to salivate, Pavlov would present them with food, placing the target piece on the canine’s tongue. After working with a particular dog for a few days, Pavlov noticed that the dog would salivate before being presented with food. The dogs drooled when Pavlov entered the room. Later they already slobbered at the mere sound of his approaching footsteps. What got Pavlov’s attention was the fact that salivation is a reflex and the dogs were displaying that reflex in the absence of a natural stimulus. This idea, that a natural reflex could be affected by learning, interested Pavlov so much that he abandoned his studies of digestion and spent the next 30 years, the remainder of his career and life, investigating this phenomenon. With his classical conditioning, Pavlov (1927) investigated the capacity of animals

to learn new stimuli and connect them to natural reflexes; allowing non - natural cues to elicit a natural reflex. Pavlov developed categories and terminology to study and describe the results of his experiments. In one set of experiments, Pavlov would ring a bell, what he referred to as a neutral stimulus. The dogs could care less about the bell and nothing happened. Then, after ringing the bell Pavlov would feed his dogs, food being the unconditioned stimulus (US). Initially, the dogs would drool only after presenting the unconditioned stimulus (US); salivation representing the unconditioned response (UR). But after this paired stimulus procedure was repeated for a while, the dogs would start to salivate at the sound of the bell alone. At this point, Pavlov referred to the dogs as being classically conditioned to salivate to the bell. Pavlov's bell now became a conditioned stimulus (CS), because it elicited salivation, the conditioned response (CR).

Pavlov postulated that further research would reveal some focus of convergence of sensory inputs with a related output and consequently spent a lot of time searching for the physical representation of memory in the nervous system that created the association between the conditioned and unconditioned stimuli. Despite the numerous cerebral lesions he made, he did not find a location in the hemispheres that, when lesioned, permanently abolished conditioned responses. Later Lashley (1950) popularized with his work on localization of memory the name "engram" for such a theoretical site of memory.

The classical conditioning paradigm has since then been applied to a wide variety of different responses, ranging from autonomic responses to fine motor responses such as the eyelid reflex. This thesis will describe two of the most widely used paradigms, i.e. eyeblink conditioning and fear conditioning.

### **1.2 Eyeblink conditioning**

Gormezano and associates developed in the 1960's a robust animal preparation that could provide the data needed to elucidate the mechanism behind classical conditioning of motor responses and the underlying associative processes (Gormezano 1960). In this model a tone is used as a CS and a puff of air aimed at the cornea of a rabbit is used as an US. The US always caused a reflexive fast closure of the eyelid (UR) and thereby a passive sweep of the nictitating membrane (NMR) over the cornea. The movement of this nictitating membrane was transduced via a small suture and a lever system to a torque free potentiometer so as to acquire accurate analog recordings of the nictitating membrane position during the trials. Repetitive presentation of the CS, temporally paired with the US resulted in the generation of a CR, a closure of the eyelid upon presentation of the CS. With the use of the rabbit eyeblink conditioning setup (or similar setups) several researchers started searching for the engram, i.e. at least the one responsible for classical conditioning of somatic muscle responses to an aversive stimulus. Two types of conditioning have been used extensively in this search. The first type is called delay conditioning, which is the simplest form. In a delay paradigm the CS precedes the US in time and both stimuli terminate together. Thus, at the moment of US presentation the CS is still active.

The second type is called trace conditioning and is somewhat more demanding in

that it requires the memory of the CS to be retained in its absence for association with the US. In trace conditioning the CS also precedes the US but is only presented briefly, followed by a stimulus free interval before the US is presented. Association can only be made when the CS event is held into memory until presentation of the US (figure 1.2).

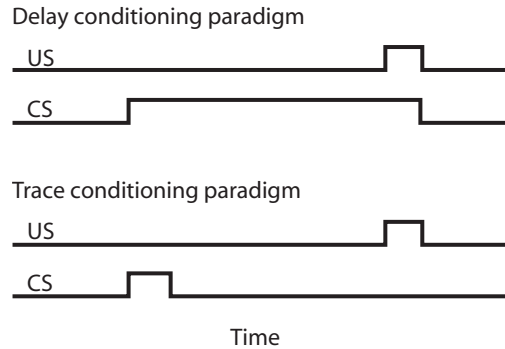


**Figure 1.2 Eyeblink conditioning paradigms.** In a delay paradigm the CS precedes the US and both stimuli terminate together. In trace conditioning the CS also precedes the US but is only presented briefly, followed by a stimulus free interval before the US is presented.

### 1.2a - *The search for the engram*

Searching for a learning and memory locus in the brain typically involves lesion studies. However, when lesions are used as a means to study whether certain brain areas are critical for a particular task one has to realize a couple of important issues. Lesions can have no effect, a temporal effect or a permanent effect. If a lesion has no effect ideally this would mean that the lesioned structure has no essential involvement with the studied behavior. This does not mean that in the normal intact brain this structure does not have any function associated with the studied behavior. For instance, the hippocampus contains neurons that show a remarkable CR predicting activity during simple delay conditioning (Berger et al. 1976). However, when the hippocampus is lesioned no apparent effect on delay conditioning has been described (Schmaltz and Theios 1972). If the lesion only has a temporary effect it becomes more complicated. After some time the initial loss of function recovers. Four mechanisms, not mutually exclusive, have been described to explain recovery of function: functional takeover, sparing, reorganization and substitution. The functional takeover hypothesis in accordance with the vicariation theory first stated by Munk (1881), postulates that after larger lesions, adaptive reorganization takes place in other regions of the same area or in other areas that may not have been originally involved in the function mediated by the injured zone. The result is a takeover of the lost function by a surviving brain area at the expense of its original function.

The idea of sparing (Lashley 1939) following the diaschisis theory of Monakow (1914) states that normal functioning of a particular brain area can be altered due to shock (loss of circulation, connectivity) caused by a lesion in an area of the brain unrelated to the studied behavior. Recovery of function then occurs when the effects of shock are reducing, since the area responsible for the studied behavior was not damaged. For example Welsh and Harvey (1989) suggested that lesions of the cerebellum induce loss of neural and muscle tone and in such a way cause a loss of learning effect on classical eyelid conditioning.

Reorganization is actually a group of mechanisms that the brain might employ to correct the damage of the lesion. In this idea the structure involved with the studied

behavior was actually damaged by the lesion but repaired by the brain resulting in a recovered behavior similar to the original behavior. These mechanisms include regeneration, sprouting, supersensitivity, unmasking and adult neural mitosis (see Chen et al. 2002; Hall 1989; Kuhn et al. 1996; Liu and Chambers 1958; Rice et al. 2003; Yarbrough and Phillis 1975).

Substitution is the idea that the original behavior is permanently damaged by the lesion but substitution of sensory cues, motor behavior or strategies can stand in for the lost function (Xerri et al. 1998).

The mechanisms described above all can result in recovery of function. This means that if, after making a lesion, an initial loss of function occurred followed by recovery, it is almost impossible to determine whether the lesion did or did not damage the essential brain area for the studied behavior. When the lesion caused a permanent loss of function, it is very tempting to assume that the lesioned brain area was critical for the studied behavior. It is, however, still possible that the lesion merely damaged passing fibers or caused some sensory, motor or motivational impairment rather than a direct loss of function. Additionally, when recovery of function does not occur one could always ask the questions: shouldn't we just wait longer? Could the behavior have been recovered, if only the conditions were better suited to promote recovery? In short, using lesion studies as inclusion or exclusion criteria for an essential brain tissue search is much more prone to false positive and false negative conclusions as one might initially think. Deficits induced by a lesion could be due to either a lack of a specific function normally supplied by the lesioned structure or a nonspecific functional change in the remaining system. Accordingly, the existence of normal function after a lesion could mean an absence of involvement of the structure in the studied behavior or could reflect parallel and redundant organization of the system or could simply be a consequence of not monitoring the parameter controlled by the lesioned structure.

The search for the engram resulted in experiments to determine the minimal brain tissue that was necessary to support a classical conditioned eyeblink reflex. Norman, Buchwald and Villablanca (Norman et al. 1977; Norman et al. 1974) made a variety of radical lesions in the cat, after which these cats were tested on their ability to learn conditioned eyelid responses. Even after complete severance of the lower brainstem via a midcollicular transection, thereby eliminating all brain functions above the brainstem, cats still learned simple delay classical conditioning. The learning however, could have been the result of a transfer of function so as to compensate for the lesion damage by using brain areas that are normally not involved. In 1987 it was shown that well trained rabbits showed a retention of classical conditioned responses after midbrain decerebration (Mauk and Thompson 1987), thus the remaining tissue contained the previously established memory.

Lesions of several brainstem and cerebellar regions have produced severe and permanent deficits in the acquisition and retention of classically conditioned eyeblink responses (McCormick et al. 1981; Norman et al. 1977; Welsh 1992; Welsh and Harvey 1989). However, the literature on the effects of these lesions and their implications is rather controversial. The difficulties with lesion studies as mentioned above might at least partly explain the large body of conflicting arguments and re-



sults in the field of classical eyeblink conditioning.

A large advance in the search for the engram was made in the 1980's. Thompson and colleagues made large unilateral lesions in the cerebellum and noted that CR's disappeared on the lesioned site without an apparent effect on UR performance (McCormick et al. 1981). Later, using very small lesions (Clark et al. 1984; Lavond et al. 1985) narrowed the location down to the deep cerebellar nuclei by demonstrating that focal lesions in the anterior interposed nucleus permanently abolished the ipsilateral CR, whereas training the unlesioned site resulted in CR's. UR performance on both eyes was similar. Interestingly the signature of the CR that can be recorded in the hippocampus was also abolished by the lesion and returned after training the unlesioned site. Lesions of the hippocampus in well-trained animals using a trace conditioning paradigm caused the learned eyeblink responses to become mal-adapted to the interval between the CS and the US (Solomon et al. 1986). This indicated a critical role for the hippocampus in trace conditioning. However, lesions of the cerebellum completely abolished trace conditioning (Woodruff-Pak et al. 1985). This, combined with the observation that hippocampal lesions have no effect on simple delay conditioning (Schmaltz and Theios 1972), led to the proposition that the basic association for classical conditioning occurs at the lower basic levels of the nervous system and when the complexity of the task increases, higher brain regions become involved (Lavond et al. 1993).

The importance of the cerebellum in classical conditioning was further strengthened by studies demonstrating that lesions in the pathway between the interposed nuclei and the motor neurons innervating the eyelid muscle caused deficits similar to lesioning the nuclei itself (Desmond et al. 1983; Rosenfield and Moore 1983; Rosenfield and Moore 1985).

Meanwhile strong criticism emerged against the hypothesis that the cerebellum is a critical structure for classical eyeblink conditioning. Some scientists reported that conditioning was actually possible without a cerebellum. Furthermore, it was argued that the effects of lesions on classical conditioning were due to the fact that the lesions caused deficits in motor performance and that the observed learning deficits were secondary to these (Kelly et al. 1990; Norman et al. 1977; Welsh 1992; Welsh and Harvey 1989; Welsh and Harvey 1991). Adding to the controversy is the fact that people who believe(d) in the cerebellum being the site of the engram were, and still are, hotly debating whether the engram is located in the deep nuclei, the cerebellar cortex or, divided over both (for review see Yeo 1991; Bloedel and Bracha 1995; Thompson and Krupa 1994). Despite the controversy, it is safe to assume that the cerebellum at least has an important role in the learning mechanisms underlying classically conditioned eyelid responses.

### **1.2b - *The cerebellum***

The cerebellum takes up only 10% of the total brain volume but contains more neurons than the rest of the brain. The cerebellar cortex contains seven types of neurons (i.e. Purkinje cells, granule cells, brush cells, Golgi cells, stellate cells, basket cells and Lugaro cells) divided over three layers. The top layer or molecular layer contains the stellate/basket inhibitory cells. The bifurcated granule cell axons run parallel

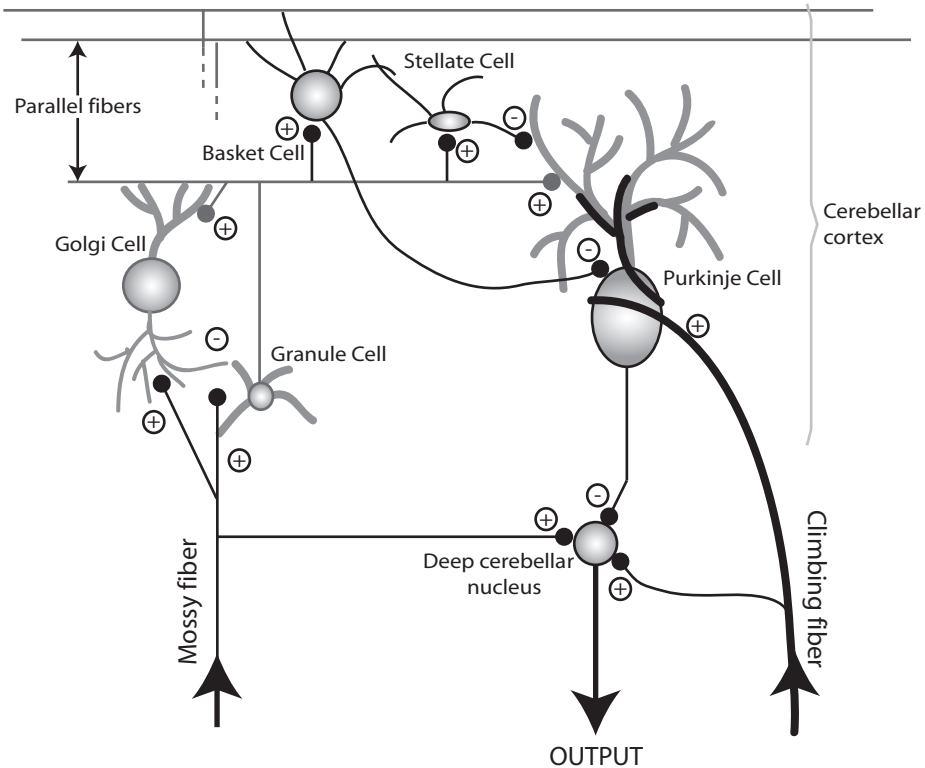


**Figure 1.3 Cerebellar architecture.** The sole output of the cerebellar cortex is formed by the Purkinje cells. They project to the deep cerebellar nuclei and receive input from two entirely different and distinct sources. The mossy fibers arise from a variety of sources including the pontine nuclei, spinal cord and dorsal column nuclei. They terminate on the granule cells, which then give rise to the parallel fibers innervating the flat, fan-shaped Purkinje cell dendritic tree. Each Purkinje cell may have up to 250,000 (in man) parallel fiber synaptic inputs. The climbing fibers arise exclusively from the inferior olive in the medulla. Each adult Purkinje cell has but one climbing fiber input, but this single fiber makes multiple synaptic contacts with one Purkinje cell. The mossy fiber inputs drive the Purkinje cell to generate simple spikes at high rates. The climbing fiber input is excitatory too, but causes a very large complex spike which dominates the Purkinje cell and temporarily silences its simple spike output. brush and Lugaro cells are left out for reasons of simplicity.

to the folia in this layer and are called parallel fibers. They span a large number of Purkinje cell dendrites which are arranged perpendicular to the parallel fiber orientation. The large cell bodies of the Purkinje cells are located in the intermediate layer, therefore called the Purkinje cell layer. Purkinje cells provide the sole output of the cerebellar cortex and inhibit their target neurons in the deep cerebellar nuclei and vestibular nuclei. The granule cell layer contains a vast number of granule cells (estimated at  $10^{11}$ ) and a few larger Golgi interneurons, Lugaro cells and brush cells. See figure 1.3 for more details, or see Voogd and Glickstein (1998) for review.

The output of the cerebellar cortex is organized in parasagittal zones (for review see Voogd and Glickstein 1998). Purkinje cells of a particular zone project to a particular cerebellar or vestibular nucleus. Climbing fibers of a particular olivary subnucleus project to a single Purkinje cell zone or to a pair of zones that share the same target nucleus. These target nuclei in turn provide an inhibitory projection to the corresponding olivary cells. Zones that receive peripheral input have been demonstrated

to show a somatotopical climbing fiber microzonation (Andersson and Oscarsson 1978; Ekerot et al. 1991; Garwicz et al. 1992). The cerebellum consists of discrete modules, each having its own connections with the inferior olive. Ekerot and colleagues have proposed (see Garwicz et al. 1998) that each microzone, or ensemble of microzones with similar climbing fiber receptive fields control a set of muscles that constitute an elemental output synergy and that the climbing fibers signal about particular aspects of activities of this set of muscles. They demonstrated that the organization of corticonuclear and nucleofugal projections of the intermediate cerebellum in cats is compatible with this hypothesis. Such a scheme would also be compatible with some hypotheses on the potential roles of the cerebellar circuitry in eyeblink conditioning.

The striking organization of the cerebellar cortex has put forward theories of cerebellar function that implicated the cerebellum as a pattern learning machine that could guide the learning of specific motor tasks (Albus 1971; Gilbert 1974; Marr 1968). The general idea of the Marr-Albus hypothesis is that activity in one input system (climbing fibers) alters the responsiveness of the Purkinje cell to activity in the second input system (mossy/ parallel fibers). Because a climbing fiber has a one to one relation with a Purkinje cell while the same Purkinje cell receives input from thousands of parallel fibers, this system is suitable for associating a large variety of different inputs with a single error event. Feedback information about ongoing movement is conveyed to the Purkinje cell via the mossy fiber/parallel fiber system. If the movement is incorrect the error will be translated in climbing fiber activity. The effectiveness of the active parallel fiber input will then be weakened by the co-active climbing fiber. It was only after Ito and Kano (1982) described the process of long term depression (LTD) that experimental evidence for the Marr–Albus theory was found.

Thus, the cerebellum is well designed to mediate associative learning processes, and its architecture has guided modelers and experimentalists to uncover its role in learning.

### **1.2c - Long Term Depression (LTD)**

Cerebellar parallel fiber LTD is a long lasting reduction in synaptic efficacy that occurs specifically at the parallel fiber- Purkinje cell synapses and can be induced by pairing parallel fiber activity with climbing fiber activity (for review see Linden and Conner 1995, Ito 2001). The process of LTD can be summarized as follows (see figure 1.4). Parallel fiber activation leads to activation of both the ionotropic,  $\alpha$ -amino-3-hydroxy-5-methylisoxazolpropionate (AMPA) receptor and the metabotropic glutamate receptor (mGluR1) on the dendritic synapses of Purkinje cells. Climbing fiber activation leads to a massive depolarization of the Purkinje cell and a large increase in intracellular free  $\text{Ca}^{2+}$ . Activation of mGluR1 leads to a G-protein coupled activation of phospholipase C (PLC), which produces di-acyl-glycerol (DAG). In addition, it converts phosphatidyl-inositol-phosphate (PIP2) into inositol-tri-phosphate ( $\text{IP}_3$ ).  $\text{IP}_3$  mediates release of  $\text{Ca}^{2+}$  from the intra-cellular  $\text{Ca}^{2+}$  stores. Increased free  $\text{Ca}^{2+}$  together with DAG activates protein kinase C (PKC), which acts on AMPA

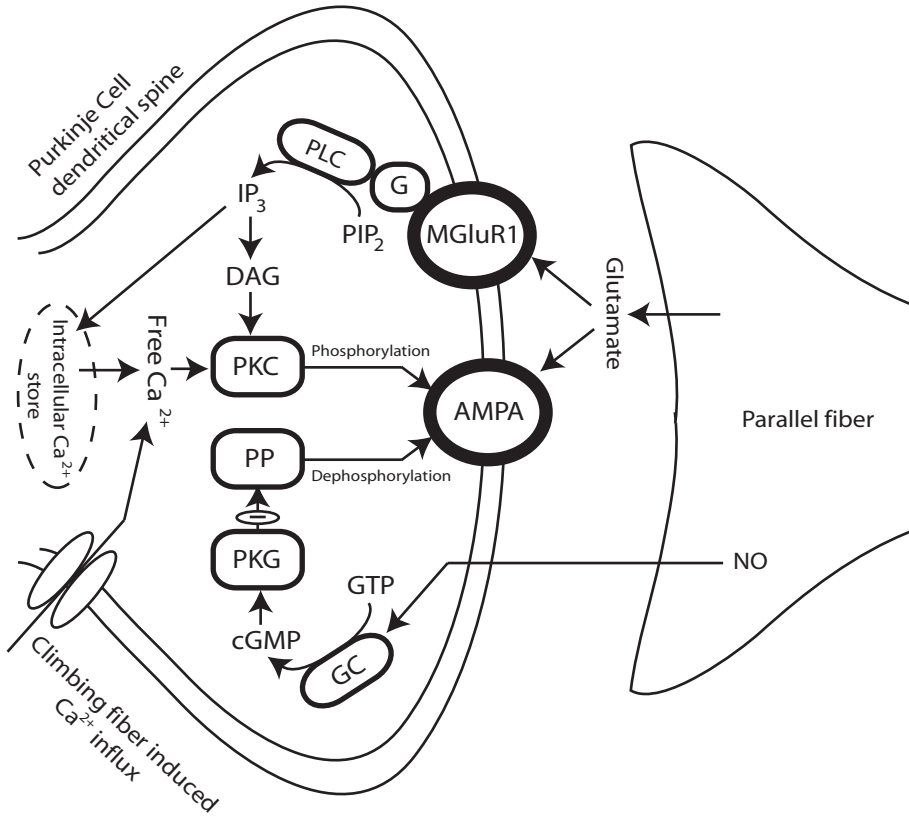


**Figure 1.4. Simplified schematic of parallel fiber LTD.** LTD normally requires simultaneous activation of AMPA and MGLuR1 receptors together with a high intracellular free  $\text{Ca}^{2+}$ . The latter is achieved by both the mGluR1 activation as well as climbing fiber induced depolarization. MGLuR1 activation also leads to production of DAG which together with high free  $\text{Ca}^{2+}$  activates PKC. The activation of PKC results in phosphorylation and internalization of AMPA receptors thereby making the Purkinje cell less excitable through this particular parallel fiber contact. AMPA,  $\alpha$ -amino-3-hydroxy-5-methylisoxazolpropionate; cGMP, cyclic guanosine-monophosphate; DAG, di-acylglycerol; G, G-protein; GC, guanylyl-cyclase; GTP, guanosine-tri-phosphate; IP<sub>3</sub>, inosi tol-tri-phosphate; MGLuR1, metabotropic glutamate receptor; PIP<sub>2</sub>, phosphatidyl-inositol-biphosphate; PKC, protein kinase C; PKG, protein kinase G; PLC, phospholipase C; PP protein phosphatase; NO, nitrous oxide.

receptors by phosphorylating a serine residue on the intracellular c-terminal end of Glur2/3 subunits. AMPA receptors with phosphorylated serine residues are internalized by a clatherin mediated endocytosis. Thus, LTD causes a reduction in selected parallel fiber synapse efficacy by down-regulating the number of AMPA receptors on the postsynaptic membrane. A second pathway is mediated by nitrous oxide (NO) (Daniel et al. 1993; Lev-Ram et al. 1995). This pathway cannot be shown in Purkinje cell cultures (Linden et al. 1995) since NO synthetase is produced by granule cells. NO is a short-living gas that through diffusion can influence about 4000 synapses in 10 ms. As such, NO has been proposed as a possible candidate for the yet unidentified mediator of heterosynaptic LTD (Reynolds and Hartell 2001). NO acts on guanylyl-cyclase (GC) which in turn converts guanosine-tri-phosphate (GTP) into cyclic guanosine-mono-phosphate (cGMP). cGMP then activates PKG which results in inhibition of protein phosphatases (PP), thereby blocking dephosphorylation of AMPA receptors. AMPA receptors are continuously phosphorylated and depho-

sporylated. LTD shifts the balance towards phosphorylation by activation of PKC and PKG.

In conjunction, the Marr-Albus model, the existence of LTD induction at the parallel fiber to Purkinje cell synapse and the impacts of the cerebellar lesions can be merged into a model for classical conditioning; in which the CS input is relayed by the mossy / parallel fiber system and the US by the climbing fiber input. Much of the work on LTD has been done *in vitro*, using stimulation protocols that would normally not induce classical conditioned responses in intact animals. However, evidence that *in vivo*, LTD at the parallel fiber/ Purkinje cell synapse indeed might be responsible for parts of the learning process underlying classical conditioning of the eyelid responses arose from the work of Schreurs and colleagues who showed that in rabbit using both *in vivo* and slice preparations 1) LTD occurred specifically when CS and US were temporally paired using natural stimulations that supported classical conditioning in intact animals; 2) membrane bound PKC is upregulated after training *in vivo*; and 3) this LTD induced by natural stimulations could be blocked by blocking PKC or intracellular  $Ca^{2+}$  (Freeman et al. 1998; Freeman et al. 1998; Schreurs et al. 1996).

### **1.2d – pathways**

This chapter reviews the pathways involved with the UR and the CR. First, the UR pathway will be described. Second, the CR pathway, or at least a summary of the most plausible suggestions will be mentioned.

#### *- The unconditioned response pathway*

The unconditioned response (UR) in classical eyeblink conditioning is one of the main nociceptive reflexes. The blink reflex was initially described in 1896 by the British human physiologist Overend. He described that tapping the forehead skin above the eyes with a stethoscope caused ipsilateral eyelid twitching while tapping the midline caused bilateral eyelid twitching. In 1901 McCarthy redefined the reflex by noting that tapping the skin overlying the supraorbital nerve with a reflex hammer elicits a usually bilateral response of the orbicularis oculi muscles. The underlying mechanisms remained uncertain until Kugelberg analysed the blink reflex in 1952 using electrophysiological techniques. He demonstrated two components in the human blink reflex. An early response, R1, which is ipsilateral to the stimulation side and has a latency of about 10 ms. The second, later response (R2) is bilateral and has a latency of about 30 ms. R2 is responsible for the actual closure of the eyelids in primate species.

The UR circuit has extensively been studied in rabbit (van Ham and Yeo 1996; van Ham and Yeo 1996), guinea pig (Pellegrini et al. 1995), cat (Holstege et al. 1986; Holstege et al. 1986) and rat (Morcuende et al. 2002) but not in mice. The neuroanatomical circuitries that have been proposed to underly the R2 component may vary among species, i.e. the circuitry proposed for cats differs from that proposed for rabbits and guinea pigs. However, they are not mutually exclusive. Figure 1.5 shows the circuitry as has been described for rabbit. Neurons receiving periocular and corneal

primary afferent input are located in the principal trigeminal nucleus (Vp), spinal trigeminal nucleus (Vs) and rostral levels of the cervical spinal cord (C) (van Ham and Yeo 1996). The R1 component is mediated by a di-synaptic pathway involving neurons in the trigeminal nucleus (principal Vp and spinal Vs) and the intermediate sub-area of the facial (VII) nucleus. The intermediate sub-area of VII contains the motoneurons innervating the musculus orbicularis oculi (MOO) which is a circular muscle around the eyes and responsible for eyelid closure. Blink related neurons located in the paratrigeminal reticular formation (RET) extensively project in a similar way as neurons in Vp. Therefore the existence of a rostral trigeminal blink area is suggested involving Vp, RET and Vs-pars oralis (not shown, for full description see van Ham and Yeo 1996)

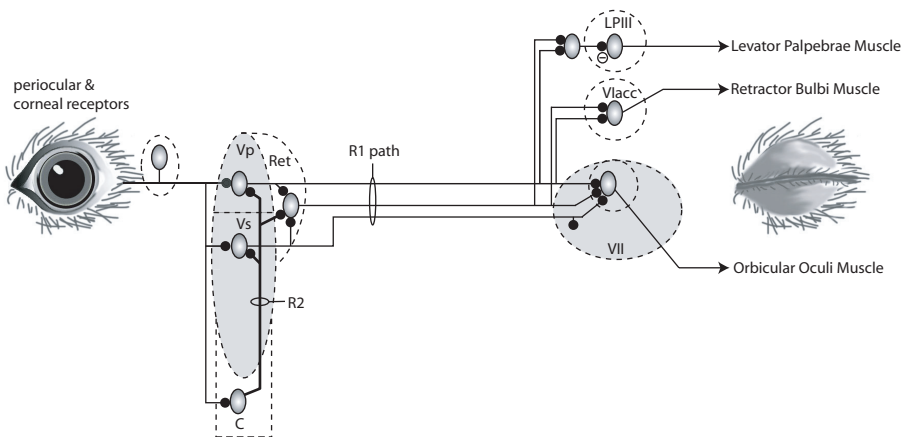


**Figure 1.5 Unconditioned response pathway as described for rabbit** (simplified and adapted from van Ham and Yeo 1996). Neurons receiving periocular and corneal primary afferent input are located in the principal trigeminal nucleus (Vp), spinal trigeminal nucleus (Vs) and rostral levels of the cervical spinal cord (C). R1 is disynaptic via Vp or Vs and blink motoneurons. Primary afferent receiving neurons in Vp activate motoneurons in the intermediate sub-area of VII and VIacc, but inhibit those in LPIII. The afferent receiving neurons in Vs project only to VII and are not restricted to the intermediate sub-area but include other facial sub-areas, thereby subserving other facial musculature. R2 is suggested to be mediated by interconnectivity between various parts in the trigeminal nucleus and rostral areas of the cervical cord.

The eyeblink does not only result from excitation of the MOO muscle. In addition, an inhibition of the antagonistic levator palpebrae muscle (i.e. the muscle that elevates the upper eyelid) is needed as well as activation of the accessory abducens nucleus (VIacc), responsible for retraction of the eyeball into the orbit. Motoneurons controlling the levator palpebrae muscle are located in the caudal contralateral oculomotor nucleus (LPIII). Inhibition of LPIII neurons is achieved by either activating local inhibitory interneurons or by separate inhibitory neurons in the trigeminal nucleus (van Ham and Yeo 1996). Neurons in Vp, Vs-pars oralis and RET are thought to provide monosynaptic connectivity to motoneurons in VII, VIacc as well as LPIII. Neurons in Vs provide connectivity to neurons in Vp and RET but also directly to motoneurons in VII. Interestingly these projections to VII are not restricted to the intermediate sub-area but included other facial sub-areas, thereby subserving other



facial musculature. In addition, these projections do not collateralize to VIacc. The primary afferents receiving neurons located in the rostral levels of the spinal cord do not project directly to motoneurons, but they exert their effects via neurons in Vs and Vp thereby creating polysynaptic pathways, that may mediate the R2 component. Based on a number of anatomical studies, Holstege and colleagues have suggested a more complex R2 pathway in the cat (figure 1.6; for full description see Holstege et al. 1986). This pathway contains two areas, one in the medulla oblongata and one in the pons that provide strong projections to the intermediate sub-area of VII. These areas are called the medullary and pontine blink premotor areas (Holstege et al. 1986; Holstege et al. 1986). These areas do not receive a direct input from the trigeminal nucleus and therefore cannot contribute to the disynaptic R1 component of the blink reflex. According to Shahani and Young (1968), the R2 component is responsible for actual closure of the eyelids (humans). Since a robust input to the blink motoneurons is necessary for such a performance, the pontine and medullary blink premotor areas are putative sources for this input (Holstege et al. 1986). Projections to these premotor areas involving the red nucleus and superior colliculus are depicted.

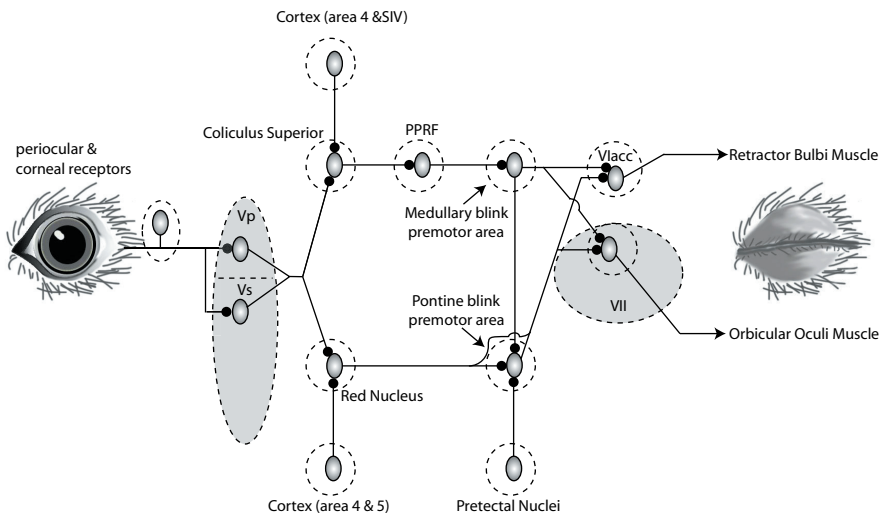


**Figure 1.6 R2 circuitry proposed for cat**, (by Holstege et al. 1986). Most of the sites and projections have been described or suggested in rabbit and rat as well. These pathways are superimposed on the R1 circuitry (not shown for simplicity).

In addition, areas projecting to the MOO motoneurons but not to VIacc motoneurons have been found at all levels of the bulbar lateral tegmental field. They probably relay input from somatic and emotional motor systems to muscles around the eye. The essential blink circuit is probably the same across mammalian species, but may be differently utilized. In rodents the R1 component contributes substantially to eyelid closure (Pellegrini et al. 1995). This difference between higher and lower mammals might be due to a stronger synaptic weighting of R1 circuitry. As in the cat it has been shown in rat that specific areas of medullary, pontine and mesencephalic reticular formations project onto MOO motoneurons. These projections were

frequently monosynaptic and larger in number than those from the trigeminal nuclei. Some of those pathways may be involved in the genesis of premotor signals related to the expression of internal emotional states, because limbic structures project to these areas through the central amygdala and hypothalamus (Holstege et al. 1986). Finally, rats display a strong monosynaptic input from auditory pathways to blink motoneurons which may explain the much more noticeable eyelid component in the auditory startle response in these animals. (Morcuende et al. 2002),

### *- The conditioned response pathway*

It is generally agreed that the cerebellum has at least an important role in classical conditioning of the eyelid response (see figure 1.7). Besides the lesion studies this notion is not only supported by lesion studies, but also by electrical stimulation studies and electrophysiological recording. Microstimulation experiments of the inferior olive have shown that the olivary climbing fibers can mediate the US, while the neurons in the pontine nuclei can well function as the CS (Mauk et al. 1986; Steinmetz et al. 1986; Steinmetz et al. 1989). Trained animals show CR's when the brachium pontis (BP, the bundle of mossy fibers entering the cerebellum) is stimulated, even when all fibers passing through the BP are lesioned before the stimulation site (Hesslow et al. 1999; Svensson et al. 1997).

The parts of the inferior olive that receive US related input from Vp and Vs are the medial portion of the dorsal accessory olive (mDAO) and the ventral leaf of the principal olive (Van Ham and Yeo 1992). Which cerebellar cortical areas are involved in classical conditioning of the eyelid response and to what extent the cerebellar cortex is responsible for CR expression is still under debate. The question remains to what extent plasticity in the cerebellar cortex and/or plasticity in the deep cerebellar nuclei (i.e. anterior interposed nucleus, AIN) are critical for classical conditioning of the eyelid response (Attwell et al. 2002; Yeo 1991; Lavond 2002; Lavond and Steinmetz 1989; Mauk and Donegan 1997; Medina et al. 2000; Medina et al. 2002).

Conditioned eyelid responses not only need to be acquired, to be effective they also need to peak at the right moment (i.e. just before the US would arrive). Different theories as to how this learning dependent timing comes about have been proposed. Learned timing could occur in the cerebellar cortex and/or in regions that project to the cerebellum via mossy fiber CS inputs. Moore and colleagues (Blazis and Moore 1991; Desmond and Moore 1991; Moore et al. 1989; Moore et al. 1986) have suggested that response timing may be mediated by mechanisms in the brainstem that lead to the timed activation of different mossy fibers at different times during the CS. This temporal code could be conveyed to the cerebellum where appropriate synapses are altered to obtain appropriately timed conditioned responses. Under certain conditions lesions of the hippocampus can alter the timing of conditioned responses (Orr and Berger 1985; Port et al. 1986), suggesting that the hippocampus can provide appropriately timed input to the cerebellum. Further, hippocampal pyramidal cells develop conditioned increases in activity that parallel the amplitude and time course of the learned behavioral responses (Berger et al. 1976; Mauk et al. 1982). These data have promoted suggestions that the hippocampus forms a "neural model" of the conditioned response and suggest the possibility that hippocampal-cerebellar



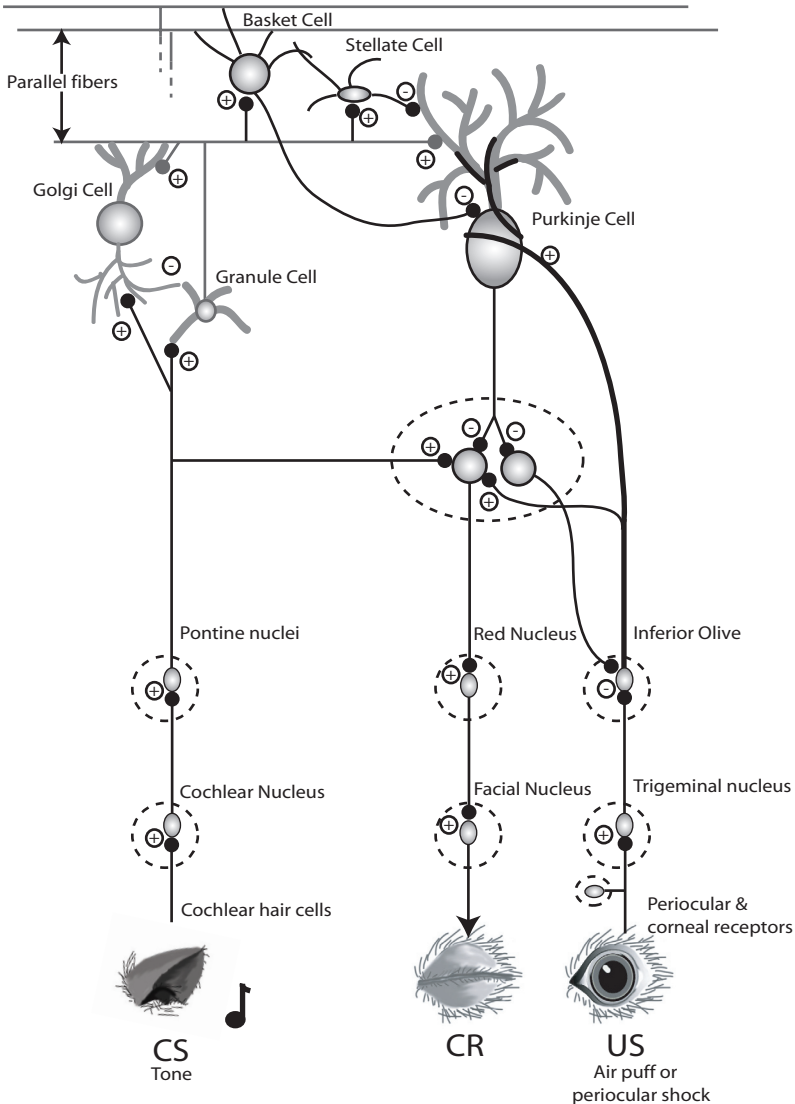


**Figure 1.7 Conditioned response pathway.** Information about the US is conveyed to the cerebellum via the trigeminal nucleus, the inferior olive and its climbing fiber system. Information about the auditory CS is transported to the cerebellum via the cochlear nucleus, pontine nuclei and the mossy fiber system. Plastic processes at sites of convergence (i.e. cerebellar nuclei, Purkinje cell) are hypothesized to underlie various aspects of the learned response. The inhibitory pathway from the deep nucleus back to the inferior olive has been claimed to mediate behavioral extinction (Kitazawa 2002; Medina et al. 2002).

interactions of some sort could influence the timing of conditioned responses. However, strong evidence has been presented that argues against this hypothesis. First, tonic activation of mossy fibers using electrical pontine stimulation as the CS results in normal response timing (Steinmetz et al. 1989; Svensson et al. 1997). Since this mossy fiber stimulation activates a fairly constant subset of mossy fibers throughout the duration of the CS, this normal timing occurs in the absence of the temporally coded mossy fiber inputs postulated by Moore and colleagues. Second, since mossy fibers send collaterals to cerebellar nuclei (Matsushita and Ikeda 1976; McCrea et al.

1977; Steinmetz and Sengelaub 1992), it seems likely that timing information would be conveyed there also. This is inconsistent with short-latency (i.e. ill timed) responses observed following cerebellar cortex lesions (Perrett et al. 1993). Together, these observations provide support for the hypothesis that the temporal discrimination involved in learned timing of conditioned responses is mediated by mechanisms within the cerebellum. Within the cerebellum two possible sites of where learned timing could develop have been proposed. Based on permanent and temporal lesion studies as well as electrophysiological recordings Yeo and colleagues argued that all aspects of conditioned responses are learned through plasticity in specific multiple cerebellar cortical areas (Attwell, 2002). In contrast, Lavond and colleagues (2002) argued that learning in the interposed nuclei can account for all the observed results of experiments on conditioning using lesions, recordings, stimulation and pharmacology. The more distributed explanation from the group of Mauk, based on experimental evidence and computer modeling (Medina et al. 2000) states that the capacity for temporally specific learning appears to be a specific property of the cerebellar cortex. In their view proper response timing would be the result of three interacting factors. 1) Connectivity in the cerebellar cortex produces variations in the different subsets of active granule cells during CS presentation; 2) parallel fiber – Purkinje cell synapses active around the moment of the climbing fiber activation will be depressed by LTD, eventually leading to a decrease in Purkinje cell activity and disinhibition of the cerebellar nuclear cell; and 3) Active parallel fiber – Purkinje cell synapses during other moments of CS presentation will be enhanced via LTP, thereby leading to an increase in Purkinje cell activity and a stronger inhibition of the cerebellar nuclear cells. Together these three phenomena would be responsible for the response shape of the conditioned response.

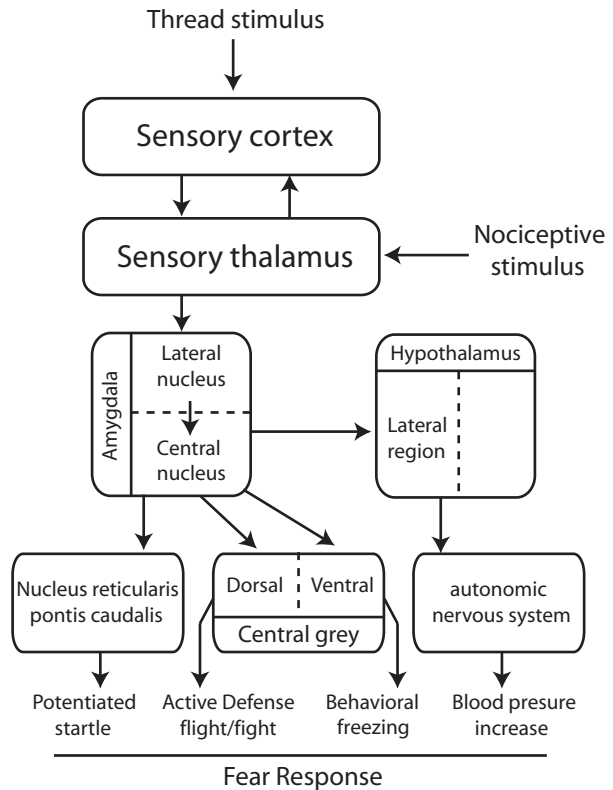
The acquisition and growth of the CR during the training time then would be the result of additional plasticity in the interposed nuclei, induced by the timed disinhibition through the Purkinje cells.

Thus, the CR pathway supports a prominent role of parallel fiber LTD but at the same time it also permits multiple other plastic processes to be involved in eyeblink conditioning.

### **1.3 Fear conditioning**

Fear is a complex emotion, but can be objectively measured in the laboratory using classical conditioning procedures in which a conditioned stimulus such as a tone is paired with an aversive stimulus, such as a footshock. Only a very small number of pairings (depending on US strength) is needed to elicit a constellation of behavior that is typically used to define a state of fear in animals. This includes a change in heart rate, blood pressure increase, vocalization, cessation of ongoing behavior and hyper-responsiveness to sensory stimuli (see fig 1.8). In a laboratory setup the most frequently used measures of fear are freezing behavior as well as the acoustic startle response.

**Figure 1.8 The fear response.** Unconditioned and conditioned aversive stimuli proceed from sense receptors to sensory cortex and/or sensory thalamus (see LeDoux 1992). The lateral nucleus of the amygdala receives input signals from the thalamus, transmitting them to the amygdala's central nucleus. There are three important connections efferent to the amygdala: a) a projection from the central amygdala to the lateral hypothalamic area that mediates the autonomic emotional response; b) projections to the midbrain central gray region, which mediates coping behaviors (see Keay and Bandler 2001); and c) a direct projection to the nucleus reticularis pontis caudalis, which modulates the startle circuit (adapted from Lang et al. 1998).



### 1.3a - behavioral freezing

In rodents freezing behavior, which is a sudden arrest of all ongoing movement (except breathing) after exposure to fearful event, is a frequently used measure to study and compare states of fear. Typically the animal is observed for a fixed period of time and behavior is scored. The state of fear is then determined as a ratio between the time the animal was freezing and the time the animal was not freezing. Since fear influences the acoustic startle response (think about the effect that watching a scary movie has on your reactivity to sudden sounds) this phenomenon has also been frequently used as a measure to study fear, usually in larger animals and humans.

### 1.3b - The acoustic startle response

The startle response is a rapid contraction of facial and skeletal muscles evoked by sudden intense acoustic, tactile or vestibular stimuli. It is the most extensive of all reflexes and can be easily observed across many mammalian species, including man. The startle response pattern consist of eyelid closure and a contraction of facial, neck and skeletal muscles, as well as an arrest of ongoing behaviors and an acceleration of the heart rate. The response pattern is suggestive of a protective function of startle against injury and of preparation for flight or fight. The startle response can be modulated by emotional states and is therefore frequently used as a tool to study a variety of aspects of emotions and emotional disorders (Davis et al. 1997; Koch 1999). The startle response can also be modified by many different forms of learning; as such it provides a meaningful tool to study cellular and molecular mechanisms of learn-

ing and plasticity in mammals (Davis et al. 1993; Lang et al. 1998). The neuronal structures underlying the startle response to acoustic stimuli have been studied intensively and include the cochlear root nucleus, the caudal pontine reticular nucleus and the output motoneurons located in the spinal cord and the facial nucleus (figure 1.9; see Koch, 1999 for review). The central sensorimotor interface of the startle is located in the pontine caudal reticular formation (PnC), which contains giant neurons that receive multimodal sensory input and project directly to facial, cranial and spinal motoneurons. Electrophysiological recording and stimulation experiments have shown that for facial components of startle, the gigantocellular nucleus of the medullary reticular formation also plays a role (Pellet 1990).

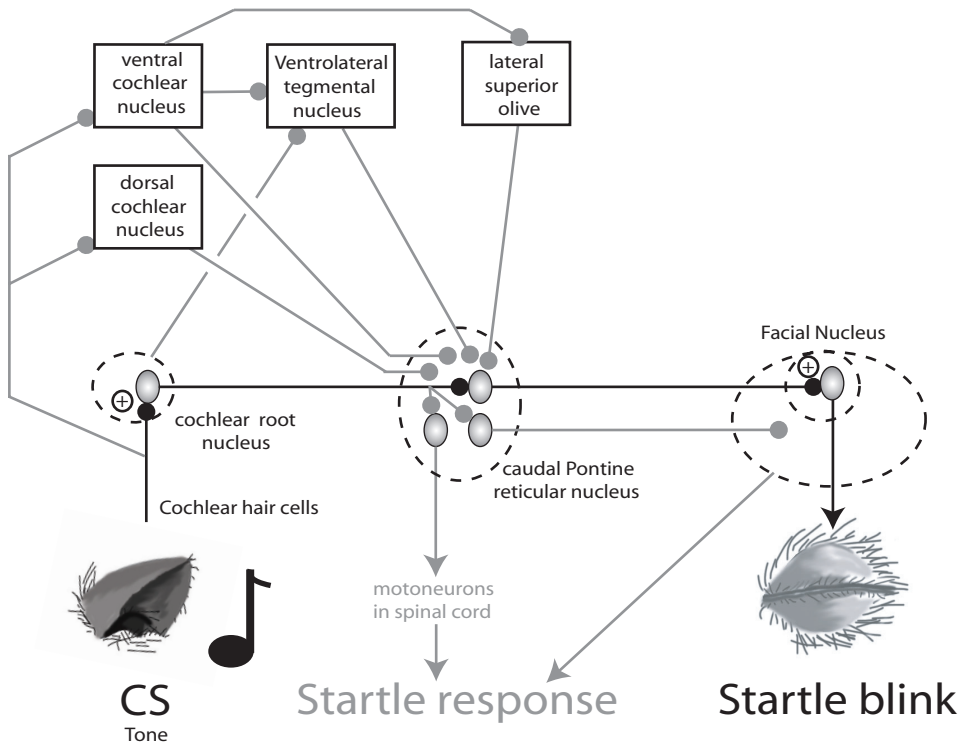


**Figure 1.9 basic simplified circuitry of the auditory startle response.** The black arrows show the fastest probable route of transmission of acoustic information to the blink motor output. The startle blink is an early component of the general startle response. The grey arrows show projections proposed to be involved in the startle response. These correlate with the multiple peaked excitatory post synaptic potentials (EPSP) recordings with constant latencies in the caudal pontine reticular nucleus.

Extracellular and intracellular single unit recordings from the rat PnC *in vivo* during acoustic stimulation revealed short latency excitatory post synaptic potentials (EPSP) of 2.6 msec and spike latency of 4.4 msec, which fit well with the short latency of the acoustic startle response (8-10 msec) (Ebert and Koch 1992; Lingenhohl and Friauf 1992; Lingenhohl and Friauf 1994). The PnC giant neurons appear to have a relatively low firing threshold and a capacity to temporally integrate various synaptic inputs. The EPSP amplitude of PnC neurons after acoustic stimulation is enhanced after electrical amygdala stimulation and reduced by a prepulse (short low amplitude acoustic stimulation < 50ms prior to the loud acoustic stimulus) or by in-

creasing the amplitude rise time of the acoustic stimulus. Interestingly, intracellular recordings have demonstrated that EPSP's from PnC neurons show multiple peaks that occur at constant latencies. This is suggestive of excitatory input to the PnC with different latencies from multiple afferent systems. Various auditory inputs to the PnC from the dorsal and ventral cochlear nucleus as well as the lateral superior olive and cochlear root nucleus have been revealed with the use of tracing studies. In addition, inputs from various other nuclei of the reticular formation have been described (for review see Koch 1998).

### **1.3c - contextual and cued fear conditioning**

As mentioned above fear can be classically conditioned. In a typical fear conditioning experiment, a rat or mouse is placed into an apparatus and receives pairings of a phasic auditory cue and electrical shock to its feet. Subsequently, when the auditory-cue conditioned stimulus is presented, the rodent will display a natural defensive response termed freezing, i.e. it becomes immobile. In addition to displaying conditioned freezing to the auditory cue (cued fear conditioning), the rodent also displays freezing to the situation or place in which the shock occurred. This phenomenon is usually referred to as contextual fear conditioning. Fear conditioned responses generally manifest themselves much more quickly than classically conditioned eyelid responses. After just 1 pairing of the CS with the US fear conditioned responses can have a profound magnitude, with retention of more than 2 weeks. Generally, cued fear conditioning seems critically dependent on the amygdala, while contextual fear conditioning additionally involves the hippocampus (for review see Medina et al. 2002; Phillips and LeDoux 1992). Lesions of the amygdala interfere with the conditioning of fear responses to both the cue and the context, whereas lesions of the hippocampus interfere with conditioning to the context but not to the cue. The amygdala seems involved in the conditioning of fear responses to simple, modality-specific conditioned stimuli as well as to complex, polymodal stimuli, while the hippocampus appears to be only involved in fear conditioning situations involving complex, polymodal events. These findings suggest a specific associative role for the amygdala and a sensory relay role for the hippocampus in fear conditioning.

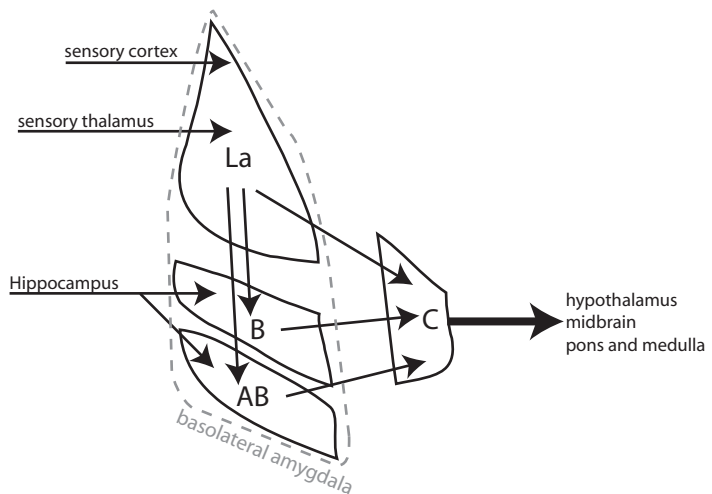
The difference between cue-explicit fear and a more generalized fear of the context in which shock occurs (e.g., the experimental chamber) is very interesting. A further distinction between cue-explicit and more generalized fear has been made by Michael Davis and colleagues. He demonstrated that potentiated startle that normally occurs in the presence of fear cues is eliminated by lesions of the central nucleus of the amygdala. Potentiated startle is also observed when rodents are placed in a naturally species-specific dangerous environment such as a brightly lit cage, analogous to humans placed in a total dark environment (Davis et al. 1997). In contrast to fear conditioning, where an initial harmless context or cue is associated with fear only after exposure to a fearful event, this potentiation effect is not dependent on training. In addition when corticotropin-releasing hormone (CRH) is injected into the cerebral ventricles of the rat, it induces a generalized state of arousal, resembling anxiety (Swerdlow et al. 1986). Unlike conditioned fear, however, CRH potentiated startle is not eliminated by lesions of the amygdala's central nucleus. Instead, this anxietylike,

CRH-driven potentiated startle appears to depend on a different structure, the bed nucleus of the stria terminalis (Lee and Davis 1997). This same bed nucleus (and not the amygdala's central nucleus) is also critical to potentiated startle occurring when rats are exposed to a brightly lit experimental chamber (Walker and Davis 1997). In short, the neurophysiological circuit for unconditioned anxietylike reactions appears to involve a different pathway from that engaged by explicit, conditioned fear cues.

### 1.3d - CS pathways

The pathways through which CS inputs reach the amygdala have been studied extensively in recent years. Much of the work has been focused on the auditory modality, which will be described briefly. The amygdala is a complex structure, consisting of about 12 subnuclei, each with different inputs and outputs and each with different functions. Although a number of different schemes have been used to label amygdala areas the scheme for the rat brain suggested by Pitkanen et al (1997) is followed here. The areas of most relevance to fear conditioning are the lateral, basal, accessory basal and central nuclei as well as the connections between these nuclei (Figure 1.10). The connections between the nuclei are indicated. However, it is important to note that connections are organized on a subnuclear level within each nuclear region. The main input from the sensory cortex and sensory thalamus terminate in the lateral nucleus; and the basal and accessory basal nuclei receive a strong projection from the ventral hippocampus (CA1 and subiculum).

**Figure 1.10. Intra-amygdalar connections involved with fear conditioning.** The areas of most relevance to fear conditioning are the lateral (La), basal (B), accessory basal (AB), central nuclei (C) and the connections between these nuclei. The lateral nucleus projects to the central, the basal and accessory basal nucleus. The basal and accessory basal nucleus both project to the central nucleus as well. Lateral, basal and accessory basal nucleus are frequently also termed basolateral complex or basolateral amygdala.



Auditory CS information reaches the lateral nucleus of the amygdala through connections from auditory processing areas in both the thalamus (medial geniculate body) and the auditory cortex (LeDoux et al. 1990; Mascagni et al. 1993)(figure 1.11). Of these two projections the direct projection from the thalamus is probably the more important one. The exact conditions under which the cortical projection is required are not known, probably they come into play when more complex auditory cues are used (Jarrell et al. 1987). Further evidence for the involvement of the lateral amygdala is given by the demonstration that damage to the lateral amygdala indeed interferes with auditory fear conditioning (Campeau and Davis 1995). As mentioned

above, rodents also show conditioned fear after reexposure to the context where the unconditioned fear evoking stimulus was presented. Besides the amygdala, the hippocampus is also critically involved in this contextual fear conditioning (Phillips and LeDoux 1992). Ventral hippocampal areas, more specifically the CA1 and subiculum regions project to the basal and accessory basal nucleus of the amygdala (Canteras and Swanson 1992; van Groen and Wyss 1990). Damage to these areas in both the amygdala and the hippocampus is known to interfere with contextual conditioning (Maren and Fanselow 1995; Bannerman et al. 2003; Richmond et al. 1999). Figure 1.11 summarizes the auditory CS and contextual CS pathways into the amygdala as well as the US pathways

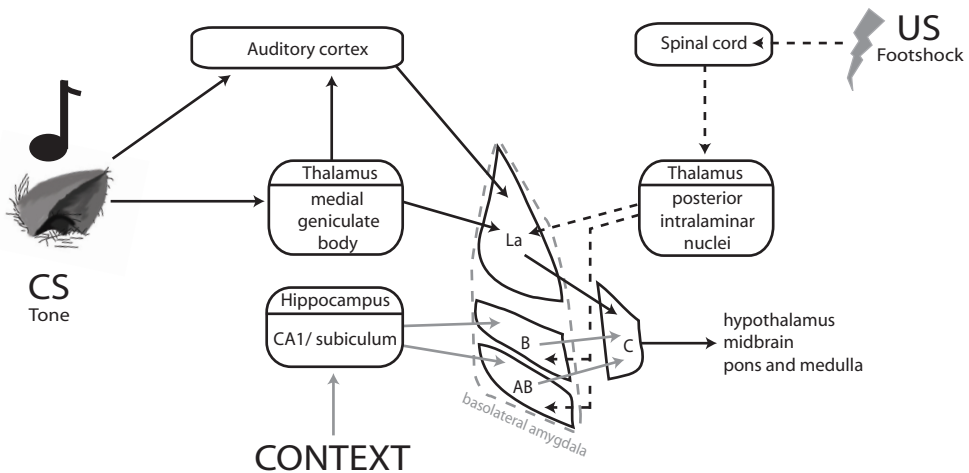


**Figure 1.11 Contextual and cued fear conditioning circuitry.** Conditioning to a tone (CS) involves projections from the auditory system to the lateral nucleus of the amygdala (La) and from La to the central nucleus of the amygdala (C, black arrows). For simplicity, single US pathways are depicted (dashed arrows). The US is transmitted to the thalamus via the spinothalamic tract and conveyed to La, B and probably AB. In contrast to tone CS, conditioning to the apparatus and other contextual cues present when the CS and US are paired involves the representation of the context by the hippocampus and the communication between the hippocampus and the basal (B) and accessory basal (AB) nuclei of the amygdala, which in turn project to C (grey arrows). As for tone conditioning, C controls the expression of the responses.

### 1.3e - US pathways

If the amygdala is the learning site for classical fear conditioning then there must be a convergence of CS and US information. Since the lateral nucleus seems to be the important target area for acoustic CS input, this would be the most obvious site where such a convergence and plasticity could exist.

The thalamic posterior intralaminar nuclei receive somatic pain inputs from the spinal cord (Cliffer et al. 1991; Ledoux et al. 1987) and in turn project to the amygdala, particularly the basolateral amygdaloid nucleus (Ledoux et al. 1987; Yasui et al. 1991). Electrical stimulation of this area is an effective unconditioned stimulus for fear conditioning similar to foot shock (Cruikshank et al., 1992). Thus, this thalamo-amygdaloid pathway may serve as a US pathway during emotional learning. However, lesions in this thalamic region did not prevent fear conditioning to a foot-shock US (Campeau and Davis 1995). Therefore parallel US pathways have been



suggested, probably involving the parietal insular cortex (see Shi and Davis 1999). Furthermore, cells in the amygdaloid lateral nucleus are responsive to nociceptive stimulation, and some of the same cells respond to auditory inputs as well (Roman-ski et al 1993). Thus, the substrate for conditioning (convergence of CS and US information) exists in the lateral nucleus, and as shown below, conditioning induces plasticity in CS-elicited responses in this area. Cortical areas that process somato-sensory stimuli, including nociceptive stimuli, project to the lateral and some other amygdala nuclei (see McDonald 1998). Parallel to the CS inputs, there is evidence that conditioning can be mediated by US inputs to the amygdala from either thalamic or cortical areas (Shi and Davis 1999). Although the basal and accessory basal nuclei of the amygdala do not receive direct CS inputs from auditory systems, they do receive inputs from the hippocampus (Canteras and Swanson 1992). The hippocampus, as described above, is necessary for forming a representation of the context, and these contextual representations, transmitted from the hippocampus to the basal and accessory basal nuclei, may be modified by the US inputs to these regions. The central nucleus of the amygdala receives nociceptive inputs from the parabrachial area (Bernard and Besson 1990) and directly from the spinal cord (Bernard and Besson 1990). Although the central nucleus does not receive inputs from sensory areas processing acoustic CSs, it is a direct recipient of inputs from the lateral, basal and accessory basal nuclei. US inputs to the amygdaloid central nucleus could be involved in higher-order integration. For example, associative responses created by CS-US convergence in the lateral or context-US convergence in the basal and /or accessory basal nucleus, after transfer to the central nucleus, might converge with and be further modified by nociceptive inputs to the central nucleus.

Finally, with respect to the intra-amygdalar pathways (see figure 1.10) it is important to note that the direct pathway from the lateral to the central nucleus is the most important for the transmission of tone CS information. Evidence for this is given by the demonstration that lesions of the basal and accessory basal nucleus do not interfere with tone CS fear conditioning (Nader et al. 2001). Thus, the basolateral amygdala is well equipped for mediating the plasticity underlying contextual and cued fear conditioning.

### ***1.3f - plasticity related to fear conditioning***

Plasticity related to fear has been studied using three methods, i.e. single unit recordings, induction of long term potentiation (LTP) and blockage of LTP. Some cells in the lateral amygdaloid nucleus are responsive to both CS and US inputs; In addition CS induced responses in these cells can be modified after pairing with the US (Quirk et al. 1997; Quirk et al. 1995). CS-US related plasticity has also been observed in other areas such as the thalamus, auditory cortex and central nucleus, but induction of plasticity in these areas all needed more training trials and had longer response latencies than observed in the lateral amygdala (Pascoe and Kapp 1985; Quirk et al. 1997; Weinberger et al. 1995). LTP is a physiological procedure pioneered in studies of the hippocampus (Bliss and Lomo 1973) and is believed to engage the cellular mechanisms similar to those that underlie natural learning (see Bliss and Collin



gridge 1993). The most extensively studied form of LTP occurs in the CA1 region of the hippocampus and involves the interaction between presynaptic glutamate and two classes of postsynaptic receptors. First, glutamate binds to AMPA receptors and depolarizes the postsynaptic cell. The depolarization allows glutamate to bind to the N-methyl-D-aspartate (NMDA) class of receptors. Calcium then flows into the cell through the NMDA channel and triggers a host of intracellular events that ultimately result in gene induction and synthesis of new proteins (Kandel 1997). These then help to stabilize the changes over long periods of time.

There have been a number of studies of LTP in the amygdala, mostly involving *in vitro* brain slices and pathways carrying information from the cortex to the lateral and basal nuclei (Chapman and Bellavance 1992; Huang and Kandel 1998). These studies have led to mixed results regarding the possible role of NMDA receptors in cortico-amygdala LTP, with some studies finding effects (Huang and Kandel 1998) and some not (Chapman and Bellavance 1992). LTP has also been studied *in vivo* in the thalamo-amygdala pathway using recordings of extracellular field potentials (Clugnet and LeDoux 1990; Rogan et al. 1997). These studies show that LTP occurs in fear processing pathways, that the processing of natural stimuli similar to those used as a CS in conditioning studies is facilitated following LTP induction, and that fear conditioning and LTP induction produce similar changes in the processing of CS-like stimuli. Although exploration of mechanisms is difficult in these *in vivo* studies, they nevertheless provide some of the strongest evidence to date in any brain system of a relation between natural learning and LTP (Barnes 1995; Eichenbaum 1995; Stevens, 1998). LTP has been found *in vivo* in the hippocampal-amygdala pathway, which is believed to be involved in context conditioning (Maren and Fanselow 1995).

The fact that blockade of NMDA receptors with the drug D,L-2-amino-5-phosphonovalerate (APV) prevents hippocampal LTP from occurring inspired researchers to attempt to prevent fear conditioning by infusion of APV into the amygdala. Initial studies were promising (Miserendino et al. 1990). NMDA receptors seemed to be involved in the plasticity underlying learning and not in the transmission of signals through the amygdala. However, subsequently both *in vivo* (Maren et al. 1996) and *in vitro* (Weisskopf and LeDoux 1999) studies have suggested that NMDA receptors also make significant contributions to synaptic transmission in pathways that provide inputs to the amygdala. Furthermore, several studies have found that blockade of NMDA receptors affects both the acquisition and the expression of fear learning (Lee and Kim 1998; Maren et al. 1996), which is more consistent with the transmission rather than the plasticity hypothesis, but others have confirmed that acquisition could be affected independently from expression (Gewirtz and Davis 1997). The contribution of NMDA receptors to fear conditioning and its underlying plasticity, as opposed to synaptic transmission in amygdala circuits, remains unresolved.

## 1.4 Scope of this thesis

The enormous amount of literature and decades of hot debate among research groups does not seem to fit the much advertized simplicity of both the classical conditioning procedure and the circuitry involved. However, it is becoming increasingly clear that the simplicity of the cerebellar circuitry should not be overestimated.

Recently, Ekerot and colleagues have demonstrated that parallel fiber receptive fields of cerebellar cortical interneurons can be adaptively modified through parallel fiber – climbing fiber conjunctive stimulation (Ekerot and Jorntell, 2003; Jorntell and Ekerot 2003). In addition, *in vitro* studies have demonstrated long-term plasticity at multiple sites in both the cerebellar cortex and deep cerebellar nucleus (see Hansel et al. 2001 for review). Plasticity has been described for parallel fiber, interneuron and climbing fiber synapses. LTD and its reverse, long term potentiation (LTP) have been shown in the Purkinje cell to nuclear cell synapse and additionally, cerebellar granular cells and nuclear cells exhibit activity dependent changes in intrinsic excitability that are non-synaptic. The totally plastic cerebellar circuit is becoming more and more likely. Attempts to solve the questions regarding if, when and how the cerebellum contributes to classical eyeblink conditioning in the normal behaving animal with techniques that involves mechanical lesions (including cooling and local infusion/injections of chemicals) will very likely be unsuccessful in such a plastic circuit. In order to truly understand what is happening with the cerebellum during classical conditioning the lesioning technique should be advanced to the molecular level. Genetic techniques nowadays make it possible to genetically alter single proteins. Such a genetic approach, combined with electrophysiology and behavioral experiments might give further insights into cerebellar functioning in associative motor learning.

This thesis primarily attempts to solve some long standing issues regarding classical eyelid conditioning. More specifically, what is the specific role of cerebellar LTD in classical eyeblink conditioning, and how does the answer change the view on cerebellar functioning on associative motor learning? The approach used in this thesis is a combination of the above mentioned genetic approach with classical conditioning experiments. The genetic techniques are by far best possible in mice because of their fast breeding and the availability of genetically well characterized inbred strains. Often gene function is tested by creating transgenic or knockout mice. In transgenic mice, artificial DNA is introduced in the genome of a mouse, which will lead to expression of the transgene in the animal. In knockout mice a targeted gene is completely deleted from the genome. The protein that was coded by this gene will no longer be expressed. When working with genetically manipulated mice potential problems might occur, not unlike those discussed above for lesion experiments. It is clear that behavior of a null mutant or transgenic animal is not only influenced by the altered or deleted gene but probably also by a number of secondary or compensating developmental or physiological changes. Therefore when a null mutant or transgenic animal has a behavioral phenotype, this does not necessarily mean that the changed behavior is indicative for the normal functioning of the altered or deleted gene. Fortunately, it is possible by using tissue specific enhancers (DNA sequences that promote gene transcription) to make e.g. cell type specific gene deletions. Although

this is very attractive, the final results might still be influenced by developmental compensatory mechanisms, since the gene will be missing throughout development. Recently, inducible gene promoters have been added to the genetic toolbox. This means that it is possible to make cell-type specific gene modifications that can be turned on or off when needed. It would then be possible to e.g. do behavioral experiments in a mouse and compare results before and after the gene was turned on. This would greatly improve the statistical power of the experiments.

In short, the genetic lesion technique suffers from similar mechanisms as the mechanical lesion studies but at least for the genetic lesion technique the technology today and in the future will provide great improvements to compensate these problems.

To be able to study the effect of genetic lesions on classical conditioning we needed a system that could reliably measure the performance of a mouse on such a learning task. Some studies using mice in eyeblink conditioning tasks already existed (Aiba et al. 1994; Bao et al. 1998; Chen et al. 1996; Kim et al. 1997; Shibuki et al. 1996). All these studies used electromyographic (EMG) recordings of the MOO muscle to assess responsiveness on the training paradigm. Attempts to repeat this procedure led to the realization that to obtain reliable EMG recordings of the MOO muscle in a mouse over a number of consecutive days is close to impossible, simply because of the small size of a mouse eyelid. We therefore developed a new system that could reliably measure eyelid position over time in mice. Since it makes use of magnetism we called it the magnetic distance measurement technique (MDMT). **Chapter 2** describes the developmental process and validation of the technique.

The previous studies using various knockout mice (mGluR1, GluR $\delta$ 2, glial fibrillary acidic protein) have supported the claim that LTD was underlying several forms of motor learning; however, this work has suffered from the limitations that the knockout technique lacks anatomical specificity and that functional compensation can occur via similar gene family members. To overcome these limitations, a transgenic mouse (called L7-PKCi) has been produced in which the pseudosubstrate PKC inhibitor, PKC [19-31], was selectively expressed in Purkinje cells under the control of the *pcp-2(L7)* gene promoter. The creation of this mouse, the effect of the transgene on LTD, normal motor behavior and VOR adaptation is described in **Chapter 3**.

**Chapter 4** demonstrates what the lack of cerebellar LTD means for the performance of L7-PKCi mouse on classical eyelid conditioning.

**Chapter 5** reports the cerebellar deficits included in the Fragile X syndrome. The syndrome is caused by a lack of a single protein called Fragile X mental retardation protein (FMRP). Hippocampal studies on a mouse model which lacks FMRP have suggested an enhancement of hippocampal LTD next to morphological differences in dendrital spines in these mice. Therefore we tested this mouse model to study the effect of lack FMRP on cerebellar morphology and tested whether also cerebellar parallel fiber LTD was enhanced. In addition, the effect of this enhanced LTD on the performance on the eyeblink conditioning task is described.

Our studies in mice using MDMT for classical eyelid conditioning indicated that only part of the behavior could be explained by the standard classical eyeblink conditioning circuitry. This realization led us to investigate and take into account the processes

and phenomenon of classical conditioning of the fear response. Large similarities between the two procedures i.e. both the stimulus presentations and behavioral measures are actually easy to recognize. We therefore created a fear conditioning setup (adapted from Anagnostaras et al. 2000) and subjected a variety of mice to this test. In **Chapter 6** we provide evidence that mice with haploinsufficiency for *Cyln2* have features reminiscent of Williams syndrome, including mild growth deficiency, brain abnormalities, hippocampal dysfunction and particular deficits in motor coordination. Dysfunction of hippocampal dependent learning was tested both at the electrophysiological level and at the behavioral level by investigating LTP-induction, contextual fear conditioning and cued-fear conditioning, respectively.

In **Chapter 7** the implications of the results from this thesis will be discussed. In addition, Important differences between mice and other animal models with regard to the eyeblink conditioning task will be discussed, as well as possible effects of fear related processes on the eyeblink performance of mice.

## 1.5 References

- Aiba, A., M. Kano, C. Chen, M. E. Stanton, G. D. Fox, K. Herrup, T. A. Zwingman and S. Tonegawa (1994). "Deficient cerebellar long-term depression and impaired motor learning in mGluR1 mutant mice." *Cell* 79(2): 377-88.
- Albus, J. S. (1971). "A theory of cerebellar function." *Math. Biosci.* 10: 25-61.
- Anagnostaras, S. G., S. A. Josselyn, P. W. Frankland and A. J. Silva (2000). "Computer-assisted behavioral assessment of Pavlovian fear conditioning in mice." *Learn Mem* 7(1): 58-72.
- Andersson, G. and O. Oscarsson (1978). "Climbing fiber microzones in cerebellar vermis and their projection to different groups of cells in the lateral vestibular nucleus." *Exp Brain Res* 32(4): 565-79.
- Attwell, P. J., M. Ivarsson, L. Millar and C. H. Yeo (2002). "Cerebellar mechanisms in eyeblink conditioning." *Ann N Y Acad Sci* 978: 79-92.
- Bannerman, D. M., M. Grubb, R. M. Deacon, B. K. Yee, J. Feldon and J. N. Rawlins (2003). "Ventral hippocampal lesions affect anxiety but not spatial learning." *Behav Brain Res* 139(1-2): 197-213.
- Bao, S., L. Chen and R. F. Thompson (1998). "Classical eyeblink conditioning in two strains of mice: conditioned responses, sensitization, and spontaneous eyeblinks." *Behav Neurosci* 112(3): 714-8.
- Barnes, C. A. (1995). "Involvement of LTP in memory: are we "searching under the street light"?" *Neuron* 15(4): 751-4.
- Berger, T. W., B. Alger and R. F. Thompson (1976). "Neuronal substrate of classical conditioning in the hippocampus." *Science* 192(4238): 483-5.
- Bernard, J. F. and J. M. Besson (1990). "The spino(trigemino)pontoamygdaloid pathway: electrophysiological evidence for an involvement in pain processes." *J Neurophysiol* 63(3): 473-90.
- Blazis, D. E. and J. W. Moore (1991). "Conditioned stimulus duration in classical trace conditioning: test of a real-time neural network model." *Behav Brain Res* 43(1): 73-8.
- Bliss, T. V. and G. L. Collingridge (1993). "A synaptic model of memory: long-term potentiation in the hippocampus." *Nature* 361(6407): 31-9.
- Bliss, T. V. and T. Lomo (1973). "Long-lasting potentiation of synaptic transmission in the dentate area of the anaesthetized rabbit following stimulation of the perforant path." *J Physiol* 232(2): 331-56.
- Campeau, S. and M. Davis (1995). "Involvement of subcortical and cortical afferents to the lateral nucleus of the amygdala in fear conditioning measured with fear-potentiated startle in

- rats trained concurrently with auditory and visual conditioned stimuli." *J Neurosci* 15(3 Pt 2): 2312-27.
- Canteras, N. S. and L. W. Swanson (1992). "Projections of the ventral subiculum to the amygdala, septum, and hypothalamus: a PHAL anterograde tract-tracing study in the rat." *J Comp Neurol* 324(2): 180-94.
- Chapman, P. F. and L. L. Bellavance (1992). "Induction of long-term potentiation in the basolateral amygdala does not depend on NMDA receptor activation." *Synapse* 11(4): 310-8.
- Chen, L., S. Bao, J. M. Lockard, J. K. Kim and R. F. Thompson (1996). "Impaired classical eyeblink conditioning in cerebellar-lesioned and Purkinje cell degeneration (pcd) mutant mice." *J Neurosci* 16(8): 2829-38.
- Chen, R., L. G. Cohen and M. Hallett (2002). "Nervous system reorganization following injury." *Neuroscience* 111(4): 761-73.
- Clark, G. A., D. A. McCormick, D. G. Lavond and R. F. Thompson (1984). "Effects of lesions of cerebellar nuclei on conditioned behavioral and hippocampal neuronal responses." *Brain Res* 291(1): 125-36.
- Cliffer, K. D., R. Burstein and G. J. Giesler, Jr. (1991). "Distributions of spinothalamic, spinohypothalamic, and spinotelencephalic fibers revealed by anterograde transport of PHA-L in rats." *J Neurosci* 11(3): 852-68.
- Clugnet, M. C. and J. E. LeDoux (1990). "Synaptic plasticity in fear conditioning circuits: induction of LTP in the lateral nucleus of the amygdala by stimulation of the medial geniculate body." *J Neurosci* 10(8): 2818-24.
- Daniel, H., N. Hemart, D. Jaillard and F. Crepel (1993). "Long-term depression requires nitric oxide and guanosine 3':5' cyclic monophosphate production in rat cerebellar Purkinje cells." *Eur J Neurosci* 5(8): 1079-82.
- Davis, M., W. A. Falls, S. Campeau and M. Kim (1993). "Fear-potentiated startle: a neural and pharmacological analysis." *Behav Brain Res* 58(1-2): 175-98.
- Davis, M., D. L. Walker and Y. Lee (1997). "Amygdala and bed nucleus of the stria terminalis: differential roles in fear and anxiety measured with the acoustic startle reflex." *Phil. Trans. R. Soc. Lond* 352: 1675-1687.
- Desmond, J. E. and J. W. Moore (1991). "Altering the synchrony of stimulus trace processes: tests of a neural-network model." *Biol Cybern* 65(3): 161-9.
- Desmond, J. E., M. E. Rosenfield and J. W. Moore (1983). "An HRP study of the brainstem afferents to the accessory abducens region and dorsolateral pons in rabbit: implications for the conditioned nictitating membrane response." *Brain Res Bull* 10(6): 747-63.
- Ebert, U. and M. Koch (1992). "Glutamate receptors mediate acoustic input to the reticular brain stem." *Neuroreport* 3(5): 429-32.

- Eichenbaum, H. (1995). "Spatial learning. The LTP-memory connection." *Nature* 378(6553): 131-2.
- Ekerot, C. F., M. Garwicz and J. Schouenborg (1991). "Topography and nociceptive receptive fields of climbing fibres projecting to the cerebellar anterior lobe in the cat." *J Physiol* 441: 257-74.
- Freeman, J. H., Jr., A. M. Scharenberg, J. L. Olds and B. G. Schreurs (1998). "Classical conditioning increases membrane-bound protein kinase C in rabbit cerebellum." *Neuroreport* 9(11): 2669-73.
- Freeman, J. H., Jr., T. Shi and B. G. Schreurs (1998). "Pairing-specific long-term depression prevented by blockade of PKC or intracellular Ca<sup>2+</sup>." *Neuroreport* 9(10): 2237-41.
- Garwicz, M., C. F. Ekerot and H. Jorntell (1998). "Organizational Principles of Cerebellar Neuronal Circuitry." *News Physiol Sci* 13: 26-32.
- Garwicz, M., C. F. Ekerot and J. Schouenborg (1992). "Distribution of Cutaneous Nociceptive and Tactile Climbing Fibre Input to Sagittal Zones in Cat Cerebellar Anterior Lobe." *Eur J Neurosci* 4(4): 289-295.
- Gewirtz, J. C. and M. Davis (1997). "Second-order fear conditioning prevented by blocking NMDA receptors in amygdala." *Nature* 388(6641): 471-4.
- Gilbert, P. F. (1974). "A theory of memory that explains the function and structure of the cerebellum." *Brain Res* 70(1): 1-18.
- Hall, S. M. (1989). "Regeneration in the peripheral nervous system." *Neuropathol Appl Neurobiol* 15(6): 513-29.
- Hansel, C., D. J. Linden and E. D'Angelo (2001). "Beyond parallel fiber LTD: the diversity of synaptic and non-synaptic plasticity in the cerebellum." *Nat Neurosci* 4(5): 467-75.
- Hesslow, G., P. Svensson and M. Ivarsson (1999). "Learned movements elicited by direct stimulation of cerebellar mossy fiber afferents." *Neuron* 24(1): 179-85.
- Holstege, G., J. Tan, J. J. van Ham and G. A. Graveland (1986). "Anatomical observations on the afferent projections to the retractor bulbi motoneuronal cell group and other pathways possibly related to the blink reflex in the cat." *Brain Res* 374(2): 321-34.
- Holstege, G., J. J. van Ham and J. Tan (1986). "Afferent projections to the orbicularis oculi motoneuronal cell group. An autoradiographical tracing study in the cat." *Brain Res* 374: 306-320.
- Huang, Y. Y. and E. R. Kandel (1998). "Postsynaptic induction and PKA-dependent expression of LTP in the lateral amygdala." *Neuron* 21(1): 169-78.
- Ito, M. (2001). "Cerebellar long-term depression: characterization, signal transduction, and functional roles." *Physiol Rev* 81(3): 1143-95.



## Chapter 1

---

- Ito, M. and M. Kano (1982). "Long-lasting depression of parallel fiber-Purkinje cell transmission induced by conjunctive stimulation of parallel fibers and climbing fibers in the cerebellar cortex." *Neurosci Lett* 33(3): 253-8.
- Jarrell, T. W., C. G. Gentile, L. M. Romanski, P. M. McCabe and N. Schneiderman (1987). "Involvement of cortical and thalamic auditory regions in retention of differential bradycardiac conditioning to acoustic conditioned stimuli in rabbits." *Brain Res* 412(2): 285-94.
- Kandel, E. R. (1997). "Genes, synapses, and long-term memory." *J Cell Physiol* 173(2): 124-5.
- Keay, K. A. and R. Bandler (2001). "Parallel circuits mediating distinct emotional coping reactions to different types of stress." *Neurosci Biobehav Rev* 25(7-8): 669-78.
- Kelly, T. M., C. C. Zuo and J. R. Bloedel (1990). "Classical conditioning of the eyeblink reflex in the decerebrate- decerebellate rabbit." *Behav Brain Res* 38(1): 7-18.
- Kim, J. J., J. C. Shih, K. Chen, L. Chen, S. Bao, S. Maren, S. G. Anagnostaras, M. S. Fanselow, E. De Maeyer, I. Seif and R. F. Thompson (1997). "Selective enhancement of emotional, but not motor, learning in monoamine oxidase A-deficient mice." *Proc Natl Acad Sci U S A* 94(11): 5929-33.
- Kitazawa, S. (2002). "Neurobiology: ready to unlearn." *Nature* 416(6878): 270-3.
- Koch, M. (1999). "The neurobiology of startle." *Prog. Neurobiol.* 59: 107-128.
- Kugelberg, E. (1952). "Facial reflexes." *Brain* 75: 385-396.
- Kuhn, H. G., H. Dickinson-Anson and F. H. Gage (1996). "Neurogenesis in the dentate gyrus of the adult rat: age-related decrease of neuronal progenitor proliferation." *J Neurosci* 16(6): 2027-33.
- Lang, P. J., M. M. Bradley and B. N. Cuthbert (1998). "Emotion, motivation, and anxiety: brain mechanisms and psychophysiology." *Biol Psychiatry* 44(12): 1248-63.
- Lashley, K. S. (1939). "The mechanism of vision. XVI. The functioning of small remnants of the visual cortex." *J. Comp. Neurol.* 70: 45-67.
- Lashley, K. S. (1950). "In search of the engram." *Society of experimental Biology, Symposium* 4: 454-482.
- Lavond, D. G. (2002). "Role of the nuclei in eyeblink conditioning." *Ann N Y Acad Sci* 978: 93-105.
- Lavond, D. G., T. L. Hembree and R. F. Thompson (1985). "Effect of kainic acid lesions of the cerebellar interpositus nucleus on eyelid conditioning in the rabbit." *Brain Res* 326(1): 179-82.
- Lavond, D. G., J. J. Kim and R. F. Thompson (1993). "Mammalian brain substrates of aversive classical conditioning." *Annu Rev Psychol* 44: 317-42.



- Lavond, D. G. and J. E. Steinmetz (1989). "Acquisition of classical conditioning without cerebellar cortex." *Behav Brain Res* 33(2): 113-64.
- LeDoux, J. E. (1992). "Brain mechanisms of emotion and emotional learning." *Curr Opin Neurobiol* 2(2): 191-7.
- LeDoux, J. E., C. Farb and D. A. Ruggiero (1990). "Topographic organization of neurons in the acoustic thalamus that project to the amygdala." *J Neurosci* 10(4): 1043-54.
- Ledoux, J. E., D. A. Ruggiero, R. Forest, R. Stornetta and D. J. Reis (1987). "Topographic organization of convergent projections to the thalamus from the inferior colliculus and spinal cord in the rat." *J Comp Neurol* 264(1): 123-46.
- Lee, H. and J. J. Kim (1998). "Amygdalar NMDA receptors are critical for new fear learning in previously fear-conditioned rats." *J Neurosci* 18(20): 8444-54.
- Lee, Y. and M. Davis (1997). "Role of the hippocampus, the bed nucleus of the stria terminalis, and the amygdala in the excitatory effect of corticotropin-releasing hormone on the acoustic startle reflex." *J Neurosci* 17(16): 6434-46.
- Lev-Ram, V., L. R. Makings, P. F. Keitz, J. P. Kao and R. Y. Tsien (1995). "Long-term depression in cerebellar Purkinje neurons results from coincidence of nitric oxide and depolarization-induced Ca<sup>2+</sup> transients." *Neuron* 15(2): 407-15.
- Linden, D. J. and J. A. Conner (1995). "Long-term synaptic depression." *Annu Rev Neurosci* 18: 319-357.
- Linden, D. J., T. M. Dawson and V. L. Dawson (1995). "An evaluation of the nitric oxide/cGMP/cGMP-dependent protein kinase cascade in the induction of cerebellar long-term depression in culture." *J Neurosci* 15(7 Pt 2): 5098-105.
- Lingenhohl, K. and E. Friauf (1992). "Giant neurons in the caudal pontine reticular formation receive short latency acoustic input: an intracellular recording and HRP-study in the rat." *J Comp Neurol* 325(4): 473-92.
- Lingenhohl, K. and E. Friauf (1994). "Giant neurons in the rat reticular formation: a sensorimotor interface in the elementary acoustic startle circuit?" *J Neurosci* 14(3 Pt 1): 1176-94.
- Liu, C. N. and W. W. Chambers (1958). "Intraspinal sprouting of dorsal root axons; development of new collaterals and preterminals following partial denervation of the spinal cord in the cat." *AMA Arch Neurol Psychiatry* 79(1): 46-61.
- Maren, S., G. Aharonov, D. L. Stote and M. S. Fanselow (1996). "N-methyl-D-aspartate receptors in the basolateral amygdala are required for both acquisition and expression of conditional fear in rats." *Behav Neurosci* 110(6): 1365-74.
- Maren, S. and M. S. Fanselow (1995). "Synaptic plasticity in the basolateral amygdala induced by hippocampal formation stimulation in vivo." *J Neurosci* 15(11): 7548-64.

Marr, D. (1968). "A theory of cerebellar cortex." *J. Physiol* 202: 437-470.

Mascagni, F., A. J. McDonald and J. R. Coleman (1993). "Corticoamygdaloid and cortico-cortical projections of the rat temporal cortex: a Phaseolus vulgaris leucoagglutinin study." *Neuroscience* 57(3): 697-715.

Matsushita, M. and M. Ikeda (1976). "Projections from the lateral reticular nucleus to the cerebellar cortex and nuclei in the cat." *Exp Brain Res* 24(4): 403-21.

Mauk, M. D. and N. H. Donegan (1997). "A model of Pavlovian eyelid conditioning based on the synaptic organization of the cerebellum." *Learn Mem* 4(1): 130-58.

Mauk, M. D., J. E. Steinmetz and R. F. Thompson (1986). "Classical conditioning using stimulation of the inferior olive as the unconditioned stimulus." *Proc Natl Acad Sci U S A* 83(14): 5349-5353.

Mauk, M. D. and R. F. Thompson (1987). "Retention of classically conditioned eyelid responses following acute decerebration." *Brain Res* 403(1): 89-95.

Mauk, M. D., J. T. Warren and R. F. Thompson (1982). "Selective, naloxone-reversible morphine depression of learned behavioral and hippocampal responses." *Science* 216(4544): 434-6.

McCormick, D. A., D. G. Lavond, G. A. Clark, R. E. Kettner, C. E. Rising and R. F. Thompson (1981). "The engram found? Role of the cerebellum in classical conditioning of nictitating membrane and eyelid responses." *Bulletin of the Psychonomic Society* 18: 103-105.

McCrea, R. A., G. A. Bishop and S. T. Kitai (1977). "Electrophysiological and horseradish peroxidase studies of precerebellar afferents to the nucleus interpositus anterior. II. Mossy fiber system." *Brain Res* 122(2): 215-28.

McDonald, A. J. (1998). "Cortical pathways to the mammalian amygdala." *Prog Neurobiol* 55(3): 257-332.

Medina, J. F., J. Christopher Repa, M. D. Mauk and J. E. LeDoux (2002). "Parallels between cerebellum- and amygdala-dependent conditioning." *Nat Rev Neurosci* 3(2): 122-31.

Medina, J. F., K. S. Garcia, W. L. Nores, N. M. Taylor and M. D. Mauk (2000). "Timing mechanisms in the cerebellum: testing predictions of a large-scale computer simulation." *J Neurosci* 20(14): 5516-25.

Medina, J. F., W. L. Nores and M. D. Mauk (2002). "Inhibition of climbing fibres is a signal for the extinction of conditioned eyelid responses." *Nature* 416(6878): 330-3.

Medina, J. F., W. L. Nores, T. Ohyama and M. D. Mauk (2000). "Mechanisms of cerebellar learning suggested by eyelid conditioning." *Curr Opin Neurobiol* 10(6): 717-24.

Miserendino, M. J., C. B. Sananes, K. R. Melia and M. Davis (1990). "Blocking of acquisition but not expression of conditioned fear-potentiated startle by NMDA antagonists in the amygdala." *Nature* 345(6277): 716-8.

Monakow, C. v. (1914). "Die lokalisation im grosshirn und der abbau der funktion durch kortikale herde." Wiesbaden, Bergmann.

Moore, J. W., J. E. Desmond and N. E. Berthier (1989). "Adaptively timed conditioned responses and the cerebellum: a neural network approach." *Biol Cybern* 62(1): 17-28.

Moore, J. W., J. E. Desmond, N. E. Berthier, D. E. Blazis, R. S. Sutton and A. G. Barto (1986). "Simulation of the classically conditioned nictitating membrane response by a neuron-like adaptive element: response topography, neuronal firing, and interstimulus intervals." *Behav Brain Res* 21(2): 143-54.

Morcuende, S., J. M. Delgado-Garcia and G. Ugolini (2002). "Neuronal premotor networks involved in eyelid responses: retrograde transneuronal tracing with rabies virus from the orbicularis oculi muscle in the rat." *J Neurosci* 22(20): 8808-18.

Munk, H. (1881). "Über die Funktionen der Grosshirnrinde. Gesammelte Mitteilungen aus den Jahren 1877-1880." Berlin: Hirshwald.

Nader, K., P. Majidishad, P. Amorapanth and J. E. LeDoux (2001). "Damage to the lateral and central, but not other, amygdaloid nuclei prevents the acquisition of auditory fear conditioning." *Learn Mem* 8(3): 156-63.

Norman, R. J., J. S. Buchwald and J. R. Villablanca (1977). "Classical conditioning with auditory discrimination of the eye blink in decerebrate cats." *Science* 196(4289): 551-3.

Norman, R. J., J. R. Villablanca, K. A. Brown, J. A. Schwafel and J. S. Buchwald (1974). "Classical eyeblink conditioning in the bilaterally hemispherectomized cat." *Exp Neurol* 44(3): 363-80.

Orr, W. B. and T. W. Berger (1985). "Hippocampectomy disrupts the topography of conditioned nictitating membrane responses during reversal learning." *Behav Neurosci* 99(1): 35-45.

Overend, W. (1896). "Preliminary note on a new cranial reflex." *Lancet* 1: 619.

Pascoe, J. P. and B. S. Kapp (1985). "Electrophysiological characteristics of amygdaloid central nucleus neurons during Pavlovian fear conditioning in the rabbit." *Behav Brain Res* 16(2-3): 117-33.

Pavlov, I. P. (1927). "Conditioned reflexes: An investigation of the physiological activity of the cerebral cortex (G.V. Anrep, translation)." London: Oxford University Press.

Pellegrini, J. J., A. K. Horn and C. Evinger (1995). "The trigeminally evoked blink reflex. I. Neuronal circuits." *Exp Brain Res* 107(2): 166-80.

Pellet J. (1990). "Neural organization in the brainstem circuit mediating the primary acoustic head startle: an electrophysiological study in the rat." *Physiol Behav* 48: 727-739.

Perrett, S. P., B. P. Ruiz and M. D. Mauk (1993). "Cerebellar cortex lesions disrupt learning-

dependent timing of conditioned eyelid responses.” *J Neurosci* 13(4): 1708-18.

Phillips, R. G. and J. E. LeDoux (1992). “Differential contribution of amygdala and hippocampus to cued and contextual fear conditioning.” *Behav Neurosci* 106(2): 274-85.

Port, R. L., A. G. Romano, J. E. Steinmetz, A. A. Mikhail and M. M. Patterson (1986). “Retention and acquisition of classical trace conditioned responses by rabbits with hippocampal lesions.” *Behav Neurosci* 100(5): 745-52.

Quirk, G. J., J. L. Armony and J. E. LeDoux (1997). “Fear conditioning enhances different temporal components of tone-evoked spike trains in auditory cortex and lateral amygdala.” *Neuron* 19(3): 613-24.

Quirk, G. J., C. Repp and J. E. LeDoux (1995). “Fear conditioning enhances short-latency auditory responses of lateral amygdala neurons: parallel recordings in the freely behaving rat.” *Neuron* 15(5): 1029-39.

Rankin, C. H., C. D. Beck and C. M. Chiba (1990). “*Caenorhabditis elegans*: a new model system for the study of learning and memory.” *Behav Brain Res* 37(1): 89-92.

Reynolds, T. and N. A. Hartell (2001). “Roles for nitric oxide and arachidonic acid in the induction of heterosynaptic cerebellar LTD.” *Neuroreport* 12(1): 133-6.

Rice, A. C., A. Khaldi, H. B. Harvey, N. J. Salman, F. White, H. Fillmore and M. R. Bullock (2003). “Proliferation and neuronal differentiation of mitotically active cells following traumatic brain injury.” *Exp Neurol* 183(2): 406-17.

Richmond, M. A., B. K. Yee, B. Pouzet, L. Veenman, J. N. Rawlins, J. Feldon and D. M. Bannerman (1999). “Dissociating context and space within the hippocampus: effects of complete, dorsal, and ventral excitotoxic hippocampal lesions on conditioned freezing and spatial learning.” *Behav Neurosci* 113(6): 1189-203.

Rogan, M. T., U. V. Staubli and J. E. LeDoux (1997). “Fear conditioning induces associative long-term potentiation in the amygdala.” *Nature* 390(6660): 604-7.

Rosenfield, M. E. and J. W. Moore (1983). “Red nucleus lesions disrupt the classically conditioned nictitating membrane response in rabbits.” *Behav Brain Res* 10(2-3): 393-8.

Rosenfield, M. E. and J. W. Moore (1985). “Red nucleus lesions impair acquisition of the classically conditioned nictitating membrane response but not eye-to-eye savings or unconditioned response amplitude.” *Behav Brain Res* 17(1): 77-81.

Schmaltz, L. W. and J. Theios (1972). “Acquisition and extinction of a classically conditioned response in hippocampctomized rabbits (*Oryctolagus cuniculus*.)” *J Comp Physiol Psychol* 79(2): 328-33.

Schreurs, B. G., M. M. Oh and D. L. Alkon (1996). “Pairing-specific long-term depression of Purkinje cell excitatory postsynaptic potentials results from a classical conditioning procedure in the rabbit cerebellar slice.” *J Neurophysiol* 75(3): 1051-60.

- Shahani, B. and R. R. Young (1968). "A note on blink reflexes." *J Physiol* 198(2): 103-104.
- Shi, C. and M. Davis (1999). "Pain pathways involved in fear conditioning measured with fear-potentiated startle: lesion studies." *J Neurosci* 19(1): 420-30.
- Shibuki, K., H. Gomi, L. Chen, S. Bao, J. J. Kim, H. Wakatsuki, T. Fujisaki, K. Fujimoto, A. Katoh, T. Ikeda, C. Chen, R. F. Thompson and S. Itohara (1996). "Deficient cerebellar long-term depression, impaired eyeblink conditioning, and normal motor coordination in GFAP mutant mice." *Neuron* 16(3): 587-99.
- Solomon, P. R., E. R. Vander Schaaf, R. F. Thompson and D. J. Weisz (1986). "Hippocampus and trace conditioning of the rabbit's classically conditioned nictitating membrane response." *Behav Neurosci* 100(5): 729-44.
- Squire, L. R. (1992). "Memory and the hippocampus: a synthesis from findings with rats, monkeys, and humans." *Psychol Rev* 99(2): 195-231.
- Stevens, C. F. (1998). "A million dollar question: does LTP = memory?" *Neuron* 20(1): 1-2.
- Steinmetz, J. E., D. G. Lavond and R. F. Thompson (1989). "Classical conditioning in rabbits using pontine nucleus stimulation as a conditioned stimulus and inferior olive stimulation as an unconditioned stimulus." *Synapse* 3(3): 225-233.
- Steinmetz, J. E., D. J. Rosen, P. F. Chapman, D. G. Lavond and R. F. Thompson (1986). "Classical conditioning of the rabbit eyelid response with a mossy-fiber stimulation CS: I. Pontine nuclei and middle cerebellar peduncle stimulation." *Behav Neurosci* 100(6): 878-87.
- Steinmetz, J. E. and D. R. Sengelaub (1992). "Possible conditioned stimulus pathway for classical eyelid conditioning in rabbits. I. Anatomical evidence for direct projections from the pontine nuclei to the cerebellar interpositus nucleus." *Behav Neural Biol* 57(2): 103-15.
- Svensson, P., M. Ivarsson and G. Hesslow (1997). "Effect of varying the intensity and train frequency of forelimb and cerebellar mossy fiber conditioned stimuli on the latency of conditioned eye-blink responses in decerebrate ferrets." *Learn Mem* 4(1): 105-15.
- Swerdlow, N. R., M. A. Geyer, W. W. Vale and G. F. Koob (1986). "Corticotropin-releasing factor potentiates acoustic startle in rats: blockade by chlordiazepoxide." *Psychopharmacology (Berl)* 88(2): 147-52.
- van Groen, T. and J. M. Wyss (1990). "Extrinsic projections from area CA1 of the rat hippocampus: olfactory, cortical, subcortical, and bilateral hippocampal formation projections." *J Comp Neurol* 302(3): 515-28.
- Van Ham, J. J. and C. H. Yeo (1992). "Somatosensory Trigeminal Projections to the Inferior Olive, Cerebellum and other Precerebellar Nuclei in Rabbits." *Eur J Neurosci* 4(4): 302-317.
- van Ham, J. J. and C. H. Yeo (1996). "The central distribution of primary afferents from the external eyelids, conjunctiva, and cornea in the rabbit, studied using WGA-HRP and B-HRP

as transganglionic tracers." *Exp. Neurol.* 142: 217-225.

van Ham, J. J. and C. H. Yeo (1996). "Trigeminal inputs to eyeblink motoneurons in the rabbit." *Exp Neurol* 142(2): 244-257.

Voogd, J. and M. Glickstein (1998). "The anatomy of the cerebellum." *Trends Neurosci* 21(9): 370-5.

Walker, D. L. and M. Davis (1997). "Double dissociation between the involvement of the bed nucleus of the stria terminalis and the central nucleus of the amygdala in startle increases produced by conditioned versus unconditioned fear." *J Neurosci* 17(23): 9375-83.

Weinberger, N. M., R. Javid and B. Lapan (1995). "Heterosynaptic long-term facilitation of sensory-evoked responses in the auditory cortex by stimulation of the magnocellular medial geniculate body in guinea pigs." *Behav Neurosci* 109(1): 10-7.

Weisskopf, M. G. and J. E. LeDoux (1999). "Distinct populations of NMDA receptors at subcortical and cortical inputs to principal cells of the lateral amygdala." *J Neurophysiol* 81(2): 930-4.

Welsh, J. P. (1992). "Changes in the motor pattern of learned and unlearned responses following cerebellar lesions: a kinematic analysis of the nictitating membrane reflex." *Neuroscience* 47(1): 1-19.

Welsh, J. P. and J. A. Harvey (1989). "Cerebellar lesions and the nictitating membrane reflex: performance deficits of the conditioned and unconditioned response." *J Neurosci* 9(1): 299-311.

Welsh, J. P. and J. A. Harvey (1991). "Pavlovian conditioning in the rabbit during inactivation of the interpositus nucleus." *J Physiol (Lond)* 444: 459-80.

Woodruff-Pak, D. S., D. G. Lavond and R. F. Thompson (1985). "Trace conditioning: abolished by cerebellar nuclear lesions but not lateral cerebellar cortex aspirations." *Brain Res* 348(2): 249-60.

Xerri, C., M. M. Merzenich, B. E. Peterson and W. Jenkins (1998). "Plasticity of primary somatosensory cortex paralleling sensorimotor skill recovery from stroke in adult monkeys." *J Neurophysiol* 79(4): 2119-48.

Yarbrough, G. G. and J. W. Phillis (1975). "Supersensitivity of central neurons--a brief review of an emerging concept." *Can J Neurol Sci* 2(3): 147-52.

Yasui, Y., C. B. Saper and D. F. Cechetto (1991). "Calcitonin gene-related peptide (CGRP) immunoreactive projections from the thalamus to the striatum and amygdala in the rat." *J Comp Neurol* 308(2): 293-310.

Yeo, C. H. (1991). "Cerebellum and classical conditioning of motor responses." *Ann N Y Acad Sci* 627: 292-304.

# Chapter 2

## Monitoring Kinetic and Frequency-Domain Properties of Eyelid Responses in Mice With Magnetic Distance Measurement Technique

S.K.E. KOEKKOEK<sup>1</sup>, W. L. DEN OUDEN<sup>1</sup>, G. PERRY<sup>2</sup>, S. M. HIGHSTEIN<sup>2</sup> AND C. I. DE ZEEUW<sup>1</sup>

<sup>1</sup>*Department of Neuroscience, Erasmus University Rotterdam, 3000 DR, Rotterdam, The Netherlands*

<sup>2</sup>*Department of Otolaryngology, Washington University School of Medicine, St. Louis, Missouri 63110*

Received 16 May 2001; accepted in final form 12 April 2002

- *J Neurophysiol* 88: 2124–2133, 2002

### List of Abbreviations

CS	: Conditioned Stimulus
EMG	: ElectroMyoGraph
FPS	: Frames Per Second
MDMT	: Magnetic Distance Measurement Technique
ISI	: Inter-Stimulus Interval (CS-US interval)
ITI	: Inter-Trial Interval
LED	: Light Emitting Diode
MLLS	: Musculus Levator Labii Superior
MOO	: Musculus Orbicularis Oculi
SD	: Standard Deviation
US	: Unconditioned Stimulus



## 2.1 Abstract

Classical eye-blink conditioning in mutant mice can be used to study the molecular mechanisms underlying associative learning. To measure the kinetic and frequency domain properties of conditioned (tone - periorbital shock procedure) and unconditioned eyelid responses in freely moving mice, we developed a method that allows adequate, absolute, and continuous determination of their eyelid movements in time and space while using an electrical shock as the unconditioned stimulus. The basic principle is to generate a local magnetic field that moves with the animal and that is picked up by either a field-sensitive chip or coil. With the use of this magnetic distance measurement technique (MDMT), but not with the use of electromyographic recordings, we were able to measure mean latency, peak amplitude, velocity, and acceleration of unconditioned eyelid responses, which equaled  $7.9 \pm 0.2$  ms,  $1.2 \pm 0.02$  mm,  $28.5 \pm 1$  mm/s, and  $637 \pm 22$  mm/s<sup>2</sup>, respectively (means  $\pm$  SD). During conditioning, the mice reached an average of 78% of conditioned responses over four training sessions, while animals that were subjected to randomly paired conditioned and unconditioned stimuli showed no significant increases. The mean latency of the conditioned responses decreased from  $222 \pm 40$  ms in *session 2* to  $127 \pm 6$  ms in *session 4*, while their mean peak latency increased from  $321 \pm 45$  to  $416 \pm 67$  ms. The mean peak amplitudes, peak velocities, and peak acceleration of these responses increased from  $0.62 \pm 0.02$  to  $0.77 \pm 0.02$  mm, from  $3.9 \pm 0.3$  to  $7.7 \pm 0.5$  mm/s, and from  $81 \pm 7$  to  $139 \pm 10$  mm/s<sup>2</sup>, respectively. Power spectra of acceleration records illustrated that both the unconditioned and conditioned responses of mice had oscillatory properties with a dominant peak frequency close to 25 Hz that was not dependent on training session, interstimulus interval, or response size. These data show that MDMT can be used to measure the kinetics and frequency domain properties of conditioned eyelid responses in mice and that these properties follow the dynamic characteristics of other mammals.

## 2.2 Introduction

Important insights have been obtained on the mechanisms underlying learning and memory by investigating the abilities of animals to condition their eyelid responses. Eyelid responses can either be conditioned in the standard way in which a conditioned stimulus (CS) such as a tone continues until the unconditioned stimulus (US) such as a corneal air-puff or an electrical shock ceases, or one can acquire so-called traceconditioned eyelid responses in which the CS and US are separated by a trace interval. The main area for memory formation and storage underlying classical eye-blink conditioning is probably the cerebellum (Hesslow and Yeo 1998; Kim and Thompson 1997; McCormick and Thompson 1984), while the critical brain regions involved in trace conditioning also include higher structures such as the hippocampus (Disterhoft et al. 1999; Thompson et al. 1996).

Initially, most of the classical conditioning studies were done in rabbits and cats see e.g., (Attwell et al. 2001; Gruart et al. 1997; Steinmetz et al. 1992). These studies did not only elucidate which parts of the brain stem and cerebellum contribute to the formation and/or storage of conditioned responses, but they also provided insight



into the framework of kinetic and frequency domain properties of both conditioned and unconditioned eyelid movements (Becker and Fuchs 1988; Evinger et al. 1991; Gruart et al. 1994, 2000a,b). Based on these findings it has been suggested that there must be a common oscillator that underlies eyelid movements (Domingo et al. 1997) and that the dominant frequency of this oscillator shows an inverse logarithmic relationship with the body weight of the type of species (Gruart et al. 2000a,b). To date the kinetic properties of eyelid movements in mice have not been described yet, and it is not known whether their eyelid oscillations follow the same relationship.

With the advent of transgenic technologies, it has become feasible to investigate the underlying mechanisms of eye-blink conditioning at the molecular level. Because the mouse is the only mammal of which embryonic stem cells are presently available that can be readily genetically manipulated for homologous recombination, this mammal is at present the preferred species to investigate the molecular mechanisms underlying learning and memory formation including those associated with eye-blink conditioning. For example, recent studies in mouse mutants were aimed at identifying the roles of mGluR1 and glial fibrillary acidic protein in the induction of cerebellar long-term depression and eye-blink conditioning (Aiba et al. 1994; Conquet et al. 1994; Shibuki et al. 1996). These studies have adopted the electromyographic (EMG) recording methods that were successfully applied for eye-blink conditioning in rabbits and cats. However, the question is whether this methodology is optimal for recording eyelid responses in mice. The much smaller size of the mouse and its facial musculature may make this preparation much more susceptible for picking up EMG activities of muscles that are not involved in the eye-blink response. For example, due to chewing or whisker movements during conditioning trials, EMG eye-blink recordings that are thought to result from activities in the musculus orbicularis oculi (MOO) may be contaminated by activities of larger surrounding muscles like the musculus masseter or musculus levator labii superior (MLLS). Such a spill-over of electrical signals may be particularly detrimental if one needs to obtain accurate recordings with an optimal spatiotemporal resolution. Moreover, for measuring position, velocity, or acceleration of conditioned and unconditioned eyelid responses, EMG recordings do have the disadvantages that they reflect muscle activities rather than directly the actual eyelid movement and that stimulus artifacts are picked up if the unconditioned stimulus (US) is delivered by an electrical shock. An alternative could be to implant a search coil in the eyelid so as to detect an inductive current during eyelid rotation by placing the subject in a homogenous magnetic field. This method has been successfully applied for eye-blink conditioning in cats and humans (Becker and Fuchs 1988; Delgado-Garcia et al. 1990; Gruart et al. 2000a; Schicatano et al. 2002), but this approach is also unlikely to be optimal for mice as this method requires the subject to be restrained. Because mice are relatively sensitive for fixation, which can evoke various sorts of unwanted emotional, nonassociative, and even associative reactions during the process of eyelid conditioning, it appears particularly relevant for mice to do eye-blink conditioning in the freely moving preparation (see also following text). We have therefore attempted to develop a method for eyeblink conditioning in mice that allows us to record their eyelid responses with a high spatiotemporal resolution in a freely moving state while

applying conditioned and unconditioned stimuli without inducing artifacts in the recording. The basic principle is to generate a local magnetic field that moves with the animal and that is picked up by either a field sensitive chip or coil; we refer to this method as the magnetic distance measurement technique (MDMT). The spatio-temporal resolution of conditioned eyelid responses recorded in mice with the use of MDMT will be directly compared with that of EMG recordings, and the use of both methods in mice will be evaluated with the use of high speed video recordings. In addition, using MDMT we will provide for the first time the framework of kinetic and frequency domain properties of conditioned and nonconditioned eyelid movements of mice that can serve as a basis for further studies in transgenic mutants.

## 2.3 Methods

### 2.3a - MDMT

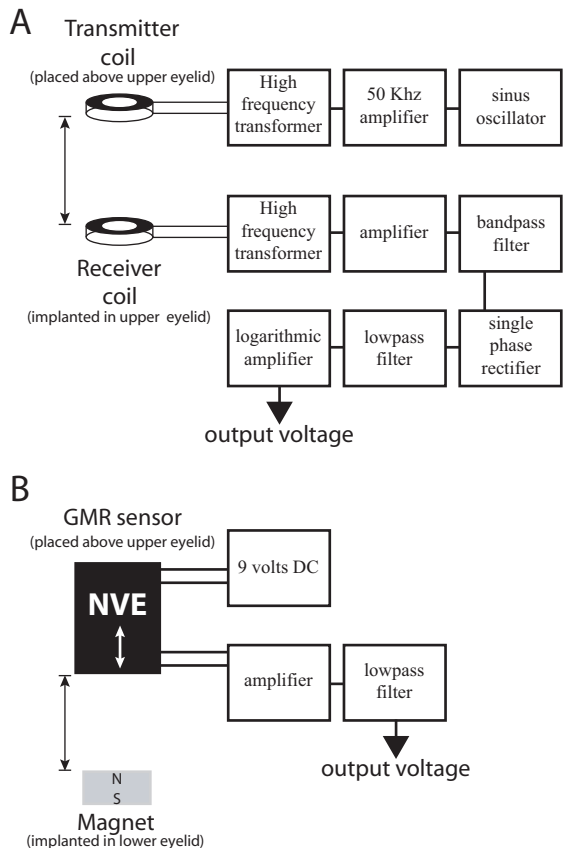
MDMT can be applied with the use of either two local coils or a magnet and a locally placed field-sensitive chip. The electronic circuitries of both possibilities are depicted in Fig. 1. In the first possibility, the magnetic field is generated by a transmitter coil (60 turns of 30 mm enameled copper wire, 1.2 mm in diameter, 0.3 mm thickness, IET, Marly, Switzerland) placed above the upper eyelid, while a eyelid receiver coil (20 turns of 30  $\mu$ m enameled copper wire, 0.8 mm in diameter, 0.2 mm thickness, IET) implanted in the upper eyelid relays an induction signal, which is dependent on the changes of the mutual position of these two coils (Fig. 2.1A). The transmitter and receiver part of the system are situated on the same electronic print layout. The transmitter part consists of a sinus oscillator serving as a current source (100 mA, 50 kHz) and an amplifier that supplies the field generating coil. The transmitter coil is connected to the amplifier via a high-frequency transformer to prevent leakage of current to the coil. The small induced voltage ( $\pm 0.5$  mV) in the receiver coil is fed into the receiver part via a high-frequency transformer after which the signal is amplified (40–90 dB). To reduce the noise of the signal it is band-pass filtered before it is single phase rectified, low-pass filtered, and fed into a logarithmic amplifier.

Because the amplifier delivers a signal proportional to the natural logarithm of the amplitude of the induced voltage, the inductance in the receiver coil changes with displacement of the eyelid (Arts and Reneman 1980; Renterghem 1983). The data are captured with the use of a CED power1401 AD converter sampling at 1 kHz coupled to an Axon Instruments Cyberamp 360 and analyzed off-line using custom written Matlab scripts. In the second possibility, the magnetic field is generated by a magnet (neodymium iron borium; 0.8 x 0.5 x 0.2 mm in size, 3 mg weight, machined using 0.8 mm disk-type magnets (Wondermagnet: [www.wondermagnet.com](http://www.wondermagnet.com)) implanted in the lower eyelid, while a giant magnetoresistive (GMR) sensorchip (NVE; AA004-MSOP) fixed above the upper eyelid picks up the strength of the magnetic field and delivers thereby a signal that depends on the position of the magnet, which has its north-south pole orientation across the width of the magnet (Fig. 1.1B). The application use of GMR sensors is comparable to that of so-called “Hall-effect” sensors (Hamiel et al. 1995; Korhonen 1991; Rodriguez et al. 2001). For details on GMR technology, see GMR technology sheet (NVE 2002). When a voltage is ap-

plied to the sensor, it returns a voltage that is determined by the strength of the magnetic field. Thus if the system is calibrated correctly, the voltage directly reflects the distance between the magnet and the sensor. System analysis of a dummy setup shows that following logarithmic conversion the sensor signal is linearly related to distances between 1.8 and 3.7 mm (< 5% deviation). The signals are captured and analyzed as described below.

The surgical procedures to prepare the animals for MDMT were as follows. Adult male (6–10 wk) C57/B6 mice were anesthetized using an oxygenated mixture of

**Figure 2.1. Organization of magnetic distance measurement technique (MDMT) devices** using either 2 minicoils or a GMR sensor chip with magnet. *A*: the MDMT device with minicoils is divided in a transmitter part and a receiver part, both of which are situated on the same print layout. The transmitter part consists of a current source (100 mA, 50 kHz) and an amplifier that supplies the field generating coil. This coil is connected to the amplifier via a high-frequency transformer to prevent leakage of current to the coil. The small induced voltage of the receiver coil is fed into the receiver part via a high-frequency transformer after which the signal is amplified (40–90 dB). To reduce noise, the signal is band-pass filtered. Subsequently, the signal is single phase rectified, low-pass filtered and fed into a logarithmic amplifier, which delivers a signal proportional to the natural logarithm of the amplitude of the induced voltage. *B*: the MDMT device with GMR sensorchip and a magnet is less complicated than the inductive system. A magnet provides an eyelid fixed constant magnetic field, which is detected by a GMR sensorchip. The chip consists out of a wheatstone bridge formed by 4 GMR resistors. Axis sensitivity (white arrow) is achieved by magnetically shielding 2 of the 4 resistors (NVE product sheet). The input voltage is provided by a 9-V battery pack, which in this configuration provides a signal change of 30 mV during eyelid closure. Amplification (x 100) and low-pass (500 Hz) filtering is done by an Axon Cyberamp 360.



nitrous oxide and halothane delivered through a cap fitting the snout ( $n = 18$ ). A pre-made connector converted from a miniature connector (SamTec; [www.samtec.com](http://www.samtec.com)) to hold 12 dual-pin connections on a 3 x 8 mm surface and a height of 3 mm was placed on the skull with the use of a pedestal of dental cement and 5 M1 screws. A coil or an in silicon embedded magnet was implanted in a pocket dissected in the eyelid. A suture wire glued to the coil or magnet was used to fixate this structure in the pocket. The pocket was closed with tissue glue. The transmission coil or sensor chip was carefully placed with the use of dental cement in an optimal position over the upper eyelid. For example, in case of the GMR sensor, optimal position was obtained when the distance between the magnet and sensor in the eyelid closed situation was 2 mm and the axis of sensitivity was aligned with the north-south axis of the magnet in the

halfway closed position. Fully opened, fully closed and halfway opened positions were repetitively measured and stored for calibration purposes. Two insulated copper wires with a diameter of 30  $\mu\text{m}$  and 0.5  $\mu\text{m}$  tinned tips were placed underneath the skin to provide the US. The tips of the wires were located close to the lateral corner of the eyelids, one in the upper and one in the lower lid. The US electrode was connected to computer controlled stimulus isolation units (Dagan S910; [www.dagan.com](http://www.dagan.com)), which created biphasic constant current electrical shocks (30 ms, 166 Hz pulses; max, 1 mA). The strength of the stimulus was controlled by an UR-based feedback mechanism so as to prevent potential induction of fear conditioning processes (Phillips and LeDoux 1992). This UR-based feedback was achieved by monitoring each UR and adjusting the stimulus strength to the minimal necessary to get full eyelid closure. The connecting cable including all wires was attached to a silicone mouse harness (Instech; [www.instechlabs.com](http://www.instechlabs.com)), which allowed the mice to move around during the experiment with relatively little discomfort since there is no torque or strain on the head. After the general surgery the animals were allowed to recover and adjust to their harnesses for > 4 days.

MDMT data were analyzed according to the following criteria. Eyelid movement larger than the mean + 3 times SD of the 500 ms pre-CS period was considered significant (minimal of 0.2 mm threshold was included). Trials with significant activity in the pre-CS period were excluded, and trials with significant activity in the CS-onset to 75 ms post CS-onset period were counted as startle responses. A conditioned response was counted if there was significant activity in the 75 ms post CS-onset to US-onset time period. During CS alone trials, this period was extended with 200 ms. Unconditioned blinks (40 trials) obtained from *session 1* and conditioned blinks (40 trials) obtained from *sessions 2–4* were used for response properties analysis. Velocity and acceleration traces were digitally computed. After low-pass filtering (-3 dB cutoff at 75 Hz), the first and second derivative of eyelid position traces were calculated. To estimate the relative strength of the different frequencies contained in eyelid responses. The power of the spectral density function of selected acceleration traces was calculated as described by Domingo et al. (1997).

### 2.3b - EMG

Electromyographic recordings were obtained with the use of 30  $\mu\text{m}$  Teflon-coated 90%/10% platinum/iridium wires (Advent Research Materials, Halesworth, U.K.) that were implanted in the MOO and MLLS ( $n = 6$ ). The tips of the electrodes (< 0.5 mm) were stripped from their Teflon coating, tinned, and hooked, and their leads were led underneath the skin toward the head connector. As a guideline for placement of the MLLS electrodes, we used the middle of the second lateral row of whiskers. Signals from the EMG electrodes were fed into two AI402 preamplifiers connected to a Cyberamp 360 (both Axon Instruments; [www.axon.com](http://www.axon.com)). The Cyberamp was attached to a CED ([www.ced.co.uk](http://www.ced.co.uk)) power1401.

EMG data were analyzed off-line using custom-written software (Spike2 and Matlab). The raw signals, which were sampled at 5,000 Hz for 1.5 s, were rectified and the 100 ms before the CS presentation to 500 ms after the CS presentation were integrated over 5-ms bins (120 bins). The detection level was defined as the mean of

the first 20 bins plus five times the SD. A constant value of 1 unit/bin was included as a conditioned response threshold (Chen et al. 1995). The trial was excluded if one of the bins in the control period exceeded the detection level. When the average unit count of the first six bins after CS onset was higher than the detection level, the response was considered to be a startle response and the trial was excluded. When at least one of the bins between *bin 31* and the bin at which the UR started crossed the detection level, the response was marked as a conditioned response. The start of the first bin that crossed the level was taken as conditioned response onset, and the start of the bin with the highest value determined peak-latency. The mean value of the bins from conditioned response onset to the unconditioned response was used as a measure of conditioned response strength. In contrast to MDMT, the strength of the US was not controlled by a feedback mechanism because of the stimulus artifact. The anesthesia and surgery were as described in the preceding text for MDMT except that the fifth screw of the pedestal was attached to pin 12 and functioned as a ground for the EMG recordings.

### 2.3c - Video

A Kodak Ektapro HS motion analyzer was used to record the eyeblinks with 1,125 frames/s (fps) at a spatial resolution of 256 x 256 pixels ( $n = 3$ ). The camera, which produced 750 numbered bitmap files per blink (TIFF format), was triggered so as to start 250 ms before CS presentation and to stop 416 ms after CS onset (250 ms ISI). During the video recordings, the head of the mouse was fixed by attaching its connector to a male connector, which in turn was fixated to a restrainer that was placed on a small platform inside a shielded box. A circular cold light source provided sufficient lighting for the camera. Two light-emitting diodes (LEDs), which were visually shielded from the mice, functioned as visual indicators for the presence of the CS and US. The images were analyzed using custom written software (Matlab). Each frame was color coded into 255 colors and smoothed by replacing the color value of each pixel with the average color value of that pixel and the eight immediately surrounding pixels. Of each recorded blink, the color range of the eyeball was determined, and each frame of that particular blink was and each frame of that particular blink was subsequently transformed into a binary picture in which all pixels had a value of 0 unless its color value was within the predefined color range of the eyeball; in that case it got a value of 1. The percentage of visible eye surface was defined as the number of 1's divided by the total number of pixels in the box area. This percentage plotted against frame time represented eyelid closure over time during the eyeblinks. With the use of another analysis program custom written in Matlab we produced a differential video sequence that was superimposed on the original images. This process resulted in a video of 50 frames (every 10<sup>th</sup> frame, starting at frame 200, ending at frame 700) where each frame showed the original image plus a color-coded image that represented changes in surface activity during the preceding 8.9 ms (10 frames at 1.125 fps). The anesthesia and surgery were as described above for MDMT except that the pedestal was adjusted for a head-fixed condition.



### **2.3d - Conditioning procedures.**

The mice (C57/B6 males) were subjected to either a paired (n = 8) or a randomly paired procedure (n = 3). Both procedures lasted 4 days during each of which only 1 session was conducted. During one session the subject received 100 trials grouped in 10 blocks. The trials were separated by a random inter-trial interval (ITI) in the range of 20 to 40 sec. The conditioned stimulus (CS) was a 1 kHz tone with an intensity of 78 dB and a duration of 380 ms (ISI + 30ms shock duration). The US electrical stimulus delivery was evaluated by analyzing the amplitude of the unconditioned response, and its strength was, if necessary, adjusted so as to obtain a full eyelid closure without a head-turn response. In the procedure of paired training each block consisted of 1 US-alone trial, 8 paired trials and 1 CS-alone trial (the 10<sup>th</sup> trial). After 4 sessions of paired training the subject was allowed to rest for 1 day, followed by 4 sessions of extinction (1 session per day). In the extinction procedure each block consisted of 1 US-alone trial (1<sup>st</sup> trial) and 9 CS-alone trials. In the randomly paired procedure the US occurred randomly in the ITI.

To reduce experimental stress and unwanted associative or non-associative responses 1) the boxes in which the training took place were sound proofed with the use of double walls filled with fine grained sand; 2) the lighting, ventilation and speakers were installed outside the electrically shielded inner layer; 3) the mice were kept in their own cages during the training process in the box; and 4) trials were performed only when the eyelid was fully opened and the mouse was not occupied with facial activities such as grooming or sniffing (during the experiment the eyelid and head were continuously monitored). A custom made script controlled the monitoring of eyelid and head, capturing of data, presentation of triggers and stimuli, and the handling of the file-system.

## **2.4 Results**

### **2.4a - Kinetic and frequency domain properties of conditioned and non-conditioned eyelid responses as determined with the use of MDMT.**

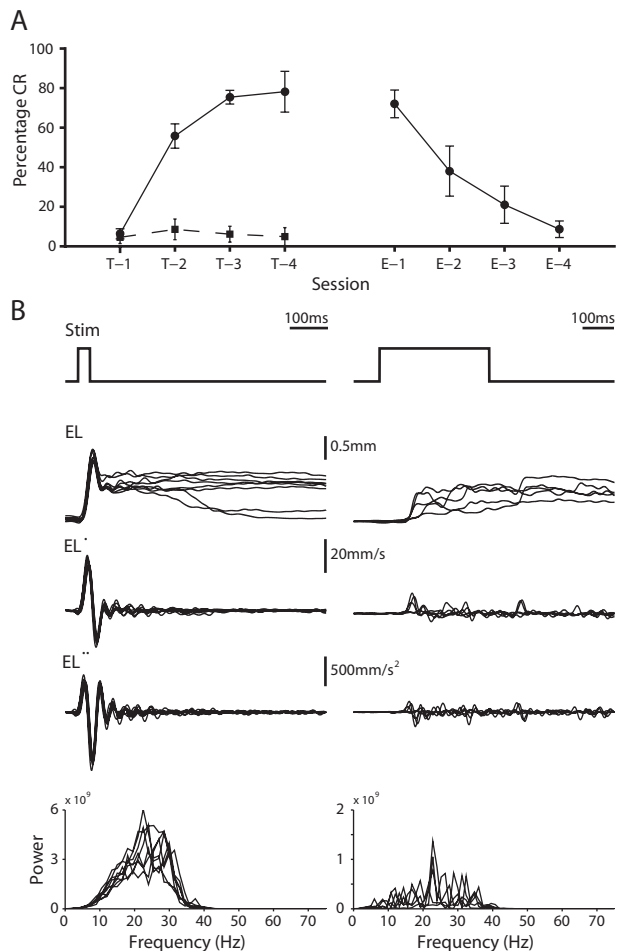
The data given below have been obtained with the use of both coil-MDMT and chip-MDMT. These two approaches differed somewhat on some practical issues such as the stability of implantation in the eyelid (coil > magnet) and the voltage signal to noise ratio (magnet-chip system > coil), but they did not show any significant difference with respect to any of the experimental data. This similarity showed that the basic technical principle of MDMT on which both approaches are based is applicable in a reliable fashion, and that the results can be pooled as done below. Eleven unrestrained C57/B6 mice were conditioned to a tone (CS) with the use of a small electrical shock as the US. The interstimulus interval (ISI) between the CS and US was 350 ms. The average percentage of conditioned responses in the CS alone trials gradually increased from  $6 \pm 2.6$  % (mean plus SEM) to  $78 \pm 10.1$  % (mean plus SEM) over four days of training (see T1 - T4 in Fig. 2.2A). In contrast, none of the animals (n = 3) that were subjected to randomly paired conditioned and unconditioned stimuli for control showed significant increases in their percentages of

conditioned responses. The conditioned responses in the animals that were trained with paired stimuli could be extinguished to pre-training levels over a period of four sessions (see E1 - E4 in Fig. 2.2A).

The unconditioned blink responses of session 1 (i.e. T1) showed a mean latency of  $7.9 \pm 0.2$  ms (mean  $\pm$  SEM, 40 trials) (Fig. 2.2B, left column). The mean peak amplitude, velocity and acceleration of these responses were  $1.2 \pm 0.02$  mm,  $28.5 \pm 1$  mm/s and  $637 \pm 22$  mm/s<sup>2</sup>, respectively. There was a significant linear relationship ( $r = 0.92$ ;  $p < 0.0001$ ) between the peak velocity and the maximum amplitude of the evoked movement (Fig. 2.3A). The mean peak amplitudes of conditioned responses of sessions 2, 3 and 4 were  $0.62 \pm 0.02$  mm,  $0.78 \pm 0.01$  mm and  $0.77 \pm 0.02$  mm (mean  $\pm$  SEM; 40 trials for each session, CS-alone trials), respectively (Fig. 2.2B, right column), while their mean peak velocities increased from  $3.9 \pm 0.3$  mm/s in session 2 to  $7.7 \pm 0.5$  mm/s in session 4.

Accordingly, the mean peak acceleration increased from  $81 \pm 7$  mm/s<sup>2</sup> to  $139 \pm 10$  mm/s<sup>2</sup>. The mean latency of the responses decreased from  $222 \pm 40$  ms in session 2 to  $127 \pm 6$  ms in session 4, while the mean peak latency of the conditioned responses increased from  $321 \pm 45$  ms to  $416 \pm 67$  ms. Although the relationship between conditioned response peak velocity and peak amplitude was significant ( $p < 0.0001$ , Fig.

**Figure 2.2. Eyeblink conditioning with the use of MDMT.** A: the percentages of the conditioned responses increase during normal paired training (●, T-1 to T-4) but not during randomly paired training (■), while the rate decreases during the extinction period (E-1 to E-4). Values are group averaged response counts; error bars indicate SE. B: examples of raw eyelid position traces are depicted as well as their 1st and 2nd derivatives, stimulus trace and power spectrum. *Left:* 8 unconditioned response (UR) recordings obtained from UR-only trials in *session 4* of an animal. The UR traces all show a high similarity resulting in a clear response profile and uniform spectrum shape. *Right:* 5 conditioned response (CR) traces obtained from conditioned stimulus (CS)-alone trials in *session 4* of the same animal. Each CR depicted here shows a different shape. The CRs can have different shapes but usually reach peak amplitude close to the end of the interstimulus interval (ISI). Due to the different shapes the power spectra are not so uniform when compared with the UR but the dominant frequency remains close to 25 Hz, suggesting that a common oscillator underlies eyelid motor system behavior. The eyelid responses were conditioned using an ISI of 350.



2.3B), the correlation coefficient was lower than that of the unconditioned responses ( $r = 0.63$ ). Oscillatory components were visible in most of the responses. Power spectra of acceleration records of both unconditioned and conditioned responses showed a dominant peak at a frequency of about 25 Hz (for unconditioned responses a mean of  $25 \pm 0.8$  Hz; for conditioned responses a mean of  $24 \pm 0.7$  Hz) (Fig. 2.2B). These dominant frequencies were not influenced by the number of the session or by the length of the ISI (for control three and four additional animals were tested with ISI's of 250 and 450 ms, respectively). Thus, the longer conditioned responses that occurred in the later training sessions were generated by an increase in the number of waves but not by a change in the dominant frequency.

### 2.4b - EMG recordings.

To find out to what extent the data obtained with MDMT differ from those obtained with EMG, and to find out whether EMG signals from the MOO can be contaminated with signals originating from surrounding muscles, we recorded simultaneously with separate EMG electrodes signals from the MOO and MLLS of adult male C57/B6 mice ( $n = 6$ ) during eyeblink conditioning. The response curves are shown in figure 2.4A. Over 4 consecutive days of training (T1 - T4) the percentage of significant responses recorded on the MOO electrodes increased to a level of 75%, while that of the MLLS electrodes increased to an average of 36%. The SD's of these percentages were significantly higher than those obtained with the use of MDMT ( $p < 0.02$ ; Student's t-test). Moreover, the percentage of conditioned responses on T1 was significantly higher than that obtained with the use of MDMT ( $p < 0.01$ ; Student's t-test). The percentage of responses recorded on the MOO electrodes could be reduced to baseline levels following 4 days of extinction,

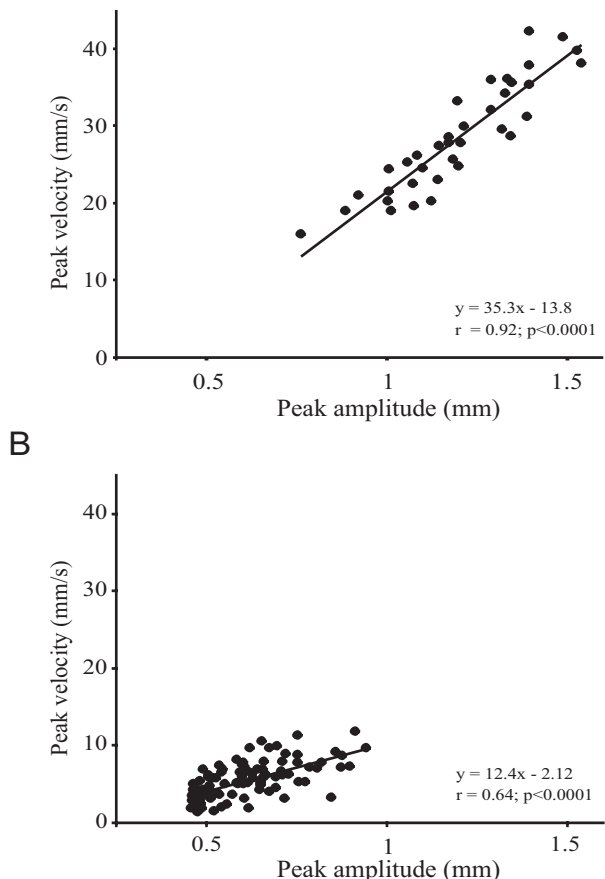


**Figure 2.3. UR and CR peak velocity as a function of maximum amplitude.** *A:* UR peak velocity is plotted against peak amplitude. There was a significant linear relationship indicating that larger responses are made by increasing the peak velocity. *B:* the same relationship but now for conditioned responses showed a much lower but still significant correlation; this is suggestive for external (outside the classical eyeblink conditioning pathway) influences on the eyelid motor system during conditioning trials



while that of the MLLS showed only a minor reduction (Fig. 2.4A, left panel). The mean sizes of the MOO responses increased and decreased consistently over consecutive days of training and extinction, respectively, while those of the MLLS already diminished to minimal levels on day 4 of the training (Fig. 2.4A, right panel). All attempts to measure frequency and time domain properties from EMG traces resulted in a large variation in the data. Thus, several data points obtained with the use of EMG recordings differed from those obtained with MDMT recordings, and the MLLS electrodes picked up a substantial percentage of responses. Together these observations raise the possibility that snout responses contaminate the eyelid recordings.

### **2.4c - Evaluation with the use of High-Speed Video Imaging.**

To find out whether snout movements can indeed contaminate eyeblink recordings in mice, and to find out to what extent the MDMT and/or EMG recordings reflect the actual kinetics of the eyelid movement, we evaluated these methods with the use of a high-speed video system by recording and analyzing conditioned and unconditioned eyelid responses in restrained mice with all three methods simultaneously ( $n = 3$ ). The spatiotemporal resolution of the video system, which operated at 1125 fps for  $256 \times 256$  pixels, appeared sufficient to reliably detect and visualize simultaneously both eyeblink movements and other facial muscle responses (Fig. 2.4B). In 37% of all trials the video analysis showed a facial response without any eyelid movement. Yet, in 43% of these cases the EMG recordings of the “MOO” detected a positive eyelid response, while none of the MDMT recordings showed a significant eyelid movement. These data indicate that non-eyelid facial movements can occur in the process of eyeblink conditioning in mice and that the muscle activities underlying these movements can contaminate EMG recordings of the MOO. This contamination is most likely due to incorrect electrode placing or wandering electrodes, even if they have been carefully placed. The superior detection of the actual displacement of the eyelid with the use of MDMT was particularly evident in trials in which irregular movements occur. Figure 2.5 shows such a trial in which the MDMT recordings correspond to those of the video recordings, while the EMG recordings diverge. The mean peak latency obtained from the MDMT recordings ( $179 \pm 10.2$  ms) was comparable with that calculated from the video traces ( $175 \pm 12.9$  ms), whereas the mean peak latency of the EMG signals was significantly lower (EMG:  $125 \pm 18.9$ ms;  $p = 0.02$  student's  $t$ -test). Thus, the fact that MDMT, but not EMG, produces results comparable to those observed with high-speed video recordings demonstrates that MDMT is suited for determination of eyelid position in mice and thus for investigation of the kinetic properties of conditioned and unconditioned responses. Interestingly, the percentage of discrete eyelid conditioned responses in the mice that had to be restrained for the stability of the video recordings was much smaller than could be expected from the recordings in the freely moving mice that have been described above. For example, in trial 300 - 400 the average percentage of discrete eyelid responses was only  $9 \pm 3$  %. These reductions held true for both numbers obtained with MDMT recordings and with EMG recordings raising the

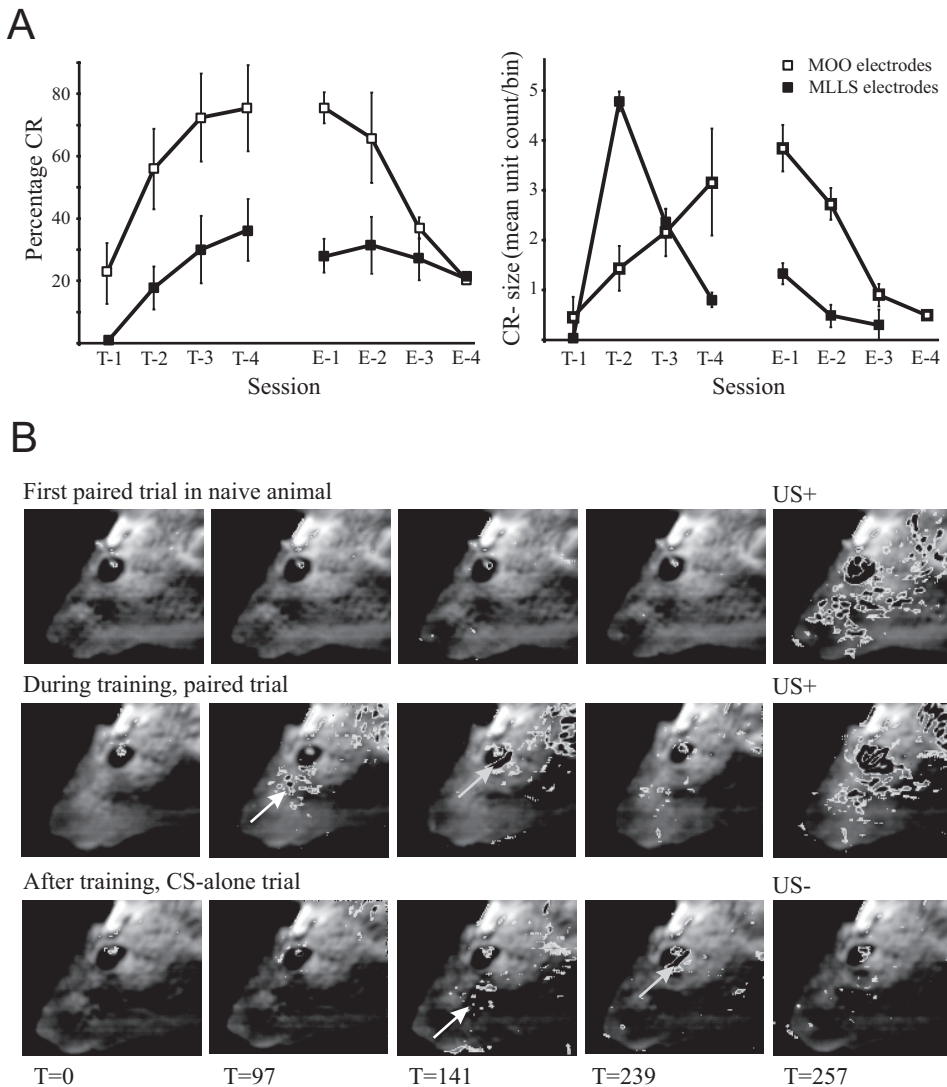


**Figure 2.4. Nondiscrete facial co-contractions displayed by video recordings and confirmed by electromyography (EMG).** *A*: the occurrence of nondiscrete facial responses in freely moving mice was quantified by recording EMG activities of both the musculus levator labii superior (MLLS) and musculus orbicularis oculi (MOO) during conditioning. *Left*: that the averaged percentage of the conditioned responses of the MLLS increased to 36% over 4 consecutive days of training (T-1 to T-4), while that of the MOO increased to a normal level of 75%. The percentage of conditioned responses recorded on the MOO electrodes could be reduced to baseline levels following 4 days of extinction, while that of the MLLS showed only a minor reduction. *Right*: the mean size of the CR of the MOO responses increased consistently over consecutive days of training, whereas those of the MLLS diminished to minimal levels on *day 4*. Thus the musculature of the snout of a freely moving mouse does show conditioning behavior with the use of an electrical shock at the eye corner as the US, but the amplitudes of its conditioned responses diminish over time. *B*: differential video frame analyses during the training confirmed that during the training process co-contractions start to occur in the facial musculature of the snout (white arrows) indicating that aspecific responses can occur that can contaminate the counts and the response properties of conditioned eyelid responses (grey arrows).

possibility that stress induced by fixation of the head and body can impair classical eyeblink conditioning. In contrast, during the same trials the percentage of non-discrete responses was on average  $87 \pm 5\%$ . In  $61 \pm 4\%$  this non-discrete response

included an eyelid response. For example, figure 2.4B (third row) shows an early non-discrete component without eyelid activity accompanied by a late eyelid only component.

## 2.5 Discussion

We present a novel method, MDMT, which allows continuous recording of eyelid position over time in freely moving mice. For the first time the response kinetics of conditioned and unconditioned eyelid responses in mice were measured and documented. Below we discuss the kinetic and oscillatory properties of eyelid responses in mice, factors in the setup that may influence the rate of conditioning in mice, and potential future applications of MDMT.

As measured with the use of MDMT the average percentage of conditioned responses in CS alone trials of freely moving mice gradually increase to 78% over four days of training, while they decrease to baseline level within four days of extinction. These percentages agree well with those obtained with the use of EMG recordings (present study; Chen et al. 1996; Conquet et al. 1994; Kishimoto et al. 2001). Yet, our combined MDMT-EMG-Video recordings demonstrated that EMG recordings in restrained mice can pick up a substantial number of false-positive conditioned responses due to snout movements, while MDMT recordings will not detect a conditioned eyelid response when the eyelid is not moving. This discrepancy in response counts suggests that when EMG electrodes are placed in the eyelid of a mouse they do not only pick up false-positive responses from surrounding musculature but also false-negative responses in cases of MOO only responses. In mice, the MOO is a thin muscle, which is much thinner than the actual eyelid and covers the bottom of the eyelid following the curve of the eyeball. Thus, as one needs EMG electrodes of a particular minimum size with a particular minimum stiffness to pick up sufficient signals over at least 4 days of training, it appears impossible to place these electrodes perfectly and permanently in the optimal site of the small MOO muscle of a mouse. The measurements done with the use of MDMT, but not EMG, provided stable and reliable data on the kinetics of eyelid movements in mice. The mean latency of their unconditioned eyelid responses equaled 7.9 ms, which is comparable to values described for rabbit (Quinn et al., 1984) and compatible with a disynaptic pathway mediating the UR (van Ham and Yeo, 1996). The mean velocity (28.5 mm/s) and acceleration ( $637 \text{ mm/s}^2$ ) that we found for eyelid movements in mice cannot be directly compared with those previously obtained in rabbits, rats and cats (see eg. Gruart et al. 1994), since we directly recorded changes in distance while our colleagues measured coil-rotations. However, the ratio between peak amplitude and peak velocity and the ratio between peak velocity and peak acceleration in mice (1 : 24 and 1 : 22) agreed well with the same values that can be obtained from rabbits (1 : 17 and 1 : 18) (Gruart et al. 2000b). In addition, the correlation coefficient of the observed linear relationship between unconditioned response peak amplitude and peak velocity in mice ( $r = 0.92$ ) is similar to that in rabbit ( $r = 0.91$ ). Thus, as described by Gruart and colleagues (2000b) for eyelid responses in rabbits, larger lid responses in mice may be predominantly achieved by increasing the velocity of the movement.

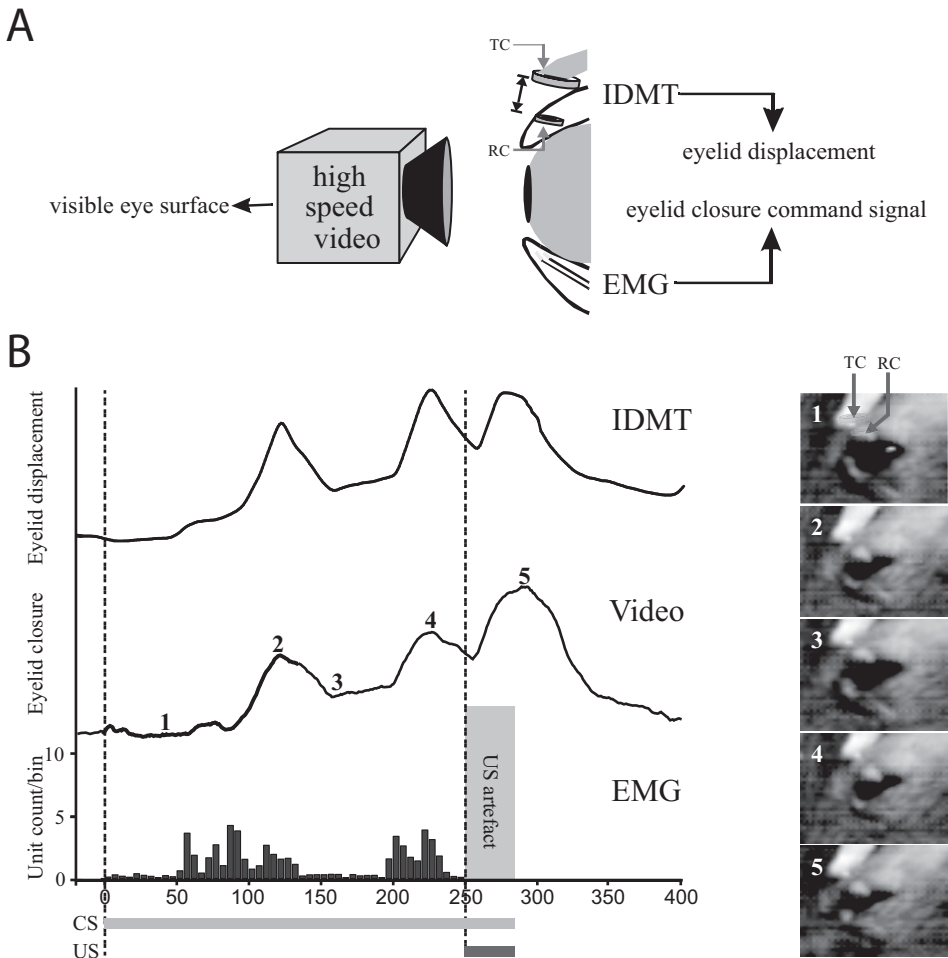


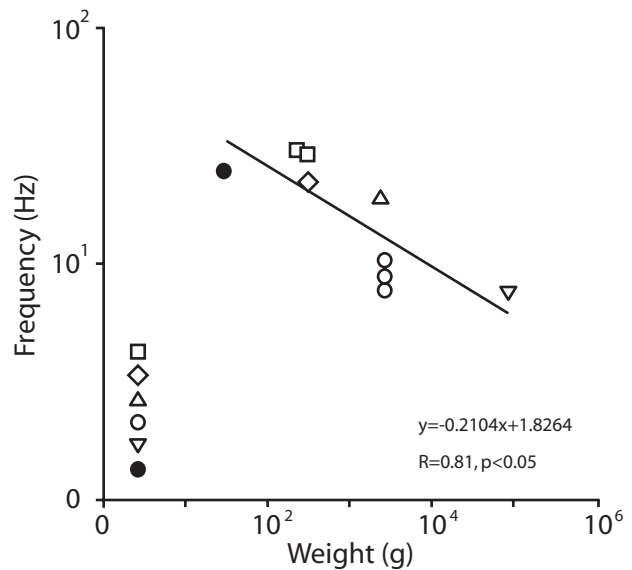
**Figure 2.5. High-speed Video evaluation.** To evaluate the spatiotemporal accuracy of the MDMT-system and to compare this accuracy with that of the EMG system, all three methods, i.e., high-speed video, MDMT (inductive system) and EMG, were applied simultaneously in the same mice. (A) Scheme showing how the three recording methods were implemented around a single eye. TC indicates Transmitter Coil (head-fixed magnetic field generator); RC indicates Receiver Coil. (B) Example of three simultaneous recordings with MDMT, high-speed video and EMG during a paired trial (from top to bottom). The MDMT signal closely follows that of the automated video signal in space and time (with regard to both onset and peak latency), while the converted EMG signal shows more variation in its amplitude and precedes the video signal at different latencies (MDMT peak velocity was 206 ms, while EMG peak latency was 89 ms) during the various parts of the trace. Note that the unconditioned response can be monitored successfully with the use of MDMT. Micrographs 1 to 5 in panel on the right correspond to numbers 1 to 5 in video trace.

On the other hand, it should be noted that species differences can occur as the ratios mentioned above for mice and rabbits diverge from those in cats (1 : 43 for the ratio between peak amplitude and peak velocity and 1 : 52 for the ratio between peak velocity and peak acceleration) (Domingo et al. 1997).

The kinetic parameters of conditioned responses in mice depended on the number of the training session. Over the trials the mean peak latency, amplitude, velocity, and acceleration of the conditioned responses increased to  $416 \pm 76$  ms,  $0.77 \pm 0.02$  mm, 56

$7.7 \pm 0.5$  mm/s and  $139 \pm 10$  mm/s<sup>2</sup>, respectively, while mean onset latency of the responses decreased to  $127 \pm 6$  ms. Peak latency and onset latency were comparable to those found in rabbits (Gruart et al. 2000b). Using an ISI of 250 ms the onset latency of well trained rabbits equaled about 130 ms and the peak latency of their conditioned responses also occurred somewhat after the ISI. The conditioned responses in mice also resembled those in cats and rabbits in that the larger conditioned responses were generated by changing the amplitude and/or number of waves (Domingo et al. 1997; Gruart et al. 2000ab). Moreover, the differences between the conditioned and unconditioned responses of mice were similar to those of rabbits and cats (see eg. Gruart et al. 2000b); for example, the conditioned responses had a slower build-up and smaller maximum amplitude than the unconditioned responses and the peak velocity of conditioned responses in trained animals was about five times smaller than that of unconditioned responses. Even though the unconditioned and conditioned eyelid responses showed differences in their kinetic properties, they still could be generated using the same common neural oscillator. Indeed, both types of responses in mice showed oscillatory components of about 25 Hz that were independent of the number of the training session and the ISI. Interestingly, this preferred frequency for mice is in line with an hypothesis by Gruart and others (2000a, b), which predicts that eyelid movements have an underlying oscillator with a dominant frequency that is related to the weight of the species (Fig. 2.6).

**Figure 2.6. Relationship between mean body weight and the dominant frequency of eyelid responses for different species.** The dominant frequency of the eyelid motor system of the mouse is depicted (F) among that of other species (open symbols) as described by Gruart et al. (2000). The regression line is recalculated and the resulting equation and R-value is shown. The fact that our data did not significantly change the correlation coefficient indicates that it is in line with the hypothesis that there is an underlying oscillator that controls eyelid movement with a frequency that can be correlated with the species mean body weight.



Thus, because of the observed differences in response kinetics between unconditioned and conditioned responses we can conclude that these responses in mice are controlled through different neural pathways but since both response types showed similar frequency domain properties they are probably generated by a common neural oscillator.

The data presented above are relevant because the kinetic and frequency domain properties of eyelid responses may differ between different strains of mice or differ-

ent types of transgenics. Insight into these differences may for example prevent false claims about cerebellar contributions to associative learning as a particular impairment in eyeblink conditioning could be caused by a performance deficit rather than a deficit that directly and specifically affects motor learning (Steinmetz, et al. 1992; Welsh and Harvey 1989). The data provided above also indicated that the context of the experimental setup can play a role in the rate of acquisition. For example, the high-speed video recordings showed that restraining the animal impairs the acquisition of discrete eyelid conditioned responses, while the total number of responses are increased. Since stress has been reported to influence classical conditioning, fixation stress may explain why conditioning of a freely moving mouse shows different results (Neufeld and Mintz 2001; Shors, et al. 1992). Potentially, fear related processes are able to influence classical conditioning experiments. At present it is unknown to what extent the eyelid motor system of mice in itself is involved in these fear related processes. However, such processes may be particularly relevant in mice since the correlation coefficient of the peak amplitude - peak velocity relation of the conditioned responses was significantly lower in mice than in rabbits (Gruart et al. 2000). In general, fear related activities may originate from direct excitatory projections from the amygdala to the eyelid motor system (Fanardjian and Manvelyan 1987) and from fear related hormonal states which can modulate brain stem controlled reflexes (Lee and Davis 1997; Shors, et al. 2000). Thus, one should attempt to avoid potential factors that may influence fear induction during eyeblink conditioning experiments in mice.

With the use of MDMT recordings in cerebellar mutants we will now be able to investigate the cellular mechanisms underlying eyelid motor performance and to properly dissect the molecular components of the cerebellar network that are responsible for the control of eyeblink conditioning. Since MDMT allows us to investigate the kinetics continuously over time, we can for example also start to investigate specific cerebellar conditioning hypotheses in which timing mechanisms play a dominant role (Mauk et al. 2000; Mauk and Ruiz 1992; Medina et al. 2000; Medina and Mauk 2000; Perrett et al. 1993). In addition, MDMT may provide a new methodological asset to the field of trace conditioning, in which interstimulus intervals and timing also play an important role (Buhusi and Meck 2000; Weiss and Thompson 1991).

### **Acknowledgements**

This study has been supported by NWO-ALW, NWO-MW, HFSP, NIH and EEC. We would like to thank Eddie Dalm and Hans vd Burg for technical assistance.



## 2.6 References

- Aiba, A., Kano, M., Chen, C., Stanton, M. E., Fox, G. D., Herrup, K., Zwingman, T. A. and Tonegawa, S. (1994) "Deficient cerebellar long-term depression and impaired motor learning in *mglur1* mutant mice". *Cell*. 79:377-388.
- Arts, T. and Reneman, R. S. Measurement of deformation of canine epicardium in vivo during cardiac cycle. *Am J Physiol*. 239:H432-H437, 1980.
- Attwell, P. J., Rahman, S. and Yeo, C. H. Acquisition of eyeblink conditioning is critically dependent on normal function in cerebellar cortical lobule hvi. *J Neurosci*. 21:5715-5722, 2001.
- Becker, W. and Fuchs, A. F. Lid-eye coordination during vertical gaze changes in man and monkey. *J Neurophysiol*. 60:1227-1252, 1988.
- Buhusi, C. V. and Meck, W. H. Timing for the absence of a stimulus: The gap paradigm reversed. *J Exp Psychol Anim Behav Process*. 26:305-322, 2000.
- Chen, C., Kano, M., Abeliovich, A., Chen, L., Bao, S., Kim, J. J., Hashimoto, K., Thompson, R. F. and Tonegawa, S. Impaired motor coordination correlates with persistent multiple climbing fiber innervation in *pkc gamma* mutant mice. *Cell*. 83:1233-1242, 1995.
- Chen, L., Bao, S., Lockard, J. M., Kim, J. K. and Thompson, R. F. Impaired classical eyeblink conditioning in cerebellar-lesioned and purkinje cell degeneration (*pcd*) mutant mice. *J Neurosci*. 16:2829-2838, 1996.
- Conquet, F., Bashir, Z. I., Davies, C. H., Daniel, H., Ferraguti, F., Bordi, F., Franz-Bacon, K., Reggiani, A., Matarese, V., Conde, F. and et al. Motor deficit and impairment of synaptic plasticity in mice lacking *mglur1*. *Nature*. 372:237-243, 1994.
- Delgado-Garcia, J. M., Evinger, C., Escudero, M. and Baker, R. Behavior of accessory abducens and abducens motoneurons during eye retraction and rotation in the alert cat. *J Neurophysiol*. 64:413-422, 1990.
- Disterhoft, J. F., Kronforst-Collins, M., Oh, M. M., Power, J. M., Preston, A. R. and Weiss, C. Cholinergic facilitation of trace eyeblink conditioning in aging rabbits. *Life Sci*. 64:541-548, 1999.
- Domingo, J. A., Gruart, A. and Delgado-Garcia, J. M. Quantal organization of reflex and conditioned eyelid responses. *J Neurophysiol*. 78:2518-2530, 1997.
- Evinger, C., Manning, K. A. and Sibony, P. A. Eyelid movements. Mechanisms and normal data. *Invest Ophthalmol Vis Sci*. 32:387-400, 1991.
- Fanardjian, V. V. and Manvelyan, L. R. Mechanisms regulating the activity of facial nucleus motoneurons--iii. Synaptic influences from the cerebral cortex and subcortical structures. *Neuroscience*. 20:835-843, 1987.

GMR technology sheet; NVE corporation; 11409 valley view road; eden prairie, mn 55344-3617; <http://www.nve.com/technical/gmr/gmr.html>;

Gruart, A., Blazquez, P. and Delgado-Garcia, J. M. Kinematic analyses of classically-conditioned eyelid movements in the cat suggest a brain stem site for motor learning. *Neurosci Lett.* 175:81-84, 1994.

Gruart, A., Guillazo-Blanch, G., Fernandez-Mas, R., Jimenez-Diaz, L. and Delgado-Garcia, J. M. Cerebellar posterior interpositus nucleus as an enhancer of classically conditioned eyelid responses in alert cats. *J Neurophysiol.* 84:2680-2690, 2000a.

Gruart, A., Pastor, A. M., Armengol, J. A. and Delgado-Garcia, J. M. Involvement of cerebellar cortex and nuclei in the genesis and control of unconditioned and conditioned eyelid motor responses. *Prog Brain Res.* 114:511-528, 1997.

Gruart, A., Schreurs, B. G., del Toro, E. D. and Delgado-Garcia, J. M. Kinetic and frequency-domain properties of reflex and conditioned eyelid responses in the rabbit. *J Neurophysiol.* 83:836-852, 2000b.

Hamiel, S. R., Bleicher, J. N., Tubach, M. R. and Cronan, J. C. Evaluation of the hall-effect sensor for determination of eyelid closure in vivo. *Otolaryngol Head Neck Surg.* 113:88-91, 1995.

Hesslow, G. and Yeo, C. Cerebellum and learning: A complex problem. *Science.* 280:1817-1819, 1998.

Lee, Y. and Davis, M. Role of the hippocampus, the bed nucleus of the stria terminalis, and the amygdala in the excitatory effect of corticotropin-releasing hormone on the acoustic startle reflex. *J Neurosci.* 17:6434-6446, 1997.

Kim, J. J. and Thompson, R. F. Cerebellar circuits and synaptic mechanisms involved in classical eyeblink conditioning. *Trends Neurosci.* 20:177-181, 1997.

Kishimoto, Y., Kawahara, S., Fujimichi, R., Mori, H., Mishina, M. and Kirino, Y. Impairment of eyeblink conditioning in glurdelta2-mutant mice depends on the temporal overlap between conditioned and unconditioned stimuli. *Eur J Neurosci.* 14:1515-1521, 2001.

Korhonen, T. Three-dimensional hall effect accelerometer for recording head movements of freely moving laboratory animals. *Physiol Behav.* 49:651-652, 1991.

Mauk, M. D., Medina, J. F., Nores, W. L. and Ohyama, T. Cerebellar function: Coordination, learning or timing? *Curr Biol.* 10:R522-525, 2000.

Mauk, M. D. and Ruiz, B. P. Learning-dependent timing of pavlovian eyelid responses: Differential conditioning using multiple interstimulus intervals. *Behav Neurosci.* 106:666-681, 1992.

McCormick, D. A. and Thompson, R. F. Cerebellum: Essential involvement in the classically conditioned eyelid response. *Science.* 223:296-299, 1984.



Medina, J. F., Garcia, K. S., Nores, W. L., Taylor, N. M. and Mauk, M. D. Timing mechanisms in the cerebellum: Testing predictions of a large- scale computer simulation. *J Neurosci.* 20:5516-5525, 2000.

Medina, J. F. and Mauk, M. D. Computer simulation of cerebellar information processing. *Nat Neurosci.* 3 Suppl:1205-1211, 2000.

Neufeld, M. and Mintz, M. Involvement of the amygdala in classical conditioning of eyeblink response in the rat. *Brain Res.* 889:112-117, 2001.

Perrett, S. P., Ruiz, B. P. and Mauk, M. D. Cerebellar cortex lesions disrupt learning-dependent timing of conditioned eyelid responses. *J Neurosci.* 13:1708-1718, 1993.

Phillips, R. G. and LeDoux, J. E. Differential contribution of amygdala and hippocampus to cued and contextual fear conditioning. *Behav Neurosci.* 106:274-285, 1992.

Quinn, K. J., Kennedy, P. R., Weiss, C. and Disterhoft, J. F. Eyeball retraction latency in the conscious rabbit measured with a new photodiode technique. *J Neurosci Methods.* 10:29-39, 1984.

Renterghem, R. J. v. Aortic valve geometry during the cardiac cycle (phd thesis). *Eindhoven, The Netherlands, Technical University Eindhoven.* 1983.

Rodriguez, F., Salas, C., Vargas, J. P. and Torres, B. Eye-movement recording in freely moving animals. *Physiol Behav.* 72:455-460, 2001.

Schicatano, E. J., Mantzouranis, J., Peshori, K. R., Partin, J. and Evinger, C. Lid restraint evokes two types of motor adaptation. *J Neurosci.* 22:569-576, 2002.

Shibuki, K., Gomi, H., Chen, L., Bao, S., Kim, J. J., Wakatsuki, H., Fujisaki, T., Fujimoto, K., Katoh, A., Ikeda, T., Chen, C., Thompson, R. F. and Itohara, S. Deficient cerebellar long-term depression, impaired eyeblink conditioning, and normal motor coordination in gfap mutant mice. *Neuron.* 16:587-599, 1996.

Shors, T. J., Beylin, A. V., Wood, G. E. and Gould, E. The modulation of pavlovian memory. *Behav Brain Res.* 110:39-52, 2000.

Shors, T. J., Weiss, C. and Thompson, R. F. Stress-induced facilitation of classical conditioning. *Science.* 257:537-539, 1992.

Steinmetz, J. E., Lavond, D. G., Ivkovich, D., Logan, C. G. and Thompson, R. F. Disruption of classical eyelid conditioning after cerebellar lesions: Damage to a memory trace system or a simple performance deficit? *J Neurosci.* 12:4403-4426, 1992.

Thompson, L. T., Moyer, J. R., Jr. and Disterhoft, J. F. Trace eyeblink conditioning in rabbits demonstrates heterogeneity of learning ability both between and within age groups. *Neurobiol Aging.* 17:619-629, 1996.

van Ham, J. J. and Yeo, C. H. Trigeminal inputs to eyeblink motoneurons in the rabbit. *Exp*

*Neurol.* 142:244-257, 1996.

Weiss, C. and Thompson, R. F. The effects of age on eyeblink conditioning in the freely moving fischer-344 rat. *Neurobiol Aging*. 12:249-254, 1991.

Welsh, J. P. and Harvey, J. A. Cerebellar lesions and the nictitating membrane reflex: Performance deficits of the conditioned and unconditioned response. *J Neurosci*. 9:299-311, 1989.

# Chapter 3

## Expression of a Protein Kinase C Inhibitor in Purkinje Cells Blocks Cerebellar LTD and Adaptation of the Vestibulo - Ocular Reflex.

Chris I. De Zeeuw<sup>1</sup>, Christian Hansel<sup>2</sup>, Feng Bian<sup>3</sup>, Sebastiaan K.E. Koekoek<sup>1</sup>, Adriaan M. van Alphen<sup>1</sup>, David J. Linden<sup>2</sup> and John Oberdick<sup>3</sup>

*1 Department of Anatomy, Erasmus University Rotterdam, P.O. Box 1738, 3000 DR, Rotterdam, The Netherlands;*

*2 Department of Neuroscience, Johns Hopkins University School of Medicine, 725 N. Wolfe Street, Baltimore, MD, 21205 3 Department of Cell Biology, Neurobiology & Anatomy/ Neuroscience Division, and the Neurobiotechnology Center, The Ohio State University, Columbus, OH, 43210.*

Received December 11, 1997; revised January 13, 1998

*Neuron* 20: 495–508, 1998

### 3.1 Abstract

Cerebellar long-term depression (LTD) is a model system for neuronal information storage which has an absolute requirement for activation of protein kinase C (PKC). It has been claimed to underlie several forms of cerebellar motor learning. Previous studies using various knockout mice (mGluR1, GluR $\delta$ 2, glial fibrillary acidic protein) have supported this claim; however, this work has suffered from the limitations that the knockout technique lacks anatomical specificity and that functional compensation can occur via similar gene family members. To overcome these limitations, a transgenic mouse (called L7-PKCi) has been produced in which the pseudosubstrate PKC inhibitor, PKC[19-31], was selectively expressed in Purkinje cells under the control of the *pcp-2(L7)* gene promoter. Cultured Purkinje cells prepared from heterozygous or homozygous L7-PKCi embryos showed a complete blockade of LTD induction. In addition, the compensatory eye movements of L7-PKCi mice were recorded during vestibular and visual stimulation. Whereas the absolute gain, phase and latency values of the vestibulo-ocular reflex and optokinetic reflex of the L7-PKCi mice were normal, their ability to adapt their vestibulo-ocular reflex gain during visuo-vestibular training was absent. These data strongly support the hypothesis that activation of PKC in the Purkinje cell is necessary for cerebellar LTD induction, and that cerebellar LTD is required for a particular form of motor learning, adaptation of the vestibulo-ocular reflex.

### 3.2 Introduction

In recent years there has been considerable interest in electrophysiological model systems of information storage in the brain such as long-term potentiation (LTP) and long-term depression (LTD). These phenomena have been proposed as candidate mechanisms to underlie memory storage in the behaving animal because they have attractive computational properties including their duration, input specificity and associativity (see Linden and Connor, 1995, for review) and because they have been manifest in regions of the brain that appear to be necessary for certain forms of behavioral learning as assessed with lesion and drug infusion studies. For example, the hippocampus, where LTP and LTD have been most extensively investigated, is necessary for certain forms of spatial learning, and the cerebellum, where a different form of LTD has been studied, is necessary for certain forms of motor learning such as associative eyeblink conditioning and adaptation of the vestibulo-ocular reflex (VOR). Unfortunately, testing the hypothesis that LTP and LTD in particular brain regions underlie specific behavioral phenomena has been a difficult endeavor.

The advent of transgenic mouse technology, in particular the use of embryonic stem cells and homologous recombination “knockout” methods, has made it possible to test the role of various signaling molecules in LTP and LTD together with behavioral analysis of the appropriate learning tasks (see Chen and Tonegawa, 1997, for review). However, there have been three major problems which have complicated the analysis of knockout mice. First, knockout mice have the gene of interest deleted from the earliest stages of development. As a result, these mice often have a complex developmental phenotype. For example, PKC $\gamma$ , mGLUR1 and GluR $\delta$ 2 knockout mice all

have cerebellar Purkinje cells that fail to undergo the normal developmental conversion from multiple to mono climbing fiber innervation in early postnatal life (Chen et al., 1995; Kano et al., 1995, 1997; Kashiwabuchi et al., 1995). Second, knockout of one gene sometimes produces compensatory upregulation in the expression of other related genes during development. In the CREB $\alpha$ - $\delta$  knockout mouse, there is compensatory upregulation of the related transcription factor CREM (Hummler et al., 1994; Blendy et al., 1996). Similarly, it has been suggested that PKC $\gamma$  knock out mice do not show impaired cerebellar motor learning due to compensation by other PKC isoforms in Purkinje cells (Chen et al., 1995). A third complicating factor is that knockout mice have the gene of interest deleted in every cell of the body, not just the cells of interest, making it more difficult to ascribe the knockout's behavioral effects to dysfunction in any one particular structure or cell type. This could be a potential problem for the analysis of behaviors such as associative eyeblink conditioning, and VOR adaptation, which are likely to require use-dependent plasticity at multiple sites, synapses received by both cerebellar Purkinje cells and their targets in the deep cerebellar or vestibular nuclei (Yeo et al., 1985; Khater et al., 1993; Raymond et al., 1996; Highstein et al., 1997; Pastor et al., 1994).

To address the latter two complications, we have undertaken a different approach. Cerebellar LTD is an attenuation of the parallel fiber-Purkinje cell synapse that occurs when parallel fiber and climbing fiber inputs to a Purkinje cell are co-activated at moderate frequencies (Ito et al., 1982; Linden and Connor, 1995). It has been suggested to underlie several forms of motor learning including adaptation of the VOR, associative eyeblink conditioning and limb load adjustment (Ito, 1982, 1989; Thompson and Krupa, 1994; Raymond et al., 1996; but see Linás et al., 1997). The induction of cerebellar LTD may be blocked by internal application of PKC inhibitors in Purkinje cells (Linden and Connor, 1991; Narasimhan and Linden, 1996). Thus, if cerebellar LTD is necessary for these particular forms of motor learning, then inhibition of PKC in cerebellar Purkinje cells would be expected to specifically interfere with them. Using the promoter of the Purkinje cell-specific gene *pcp-2(L7)* (Oberdick et al., 1990), transgenic mice have been created in which a selective inhibitor to a broad range of PKC isoforms (House and Kemp, 1987; Linden and Connor, 1991) is chronically overexpressed. This strategy ensures that in L7-PKCi mice, PKC inhibition will be restricted to Purkinje cells, and that compensation via upregulation of different PKC isoforms will not succeed in blunting the biochemical effect of the transgene. We have subjected these mice to biochemical, anatomical, electrophysiological and behavioral analysis to test the hypotheses that PKC activation is required for LTD induction and that LTD induction is required for adaptation of the vestibulo-ocular reflex.

### 3.3 Experimental procedures

#### 3.3a - Production of L7-PKCi Mice

The L7-PKCi vector was constructed by insertion of a 54 bp. synthetic double-

stranded DNA fragment into the BamHI site of pL7 $\Delta$ AUG (Smeyne et al., 1995). No protein epitope tag was included in this construct because of unpredictable effects on peptide function. The sequences of the two complementary 50 bp. oligonucleotides are as follows:

PKCI sense, 5'-GATCATGAGGTTCCGCCAGGAAGGGCGCCCTGAGGCAGAAGAACGTGTAAG-3';

PKCI anti, 3'-TACTCCAAGCGGTCTCTCCCGCGGGACTCCGTCTTCTTGCACATTCTAG-5'.

The resulting plasmid was digested with HindIII and EcoRI, and the linearized construct was separated from the pGEM3 base plasmid by electrophoresis followed by electroelution. This purified fragment was used for injection into mouse embryos. The antisense oligo used to make the PKCI fragment was used as probe in the Northern blot and *in situ* hybridization analyses. Northern blots were prepared as previously described (Bian et al., 1996).

### 3.3b - Mouse Strains

The L7-PKCI founder mice were generated in the FVB/N strain (Taconic). Initial physiology and LTD tests were performed on homozygotes and heterozygotes in this strain background. As this strain is albino, F2 heterozygotes were crossed into a pigmented hybrid strain (B6C3F1 hybrids; Jackson Laboratory) for behavioral studies. The results reported here represent data collected from first generation pigmented animals as well as second and third generations; each successive generation was produced from a cross between a transgenic heterozygote and a stock wild-type B6C3F1 hybrid (thus yielding wild-type and transgenic littermates). Positive transgenic mice were identified by PCR using DNA prepared from tail biopsies. To confirm the cell physiological data were in the same strain as was used for the behavioral studies, second generation pigmented heterozygotes were mated to produce homozygotes in a complex B6C3F1 substrain. These were subsequently mated to B6C3F1 wild-type stock animals to produce heterozygous embryos for primary dissociated cultures and cell electrophysiological studies. All anatomical characterizations were performed in the B6C3F1 hybrid background.

### 3.3c - Anatomical Analysis of L7-PKCI Mice

#### - *In situ* hybridization.

The *in situ* hybridization procedure was as reported previously (Smeyne et al., 1995; Bian et al., 1996). Antisense PKCI probe was end “tailed” with [<sup>35</sup>S]dATP using terminal deoxynucleotidyl transferase. After development of photographic emulsion-dipped slides sections were counterstained with cresyl violet. Images in Figure 2 were captured off of a Zeiss Axiophot microscope using an Optronix video camera and IPLab Spectrum software (Signal Analytics Corp., Virginia).

#### - *Immunocytochemistry and L7- $\beta$ -gal analysis.*

Sections were reacted and processed with antibodies to L7, calbindin, and zebrin II (courtesy of Dr. Richard Hawkes) using methods reported previously (Baader et al.,

1997). Sections were processed histochemically for NADPH-diaphorase as before (Schilling et al., 1994). L7-PKCi mice of line 1 were crossed to L7BG3 mice for analysis of L7- $\beta$ -gal banding patterns. The latter transgenic mouse carries an L7-lacZ fusion transgene with a truncated (0.5 kb) promoter as previously described (Oberdick et al., 1993). Tissues were processed for lacZ in whole mount as reported previously (Oberdick et al., 1993).

- *Cell counts and area measurements.*

For area measurements and Purkinje cell counts, 18 $\mu$ M sagittal frozen sections were prepared on a cryostat (every fourth section was collected) and stained with cresyl violet. Four sections at the midline and four sections in the hemispheres (at the point just lateral to where lobule X disappears) were analyzed. Area measurements were made using IPLab Spectrum software (Signal Analytics Corp., Virginia). The area measurements were confirmed in a second pair of animals. Purkinje cell density measurements were made by using IPLab software to define a linear segment in the Purkinje cell layer in the region to be counted. Three sections were counted from the cerebellar midline of both a wild-type and an L7-PKCi mouse, and three regions were counted in each section, the anterior lobe fissure between lobules III and IV/V, the central lobe fissure between lobules VII and VIII, and lastly the fissure between lobules IX and X. The numbers in the text are averages of all sections and all regions (nine counting events per genotype).

- *Electron microscopy.*

The cerebella of three L7-PKCi mice (B6C3F1, line 1) and three wild type littermates were processed for electron microscopy as described (De Zeeuw et al., 1997). In short, the mice were anaesthetized with Nembutal (60 mg/kg) and perfused transcardially with 10 ml 0.9% saline in 0.1 M cacodylate buffer at pH 7.3, followed by 25 ml of 3% glutaraldehyde and 1% paraformaldehyde in the same buffer. The cerebella were sectioned in three different directions (i.e. sagittally, coronally, and transversely) on a Vibratome at 70  $\mu$ m, osmicated, block stained in uranyl acetate, directly dehydrated in dimethoxypropane and embedded in Araldite. Guided by observations made in the semithin sections, pyramids of different cerebellar lobules were prepared. From these tissue blocks ultrathin sections were cut and mounted on Formvar coated nickel grids; most of these grids were processed for standard electron microscopy, but some were processed for GABA-immunocytochemistry (for details, see De Zeeuw et al., 1989). The latter grids were rinsed in a solution of 0.5 M tris buffer containing 0.9% NaCl and 0.1% Triton-X100 at pH 7.6 (TBST), and incubated overnight at 4°C in a droplet of GABA antiserum (1:1000 in TBST). The GABA antiserum was generously supplied by Dr. R.M. Buijs (Buijs et al., 1987). The next day the grids were rinsed twice with TBST (pH 8.2) and incubated for one hour at room temp in a droplet of goat anti-rabbit IgG labeled with 15 nm gold particles (Aurion) diluted 1:25 in TBST. All grids were washed twice with TBST (pH 7.6) and distilled water, counterstained with uranyl acetate and lead citrate, and examined in a Philips electron microscope (CM-100). Random samples of parallel fiber terminals and GABAergic interneuron terminals were collected from at least three non-serial ultrathin sections obtained from at least two embedded tissue blocks



of the vestibulocerebellum of each animal.

### **3.3d - L7-PKCi Purkinje Cells in Culture**

Embryonic mouse cerebellar cultures were prepared and maintained according to the method of Schilling et al. (1991). Cultures were maintained in vitro for 8-16 days at the time of use in electrophysiological experiments. Patch electrodes were attached to Purkinje cell somata and were used to apply a holding potential of -80 mV. Iontophoresis electrodes (1  $\mu\text{m}$  tip diameter) were filled with glutamate (10 mM, in 10 mM HEPES, pH 7.1 with NaOH) and were positioned  $\sim 20 \mu\text{m}$  away from large-caliber dendrites. Test pulses were delivered using negative current pulses (600-800 nA, 30 to 110 msec duration) applied at a frequency of 0.05 Hz. After acquisition of baseline responses, 6 conjunctive stimuli were applied at 0.05 Hz, each consisting of a glutamate test pulse combined with a 3 sec long depolarization step to 0 mV, timed so that the depolarization onset preceded the glutamate pulse by 500 msec. Cells were bathed in a solution that contained (in mM) NaCl (140), KCl (5),  $\text{CaCl}_2$  (2),  $\text{MgCl}_2$  (0.8), HEPES (10), glucose (10), tetrodotoxin (0.005), and picrotoxin (0.1), adjusted to pH 7.35 with NaOH, which flowed at a rate of 0.5 ml/min. The recording electrode contained CsCl (135), HEPES (10), EGTA (1), and  $\text{Na}_2\text{-ATP}$  (4), adjusted to pH 7.35 with CsOH. Patch electrodes yielded a resistance of 3-5 M $\Omega$  when measured with the internal and external salines described above. Membrane currents were recorded with an Axopatch 200A amplifier in resistive voltage-clamp mode, lowpass filtered at 5 kHz, and stored on a chart recorder. For potassium current recordings (Figure 4)  $\text{CaCl}_2$  was removed from the external saline and the internal saline contained KCl (140), EGTA (11),  $\text{CaCl}_2$  (1), HEPES (10) and  $\text{Na}_2\text{-ATP}$  (2), adjusted to pH 7.35 with KOH. These currents were lowpass filtered at 2 kHz and digitized at 5 kHz using Axodata software (Axon Instruments). Fura-2 ratio imaging of intracellular free Ca was accomplished by measuring the background corrected fluorescence ratio at 340 and 380 nm excitation using a cooled CCD camera system as previously described (Linden et al., 1995). Exposure times were 100-400 msec per single wavelength image. Experiments were conducted at room temperature.

### **3.3e - Eye Movement Recordings**

Eye movements were recorded with the use of the search coil method for mice (Koekkoek et al. 1997; De Zeeuw et al., in press). General anesthesia was induced and maintained with a mixture of Ketamine (50 mg/ml) and Xylazine (2.8 mg/ml) in sodium chloride (3.6 mg/ml). The initial dose was 0.07 ml IP supplemented with 0.03 ml IP every 35 minutes. After an incision was made in the skin, four holes with a diameter of 0.8 mm were drilled in the parietal and frontal bones, and stainless steel screws (M1, 3.75 mm long) were dipped in cyanoacrylate and screwed into the holes. A pedestal made of dental cement (Simplex Rapid, Austenal Dental Products LTD, England) containing two M3 fixation bolts and a two pin connector was mounted on top of the screws with dental cement so that the flat top surface of the pedestal was placed at an angle of 15 degrees with the nasal bone. The next day the animals were reanesthetised with Halothane (1 part  $\text{O}_2$ , 2 parts  $\text{N}_2\text{O}$ , and 2% Fluothane at a flow



of 1.5 liters per minute; Zeneca, Ridderkerk), local eye anesthesia (Novesine; 0.4%, Bournonville-Pharma B.V., The Netherlands) was applied, and a pre wound eye coil (2.8 mm outside diameter; Sokymat SA, Switzerland) made of 80 windings of 25  $\mu\text{m}$  isolated brass wire (resistance of 25 to 35 Ohm) was placed flat on the eye and carefully positioned in such a way that the pupil was located exactly in the center of the coil. The coil was fixed on the sclera with 3 10-0 Ethilon monofilament sutures and the wrapped coil wires were led underneath the skin towards the connector. Directly after surgery the mouse was put in a restrainer with its pedestal surface fixed at 45 degrees to the earth's horizontal (i.e. the angle between the nasal bone and the earth's horizontal was 60 degrees) inside an electromagnetic measurement system (Skalar Medical). While the head-fixed animal was still anesthetized the eye coil was calibrated in two different manners: by rotating the animal inside the fixed coil system as well as by rotating the coil system around the animal fixed in space. Subsequently, the animal was allowed to recover, and the recordings were started as soon as the animal was fully alert. The optokinetic and vestibular stimuli were given with the use of a servo-controlled turntable and a drum with different black and white stripes with a width corresponding to a visual angle of the mouse of 4 degrees. The diameter and height of the drum were 24 cm and 20 cm, respectively. When the eye of the mouse was positioned in the center of the drum, the visual field provided by the drum extended from 33 degrees below to 90 degrees above the horizontal plane through the eye of the mouse. The stimulus frequency and amplitude were controlled by a personal computer with the use of the Spike2 for Windows Sequencer program and a CED machine (G. Smith; Cambridge Electronics Design). Eye, table, and drum position were monitored on storage oscilloscopes and recorded on-line using the CED 1401 signal capture device and Spike2 for Windows. The stimulus protocols included optokinetic stimulation and table stimulation in the dark and light, both before and after visuo-vestibular training. We used alternating constant velocity stimulation to measure the latency, and sinusoidal stimulation to measure the gain and phase of the eye movements. All tests were performed at frequencies and with peak velocities ranging from 0.1 Hz to 0.8 Hz, and 3 deg/s to 9 deg/s, respectively. Each protocol contained at least twelve cycles enabling us to average gain, latency and phase values over at least three cycles without saccadic eye movements. Adaptation was induced by rotating the drum at 0.4 Hz either in counterphase (gain increase) or in phase (gain suppression) with the turntable at twice the amplitude (6 deg/s) for one hour. The effects of the adaptation were measured during VOR in the dark. All values were analyzed off-line using the Ced-Anal program for Windows according to standard procedures (De Zeeuw et al., 1995).

### **3.3f - Slice Preparations from L7-PKCi Cerebella**

Sagittal slices of the cerebellar vermis (200-250  $\mu\text{m}$  thick) were prepared from P21-P35 mice of the B6C3F1 strain. Following a recovery period, they were placed in a submerged chamber perfused with a bath solution containing (in mM): 124 NaCl, 5 KCl, 1.25  $\text{Na}_2\text{HPO}_4$ , 2  $\text{MgSO}_4$ , 2  $\text{CaCl}_2$ , 26  $\text{NaHCO}_3$  and 10 D-glucose bubbled with 95%  $\text{O}_2$  / 5%  $\text{CO}_2$  at room temperature. Recording was performed using the visualized whole-cell patch-clamp technique. Recording pipettes (resistance 2-3 M $\Omega$ )

were filled with a solution containing (in mM): 9 KCl, 10 KOH, 120 K gluconate, 3.48 MgCl<sub>2</sub>, 10 HEPES, 4 NaCl, 4 Na<sub>2</sub>ATP, 0.4 Na<sub>3</sub>GTP and 17.5 sucrose. Membrane currents were recorded with an Axoclamp-2A amplifier in continuous SEVC mode. Climbing fibers were stimulated in the white matter / granule cell layer using a monopolar tungsten electrode.

### **3.3g - Motor Coordination Tests**

The rotorod tests were performed according to the protocol described by Chen et al. (1995). The rotorod consists of a smooth plastic roller (8 cm diameter, 14 cm long) flanked by two large round plates (30 cm diameter) to prevent animals from escaping. A mouse was placed on the roller, and the time remained on the stationary or rotating roller was measured. A maximum of 60 sec was allowed for each animal for all motor skill tests. The thin rod consists of a smooth plastic rod (1.5 cm diameter, 50 cm long) held horizontally on both ends. A mouse was placed in the midpoint of the rod, and the time it remained on the rod was measured.

## **3.4 Results**

### **3.4a - Construction of L7-PKCi Mice**

A minigene (PKCi) was made by hybridization of two complementary synthetic oligonucleotides, each 50 bases in length, producing a double-stranded product with 5' overhangs compatible with BamHI restriction sites (see Experimental Procedures). This fragment was cloned into the BamHI site of the Purkinje cell expression vector, L7ΔAUG (Smeyne et al., 1995), in which all possible translational initiation sites were removed (Figure 3.1A). The minigene, if expressed, would encode a 13 amino acid peptide (not including the start methionine) corresponding in sequence to PKC[19-31] (Figure 3.1B), a slightly truncated version of the pseudosubstrate domain of PKC, PKC[19-36] (House and Kemp, 1987; Linden and Connor, 1991). This slightly truncated version has been demonstrated *in vitro* to be a more potent inhibitor of PKC (by ~60%) than the longer version, but both were shown by biochemical assay to selectively block the complete range of isotypes present in PKC purified from whole brain (House and Kemp, 1987). The coding portion of the minigene was optimized for mouse codon usage. The entire L7-PKCi construct was linearized with HindIII and EcoRI and injected into fertilized mouse eggs using previously described methods (Oberdick et al., 1990).

Six positive transgenic mouse lines (FVB/N background) were identified by PCR analysis of DNA prepared from tail biopsies. Animals from all lines showed no gross behavioral deficits, displaying fluid and well-coordinated gross motor skills. By Northern blot analysis of total cerebellar RNA, two lines revealed no detectable expression of the transgene. The other four showed variable levels of expression (Figure 1C). Although the precise time course of L7-PKCi transgene expression has not been determined here, it should be noted that endogenous L7 and its transgene

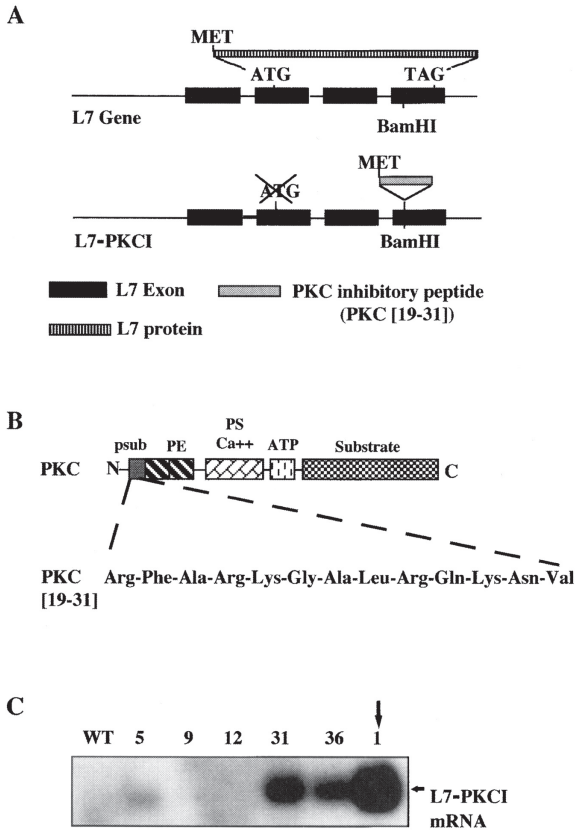


**Figure 3.1 Construction and expression of the L7-PKCi trans-gene.** A) The normal L7 gene is shown at the top. The L7-PKCi transgene construct (bottom) was made by insertion of a synthetic mini-gene coding for the peptide PKC[19-31] into the BamHI site of the vector L7 $\Delta$ AUG (Smeyne et al. 1995). The latter vector is a version of the L7 gene in which all potential start codons (ATG) in all reading frames were eliminated by PCR from all L7 exons so that translation may only be initiated from a start codon (MET) provided within cDNAs inserted into the unique BamHI cloning site. B) Structure of the prototypical PKC and sequence of PKC[19-31]. This inhibitory peptide is part of the N-terminal pseudosubstrate domain (psub) of most PKC isoforms and negatively regulates PKC catalytic activity by mimicking substrate. Schematic was adapted from Newton, 1995. PE=phorbol ester activation domain; PS=phosphatidylserine and Ca binding domain; ATP=ATP binding domain. C) Northern blot analysis of RNA prepared from cerebella of wild-type (WT) and various L7-PKCi transgenic mouse lines. The blot was probed with a  $^{32}$ P-labeled antisense oligonucleotide corresponding to the PKC[19-31] minigene. The line with highest expression (line 1, arrow) was used for all experiments described here, and the cell physiological data were confirmed in the next highest expressor (line 31).

derivatives such as L7- $\beta$ gal have been reported to be first detectable at embryonic day 15 and are continuously expressed into adulthood (Oberdick et al., 1993; Baader et al., 1997). Thus, it is expected that the L7-PKCi transgene would become activated only after the final generation of Purkinje cells, but during their early differentiation and maturation.

The data reported below were collected using the highest expressor (line 1) and/or the second highest expressor (line 31); the expression level of PKC[19-31] mRNA in line 31 is  $\sim$ 30% of that in line 1 (Figure 1C). Expression of the inhibitory peptide in Purkinje cells was confirmed by an electrophysiological assay of a phorbol ester-dependent effect which is attenuated in cerebellar cultures prepared from L7-PKCi mice (see below).

### 3.4b - Anatomical Analysis of L7-PKCi Mice

By *in situ* hybridization, expression of the transgene mRNA was revealed to be specifically and abundantly localized to cerebellar Purkinje cells (Figure 3.2). No detectable expression was observed in any other brain region. All cerebellar laminae of L7-PKCi mice appeared to be of normal size and arrangement, and foliation was normal (Figure 3.1-2C,D and G,H). Immunohistochemical staining with antibodies to the proteins calbindin (CaBP) (Jande et al., 1981) and L7 (Oberdick et al., 1988) revealed normal Purkinje cell morphology, number, and density in L7-PKCi mice as compared to wild-types. The average area of cerebellar sections at the midline



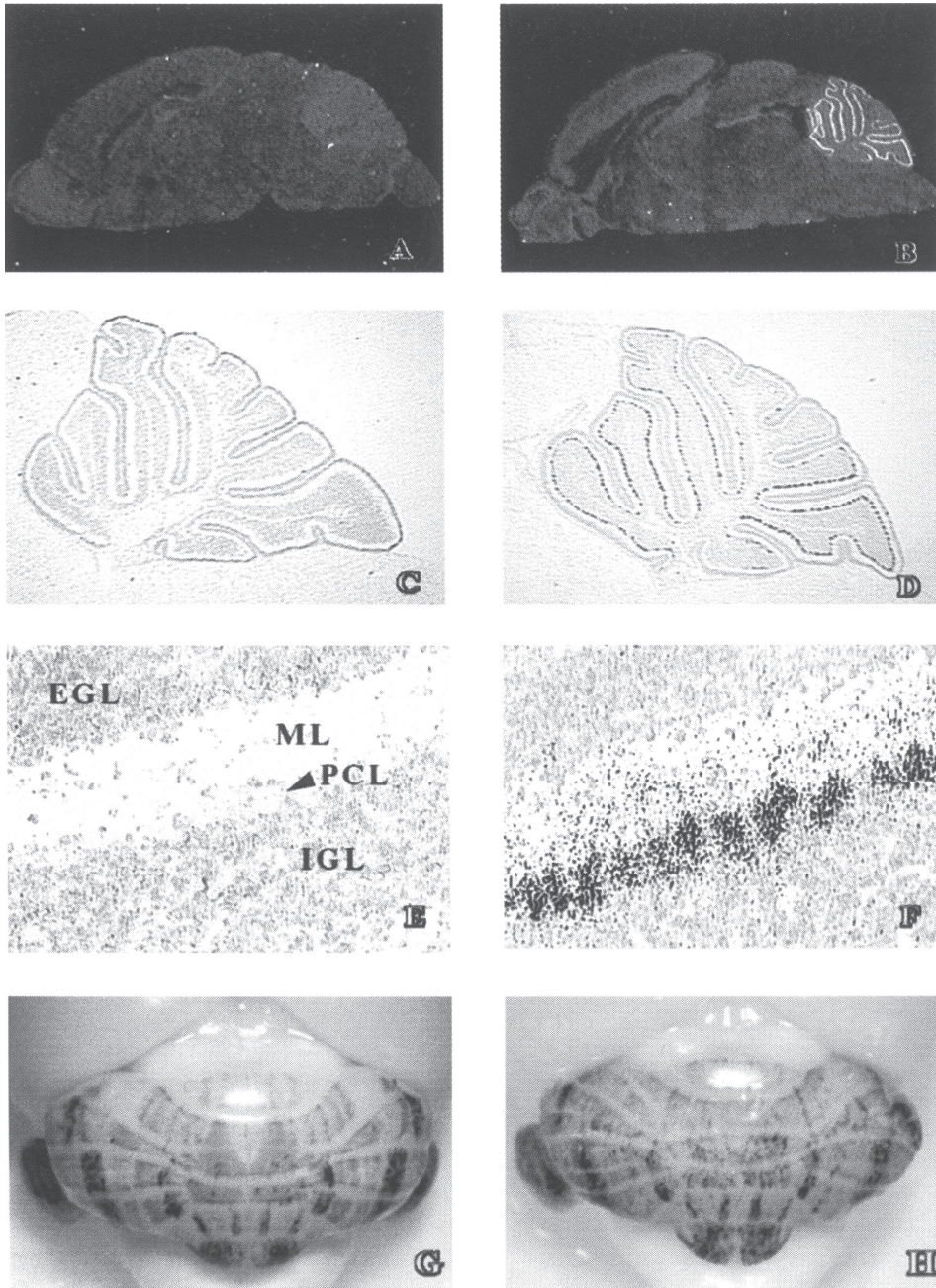


**Figure 3.2 Purkinje cell-specific expression of the L7-PKCi transgene and lack of effect on cerebellar morphology.** In situ hybridization was performed on sections of L7-PKCi and wt mouse brain using  $^{35}\text{S}$ -labeled PKCi antisense oligonucleotide probe. Hybridization signal is undetectable in wt sections at all magnifications (A,C,E) but is clearly detectable in the Purkinje cell layer of L7-PKCi sections (B,D,F). Panels A and B are dark-field views whereas panels C-F are bright-field. Grains in the molecular layer in panel F are localized to Purkinje cell dendrites as reported previously for endogenous and transgene versions of the *L7* mRNA (Bian et al., 1996). (G and H) Whole mount views of L7βG3 expression in wt (G) and L7-PKCi transgenics (H). The gross pattern of sagittal bands (blue-green β-gal stain) is unchanged. Likewise, the pattern of lobulation and fissurization is unchanged.

Magnifications: 12.5X (A,B); 30X (C,D); 200X (E,F). Abbreviations: EGL = external germinal layer; ML = molecular layer; PCL = Purkinje cell layer; IGL = internal granule cell layer.

was  $7.9 \pm 0.4 \text{ mm}^2$  in wild-type versus  $7.7 \pm 0.4 \text{ mm}^2$  in L7-PKCi mice, and in the hemispheres  $6.2 \pm 0.5 \text{ mm}^2$  in wild-type versus  $5.6 \pm 0.3 \text{ mm}^2$  in L7-PKCi mice. The Purkinje cell density at the midline was measured to be  $31 \pm 6 \text{ PCs/mm}$  in the wild-type and  $34 \pm 6 \text{ PCs/mm}$  in L7-PKCi mice. Thus, none of these measures in L7-PKCi mice shows any significant difference from wild-type.

The cerebellum is divided into a series of sagittally-oriented modules, which can be revealed by tracing patterns of afferent and efferent projections as well as by electrophysiological properties of the Purkinje cell responses (Voogd and Bigaré, 1981; De Zeeuw et al., 1994). In L7-PKCi mice, a number of Purkinje cell markers that identify sagittal zones within the cerebellar cortex (L7- $\beta$ gal, Oberdick et al., 1993; zebrin II, Leclerc et al., 1992) were shown to have normal patterns of expression, and similarly, sagittally-organized granule cell patches that have been suggested to be dependent upon the pattern of mossy fiber innervation (nNOS, Schilling et al., 1994) were observed to be unaffected. These observations are summarized in Figure 3.2 G,H in which the pattern of expression of a truncated version of L7- $\beta$ gal is compared in wild-type and L7-PKCi backgrounds. Although subtle differences can be seen, these cannot be distinguished from effects due to individual and strain variability at this time. Nevertheless, it is quite clear that the gross pattern of sagittal banding is normal in L7-PKCi mice. Likewise, electron microscopic analysis of the neurons

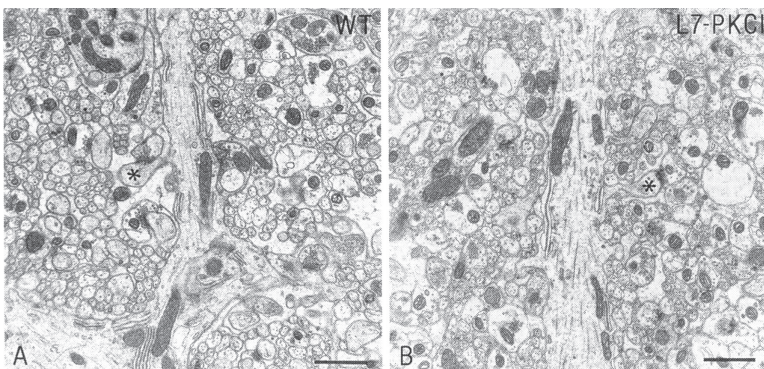


**Figure 3.3 Ultrastructure of parallel fiber synapses onto the Purkinje cell is indistinguishable.** The electron micrographs are from sagittal sections of the molecular layer in the vestibulocerebellum of wild types (A) and L7-PKCi mutants (B). Asterisks indicate the morphology of a Purkinje cell spine innervated by an asymmetric synapse. Scale bars indicate 1  $\mu\text{m}$ .

and interneurons in the cerebellar cortex in L7-PKCi mice showed no obvious abnormalities; although the total surface area comprised by microglia may be somewhat larger in the mutant, the ultrastructural characteristics of the Purkinje cell dendritic trees and spines as well as their innervation by parallel fibers and GABAergic interneurons appeared both morphologically and numerically normal (Figure 3.3). In both wild types and L7-PKCi mutants, the majority of the terminals in the molecular layer of the cortex in the vestibulocerebellum contained clear round vesicles and established asymmetric synapses with Purkinje cell spines. The average density of these presumptive parallel fiber synapses was  $22 \pm 2.4$  per  $100 \mu\text{m}^2$  and  $19 \pm 2.8$  per  $100 \mu\text{m}^2$  in the wild types and L7-PKCi mutants, respectively. This difference



was not significantly different. These findings suggest that the intrinsic patterning of Purkinje cells as well as the regulated patterning of mossy fiber - parallel fiber afferents are unaffected by L7-PKCi expression. However, it should be cautioned that while obvious alterations in the circuitry of the cerebellar cortex layer could not be seen, it is possible that there are subtle alterations of circuitry or subcellular structure that might elude the present morphological analysis (see Figure 3.8).

### 3.4c - Electrophysiology of Purkinje Cells in Culture

When dispersed cultures were prepared from the cerebella of embryonic L7-PKCi and wild-type (wt) mice, no gross differences in cell morphology (size, number or ratio of cell types, degree or pattern of neurite outgrowth, degree of clustering) could be observed at the level of light microscopy (data not shown). Examination of a number of basal electrophysiological parameters, revealed no significant differences between L7-PKCi and wt Purkinje cells. These included  $V_m$  (B6C3F1 wt =  $-70 \pm 4$  mV, n=6; L7-PKCi-(1) hetero / B6C3F1 =  $-73 \pm 4$  mV, n=7; L7-PKCi-(31) hetero / FVB/N =  $-69 \pm 5$  mV, n=5),  $R_{input}$  (B6C3F1 wt =  $150 \pm 26$  M $\Omega$ , n=6; L7-PKCi-(1) hetero / B6C3F1 =  $159 \pm 31$  M $\Omega$ , n=7; L7-PKCi-(31) hetero / FVB/N =  $145 \pm 38$  M $\Omega$ , n=5), mEPSC frequency (B6C3F1 wt =  $9.2 \pm 3.0$  sec $^{-1}$ , n=8; L7-PKCi-(1) hetero / B6C3F1 =  $8.5 \pm 2.6$  sec $^{-1}$ , n=8; L7-PKCi-(31) hetero / FVB/N =  $9.6 \pm 3.6$  sec $^{-1}$ , n=6) and mEPSC amplitude (B6C3F1 wt =  $22 \pm 6$  pA, n=8; L7-PKCi-(1) hetero / B6C3F1 =  $21 \pm 6$  pA, n=8; L7-PKCi-(31) hetero / FVB/N =  $22 \pm 7$  pA, n=6). mEPSC frequency and amplitude were measured over a 500 sec recording period at a holding potential of -80 mV.

It is important to determine whether the PKCi peptide is expressed at sufficiently high levels to strongly inhibit PKC activity in Purkinje cells. A downside of the present anatomical specificity of transgene expression is that standard biochemical assays cannot always be employed even on carefully microdissected tissue. For example, even in microdissected cerebellar cortex, the Purkinje cells contribute only a minority of total PKC activity. Thus, strong inhibition of this PKC activity in Purkinje cells becomes difficult to detect in a background of PKC activity from other cell types. To circumvent this problem, we have utilized an electrophysiological assay. Activation of PKC by exogenous compounds such as phorbol esters and synthetic diacylglycerols has been shown to attenuate voltage-gated potassium currents in a number of cell types (Farley and Auerbach, 1986; Grega et al., 1987; Doerner et al., 1988), including rat cerebellar Purkinje cells grown in culture (Linden et al., 1992). We have replicated this observation using B6C3F1 wt mouse Purkinje cells (Figure 3.4) and have shown that the attenuation produced by phorbol ester (phorbol-12,13-dibutyrate, 300 nM;  $41 \pm 3.3\%$  attenuation of peak current, n=6 cells) is strongly blocked by a PKC inhibitor (chelerythrine, 10  $\mu$ M;  $7 \pm 2.8\%$  attenuation of peak current, n=5 cells).

The potassium current elicited in these recording conditions is likely to be predominantly composed of delayed outward rectifier current, although a contribution of A-current to the peak component is also possible. The attenuation seen herein takes the form of a decrease in conductance without an associated change in the voltage-dependence of activation (data not shown). Most importantly, application of

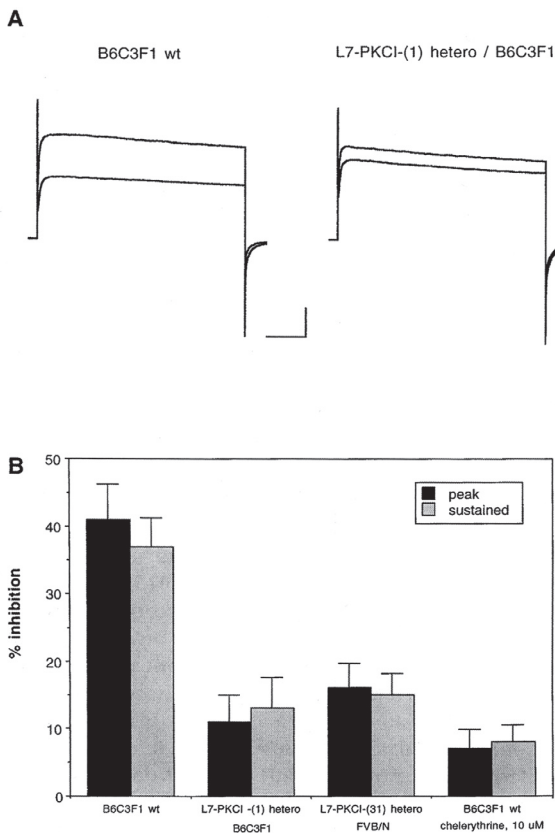


**Figure 3.4 Attenuation of potassium currents by an exogenous PKC activator is blocked in L7-PKCi Purkinje cells.** A) Families of outward currents were evoked by step depolarizations from a holding potential of -90 mV. The currents illustrated here were evoked with depolarizing steps to +40 mV and are single representative traces recorded immediately before (larger traces) and 10 min after the application of the PKC activator, phorbol-12,13-dibutyrate (300 nM) in the bath (smaller traces). Scale bars = 1 nA, 50 msec. B) Summary graphs showing the degree of attenuation produced by phorbol-12,13-dibutyrate (300 nM) upon both the peak and sustained components of the outward current. B6C3F1 wt, n=6; L7-PKCi-(1) hetero / B6C3F1, n=5; L7-PKCi-(31) hetero / FVB/N, n=6; chelerythrine / B6C3F1 wt, n=5.

phorbol-12,13-dibutyrate to Purkinje cells derived from either L7-PKCi-(1) hetero / B6C3F1 or L7-PKCi-(31) hetero / FVB/N mice produced only a minimal attenuation of the potassium current ( $11 \pm 3.9\%$ , and  $16 \pm 3.6\%$  attenuation of peak current respectively, n=5 cells/group), indicating that the expression of the PKCi peptide in these Purkinje cells is sufficient to strongly inhibit PKC.

If the induction of cerebellar LTD requires PKC activation, then this process should be blocked in L7-PKCi Purkinje cells. Cerebellar LTD was measured in voltage-clamped Purkinje cells in culture using a method in which parallel fiber stimulation was replaced by iontophoretic glutamate pulses and climbing fiber stimulation was replaced by direct depolarization of the Purkinje cell (Linden et al., 1991; see Linden, 1996, for review). Following acquisition of baseline responses, glutamate/depolarization conjunctive stimulation was applied and glutamate test pulses were resumed to monitor the time-course of Purkinje cell responses (Figure 3.5A). This treatment reliably induced LTD in Purkinje cells derived from two different strains of wt mice, B6C3F1, a pigmented strain and FVB/N, an albino strain. In contrast, LTD was strongly attenuated in L7-PKCi Purkinje cells derived from either heterozygotes in the B6C3F1 (line 1) or FVB/N (line 31) background or homozygotes in the FVB/N (line 1) background. The effects were most prominent in the cells obtained from the homozygous animals, but all Purkinje cells derived from the different transgenic cell lines or backgrounds revealed the same aberrations; all transgenic L7-PKCi mice showed a severe impairment of LTD induction.



To more accurately interpret the inhibitory effect of the L7-PKCi transgene on LTD induction, it became necessary to screen L7-PKCi Purkinje cells to determine if they had altered properties that might be expected to impact cerebellar LTD independent of a direct effect on PKC.

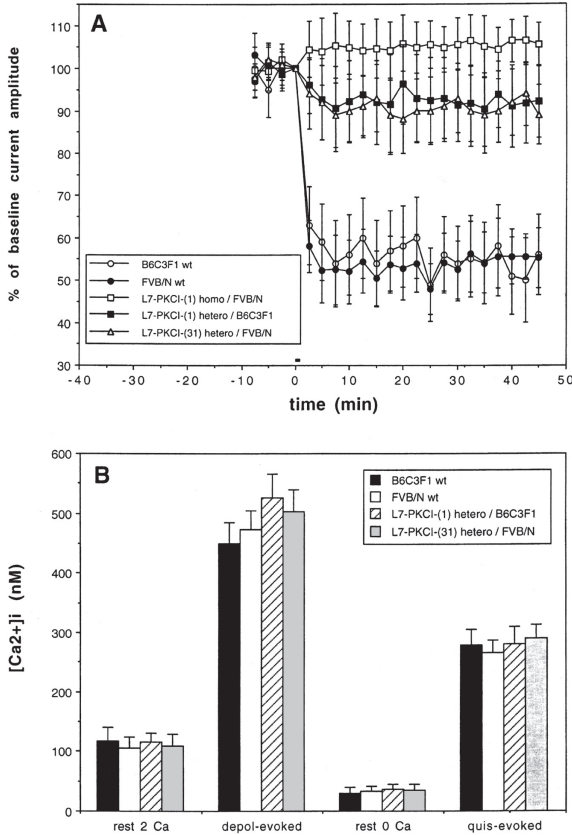


**Figure 3.5 Induction of cerebellar LTD is suppressed in cultured Purkinje cells derived from L7-PKCi mice.** A) Following acquisition of baseline responses to glutamate test pulses, glutamate/depolarization conjunction was applied at t=0 min. LTD is induced in wild type (wt) Purkinje cells of either the B6C3F1 (n=7 cells) or the FVB/N mouse (n=5). Purkinje cells derived from both homozygous L7-PKCi mice produced in a FVB/N background (n=5) and heterozygous L7-PKCi mice produced in a B6C3F1 background (line 1; n=6) or FVB/N background (line 31; n=6) showed strong suppression of LTD. B) Control experiments to determine if PKCi expression produces its suppression of LTD induction through effects on Ca<sup>2+</sup> influx and/or mobilization. Peak Ca<sup>2+</sup> transients were measured in proximal dendritic shafts of fura-2 loaded Purkinje cells grown in culture. Ca<sup>2+</sup> transients evoked by a 3 sec depolarization to 0 mV in normal (2 mM) external Ca<sup>2+</sup> were measured as an index of voltage-gated Ca<sup>2+</sup> channel function. Ca<sup>2+</sup> transients evoked by a pulse of 100 mM quisqualate in 0 Ca<sup>2+</sup>/0.2 mM EGTA external saline (6 psi, 2 s) were measured as an index of mGluR1 function. Heterozygous L7-PKCi mice produced in a B6C3F1 (line 1) or FVB/N (line 31) background were not significantly different from wild type controls in either measure (n=5 cells/group for depolarization-evoked Ca<sup>2+</sup> influx and n=10 cells/group for quisqualate-evoked Ca<sup>2+</sup> mobilization).

As voltage-gated Ca<sup>2+</sup> channels (Sakurai, 1990; Linden et al., 1991; Konnerth et al., 1992) and mGluR1 receptors (Aiba et al., 1994; Conquet et al., 1994; Shigemoto et al., 1994) are known to be necessary for LTD induction, L7-PKCi Purkinje cells were screened to determine if they had alterations in either of these two signaling systems. Fura-2 microfluorimetry was used to assess depolarization-evoked Ca<sup>2+</sup> influx in normal Ca<sup>2+</sup> external saline (2 mM), as an index of voltage-gated Ca channel function, and quisqualate-evoked Ca<sup>2+</sup> mobilization in Ca<sup>2+</sup>-free external saline as an index of mGluR1 function. Figure 5B illustrates that neither basal Ca<sup>2+</sup>, nor increases evoked by Ca<sup>2+</sup> influx via voltage-gated channels, nor Ca<sup>2+</sup> mobilization via mGluR1 receptors is significantly altered in L7-PKCi heterozygotes in a B6C3F1 (line 1) or FVB/N (line 31) background.

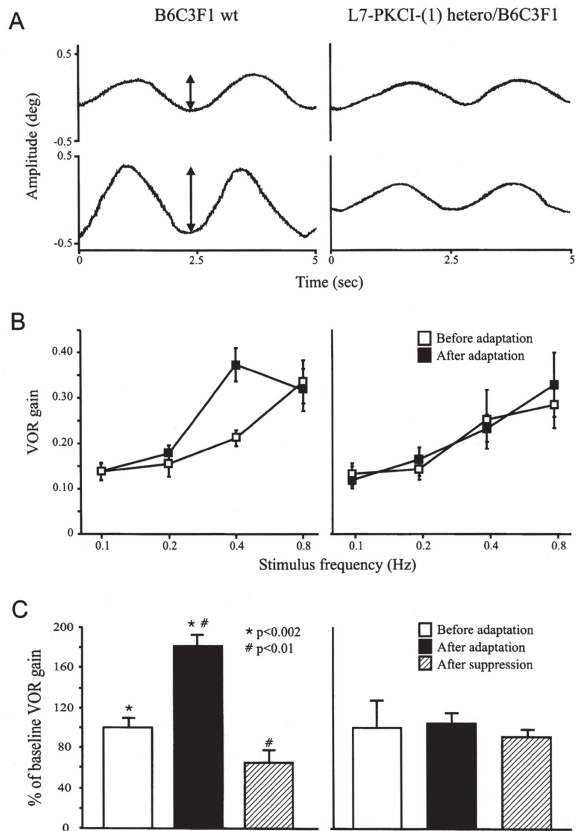
### 3.4d - Compensatory Eye Movements of L7-PKCi Mice

VOR adaptation is affected. To determine whether L7-PKCi mice can show cerebellar motor learning we investigated whether these mice adapt the gain of their VOR

during visuo-vestibular training. Heterozygous L7-PKCi mice ( $n=8$ ) and wild type littermates ( $n=10$ ) in the B6C3F1 (line 1) background were subjected to a training period of one hour of sinusoidal table stimulation (0.4 Hz; 3 deg/s peak velocity) and 180 degrees out-of-phase drum stimulation (0.4 Hz; 3 deg/s peak velocity). The average gain of the eye movements of wild type mice during VOR in the dark at 0.4 Hz increased significantly ( $p<0.002$ ; Mann-Whitney Rank Sum Test) from  $0.21 \pm 0.02$  (mean  $\pm$  SE) before the training to  $0.38 \pm 0.04$  after the training (thus, an average increase of 81%; for example, see Figure 3.6A).

**Figure 3.6 VOR adaptation is impaired in L7-PKCi mice.** A) The left panel illustrates

the eye movements of a B6C3F1 wt mouse during turntable rotation at 0.4 Hz (peak velocity 3 deg/s) in the dark (VOR) before (top) and after (bottom) one hour of visuo-vestibular training. The right panel illustrates the eye movements of a L7-PKCi(1) hetero / B6C3F1 littermate during the same protocols. Note that the gain of the wild type animal increases after the training (compare lengths of the arrows), whereas the gain of the mutant remains the same. B) The adaptation of the gain is frequency specific. The increase of the VOR gain occurred only at 0.4 Hz, the frequency at which the training was performed. C) The VOR gain increase of the wild type at 0.4 Hz after adaptation could be converted into a decrease of the gain after subjecting the animal to a suppression protocol (one hour of optokinetic stimulation in phase with turntable stimulation, left panel). In L7-PKCi mice, however, gain suppression was not possible (right panel). Thus, mice can increase or decrease their VOR gain following visuo-vestibular training in a frequency specific manner, but this adaptation only can occur only in the absence of the PKCI transgene. Note that in A) the amplitude of the eye movement is given in degrees; in B) the absolute gain values are presented; and in C) the gain values are presented as percentages of the baseline gain (set at 100%) at the beginning of the adaptation or suppression training protocol.



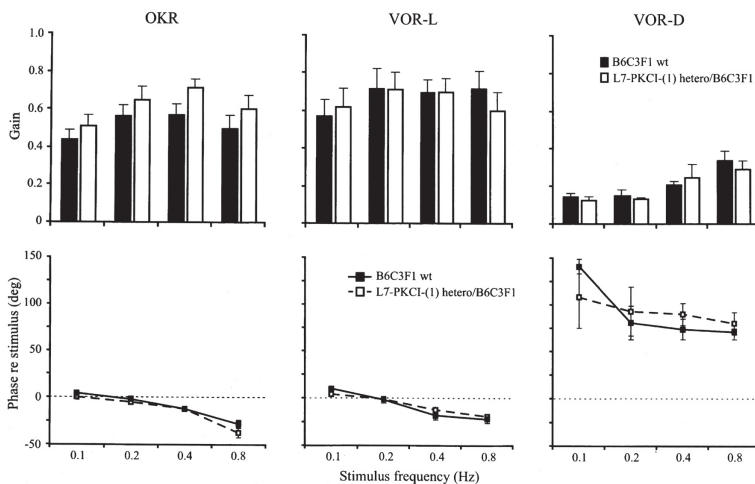
In contrast, the average gain of the eye movements of L7-PKCi mice during this protocol did not change significantly (from  $0.25 \pm 0.07$  to  $0.23 \pm 0.03$ ). The change in VOR gain after visuo-vestibular training as observed in the wild types was frequency specific (Figure 3.6B); the VOR gains at 0.1 Hz, 0.2 Hz, and 0.8 Hz were not significantly affected by the training. The adaptation only occurred at 0.4 Hz, the frequency at which the vestibular and visual stimuli were provided. After the training protocol that was aimed at increasing the VOR gain, the same mice were subjected to a so-called suppression protocol in which the drum moved for one hour in phase with the table (both at 0.4 Hz; table and drum, 3 and 6 deg/s peak velocity, respectively). In wild type mice this suppression protocol reduced the gain during VOR in the dark at 0.4 Hz significantly to 61% of the starting value ( $p<0.01$ ; Mann-

Whitney Rank Sum Test), whereas in L7-PKCi mice no alterations of the VOR gain were observed (Figure 3.6C). This effect was also frequency specific. We conclude from these experiments that VOR adaptation in B6C3F1 wild type mice is frequency specific, that VOR adaptation can lead to both an increase and a decrease of the gain, and that both of these forms of VOR adaptation are attenuated by expression of the PKCI transgene in Purkinje cells.

### 3.4e - General eye movement performance is not impaired

To determine whether the impaired VOR adaptation of the L7-PKCi mice is accompanied by general deficits in eye movement performance, we investigated the gain and phase during sinusoidal optokinetic and vestibular stimulation at different frequencies (0.1 Hz, 0.2 Hz, 0.4 Hz, and 0.8 Hz) and peak velocities (3 deg/s, 6 deg/s, and 9 deg/s). All gain and phase values of the eye movements of the L7-PKCi mice (B6C3F1 background, line 1; n=8) during the optokinetic reflex (OKR), VOR in the light (VOR-L), and VOR in the dark (VOR-D) were not significantly different from those of wild type littermates (n=10) over the range of frequencies and peak velocities examined (Figure 3.7). In the light (OKR and VOR-L), the gain of the eye movement of both mutants and wild types was generally above 0.5, the phase of the eye movement was lagging behind that of the stimulus, and the variations were small. In the dark (VOR-D), the gain of the eye movement of the animals was always below 0.5, the phase of the eye movement was leading that of the table, and the variations were relatively large as a consequence of the absence of visual stabilization. In addition, we investigated whether the latency of the optokinetic response to velocity step stimulation (0.1 Hz, 3 deg/s) was affected in mutants. The turnaround of the optokinetic response of the L7-PKCi mice followed on average  $112 \pm 8$  msec

**Figure 3.7 General eye movement performance is not impaired in L7-PKCi mice.** The gain (top) and phase (bottom) values of L7-PKCi(-1) hetero / B6C3F1 mice (n=8) and B6C3F1 wt littermates (n=10) were determined during OKR (left panel), VOR in the light (VOR-L; middle panel), and VOR in the dark (VOR-D; right panel) at four different stimulus frequencies. The gain and phase values of the L7-PKCi(-1) hetero / B6C3F1 mice did not



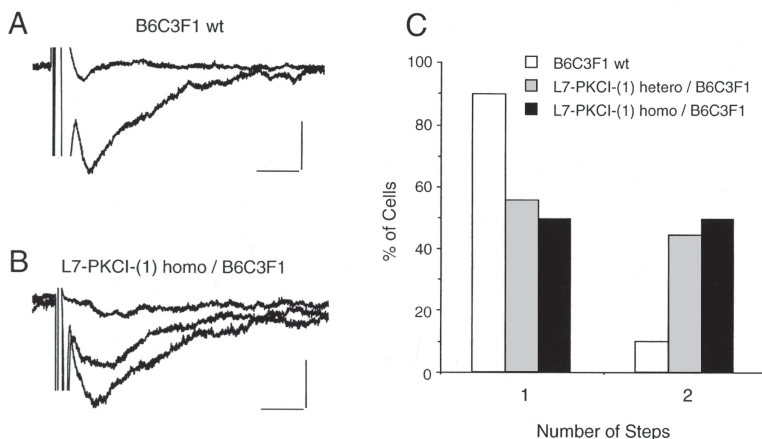
differ significantly from those of the B6C3F1 wts during any of the stimulus protocols. Thus, L7-PKCi mice are, as demonstrated in figure 6, unable to adapt their VOR gain during an hour of visuo-vestibular training, but their initial gain values before the training are apparently indistinguishable from those of wild types. The phase values as presented in this figure did not change after the training sessions.

(mean  $\pm$  SE) after the turnaround of the drum. This value was also not significantly different from the average latency of the eye movement response of the wild types ( $105 \pm 10$  msec). Thus, we conclude that the eye movement performance of L7-PKCi mice is not affected in that the amplitude (gain) and timing (phase and latency) of their compensatory eye movements are normal.

### 3.4f - Climbing Fiber Innervation of Purkinje Cells in L7-PKCi mice

It has previously been demonstrated that the global knock out of any one of a number of signaling molecules expressed in Purkinje cells results in an impairment of the developmental conversion from multiple to single innervation of Purkinje cells by climbing fibers (Kano et al., 1997; Kashiwabuchi et al., 1995). Of particular interest to the present study was the finding that this occurred in the global knockout of PKC $\gamma$  (Chen et al., 1995; Kano et al., 1995). To determine whether sustained multiple climbing fiber innervation occurred in L7-PKCi mice, climbing fiber-evoked EPSCs were measured in whole cell recordings from Purkinje cells in sagittal slices prepared from the vermis of L7-PKCi / B6C3F1 mice (line 1, age P21-P35) and age-matched B6C3F1 wt controls. Purkinje cells were voltage-clamped at holding potentials positive to the resting potential and climbing fiber-mediated EPSCs were evoked by applying stimuli of varying intensities to the underlying white matter. Due to the all-or-none characteristics of climbing fiber responses, the number of discrete EPSC steps with varying stimulation strength can be used as an indicator for the number of climbing fibers innervating a Purkinje cell. The degree of multiple climbing fiber innervation of Purkinje cells in L7-PKCi transgenic mice was higher than in wild types (Figure 3.8).

**Figure 3.8 Impaired elimination of multiple climbing fiber innervation of Purkinje cells in L7-PKCi mice.** To measure climbing fiber-mediated EPSCs and to suppress complex spikes the Purkinje cells were voltage-clamped at holding potentials positive to the resting potential, typically between -30 mV and -40 mV. A) Example of a B6C3F1 wt Purkinje cell (P32) innervated by a single climbing fiber (holding potential: -40 mV). B) Example of a L7-PKCi



homozygous Purkinje cell (P32) innervated by two climbing fibers (holding potential: -30 mV). In panels A and B, averages of 3-8 responses are shown at each threshold intensity. The scale bars represent 10 ms and 0.5 nA. (C) Summary histogram indicating the proportion of single and double climbing fiber innervation in B6C3F1 wt (n=10), L7-PKCi(1) homo / B6C3F1 (n=6) and L7-PKCi(1) hetero / B6C3F1 (n=9) mice. No higher order innervation (triple, quadruple, etc.) was seen.

In slices prepared from both heterozygous (4/9 cells) and homozygous (3/6 cells) L7-PKCi(1) / B6C3F1 mice, approximately half of the Purkinje cells were innervated by two climbing fibers, whereas in B6C3F1 wts only 1/10 cells received a double innervation at this age. We did not observe multiple climbing fiber innervation of a higher order (triple, quadruple, etc.). The observation that there is a higher degree of multiple climbing fiber innervation of Purkinje cells in L7-PKCi transgenic mice suggests that PKC activity intrinsic to the Purkinje cell is involved in the synapse elimination process leading to the typical 1:1-innervation ratio in adult wild-type mice.

### 3.4g - General Motor Performance of L7-PKCi Mice

The impaired elimination of the multiple climbing fiber innervation of Purkinje cells in the PKC $\gamma$  knock out mice has been related to a concomitant impairment of motor performance as revealed by rotorod tests (Chen et al., 1995). Since the L7-PKCi mice also show sustained multiple climbing fiber innervation during adulthood, we subjected them to the same series of rotorod tests as were used previously to analyze the PKC $\gamma$  knock out mice. The duration in which the animals remained on the apparatus (retention duration) was determined using L7-PKCi mice (B6C3F1 strain, line 1; n=8) and wt littermates (n=10) on the stationary rotorod, the running rotorod, and the stationary horizontal thin rod. 6 trials were conducted. In none of these tests did the L7-PKCi mice differ significantly from the wild types (Figure 3.9).

In all three tests the retention duration of both the L7-PKCi and the wild type mice gradually increased over 6 trials from approximately 15 s to 50 s. As a positive control we subjected adult *lurcher* mice (B6CBACa, n=6), which lack Purkinje cells (Caddy and Biscoe, 1979), to the same rotorod tests. These mice completely lacked the ability to control their movements; in all three tests their average retention duration remained between 0 and 10 sec. We conclude from these experiments that sustained multiple climbing fiber innervation, of the magnitude seen here, does not necessarily result in impaired motor coordination.

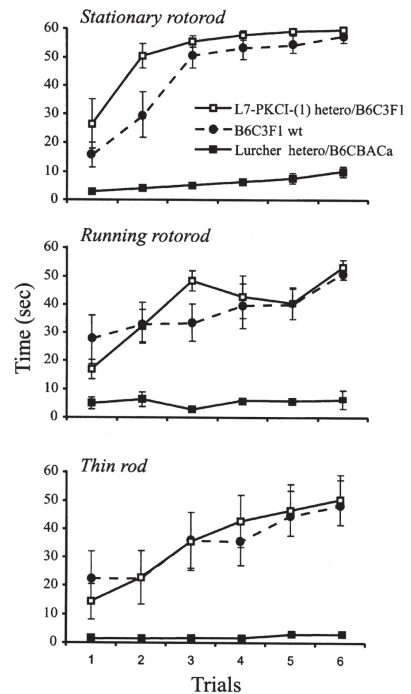


**Figure 3.9** L7-PKCi mice show no general motor coordination deficits. L7-PKCi(1) hetero / B6C3F1 mice (n=8); and B6C3F1 wt littermates (n=10) were put on the stationary rotorod (top), the running rotorod (middle), and the stationary horizontal thin rod (bottom) for a maximum of 60 sec for each trial. In all tests the duration of retention on the apparatus gradually increased over the 6 trials for both groups. In none of the tests did the duration of retention of the L7-PKCi mice differ significantly from the wts. For comparison, the staying duration times of *lurcher* mice, which show severe impairment of motor coordination, have been added.



### 3.5 Discussion

The main finding of this study is that specific expression of a protein kinase C inhibitory peptide in the Purkinje cells of a transgenic mouse (L7-PKCi) resulted in nearly complete suppression of both cerebellar LTD as assessed in culture and adaptation of the VOR in the intact, behaving animal. The phenotype of these animals was remarkably delimited. Basal electrophysiological and morphological features of Purkinje cells were unaltered (with one notable exception discussed below). Likewise, these mice showed normal motor coordination as measured by their ability to display normal eye movement reflexes (OKR and VOR) as well as by several tests of gross motor coordination (rotorod, thin rod). Their behavioral deficit appeared to be limited to a particular form of motor learning: adaptation of the VOR. While there are a number of important limitations to the interpretation of this finding, we believe that it stands as the most compelling evidence to date in favor of the hypothesis that cerebellar LTD is necessary for this form of motor learning.

To control for the effects of genetic background and insertion site, electrophysiological measurements were made using mice constructed in two different genetic backgrounds, B6C3F1 hybrid and FVB/N inbred strains, using two independently derived transgenic lines, 1 and 31. In spite of the fact that line 31 expressed the L7-PKCi product at about 30% of the level of line 1, similar results were found in terms of our electrophysiological index of PKC inhibition (attenuation of the effect of phorbol ester on voltage-gated  $K^+$  currents, Figure 4). These values were slightly, although not significantly, higher than that produced by a saturating concentration of an exogenous PKC inhibitor (chelerythrine, 10  $\mu$ M). This suggests that the concentrations of PKCI produced in the Purkinje cells of both line 1 and line 31 mice are likely to be saturating. No significant differences were seen between L7-PKCi mice as a function of the line or genetic background. These include the amplitude of LTD, several basal properties of Purkinje cells, as well as depolarization- and mGluR-evoked Ca transients. Interestingly, the suppression of LTD in cultured Purkinje cells from L7-PKCi-(1) homozygous / FVB/N mice was slightly more complete than that in cells from L7-PKCi-(1) heterozygous / FVB/N mice. It is unclear if this is related to expression levels of the PKCI peptide or more complex side-effects.

The most salient aspect of the present behavioral analysis is the specificity of the phenotype in the L7-PKCi mice; VOR adaptation was robustly affected, whereas the general eye movements and general motor performance were not impaired. When the visuo-vestibular training was done at a relatively high frequency, as in the present study (cf. Koekkoek et al., 1997), the VOR adaptation in wild type mice was frequency specific. This frequency specific adaptive effect has also been described for higher mammals such as cats and primates (Lisberger et al., 1983; Powell et al., 1991). This specificity of VOR adaptation might possibly be related to the fact that LTD is restricted to those parallel fiber-Purkinje cell synapses that were activated during LTD induction (Ekerot and Kano, 1985; Linden, 1994; but see Hartell, 1996). Certain mossy fibers and parallel fibers may very well be clustered in groups that carry particular head velocity signals, so that LTD will only occur at the Purkinje cell dendritic sites that are innervated by those parallel fibers activated under the stimulus frequency used for the training. This is consistent with the "flocculus hy-

pothesis” of Ito (1982) and co-workers.

While the main finding of this study is that specific blockade of cerebellar LTD correlates with specific blockade of VOR adaptation, it is also useful to consider the range of motor behaviors that remain intact when cerebellar LTD is blocked. The fact that the initial gain values of the L7-PKCi mice during all protocols, i.e. OKR, VOR in the light, and VOR in the dark, were normal, indicates that cerebellar LTD is not necessary for normal eye movement performance. Apparently, there is sufficient plasticity in the brainstem of the L7-PKCi mouse to obtain normal gain values when prolonged periods of training are available (Khater et al., 1993; Lisberger, 1994). Therefore, we hypothesize that it is only when the VOR adaptation has to occur rapidly (in our protocol, one hour), that PKC activity and LTD are necessary. Similarly, the general motor performance as revealed by initial performance in the rotorod and thin rod tests is not affected even though LTD is abolished. Thus, in contrast to previous reports (e.g. Aiba et al., 1994), it is unlikely that a lack of LTD can explain cerebellar ataxia. Furthermore, L7-PKCi animals improve with repeated trials of these tasks in a manner that is indistinguishable from wild type controls. Thus, these forms of motor learning are unlikely to require cerebellar LTD. It will be useful to expand the behavioral analysis to other motor learning tasks, particularly associative eyeblink conditioning.

The role of LTD in cerebellar motor learning, as proposed in the Marr-Albus-Ito theories has remained controversial (Llinás, 1981; Lisberger, 1988; De Schutter, 1995 and 1997; Simpson et al., 1996; Llinás et al., 1997). This debate is partly due to the fact that lesion studies have often been difficult to interpret. For example, lesions of the flocculus of the vestibulocerebellum, which is the region controlling compensatory eye movements, do not only affect VOR adaptation, but also the general eye movement performance such as its phase dynamics or latencies (Robinson, 1976; Zee et al., 1981; Ito et al., 1982; Nagao, 1983; Koekkoek et al., 1997). Similarly, although homologous recombination knockout technology has made it possible to test the role of various signaling molecules in cerebellar LTD, it has been difficult to rule out contributions from non-cerebellar systems or from multiple neuronal types within the cerebellum to behavioral phenotypes. For example, while mice null for the genes encoding mGluR1 (Aiba et al., 1994; Conquet et al., 1994), GluR $\delta$ 2 (Funabiki et al., 1995; Kashiwabuchi et al., 1995) and glial fibrillary acidic protein (Shibuki et al., 1996) all showed impaired cerebellar LTD and motor learning, the first two showed motor coordination deficits when the last did not. In none of these mutants was the cerebellar cortex the only brain location modified. Thus, mechanical and/or genetic lesion studies often result in conflicting behavioral deficits that may be explained by the complexity of cellular targets.

Another problem that has hindered investigations on the role of LTD in cerebellar motor learning is isotypic compensation. In this respect the PKC $\gamma$  knockout mouse is probably the most relevant. Despite the abundance of PKC $\gamma$  in Purkinje cells, neither LTD induction nor associative eyeblink conditioning are impaired in these knockout mice (Kano et al., 1995). This fact may be due to compensation by one or more of the five other PKC isoforms (PKC $\alpha$ ,  $\beta$ I,  $\delta$ ,  $\epsilon$  and  $\zeta$ ) that have been reported by various laboratories to occur in Purkinje cells (Young, 1988; Shimohama et al.,



1990; Wetsel et al., 1992; Chen and Hillman, 1993; Merchenthaler et al., 1993; Garcia and Harlan, 1997).

While these two major difficulties may have been alleviated in L7-PKCi mice, there are several caveats that should be sounded about the interpretation of the present results. First, while expression of the L7-PKCi transcript could be detected using *in situ* hybridization only in cerebellar Purkinje cells, it is possible that it is expressed at very low levels in other regions as well. For example, the endogenous L7 gene is also expressed in retinal bipolar neurons (Oberdick et al., 1990). However, because L7-driven transgene expression in the retina is only rarely observed using the L7 $\Delta$ AUG vector (unpublished observations), L7-PKCi expression in the retina of both lines reported here is undetectable, and the optokinetic responses of transgenics were totally normal, this possibility is remote. Second, it cannot be absolutely determined whether the blockade of LTD in the L7-PKCi mouse results directly from inhibition of PKC. While strong expression of the PKCi transcript is found in Purkinje cells, and while voltage-gated K<sup>+</sup> currents in L7-PKCi Purkinje cells show the same response to a PKC activator as do wt Purkinje cells treated with an exogenously applied PKC inhibitor, the PKCi effect could be mediated by a secondary pathway not considered in this report (e.g., the NO/cGMP cascade, Lev-Ram et al., 1997; see Linden, 1996 for review). Third, the one basal physiological abnormality that we have found in L7-PKCi mice is that about 50% of the Purkinje cells show a persistent multiple climbing fiber innervation, raising the possibility that this could be a cause of their failure to demonstrate VOR adaptation. We believe this to be unlikely because the PKC $\gamma$  knockout mouse shows multiple climbing fiber innervation with normal cerebellar LTD and no motor learning deficit (Chen et al., 1995; Kano et al., 1995). Finally, while our search for basal abnormalities in the physiology and anatomy of the cerebellar cortex has been extensive, many of the experiments have been performed in a culture system, which limits the type of information obtained. It will be instructive to measure some physiological parameters of Purkinje cells (simple and complex spike firing rates, for example) *in situ*, particularly in the behaving animal.

Persistent innervation of Purkinje cells by multiple climbing fibers is a phenotype which is found in a fairly large number of both naturally occurring and induced mutant mice. In the PKC $\gamma$  knockout mouse, this abnormality results from a diminished regression of multiple climbing fiber innervation in the third postnatal week (Kano et al., 1995), which is when PKC $\gamma$  expression in Purkinje cells reaches its highest level (Yoshida et al., 1988; Huang et al., 1990). It was also noted that the number of parallel fibers innervating Purkinje cells in PKC $\gamma$  mice is normal. This is different from spontaneous mutants such as the *weaver* (Crepel and Mariani, 1979), *reeler* (Mariani et al., 1977), and *staggerer* mutant mice (Crepel et al., 1980), as well as the GluR $\delta$ 2 knockout mouse (Kashiwabuchi et al., 1995) in which the number of parallel fibers is substantially reduced. These observations led Kano et al. (1995) to propose that PKC $\gamma$  may act as a downstream element in the signal cascade inside Purkinje cells necessary for the elimination of surplus climbing fiber synapses. The present observation, that chronic inhibition of PKC in Purkinje cells leads to persistent multiple climbing fiber innervation of Purkinje cells without affecting the morphology of

parallel fiber input, is consistent with this hypothesis.

The level of multiple climbing fiber innervation in adult L7-PKCi mice is comparable to that of adult PKC $\gamma$  mutants. In adult L7-PKCi mice 47% of the Purkinje cells are innervated by two climbing fibers, while in the PKC $\gamma$  knock out 41% of the Purkinje cells are innervated by two or three (<5%) climbing fibers (Kano et al., 1995). The persistent multiple climbing fiber innervation in PKC $\gamma$  mutant mice has been suggested to underlie their impaired motor coordination (Chen et al., 1995). This association is supported by reports of impaired motor coordination in mGluR1 (Aiba et al., 1994; Conquet et al., 1994) and GluR $\delta$ 2 (Kashiwabuchi et al., 1995) mutant mice, in which, respectively, 25% and 46% of the Purkinje cells receive a multiple climbing fiber innervation. Conversely, glial fibrillary acidic protein knockout mice, which have impaired cerebellar LTD, show normal mono climbing fiber innervation and motor coordination (Shibuki et al., 1996). However, the present study demonstrates that a persistent multiple climbing fiber innervation does not necessarily result in impaired motor coordination. The adult L7-PKCi mutant mice do not show any sign of ataxia, and they display normal motor coordination skills in two different sets of tests, the eye movement tests and the rotarod / thin rod tests. One of the reasons for this discrepancy may be related to the fact that the other induced mutants are global knock outs, in which brain locations other than the cerebellar Purkinje cell are affected. For example, PKC $\gamma$  is also expressed in the hippocampus, amygdala, and cerebral cortex (Huang et al., 1989), GluR $\delta$ 2 is also expressed in the cingulate cortex and hippocampus (Lomeli et al., 1993), and mGluR1 is also expressed in the olfactory bulb, hippocampus, lateral septum, thalamus, globus pallidus, preoptic nucleus, substantia nigra, dorsal cochlear nucleus, striatum, islands of Calleja, cerebral cortex, mammillary nuclei, red nucleus, and superior colliculus (Shigemoto et al., 1992). Thus, it is likely that the defects in motor coordination seen in these global knockouts are not solely a result of multiple climbing fiber innervation, and may reflect dysfunction in other brain regions. Another explanation for the robust motor coordination deficits in mice deficient in mGluR1 or GluR $\delta$ 2 could be that their Purkinje cells have additional intrinsic deficits apart from the multiple climbing fiber innervation. However, it should be cautioned that rotarod/ thin rod tests do not comprise a complete assay of motor coordination. While performance of GluR $\delta$ 2 and PKC $\gamma$  knock outs versus L7-PKCi mice on these tests are dramatically different, it remains formally possible that there is a more sensitive test that would reveal motor coordination impairments in all three types of animal.

The present strategy has produced a transgenic mouse which bypasses two of the problems inherent in conventional gene knockouts: anatomical specificity and functional compensation from other members of the gene family. Another way to overcome the problem of anatomical specificity has been to use the phage P1-derived Cre/loxP recombination system, which allows the creation of a subregion and cell type restricted gene knockout. This has been demonstrated in a study which examined the role of NMDAR1 receptors of hippocampal CA1 pyramidal cells in the formation of spatial memory (Tsien et al., 1996a,b; Stevens, 1996). However, generating such mutants demands laborious screening of numerous cell lines, and this approach does not reduce the possibility that compensatory mechanisms of other

related genes come into play. Both the present strategy and the Cre/loxP strategy will benefit greatly from coupling to inducible promoters (Mayford et al., 1996), which should attenuate the remaining problem of developmental side-effects.

#### Acknowledgments

The authors would like to thank J. v.d. Burg, R. Hawkins, E. Goedknecht, E. Dalm, D. Gurfel and E. Bugarin for technical assistance, J. Parker-Thornburg for construction of the L7-PKCi transgenic mouse lines, S. Baader for statistical analysis of cerebellar morphology, W. Russo and L. Eastman for animal care, and C. Aizenman and K. Takahashi for useful discussion. This research was supported by the Life Sciences Foundation (SLW; no. 805-33.310-p; C.I.D.Z.), which is subsidized by the Netherlands Organization for Scientific Research (NWO), by a NWO project grant (no. 903-68-361; C.I.D.Z.), by PHS MH51106, the Develbiss Fund, the McKnight Foundation and the National Alliance for Research on Schizophrenia and Depression (D.J.L.), by the Deutsche Forschungsgemeinschaft (C.H.), and by NIH 1RO1NS33114 and NSF IBN-9309611 (J.O).

### 3.6 References

Aiba, A., Kano, M., Chen, C., Stanton, M.E., Fox, G.D., Herrup, K., Zwingman, T.A., and Tonegawa, S. (1994). Deficient cerebellar long-term depression and impaired motor learning in mGluR1 mutant mice. *Cell* 79, 377-388.

Baader, S.L., Sanlioglu, S., Berrebi, A.S., Parker-Thornburg, J., and Oberdick, J. (1997) Ectopic overexpression of Engrailed-2 in cerebellar Purkinje cells causes restricted cell loss and retarded external germinal layer development at lobule junctions. *J. Neurosci.* In press.

Bian, F., Chu, T., Schilling, K., and Oberdick, J. (1996) Differential mRNA transport and the regulation of protein synthesis: selective sensitivity of Purkinje cell dendritic mRNAs to translational inhibition. *Mol. Cell. Neurosci.* 7, 116-133.

Blendy J.A., Kaestner, K.H., Schmid, W., and Schutz, G. (1996) Targeting of the CREB gene leads to up-regulation of a novel CREB mRNA isoform. *EMBO J.* 15, 1098-1106.

Buijs, R.M., Van Vulpen, E.H.S. and Geffard, M., (1987) Ultrastructural localization of GABA in the supraoptic nucleus and the neural lobe. *Neurosci.* 20, 347-355.

Caddy, K.W.T. and Biscoe, T.J. (1979) Structural and quantitative studies on the normal C3H and lurcher mutant mouse. *Phil. Trans. R. Soc. (Lond.)* 287, 167-201.

Chen, C. and Tonegawa, S. (1997) Molecular genetic analysis of synaptic plasticity, activity-dependent neural development, learning and memory in the mammalian brain. *Ann. Rev. Neurosci.* 20, 157-184.

Chen, C., Kano, M., Chen, L., Bao, S., Kim, J.J., Hashimoto, K., Thompson, R.F., and Tonegawa, S. (1995). Impaired motor coordination correlates with persistent multiple climbing fiber innervation in PKC $\gamma$  mutant mice. *Cell* 83, 1233-1242

Chen, S. and Hillman, D. (1993) Compartmentation of the cerebellar cortex by protein kinase C delta. *Neuroscience* 56, 177-188.

Conquet, F., Bashir, Z.I., Davies, C.H., Daniel, H., Ferraguti, F., Bordi, F., Franz-Bacon, K., Reggian, A., Matarrese, V., Conde, F., Collingridge, G.L., and Crépel, F. (1994). Motor deficit and impairment of synaptic plasticity in mice lacking mGluR1. *Nature* 372, 237-242.

Crépel, F., Delhaye-Bouchaud, N., Guastavina, J.M., and Sampaio, I. (1980) Multiple innervation of cerebellar Purkinje cells by climbing fibers in staggerer mutant mouse. *Nature* 283, 483-484.

Crépel, F. and Mariani, J. (1976) Multiple innervation of Purkinje cells by climbing fibers in the cerebellum of the weaver mutant mouse. *J. Neurobiol.* 7, 579-582.

De Schutter, E. (1995) Cerebellar long-term depression might normalize excitation of Purkinje cells: a hypothesis. *Trends Neurosci.* 18, 291-295.

De Schutter, E. (1997) A new functional role for cerebellar long-term depression. *The Cer-*

ebellum: From Structure to Control, De Zeeuw, Strata and Voogd (Eds). Prog. Brain Res. 114, 529-542.

De Zeeuw, C. I., Wylie, D. R., DiGiorgi, P. L. and Simpson, J. I. (1994) Projections of individual Purkinje cells of identified zones in the flocculus to the vestibular and cerebellar nuclei in the rabbit. *J Comp Neurol.* 349, 428-47.

De Zeeuw, C. I., Wylie, D. R., Stahl, J. S. and Simpson, J. I. (1995) Phase relations of Purkinje cells in the rabbit flocculus during compensatory eye movements. *J. Neurophysiol.* 74, 2051-2063.

De Zeeuw, C. I., Koekkoek, S. K. E., Wylie, D. R. W. and Simpson, J. I. (1997) Association between dendritic lamellar bodies and complex spike synchrony in the olivocerebellar system. *J. Neurophysiol.* 77, 1747-1758.

De Zeeuw, C. I., Holstege, J. C., Ruigrok, T. J. and Voogd, J. (1989) Ultrastructural study of the GABAergic, cerebellar, and mesodiencephalic innervation of the cat medial accessory olive: anterograde tracing combined with immunocytochemistry. *J. Comp. Neurol.* 284, 12-35.

Doerner, D., Pitler, T.A. and Alger, B.E. (1988) Protein kinase C activators block specific calcium and potassium current components in isolated hippocampal neurons. *J. Neurosci.* 8, 4069-4078.

Ekerot, C.-F. and Kano, M. (1985) Long-term depression of parallel fibre synapses following stimulation of climbing fibres. *Brain Res.* 342, 357-360.

Farley, J. and Auerbach, S. (1986) Protein kinase C activation induces conductance changes in Hermissenda photoreceptors like those seen in associative learning. *Nature* 319, 220-223.

Funabiki, K., Mishina, M. and Hirano, T. (1995) Retarded vestibular compensation in mutant mice deficient in  $\delta 2$  glutamate receptor subunit. *NeuroReport* 7, 189-192.

Garcia, M.M. and Harlan, R.E. (1997) Protein kinase C in central vestibular, cerebellar, and precerebellar pathways of the rat. *J. Comp. Neurol.* 385, 26-42

Grega, D.S., Werz, M.A., Macdonald, R.L. (1987) Forskolin and phorbol esters reduce the same potassium conductance of mouse neurons in culture. *Science* 235, 345-348.

Hartell, N.A. (1996) Strong activation of parallel fibers produces localized calcium transients and a form of LTD that spreads to distant synapses. *Neuron* 16, 601-610.

Highstein, S. M., Partsalis, A. and Arian, R. (1997) Role of the Y-group of the vestibular nuclei and flocculus of the cerebellum in motor learning of the vestibulo-ocular reflex. *The Cerebellum: From Structure to Control*, De Zeeuw, Strata and Voogd (Eds). Prog. Brain Res. 114, 383-401.

House, C. and Kemp, B.E. (1987) Protein kinase C contains a pseudosubstrate prototope in its regulatory domain. *Science* 238, 1726-1728.

Huang, F.L., Yoshida, Y., Nakabayashi, H., Friedman, D.P., Ungerleider, L.G., Young, W.S. 3d., and Huang, K.P. (1989) Type I protein kinase C isozyme in the visual-information-processing pathway of monkey brain. *J. Cell. Biochem.* 39, 401-10.

Huang, F.L., Young, W.S.3d., Yoshida, Y., and Huang, K.P. (1990) Developmental expression of protein kinase C isozymes in rat cerebellum. *Dev. Brain Res.* 52, 121-130.

Hummler E., Cole, T.J., Blendy, J.A., Ganss, R., Aguzzi, A., Schmid, W., Beermann, F., and Schutz, G. (1994) Targeted mutation of the CREB gene: compensation within the CREB/ATF family of transcription factors. *Proc. Natl. Acad. Sci. USA.* 91(12), 5647-5651.

Ito, M. (1982). Cerebellar control of the vestibulo-ocular reflex-around the flocculus hypothesis. *Ann. Rev. Neurosci.* 5, 275-296.

Ito, M., Jastreboff, P. J. and Miyashita, Y. (1982) Specific effects of unilateral lesions in the flocculus upon eye movements in albino rabbits. *Exp. Brain Res.* 45, 233-42.

Ito, M. (1989). Long-term depression. *Ann. Rev. Neurosci.* 12, 85-102.

Jande, S.S., Maler, L., and Lawson, D.E.M. (1981) Immunohistochemical mapping of vitamin D-dependent calcium-binding protein in brain. *Nature* 294, 765-767.

Kano, M., Hashimoto, K., Chen, C., Abeliovich, A., Aiba, A., Kurihara, H., Watanabe, M., Inoue, Y.L., and Tonegawa, S. (1995). Impaired synapse elimination during cerebellar development in PKC $\gamma$  mutant mice. *Cell* 83, 1223-1231.

Kano, M., Hashimoto, K., Kurihara, H., Watanabe, M., Inoue, Y., Aiba, A. and Tonegawa, S. (1997). Persistent multiple climbing fiber innervation of cerebellar Purkinje cells in mice lacking mGluR1. *Neuron* 18, 71-79.

Kashiwabuchi, N., Ikeda, K., Araki, K., Hirano, T., Shibuki, K., Takayama, C., Inoue, Y., Kutsuwada, T., Yagi, T., Kang, Y., Aizawa, S., and Mishina, M. (1995). Impairment of motor coordination, Purkinje cell synapse formation, and cerebellar long-term depression in GluR $\delta$ 2 mutant mice. *Cell* 81, 245-252.

Khater, T. T., Quinn, K. J., Pena, J., Baker, J. F. and Peterson, B. W. (1993) The latency of the cat vestibulo-ocular reflex before and after short- and long-term adaptation. *Exp. Brain Res.* 94, 16-32.

Koekkoek, S.K.E., A.M. v. Alphen, N. Galjart, J. v.d. Burg, F. Grosveld, and C.I. De Zeeuw (1997) Gain adaptation and phase dynamics of compensatory eye movements in mice. *Genes and Function.* 1, 175-190.

Konnerth, A., Dreessen, J., and Augustine, G.J. (1992) Brief dendritic calcium signals initiate long-lasting synaptic depression in cerebellar Purkinje cells. *Proc. Natl. Acad. Sci.* 89, 7051-7055.

Krupa, D. J., Thompson, J. K. and Thompson, R. F. (1993) Localization of a memory trace in the mammalian brain. *Science.* 260, 989-91.

Leclerc, N., Schwarting, G.A., Herrup, K., Hawkes, R., and Yamamoto, M. (1992) Compartmentation in mammalian cerebellum: Zebrin II and P-path antibodies define three classes of sagittally organized bands of Purkinje cells. *Proc. Natn. Acad. Sci USA* 89, 5006-5010.

Lev-Ram, V., Jiang, T., Wood, J., Lawrence, D.S., and Tsien, R.Y. (1997) Synergies and coincidence requirements between NO, cGMP, and Ca<sup>2+</sup> in the induction of cerebellar long-term depression. *Neuron* 18, 1025-1038.

Linden, D.J. (1994) Input-specific induction of cerebellar long-term depression does not require presynaptic alteration. *Learning & Memory* 1, 121-128.

Linden, D.J. (1996). Cerebellar long-term depression as investigated in a cell culture preparation. *Behav. and Brain Sci.* 19, 339-346 & 482-487.

Linden, D.J., and Connor, J.A. (1991). Participation of postsynaptic PKC in cerebellar long-term depression in culture. *Science* 254, 1656-1659.

Linden, D.J., and Connor, J.A. (1995). Long-term synaptic depression. *Ann. Rev. Neurosci.* 18, 319-357.

Linden, D.J., Dawson, T.M. and Dawson, V.L. (1995). An evaluation of the nitric oxide/ cGMP/ cGMP-dependent protein kinase cascade in the induction of cerebellar long-term depression in culture. *J. Neurosci.* 15, 5098-5105.

Linden, D.J., Dickinson, M.H., Smeyne, M., and Connor, J.A. (1991). A long-term depression of AMPA currents in cultured cerebellar Purkinje neurons. *Neuron* 7, 81-89.

Linden DJ., Smeyne M., Sun SC., and Connor JA. (1992) An electrophysiological correlate of protein kinase C isozyme distribution in cultured cerebellar neurons. *J. Neurosci.* 12, 3601-3608.

Lisberger, S.G. (1988) The neural basis for learning of simple motor skills. *Science* 242, 728-735.

Lisberger, S. G. (1994) Neural basis for motor learning in the vestibuloocular reflex of primates. III. Computational and behavioral analysis of the sites of learning. *J Neurophysiol.* 72, 974-98.

Lisberger, S. G., Miles, F. A. and Optican, L. M. (1983) Frequency-selective adaptation: evidence for channels in the vestibulo-ocular reflex? *J. Neurosci.* 3, 1234-44.

Llinás, R., Lang, E.J. and Welsh, J.P. (1997) The cerebellum, LTD. and memory: alternative views. *Learning & Memory* 3, 445-455.

Lomeli, H., Sprengel, R., Laurie, D.J., Kohr, G., Herb, A., Seeburg, P., Wisden, W. (1993) The rat delta-1 and delta-2 subunits extend the excitatory amino acid receptor family. *FEBS Lets.* 315, 318-322.

Mariani, J., Crépel, F., Mikoshiba, K., Changeux, J.P., and Sotelo, C. (1977) Anatomical,



physiological, and biochemical studies of the cerebellum from reeler mutant mouse. *Phil. Trans. R. Soc. Lond.* 281, 1-28.

Mayford, M., Bach, M.E., Huang, Y.-Y., Wang, L., Hawkins, R.D. and Kandel, E.R. (1996). Control of memory formation through regulated expression of a CaMKII transgene. *Science* 274, 1678-1683.

Merchenthaler, I., Liposits, Z., Reid, J.J. and Wetsel, W.C. (1993) Light and electron microscopic immunocytochemical localization of PKC $\gamma$  immunoreactivity in the rat central nervous system. *J. Comp. Neurol.* 336, 378-399.

Nagao, S. (1983) Effects of vestibulocerebellar lesions upon dynamic characteristics and adaptation of vestibulo-ocular and optokinetic responses in pigmented rabbits. *Exp. Brain Res.* 53, 36-46.

Narasimhan, K. and Linden, D.J. (1996) Defining a minimal computational unit for cerebellar long-term depression. *Neuron* 17, 333-341.

Newton, A.C. (1995) Protein kinase C: structure, function, and regulation. A Minireview. *J. Biol. Chem.* 270, 28495-28498.

Oberdick, J., Levinthal, F., and Levinthal, C. (1988) A Purkinje cell differentiation marker shows a partial sequence homology to the cellular *sis*/PDGF2 gene. *Neuron* 1, 367-376.

Oberdick, J., Smeyne, R.J., Mann, J.R., Zackson, S., and Morgan, J.I. (1990) A promoter that drives transgene expression in cerebellar Purkinje and retinal bipolar neurons. *Science* 248, 223-226.

Oberdick, J., Schilling, K., Smeyne, R.J., Corbin, J.G., Bocchiaro, C., and Morgan, J.I. (1993) Control of segment-like patterns of gene expression in the mouse cerebellum. *Neuron* 10, 1007-1018.

Pastor, A. M., de la Cruz, R. R., and Baker, R. (1994) Cerebellar role in adaptation of the goldfish vestibuloocular reflex. *J. Neurophysiol.* 72, 1383-94.

Powell, K.D., Quinn, K.J., Rude, S.A., Peterson, B.W., and Baker, J.F. (1991) Frequency dependence of cat vestibulo-ocular reflex direction adaptation: single frequency and multi-frequency rotations. *Brain Research.* 550, 137-141.

Raymond, J.L., Lisberger, S.G and Mauk, M.D. (1996) The cerebellum: a neuronal learning machine? *Science* 272, 1126-1131.

Robinson, D. A. (1976) Adaptive gain control of vestibuloocular reflex by the cerebellum. *J. Neurophysiol.* 39, 954-969.

Sakurai, M. (1990) Calcium is an intracellular mediator of the climbing fiber in induction of cerebellar long-term depression. *Proc. Natl. Acad. Sci. USA* 87, 3383-3385.

Schilling, K., Dickinson, M., Connor, J.A. and Morgan, J.I. (1991). Electrical activity in cerebellar cultures determines Purkinje cell dendritic growth patterns. *Neuron* 7, 891-902.

- Schilling, K., Schmidt, H.H.H.W., and Baader, S.L. (1994) Nitric oxide synthase expression reveals compartments of cerebellar granule cells and suggests a role for mossy fibers in their development. *Neuroscience* 59, 893-903.
- Shibuki, K., Gomi, H., Chen, L., Bao, S., Kim, J. J., Wakatsuki, H., Fujisaki, T., Fujimoto, K., Katoh, A., Ikeda, T., Chen, C., Thompson, R. F. and Itohara, S. (1996) Deficient cerebellar long-term depression, impaired eyeblink conditioning, and normal motor coordination in GFAP mutant mice. *Neuron*. 16, 586-599.
- Shigemoto, R., Abe, T., Nomura, S., Nakanishi, S., and Hirano, T. (1994) Antibodies inactivating mGluR1 metabotropic glutamate receptor block long-term depression in cultured Purkinje cells. *Neuron* 12, 1245-1255.
- Shimohama, S., Saitoh, T. and Gage, F.H. (1990) Differential expression of protein kinase C isozymes in rat cerebellum. *J. Chem. Neuroanat.* 3, 367-375.
- Simpson, J. I., Wylie, D. R. and De Zeeuw, C. I. (1996) On climbing fiber signals and their consequence(s). *Behav Brain Sciences*. 19, 380-394.
- Smeyne, R.J., Chu, T., Lewin, A., Bian, F., Sanlioglu, S., Kunsch, C., and Oberdick, J. (1995) Local control of granule cell generation by cerebellar Purkinje cells. *Mol. Cell. Neurosci.* 6: 230-251.
- Stevens, C.F. (1996) Spatial learning and memory: the beginning of a dream. *Cell* 87, 1147-1148.
- Thompson, R.F., and Krupa, D.J. (1994). Organization of memory traces in the mammalian brain. *Ann. Rev. Neurosci.* 108, 44-56.
- Tsien, J.Z., Huerta, P.T. and Tonegawa, S. (1996a) The essential role of hippocampal CA1 NMDA receptor-dependent synaptic plasticity in spatial memory. *Cell* 87, 1327-1338.
- Tsien, J.Z., Chen, D.F., Gerber, D., Tom, C., Mercer, E.H., Anderson, D.J., Mayford, M., Kandel, E.R. and Tonegawa, S. (1996b) Subregion- and cell type-restricted gene knockout in mouse brain. *Cell* 87, 1317-1326.
- Voogd, J. and Bigaré, F. (1980) Topographical distribution of olivary and cortico nuclear fibers in the cerebellum: a review. In *The inferior Olivary Nucleus: Anatomy and Physiology*, J. Courville, ed., Raven Press, NY. pp. 207-235.
- Wetsel, W.C., Khan, W.A., Merchenthaler, I., Rivera, H., Halpern, A.E., Phung, H.M., Nego-Vilar, A. and Hannun, Y.A. (1992) Tissue and cellular distribution of the extended family of protein kinase C isozymes. *J. Cell Biol.* 117, 121-133.
- Yeo, C.H., Hardiman, M.J., and Glickstein, M. (1985) Classical conditioning of the nictitating membrane response of the rabbit: 1. Lesions of the cerebellar nuclei. *Exp. Brain Res.* 60:87-98.
- Yoshida, Y., Huang, F.L., Nakabayashi, H., and Huang, K.P. (1988) Tissue distribution and

developmental expression of protein kinase C isozymes. *J. Biochem. Chem.* 20, 9868-9873.

Young, W.S. III (1988) Expression of three (and a putative four) protein kinase C genes in brains of rat and rabbit. *J. Chem. Neuroanat.* 1, 177-194.

Zee, D. S., Yamazaki, A., Butler, P. H. and Gucer, G. (1981) Effects of ablation of flocculus and paraflocculus of eye movements in primate. *J. Neurophysiol.* 46, 878-99.

# Chapter 4

## Cerebellar LTD and Learning-Dependent Timing of Conditioned Eyelid Responses

S.K.E. Koekkoek, H.C. Hulscher, B.R. Dortland, R.A. Hensbroek,  
Y.Elgersma, T.J.H. Ruigrok, C.I.De Zeeuw

*Department of Neuroscience, Erasmus University Rotterdam, 3000 DR, Rotterdam, The Netherlands.*

received 24 June 2003; accepted 6 August 2003

- *Science* 301: 1736-1739, 2003

## 4.1 Abstract

Mammals can be trained to make a conditioned movement at a precise time, which is correlated to the interval between the conditioned stimulus and unconditioned stimulus during the learning. This learning-dependent timing has been shown to depend on an intact cerebellar cortex, but which cellular process is responsible for this form of learning remains to be demonstrated. Here, we show that protein kinase C–dependent long-term depression in Purkinje cells is necessary for learning-dependent timing of Pavlovian conditioned eyeblink responses.

## 4.2 Introduction

Precise timing of movements is crucial for survival, and the central nervous system continuously tries to optimize this timing. Timing of movements can be learned, for example, by conditioning an eyelid response to a conditioned stimulus (CS), such as a tone, which continues until an unconditioned stimulus (US), such as an electrical shock or a corneal air puff, ceases. In this paradigm, the timing of the eyelid response is ultimately determined by the interstimulus interval (ISI) between the onset of the CS and the onset of the US. The exact timing of conditioned responses depends on plasticity in the cerebellar cortex (1–3). Yet, it is not clear which cellular processes are responsible for the timing properties of conditioned responses. Several mutant mice have been bred in which induction of long-term depression (LTD) (4) at the parallel fiber–Purkinje cell synapse is impaired, but so far it has not been possible to investigate whether this form of LTD contributes to learning-dependent timing (5–7). The deficit in these mutants either was not cell-specific or was contaminated by aberrations in motor performance, and/or the temporospatial resolution of the eyelid recording method was insufficient to detect timing differences in mice. Here, we used transgenic mice in which parallel fiber LTD is impaired in Purkinje cells *in vitro* and *in vivo* by the inhibition of protein kinase C (PKC) and in which no motor performance or excitability deficits have been detected (L7-PKCi mutants) (8–10). We subjected wild-type mice and the transgenic mice to a novel method of eyelid recording, the magnetic distance measurement technique (11). This method allows us to determine accurately the position of the eyelid of a mouse over time by generating a local magnetic field that moves with the eyelid and that is picked up by an aligned field–sensitive chip while the animal is freely moving.

## 4.3 Methods

Adult L7-PKCi mutants (C57/Bl6 background;  $n = 24$ ) and wild-type littermates ( $n = 24$ ) were anesthetized with an oxygenated mixture of nitrous oxide and halothane, and a premade connector (SamTec; [www.samtec.com](http://www.samtec.com)) was placed with a pedestal of dental cement on the skull. A magnet embedded in silicon was implanted in a pocket dissected in the eyelid and a giant magnetoresistive sensor chip (NVE; [www.nve.com](http://www.nve.com)) was placed over the upper eyelid

such that the distance between the magnet and sensor was 2 mm when the eyelid was closed and the axis of sensitivity was aligned with the north-south axis of the magnet when the eyelid was halfway closed. Two insulated copper wires with a diameter

94

of 30  $\mu\text{m}$  were placed underneath the skin that was close to the lateral corner of the eyelids to provide the US. The US electrodes were connected to computer controlled stimulus-isolation units (Dagan S910; www.dagan.com), which created biphasic constant-current electrical shocks (30 ms, 166-Hz pulses). The strength of the shocks was controlled by an unconditioned response– based feedback mechanism (with a maximum shock strength of 1 mA) to prevent fear-conditioned responses (11). The eyelid responses of the wild-type mice and L7-PKCi mutants were conditioned to a tone as the CS (10 kHz, gradually increased over 40 ms to 78 dB) during daily training sessions of 10 blocks of 10 trials. The blocks consisted of 1 US-alone trial, 8 paired trials, and 1 CS-alone trial, and the trials were separated by a random intertrial interval in the range of 20 to 40 s (11). In the first group of experiments, the onsets of the CS and US were separated by an ISI of 350 ms.

#### 4.4 Results

After four paired training sessions (T-1 to T-4) the percentage of conditioned responses, their average peak amplitude, and their average peak velocity in wild types reached levels of 80%, 0.68 mm, and 32.6 mm/s, respectively, whereas those in LTD-deficient mice had values of only 30%, 0.44 mm, and 19.6 mm/s, respectively (Fig. 4.1 and 4.2).

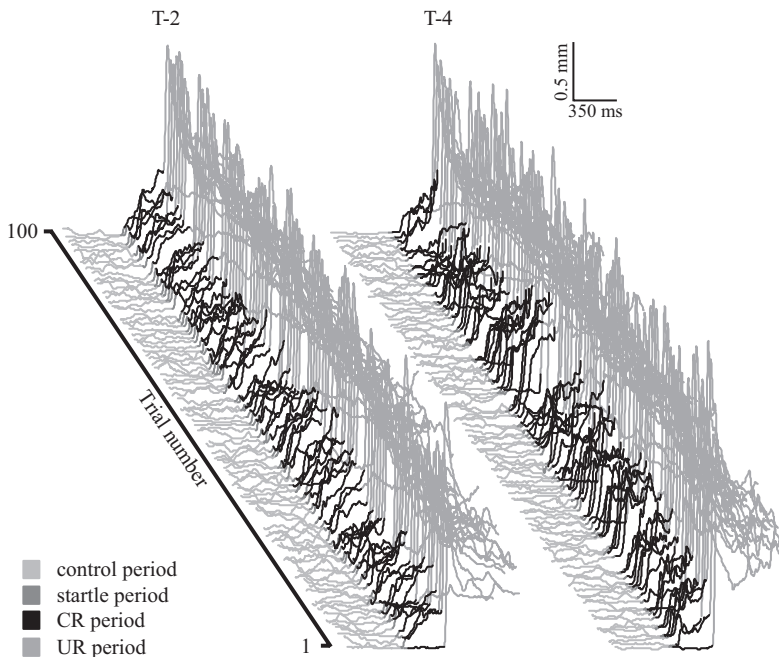


**Figure 4.1.** Average data sets for training sessions T-2 and T-4, in which each trace represents the response of wild-type (wt) animals for a particular trial.

All of these values were significantly different ( $P < 0.01$  for all three values; multivariate analysis of variance (MANOVA) for repeated measures; adjusted for multiple

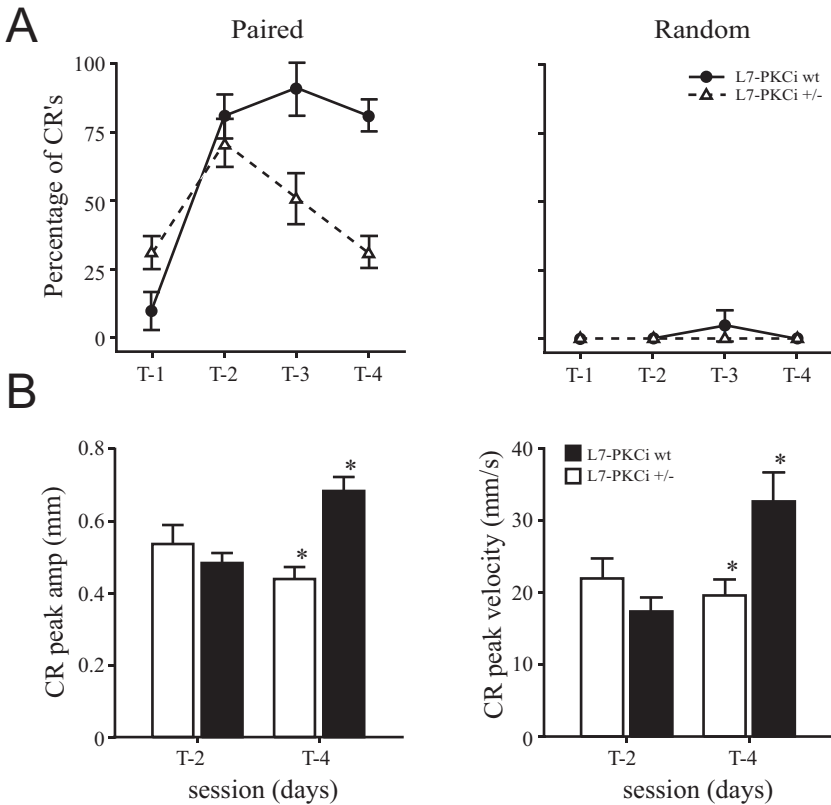


**Figure 4.2. Blockage of LTD in L7-PKCi mutants leads to a reduced rate of conditioned responses and a reduced peak amplitude and peak velocity after four daily training sessions (T-1 to T-4).** (A) The mean percentages ( $\pm$ SEM) of significant CRs over four days of either paired (left) or unpaired (right) training for L7-PKCi transgenic mice and their wild-type littermates ( $n = 10$  and  $n = 5$  in both groups for paired and unpaired training, respectively). (B) As compared with L7-PKCi mutants, wild-type animals showed a significantly increased peak amplitude ( $P < 0.01$ ; \* in left panel) and a significantly increased peak velocity ( $P < 0.01$ ; \* in right panel) at T-4 but not at T-2.

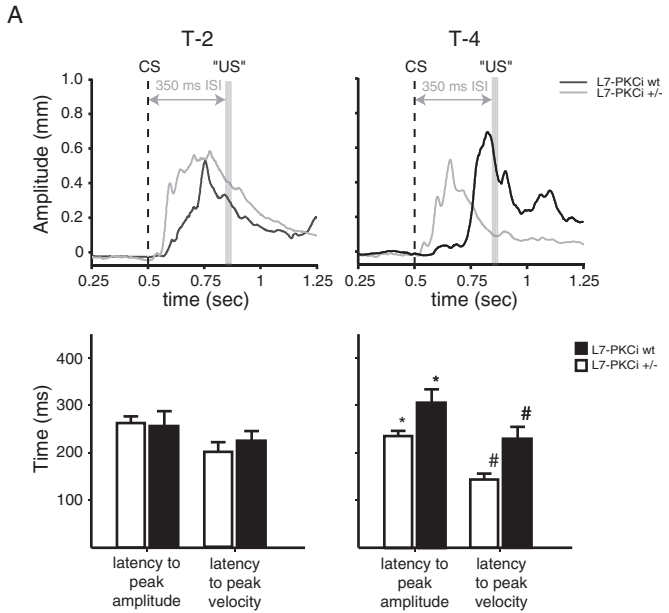
comparisons by Bonferroni correction). The percentage of conditioned responses and the peak amplitude and peak velocity in the mutants were not significantly different from those of wild types during the first two training sessions. When the CS and US were randomly paired instead of paired with a fixed ISI, neither the wild types nor the mutants showed a significant increase of conditioned responses during the training. After three subsequent daily extinction sessions, all conditioned responses disappeared in the wild-type and LTD deficient mice.

The timing properties of the conditioned responses showed the same pattern as the rate of conditioning. Although the latency to the peak of the amplitude of the conditioned eyelid response in wild types was still indistinguishable from that of the mutant after the second training session T-2, it was significantly longer than that of the mutant at T-4 ( $P < 0.05$ ; MANOVA) (Fig. 3.2-3A). The same relation held true for the latency to the peak of the velocity of the conditioned eyelid response ( $P < 0.01$ ; MANOVA). When the training sessions were continued for another 2 days, the timing of the conditioned responses in the mutant did not improve (the intervals between the peak amplitude and the US on day 5 and day 6 remained as high as

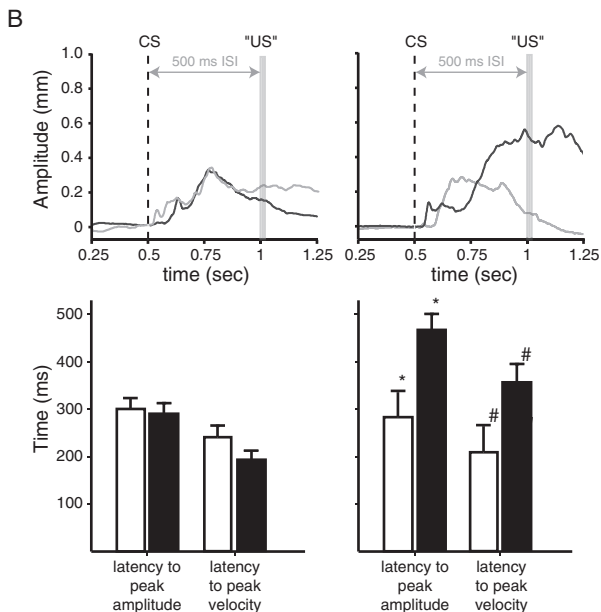


243 and 259 ms, respectively). Moreover, the timing of the remaining conditioned responses in wild types during extinction sessions gradually returned to baseline levels, whereas those in the mutants remained fixed. Thus the timing of the eyelid response of wild types can be optimized effectively by training such that the peak is at the moment of the US onset, whereas that of LTD-deficient mutants is fixed during both conditioning and extinction. The latencies to the onset of the eyelid responses were not influenced by the training. If the timing is LTD-dependent, then the latencies to peak amplitude and peak velocity in the L7-PKCi mutant should not be

**Figure 4.3 Blockage of LTD in L7-PKCi mutants prevents learning dependent timing.** (A) Examples of average data sets for training sessions T-2 and T-4, showing the average CS-alone responses of a wild-type animal (black) and a L7-PKCi mutant (grey) (top). At T-4 but not at T-2, the wild-type animal shows well-timed responses around the moment when the US is supposed to take place. In contrast, the peak of the response of the LTD-deficient L7-PKCi mutant remains fixed in time over the training sessions. The average latencies to peak amplitude and peak velocity do not differ between wild types and mutants at T-2, but both values differ significantly at T-4 ( $P < 0.05$  and  $0.01$ , indicated by \* and #, respectively; bars represent mean and SEM;  $n = 10$  for both groups) (bottom).



(B) When the CS-US interval is extended to 500 ms, the wild types (black) but not the mutants (grey) adapt the timing of their conditioned eyelid responses accordingly (top). Similar to the responses with an ISI of 350 ms, wild types and transgenics show responses with comparable timing characteristics at T-2 (left), whereas the latency to peak amplitude and latency to peak velocity of their responses are significantly different at T-4 ( $P < 0.02$  and  $P < 0.05$ , indicated by \* and #, respectively) (right). Bars represent mean and SEM ( $n = 3$  for both groups).



influenced by the length of the ISI. Indeed, increasing the ISI from 350 to 500 ms did not significantly elevate the mutants' latency to peak amplitude or to peak velocity ( $P < 0.93$  for both values; MANOVA) at T-4 (Fig. 4.3B).

In contrast, the same increase of the ISI in wild types robustly increased their average latency to peak amplitude by 167 ms and increased their latency to peak velocity by 141 ms ( $P < 0.02$  and  $P < 0.05$ , respectively; MANOVA). These data show that well-timed eyelid movements can be learned in wild-type mice but not in mice in which cerebellar LTD is blocked by the inhibition of PKC. Yet, to draw the conclusion that cerebellar LTD contributes to learning-dependent timing, it has to be shown that part of the learning that occurs in the L7-PKCi mutant does indeed have a cerebellar origin and that the well-timed components of the eyelid movements in wild types cannot occur without an intact cerebellum. We therefore investigated the conditioned responses in mutants and wild types in which the anterior interposed cerebellar nuclei were lesioned bilaterally with the use of pressure injections of 200 mmol of N-methyl-Daspartate after they were trained. Although the number of responses was substantially reduced, both the L7-PKCi mutants and the wild types displayed remnant conditioned responses after the lesions (Figure 4.4). However, the peak amplitudes were significantly reduced in both groups ( $P < 0.01$  and  $P < 0.05$  for wild types and mutants, respectively). Moreover, the mean latencies to peak amplitude and peak velocity were significantly reduced in the wild types ( $P < 0.005$ ).

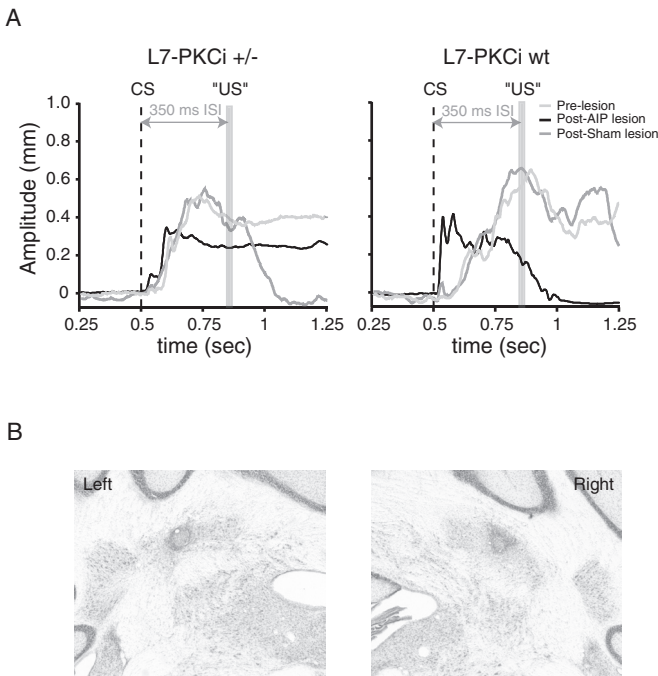


**Figure 4.4 CR Timing properties are cerebellar dependent.**

Lesions of anterior interposed cerebellar nuclei (AIP) in trained animals show that conditioned responses in both L7-PKCi mutants and wild-type mice are composed of both cerebellar and extracerebellar components and that the cerebellar component is necessary for the timing of the eyelid response. (A) Average data sets of CS-alone responses at T-4 before the lesions (light grey) and after the lesions (black) or a sham operation (dark grey) in mutants and wild types ( $n=3$  in all cases). Conditioned responses still occur after lesions of the cerebellar nuclei in both wild types and mutants, but the amplitudes of these responses are in both cases substantially higher with intact cerebellar nuclei. (B) Example of lesions placed in the left and right anterior interposed cerebellar nucleus of a wild-type mouse; lesions can be recognized by the dark grey circumscribed areas in the center.

## 4.5 Discussion

Our study provides evidence for a solution to a long-standing issue in the field of classical eyelid conditioning, i.e., whether LTD contributes to the temporal shaping of conditioned responses (12–14). Although not all components of eyelid conditioning in mice are under cerebellar control, the data demonstrate that mice without parallel fiber LTD show cerebellum-dependent conditioned responses that lack any form of temporal adaptive capacity. One cannot exclude the possibility that climbing fiber LTD, which also depends on PKC activity *in vitro* (15), is also affected in the L7-PKCi mutants. However, parallel fiber LTD but not climbing fiber LTD can be visualized with optical imaging *in vivo*, and the L7-PKCi mutant shows no induction of parallel fiber LTD *in vivo* (10). This evidence indicates that learning-dependent timing is probably mediated by PKC-dependent parallel fiber LTD. During the learning of well-timed movements, the efficacy of a specific set of parallel fiber–Purkinje cell synapses may be diminished by LTD induction so that, ultimately, different ISIs trigger different time rings of different sets of granule cells and Purkinje cells (14, 16), which in turn may lead to the induction of long-term potentiation or to an increase in the intrinsic excitability of the cerebellar nuclei target neurons (17). A similar mechanism, in which timing properties are related to input specificity of Purkinje cells, has been proposed for adaptation of the vestibuloocular reflex (VOR) (8). Indeed, blockage of LTD impairs the level of VOR adaptation after a few hours of visuovestibular training in a frequency-specific fashion, whereas the adaptation becomes non-frequency-specific when mechanisms other than LTD can come into play (8, 18). Thus, it may be a general concept for cerebellar motor learning that LTD does not only control the amplitude of trained movements but also their timing by means of an input specific mechanism.

### Acknowledgements

We thank E. Dalm and J. v. d. Burg for technical assistance. Supported by the Dutch Research Council for Medical Sciences (PIONIER and ZON-MW), Life Sciences (ALW), and the European Community (EEC) (C.I.D.Z.).

## 4.6 References

1. S. P. Perrett, B. P. Ruiz, M. D. Mauk, *J. Neurosci.* 13, 1708 (1993).
2. K. S. Garcia, M. D. Mauk, *Neuropharmacology* 37, 471 (1998).
3. J. F. Medina, W. L. Nores, M. D. Mauk, *Nature* 416, 330 (2002).
4. M. Ito, *Annu. Rev. Neurosci.* 12, 85 (1989).
5. A. Aiba et al., *Cell* 79, 377 (1994).
6. M. Miyata et al., *Eur. J. Neurosci.* 13, 1945 (2001).
7. K. Shibuki et al., *Neuron* 16, 587 (1996).
8. C. I. De Zeeuw et al., *Neuron* 20, 495 (1998).
9. J. Goossens et al., *J. Neurosci.* 21, 5813 (2001).
10. W. Gao et al., *J. Neurosci.* 23, 1859 (2003).
11. S. K. E. Koekkoek, W. L. Den Ouden, G. Perry, S. M. Highstein, C. I. De Zeeuw, *J. Neurophysiol.* 88, 2124 (2002).
12. C. Yeo, G. Hesslow, *Trends Cogn. Sci.* 2, 322 (1998).
13. K. S. Garcia, P. M. Steele, M. D. Mauk, *J. Neurosci.* 19, 10940 (1999).
14. D. Buonomano, M. D. Mauk, *Neural Comput.* 6, 38 (1994).
15. C. Hansel, D. Linden, *Neuron* 26, 473 (2000).
16. W. M. Kistler, C. I. De Zeeuw, *Cerebellum* 2, 44 (2003).
17. C. D. Aizenman, P. B. Manis, D. J. Linden, *Neuron* 21, 827 (1998).
18. A. M. van Alphen, C. I. De Zeeuw, *Eur. J. Neurosci.* 16, 486 (2002).

# Chapter 5

## Enhanced LTD at enlarged Purkinje cell spines causes motor learning deficits in fragile X syndrome

S.K.E. Koekkoek<sup>1</sup>, K. Yamaguchi<sup>2</sup>, W. De Graaf<sup>1</sup>, B.R. Dortland<sup>1</sup>, T.J.H. Ruigrok<sup>1</sup>, C.E. Bakker<sup>3</sup>, B.A. Oostra<sup>3</sup>, S. Itohara<sup>2</sup>, T. Ikeda<sup>2</sup>, C.I. De Zeeuw<sup>1\*</sup> and M. Ito<sup>2</sup>

*1 Department of Neuroscience, Erasmus MC, PO Box 1738, 3000 DR Rotterdam, The Netherlands*

*2 Laboratory for Memory and Learning and Laboratory for Behavior Genetics, Brain Science Institute, RIKEN, Wako, Saitama 351-0198, Japan*

*3 Institute of Clinical Genetics; Erasmus MC, PO Box 1738, 3000 DR Rotterdam, The Netherlands*

Submitted

## 5.1 Abstract

Abnormalities in the cerebral cortex and hippocampus contribute to cognitive deficits of fragile X syndrome. The roles of cerebellar deficits have not been investigated. Here, we demonstrate that Purkinje cells of *Fmr1* null-mutants show elongated spines and enhanced LTD induction at the parallel fiber synapses that innervate these spines. The mutants show impaired cerebellar delay eyeblink conditioning in that the percentage of conditioned responses as well as their peak amplitude and velocity are reduced. Lesions of the cerebellar nuclei of trained fragile X mice show that apart from their initial enhanced startle reflex all later components of their eyeblink responses are controlled by the cerebellum. Due to the unique aberration in cerebellar plasticity and conditioning parameters these data suggest that an optimal instead of a maximum level of LTD is essential for cerebellar motor learning and that cerebellar deficits can contribute to cognitive symptoms in fragile X patients.

## 5.2 Introduction

Fragile X syndrome is the most common monogenic cause of mental retardation<sup>1,2</sup>. Clinically, it is characterised by mental retardation, hyperactive behavior and attention deficits, facial abnormalities and macro-orchidism<sup>3</sup>. The gene involved is the fragile X mental retardation 1 gene, *Fmr1*<sup>4,5</sup>. In patients affected with fragile X syndrome the polymorphic CGG repeat of this gene reaches over 200 units, which in turn causes methylation of the promoter region of *Fmr1* and thereby functionally inactivates the gene. Due to inactivation of *Fmr1* its protein FMRP is absent in patients, while it is normally expressed in a panneuronal fashion<sup>6</sup>.

The knockout mouse of *Fmr1* shows behavioral and cognitive abnormalities comparable to the symptoms found in fragile X patients and several of them can be linked to a dysfunction of a particular brain region<sup>7</sup>. For example, their enhanced startle responses to auditory stimuli and their reduced freezing behavior in response to contextual and conditional fear stimuli indicate a malfunction of their amygdala<sup>8-10</sup>. Similarly, the tendency of the knockout mice to show a deficiency in their ability to learn the position of a hidden escape platform in a water maze task suggests hippocampal dysfunction(s)<sup>11,12</sup>. To date the potential contribution of cerebellar dysfunctions to cognitive deficits in fragile X patients has not been elucidated.

The pathological cellular mechanisms that may underlie the cortical behavioral and cognitive deficits are probably related to dysfunctions at the level of dendritic spines and their input. The dendritic spines of pyramidal cells of both fragile X patients and *Fmr1* knockout mice are unusually long and irregular<sup>13-15</sup>. Since these spines appear morphologically immature, FMRP has been suggested to be involved in spine maturation and pruning as well as synaptogenesis<sup>14</sup>. Indeed, FMRP and *Fmr1* mRNA are present in spines and/or dendrites, and FMRP is translated in response to activation of metabotropic glutamate receptors (mGluR) type 1 in synaptoneuroosomes<sup>16</sup>. The function of FMRP as an inhibitor of translation of bound mRNAs in vitro, including its own mRNA, indicates that FMRP may act as a regulator of activity-dependent translation in synapses<sup>17</sup>. This possibility is supported by the finding that the induc-

tion of mGluR1-dependent long-term depression (LTD) is enhanced in pyramidal cells of the hippocampus in *Fmr1* knockout mice<sup>18</sup>. Thus, altered hippocampal LTD in fragile X patients may interfere with a normal formation and maintenance of synapses required for particular cognitive functions.

Metabotropic GluR1-dependent LTD can also be induced at the parallel fiber to Purkinje cell synapse in the cerebellum<sup>19,20</sup>. Absence of FMRP in Purkinje cells could therefore also cause morphological and functional deficits in the cerebellum<sup>21,22</sup>. To investigate this possibility we investigated whether cerebellar Purkinje cells in *Fmr1* knockout mice have abnormal spine morphology, whether parallel fiber LTD can be induced normally in these cells, and whether *Fmr1* knockout mice can condition their eyeblink responses<sup>23,24</sup>.

## 5.3 Experimental procedures

### 5.3a - Histology

The morphology of Purkinje cells was investigated following labeling with injections of biotinylated dextrane amine (BDA) or with immunocytochemistry against Calbindin. BDA-injections (10% in 0.1M phosphate buffer) were made in the cerebellar nuclei of *Fmr1* mutants and wild types with a single barrel glass micropipette with a tip diameter of 4  $\mu\text{m}$  to retrogradely fill Purkinje cells. Location of the cerebellar nuclei was verified by electrophysiological recordings directly through the pipette. After the iontophoretic BDA injections the animals were allowed to recover for 5 days and subsequently anaesthetized (Nembutal; 50 mg/kg) and transcardially perfused with 4% paraformaldehyde in 0.1M phosphate buffer. The brains were removed, cryoprotected in sucrose, embedded in gelatin, and cut on a cryotome in sagittal 75  $\mu\text{m}$  thick sections. The sections were reacted with the ABC complex and diaminobenzidine to visualize the BDA, mounted on glass slides, coverslipped, and investigated under the light microscope at 100x magnification.

Calbindin-immunocytochemistry was performed on 100  $\mu\text{m}$  sagittal Vibrotome sections of mutants and wild types that were anaesthetized (Nembutal; 50 mg/kg) and perfused with 4% paraformaldehyde and 1% glutaraldehyde in 0.12 M sodium cacodylate buffer). After treatment with 10% normal goat serum in 0.1 M Tris-buffered saline (TBS), the sections were incubated with rabbit anti-calbindin antibody diluted 1:1000 in 0.1 M TBS for 72 hours, rinsed with Goat anti-rabbit-biotine for 90 minutes, and ultimately reacted with avidine-biotine-peroxidase and diaminobenzidine for visualization of the antigen. Some of the sections were mounted, coverslipped, and investigated under the light microscope, while others were directly processed for electron microscopy. The sagittal Vibratome sections stained for Calbindin that were used for electron microscopy were osmicated, dehydrated, embedded in Durcupan, cut into ultrathin sections (50 - 70 nm), mounted on uncoated copper grids, and double stained with uranyl acetate and lead citrate as described by<sup>54</sup>.

For the analyses of the morphology and density of Purkinje cell spines the dendrites carrying these spines were divided into two categories. One category was formed by dendrites that had a diameter bigger than 1.5  $\mu\text{m}$  (proximal category), while the



other category had a diameter smaller than 1.5  $\mu\text{m}$  (distal category). These dendritic fragments and their spines were reconstructed and analysed using programs by Neurolucida, NeuroExplorer and analySIS. Spine density (spines/ $\mu\text{m}$ ) was calculated by dividing the total number of spines per dendrite by the length of the dendrite. Total spine length was calculated by measuring the distance between the tip of the spine head and the base of the spine neck. Spine head length was measured by multiplying the distance from the tip of the spine to the head diameter-intersection line by a factor two. The head diameter-intersection line is the line that crosses perpendicularly the longitudinal axis of a spine at the point where the diameter of the head is biggest. Spine neck length was calculated by subtracting the spine head length from the total spine length.

### 5.3b - Cell physiology

Cerebellar slices were prepared from wild type and *Fmr1* mutant mice following a general procedure<sup>55</sup>. Briefly, the mice (P21-48) were anaesthetized with ether and decapitated. The cerebellum was excised and immersed in ice-cold saline containing (in mM) 125 NaCl, 2.5 KCl, 2 CaCl<sub>2</sub>, 1 MgSO<sub>4</sub>, 1.25 NaH<sub>2</sub>PO<sub>4</sub>, 26 NaHCO<sub>3</sub> and 20 glucose, and bubbled with 95% O<sub>2</sub> and 5% CO<sub>2</sub>. Sagittal slices of 300  $\mu\text{m}$  thickness were prepared from the cerebellar vermis in tetrodotoxin (1  $\mu\text{M}$ ) containing saline using a Vibratome slicer (Dosaka, Japan) and kept at room temperature (23-25°C) for at least 1 hr in normal saline. The recording chamber was perfused with oxygenized saline containing 100  $\mu\text{M}$  picrotoxin at a rate of 2 ml/min. Slice-patch recordings (Edwards et al., 1989; Llano et al., 1991) of Purkinje cells under visual control using a 40x water-immersion objective attached to an upright Nikon microscope (Eclipse E600FN) were obtained at 31.0  $\pm$  1.0°C. Whole-cell patch-clamp recordings were obtained from the somata of Purkinje cells using borosilicate pipettes (resistance, 3-5 M $\Omega$ ) filled with an internal solution containing (in mM) 60 CsCl, 40 D-gluconate, 20 TEA-Cl, 1 EGTA, 4 MgCl<sub>2</sub>, 4 Na<sub>2</sub>-ATP, 0.4 Na<sub>3</sub>-GTP and 30 HEPES. We adjusted the pH to 7.20 by adding approximately 40 mM CsOH. Membrane potential was held at -70 mV. Membrane current was recorded with a Multiclamp700A amplifier (Axon). Stimulation and on-line data acquisition were performed using pClamp 9 software (Axon). Signals were filtered at 3 KHz and digitized at 10 KHz. Access resistance and membrane capacitance were constantly monitored by applying a small hyperpolarizing voltage step (2 mV, 100 ms). When access resistance increased or decreased during conjunctive stimulation or even spontaneously, positive or negative air pressure was applied through a recording pipette in order to recover the initial value of access resistance. Purkinje cells that showed changes in access resistance of more than + 10 % were excluded for analysis. Parallel fibers (PFs) and climbing fibers (CFs) were focally stimulated by applying pulses (duration, 0.1 ms) to a slice through glass pipettes (tip diameter, 5-10  $\mu\text{m}$ ) positioned on the surface of the slice in the middle of the molecular layer and in the granule cell layer, respectively. All experiments were conducted and analyzed blindly with respect to the genotype of the animals.

### 5.3c - Eyeblink conditioning

Wild type and *Fmr1* mutant mice were prepared for eyeblink conditioning according to the MDMT procedure with the magnet-sensor chip combination as described in detail by Koekkoek et al.<sup>23</sup>. In short, mice were anaesthetized using an oxygenated mixture of nitrous oxide and halothane and a pre-made connector (modified from SamTec; www.samtec.com) was placed on the skull with the use of a pedestal of dental cement and 5 M1 screws. A sensor chip linked to the connector (NVE corporation; www.nve.com; AA004-MSOP) was placed in a standard position over the upper eyelid, while a magnet was glued on the lower eyelid. The magnet was placed such that the distance between the magnet and sensor was 2 mm when the eyelid was completely closed and that the axis of sensitivity was aligned with the north-south axis of the magnet when the eyelid was halfway closed. Fully opened, fully closed and halfway opened positions were repetitively measured and stored for calibration purposes. Mice were subjected to either a paired or a randomly paired procedure; both procedures lasted 4 days during each of which 1 session was conducted. During 1 session the subject received 64 trials grouped in 8 blocks. The trials were separated by a random inter-trial interval (ITI) ranging from 20 to 40 sec. In the procedure of paired training each block consisted of 1 US-alone trial, 6 paired trials and 1 CS-alone trial (the 8th trial). After 4 sessions (day T-1 to T-4) of paired training the subject was allowed to rest for 1 day, followed by 2 sessions of extinction (E-1 and E-2, 1 session per day). In the extinction procedure each block consisted of 1 US-alone trial (1st trial) and 7 CS-alone trials. In the randomly paired procedure the US occurred randomly in the ITI, while the CS was given as in the paired trials. In the analyses of the eyelid movements we considered a movement as a significant eyelid response when its amplitude was greater than the mean + 3 SD's of the amplitude of the movements that occurred in the 500 ms period before the onset of the CS. Such a response was considered to contain a startle response when movement occurred within the 60 ms period directly after the onset of the CS, when significant movement occurred after this period, it was counted as a conditioned response.

## 5.4 Results

### 5.4a - Morphology of Purkinje cells

As revealed by both calbindin immunocytochemistry and intracellular labeling with biotinylated dextran amine (BDA) the dendritic arborization and axons of Purkinje cells of *Fmr1* knockout mice appeared normal at the light microscopic level (Figures 5.1A, B and C). The ramifications of the dendrites were not different when analyzed with topological analyses that provide values for the symmetry of arborizations<sup>25</sup>. The spine densities of distal dendrites with an average diameter smaller than 1.5  $\mu\text{m}$  were  $1.22 \pm 0.30$  spines/ $\mu\text{m}$  (mean  $\pm$  SD) and  $1.18 \pm 0.27$  spines/ $\mu\text{m}$  (mean  $\pm$  SD) in *Fmr1* knockouts ( $n = 7$ ) and wild types ( $n = 7$ ), respectively. Likewise, the spine density in dendritic fragments with an average diameter bigger than 1.5  $\mu\text{m}$  (proximal category) was  $1.26 \pm 0.27$  spines/ $\mu\text{m}$  (mean  $\pm$  SD) in *Fmr1* knockouts and  $1.22 \pm 0.20$  spines/ $\mu\text{m}$  (mean  $\pm$  SD) in wild types. Thus, unlike the pyramidal cells in ce-

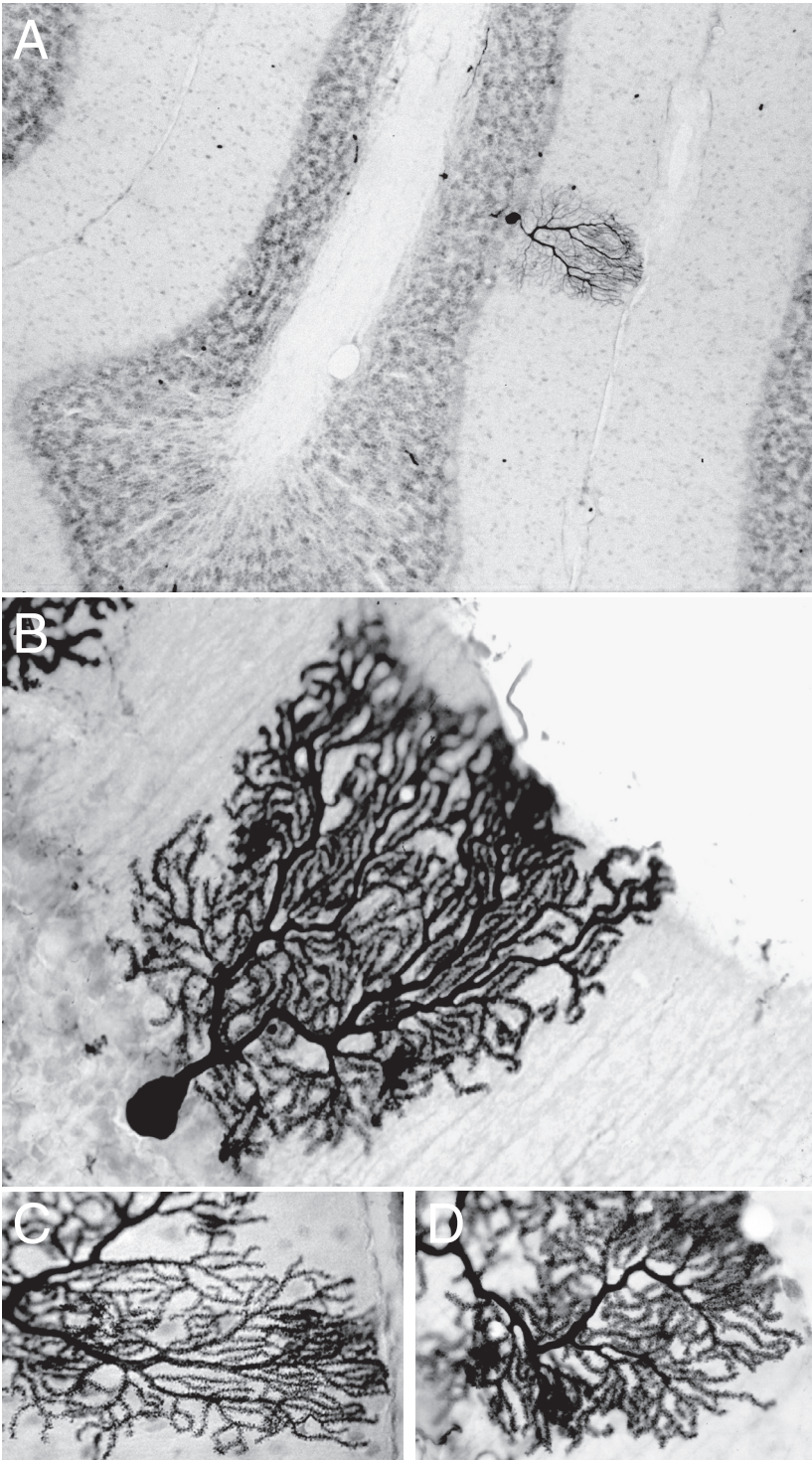


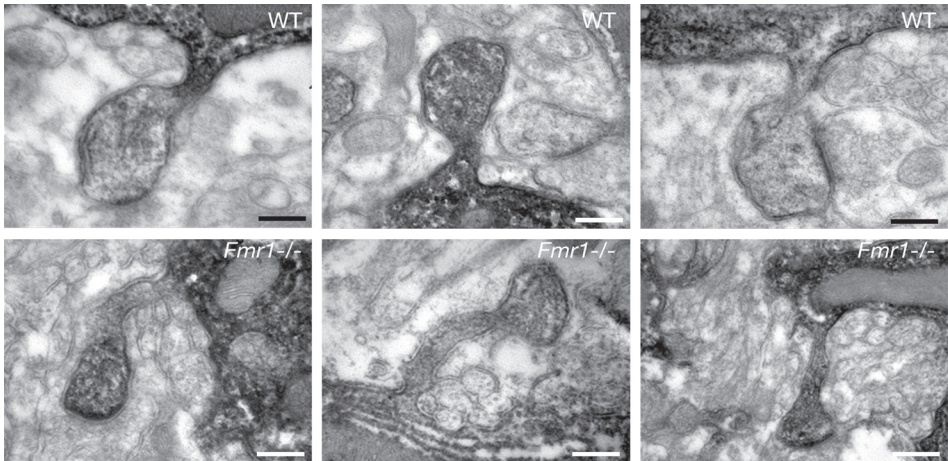
**Figure 5.1 Dendritic arborization of the Purkinje cells in *Fmr1* mutants is normal.** Panels show light microscopic images of the dendritic trees of Purkinje cells in wild types (A, C) and *Fmr1* mutants (B, D) that are retrogradely labeled with BDA. Both the topology of the Purkinje cell dendrites and the density of their spines are normal.



rebral cortical areas the spine density of cerebellar Purkinje cells in *Fmr1* knockouts did not differ significantly from that in their wild type littermates (distal vs distal  $p > 0.5$ ; proximal vs proximal  $p > 0.5$ ; total vs total  $p > 0.5$ ; student t-test).

In contrast, the shape of the spines of Purkinje cells in *Fmr1* knockout mice (Figure 5.2 bottom panels) differed from that in wild type mice (Figure 5.2 top panels). Electron microscopic analysis of calbindin stained Purkinje cells showed that their spines were more irregular and longer. The average lengths of the spine head and spine neck in *Fmr1* knockouts ( $0.56 \pm 0.05 \mu\text{m}$  and  $0.63 \pm 0.18 \mu\text{m}$ , respectively;  $n = 4$ ) were significantly longer than those in wild types ( $0.50 \pm 0.04 \mu\text{m}$  and  $0.46 \pm 0.15 \mu\text{m}$ , respectively;  $n = 4$ ) ( $p < 0.05$  and  $p < 0.001$  for heads and necks, respectively; student t-test) (Figure 5.2B). The spine head diameter, spine head length/spine head diameter ratio, average spine neck diameter and minimal spine neck diameter of *Fmr1* knockouts were not significantly different from those of wild types. Finally, electron microscopic analyses of the spine densities did not reveal any difference either among mutants and wild types.

A



B

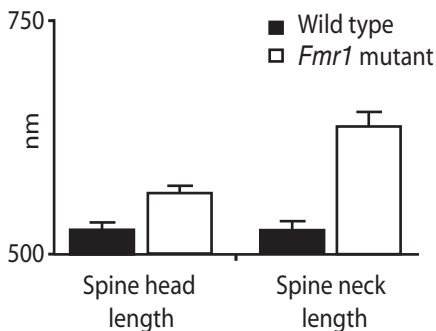


**Figure 5.2 Ultrastructural characteristics of Purkinje cell spines in *Fmr1* mutants are abnormal.**

Panel A shows electron microscopic images of the morphology of individual Purkinje cell spines in wild types (top panels) and *Fmr1* mutants (bottom panels) that are labeled following immunocytochemistry with the use of an antibody against calbindin. Note the longer and more irregularly shaped spines in *Fmr1* mutants. Scale bars in micrographs of the wild types represent 271 nm, 283 nm, and 260 nm, respectively (from left to right). Scale bars in micrographs of the *Fmr1* mutants represent 297 nm, 309 nm, and 321 nm, respectively (from left to right). B shows histograms of average lengths (+ SD) of spine heads and spine necks in *Fmr1* mutants ( $n = 194$ ) and wild types ( $n = 204$ ), respectively.

### 5.4b - LTD induction in Purkinje cells

Since Purkinje cell spines are the prime target for parallel fibers (PF), the abnormal morphology of their spines in *Fmr1* knockouts raised the question as to whether the synaptic efficacy and induction of LTD at this input are normal in the absence of FMRP.

After reaching stable recordings of EPSC's during PF stimulation at 0.2 Hz for 10 min, PF stimuli and depolarizing pulses (duration, 140 msec; -70 to +10 mV) were conjunctively applied at 1 Hz for 5 min<sup>26</sup>. Figure 5.3A shows that this conjunctive stimulation induced LTD in both wild types ( $n = 7$ ) and mutant mice ( $n = 6$ ) as represented by a significant reduction in PF-EPSC. Figure 5.2A also shows that hyperpolarizing-pulse-evoked currents hardly changed implying that conjunctive stimulation does not affect access resistance, input resistance or membrane capacitance; the change in access resistance after conjunctive stimulation was no more than 2% on average in the cells used for analyses (10 wild type and 10 mutant Purkinje cells). During the 15-minute period from 21 to 35 minutes after the onset of conjunctive stimulation the mean amplitude of the PF-EPSCs was reduced to  $70.4 \pm 1.3$

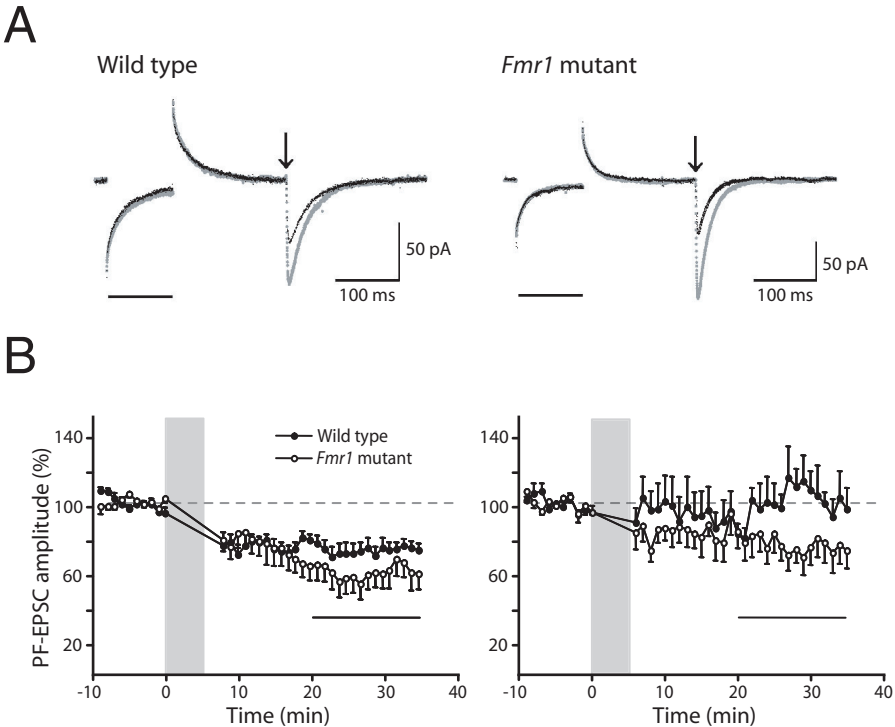


**Figure 5.3** LTD induction is enhanced in Purkinje cells of *Fmr1* mutants. A, superimposed PF-EPSCs in two of the Purkinje cells recorded before conjunctive stimulation and 33 min (wild type) or 31 min (*Fmr1* mutant) after conjunctive stimulation, each trace representing an average of 12 traces. Note the stronger reduction of the PF-EPSCs after PF stimulation in the mutant. Horizontal bars indicate hyperpolarizing pulses (2 mV, 100 ms) used for monitoring access resistance and input resistance, while downward arrows indicate moments of PF stimulation. Left panel of B plots the amplitude of PF-EPSC against time before and after conjunctive stimulation averaged for 10 cells from 7 wild type mice and 10 cells from 6 mutant mice. In each of these cells, 12 records successively acquired at 0.2 Hz were averaged to obtain PF-EPSC values for every minute. The shaded column indicates the period of conjunctive stimulation. Vertical bars extending from the plotted points either upward or downward indicate SEM. Right panel of B plots PF-EPSC against time for repetitive stimulation of PFs alone.

% in the wild types and to  $60.7 \pm 2.3$  % in the mutants.

Thus, while no significant anomaly was recognized in spike potential, PF-EPSC, resting potential or input resistance in mutant Purkinje cells, the induction of LTD in these cells was significantly enhanced as compared to that in the wild types ( $p < 0.01$ ; Duncan New Multiple Range Test by Super-ANOVA software) (Fig. 5.3B).

To find out whether this difference after conjunctive parallel fiber - climbing fiber stimulation can be attributed solely to changes in the parallel fiber to Purkinje cell synapse we also tested the effect of repetitive stimulation of PFs alone at 1 Hz for 5 minutes. Indeed this stimulus paradigm induced depression to  $75.6 \pm 2.5$  % of the baseline values in *Fmr1* mutants, while it did not cause a significant change ( $102.1 \pm 3.2$  %) in PF-EPSCs of Purkinje cells in wild types (Figure 5.3C). In these experiments too the difference among wild types and mutants was greatest 20 minutes after onset of the tetanus protocol. Thus, LTD induction following repetitive stimulation of parallel fibers alone in mutant mice is comparable to that following conjunctive stimulation in wild type mice ( $p > 0.05$  ANOVA), but smaller than that following conjunctive stimulation in *Fmr1* mutant mice ( $p < 0.01$ ) (compare Figures 5.3B and C). Hence, the depression of PF-EPSCs that normally only occurs when a large bundle of parallel fibers is stimulated<sup>27</sup> can be induced in *Fmr1* mutant mice by stimulation of a PF bundle of just a moderate size. This increased sensitivity probably explains the cause of the enhanced induction of LTD following conjunctive stimulation in *Fmr1* mutant mice, because the parallel fiber-alone-induced depression probably adds substantially to the normal conjunction-induced LTD. In fact, quantitatively the data indicate that enhancement of homosynaptic depression in parallel fibers could be the primary effect of FMRP-deficiency at the electrophysiological level. To estimate whether presynaptic release probability is depressed in the parallel fiber-induced depression, we examined paired pulse facilitation of PF-EPSC's at 50 ms intervals<sup>28</sup>. Paired-pulse facilitation increased the PF-EPSC's up to  $159.8 \pm 9.4$  % and  $145.0 \pm 5.4$  % in wild types ( $n = 12$ ) and mutants ( $n = 11$ ), respectively. This difference was not significant ( $p > 0.19$ , t-test). These data suggest that the enhanced cerebellar LTD of PF-EPSC's in *Fmr1*-deficient mice is probably not due to a change in a presynaptic release probability in parallel fiber terminals.

Since the parallel fiber input to the dendritic arbor of a Purkinje cell competes with its climbing fiber (CF) input<sup>29,30</sup>, it might be possible that the morphologically and functionally abnormal parallel fiber inputs in *Fmr1* mutants are related to an abnormal CF input. We therefore investigated the strength and depression of CF-EPSC's and we examined whether the *Fmr1* mutants suffer from a persistent multiple CF input<sup>31,32</sup>. The CF-EPSC's in mutant Purkinje cells did not show any significant anomaly; the absolute strength was indistinguishable from that in the wild type and the paired-pulse depression of the CF-EPSC's was  $81.7 \pm 1.8$  % in Purkinje cells ( $n = 7$ ) of the mutants as compared to  $77.5 \pm 2.3$  % ( $n = 7$ ) in the wild type ( $p > 0.16$ , t-test). With regard to the number of CF inputs per Purkinje cell we found that 60.4 % of the Purkinje cells ( $n = 48$ ) in wild types tested at P21-48 showed a single-CF innervation, while double- and triple-CF innervations were observed in 35.4 % and 4.2 % of the cases, respectively. In mutant mice, single-, double- and triple-CF innervations were observed in 75.6 %, 22.2 % and 2.2 % of the Purkinje cells ( $n = 45$ ) tested,

respectively. The percentage of single-CF innervation was significantly higher in the mutant than in the wild type ( $\chi$  square test,  $p < 0.01$ ). Thus, the climbing fiber input to Purkinje cells in the *Fmr1* mutant does not show any sign of a pre- or postsynaptic deficit, and their development does not show any sign of a delay; in contrast, to our surprise, the normal development from multiple to mono-climbing fiber innervation is accelerated.

### 5.4c - Eyeblink conditioning

Since the *Fmr1* null-mutant shows enhanced LTD and since parallel fiber LTD is thought to underlie various forms of cerebellar motor learning such as classical conditioning and adaptation of the vestibulo-ocular reflex<sup>24,33</sup>, it is interesting to find out whether this type of behavior is specifically affected in the mutants. We therefore subjected the animals during four paired training sessions to a classical motor learning task in which the eyelids are conditioned to a tone using the magnetic distance measurement technique (MDMT)<sup>23</sup>. Compared to wild types the *Fmr1* mutants showed significant deficits in both the peak amplitude and peak velocity of their conditioned responses during training sessions T3 and T4 but not during T1 and T2 (at both T3 and T4  $p < 0.05$ ; t-test) (Fig 5.4 A and B). In addition, the percentage of their conditioned responses was significantly reduced at T2, T3, and T4 ( $p < 0.05$  for days T-2, T-3 and T-4 using the t-test;  $p < 0.005$  using MANOVA for repeated measures on the whole training period, Bonferroni corrected). In contrast, the latencies to the onset and peak amplitude of the conditioned responses were not significantly affected in the mutant (data not shown). When the CS and US were randomly paired virtually no conditioned responses were observed (Fig. 5.4C; right panel). After two sessions of extinction the percentages of conditioned responses in both wild types and *Fmr1* mutants were significantly reduced (data not shown).

Since FMRP is also expressed in various types of neurons outside the cerebellum, extracerebellar differences among mutants and wild types may also contribute in part to the differences in conditioned responses. For example, expression of FMRP in motoneurons may result in different kinetics of the eyeblink responses, while expression in pyramidal cells in the amygdala may affect conditioned responses<sup>34</sup> and additionally can enhance a startle component. We therefore further analyzed both the kinetics of the unconditioned responses, the conditioned responses and the auditory startle responses. When we plot the amplitudes of the unconditioned responses against their peak velocities the slope and R-squared values of this correlation in the mutant are indistinguishable from those in the wild type (Figure 5.5). These similarities hold for unconditioned responses of both paired trials and trials with only the US. Thus, we can exclude the possibility that differences in sensitivity for the US among *Fmr1* mutants and wild types contribute to the differences in conditioned responses. In contrast, analyses of the initial 60 ms periods of the conditioned responses following the onset of the tone did reveal differences. As shown in figure 5.6 during all training sessions both peak amplitude and peak velocity of the startle responses of *Fmr1* mutants were significantly higher than those of wild types ( $p < 0.001$ , t-test). Moreover, the percentage of startle responses was also significantly increased during all sessions in the *Fmr1* mutant group ( $p < 0.05$ , MANOVA). Thus,



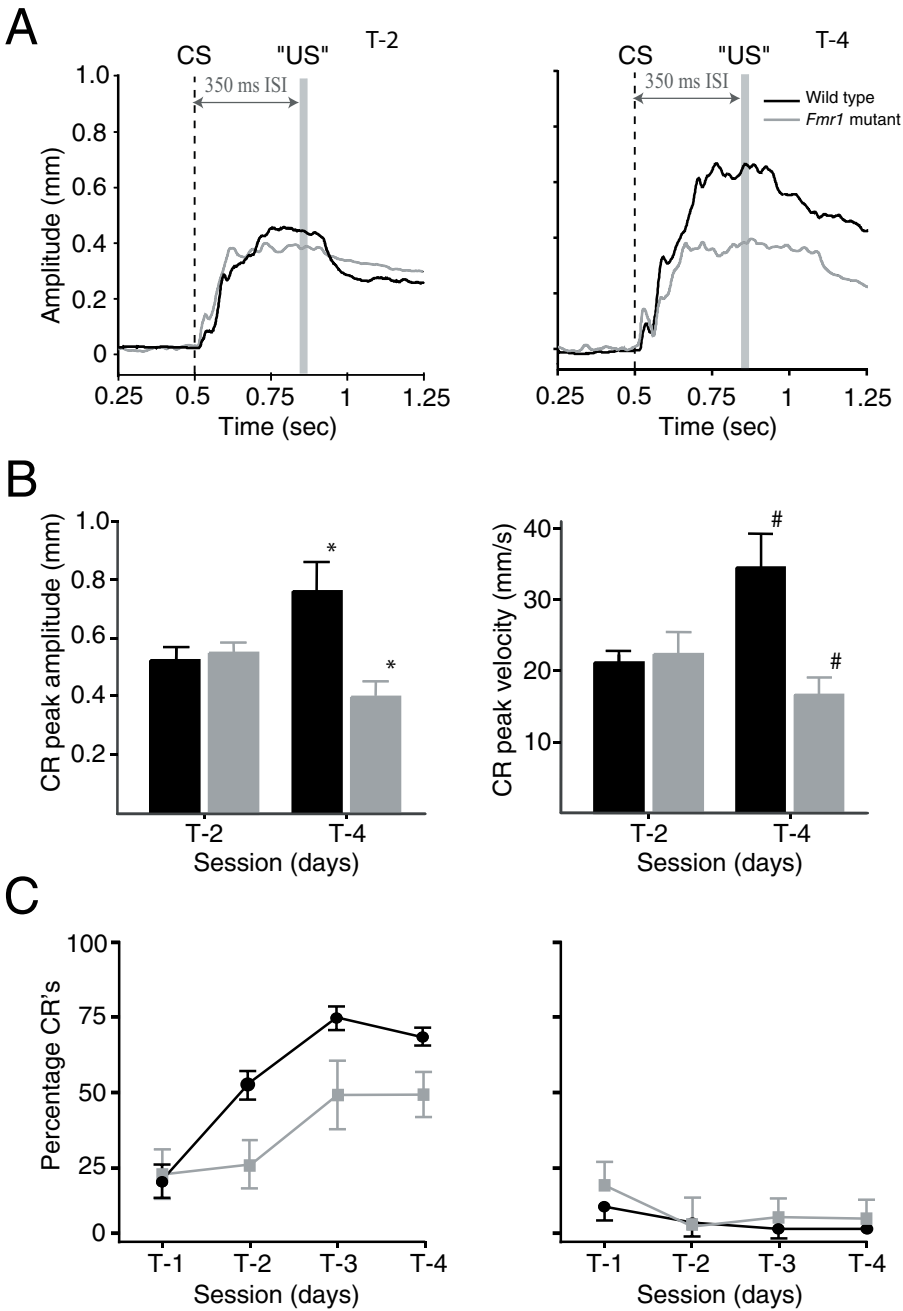


**Figure 5.4 Eyeblink conditioning is impaired in *Fmr1* mutants.** A, examples of data sets for training sessions T-2 (left) and T-4 (right) showing the average amplitude of CS-alone responses of a wild type animal (black) and a *Fmr1* mutant (grey). Note that at T-4, both the wild type animal and the *Fmr1* mutant show well timed responses around the moment when the US is supposed to take place ("US"), while the size of the response of the *Fmr1* mutant remains fixed in amplitude over the training sessions. B, histograms showing peak amplitudes and peak velocities at T-2 and T-4. In contrast to *Fmr1* mutants, wild type animals show a significantly increased peak amplitude and peak velocity at T-4 ( $p < 0.05$  \* and #) but not at T-2. C, the mean percentages (+ SEM) of significant conditioned responses over four days of either paired (left) or unpaired (right) training for *Fmr1* mutants ( $n = 10$ ) and wild types ( $n = 9$ ). These data show that *Fmr1* mutants cannot improve the percentage of their conditioned responses during the training as well as wild types.

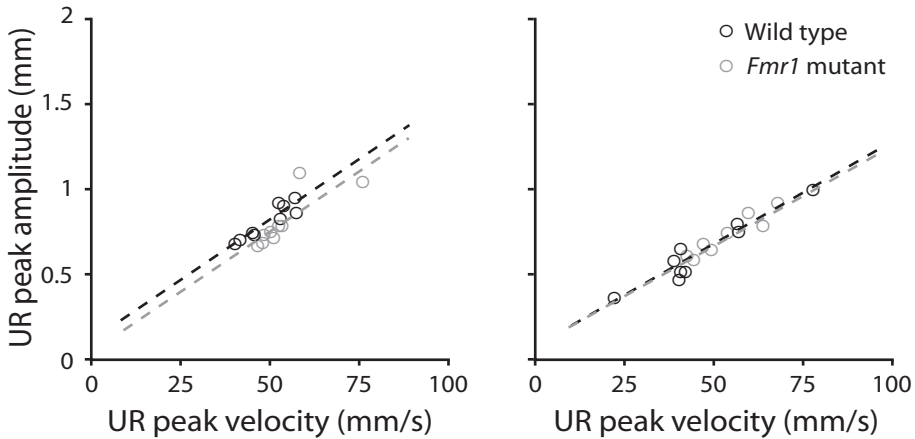


**Figure 5.5 Kinetics of unconditioned responses are unaffected in *Fmr1* mutants.** The left panel shows amplitudes of unconditioned responses of *Fmr1* mutants and wild types against their peak velocities during paired training. The right panel shows the same data but during unpaired training.

these altered startle responses, which are known to be evoked and controlled by higher brain structures such as the amygdala<sup>35</sup>, indicate a more sensitive amygdala function, which by itself may cause indirectly quantitative differences in the conditioned responses in *Fmr1* mutants. Yet, these influences would increase rather than decrease the overall peak amplitude and peak velocity of the conditioned responses in the mutants. It appears therefore unlikely that the impaired conditioned responses as observed in the later stages of the training sessions can be attributed to such non-cerebellar sources. If the differences in conditioned eyeblink responses among *Fmr1* mutants and wild types result indeed predominantly from aberrations in the cerebellar cortex, lesions of the sole output of the cerebellum, i.e. the deep cerebellar nuclei, should severely impair the conditioned responses of both mutants and wild types and they should minimize their differences in remnant conditioned responses. Figure 5.7 illustrates the impact of bilateral lesions of the anterior interposed nuclei, which are known to mediate signaling in eyeblink responses<sup>24</sup>. The data show in both mutants and wild types that both the peak amplitude and peak velocity of the later compo-

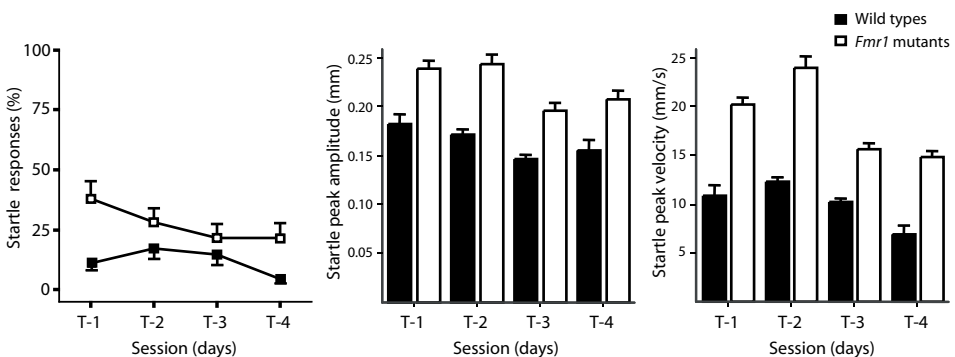


**Figure 5.6 Startle responses are enhanced in *Fmr1* mutants.** Left panel shows the percentage of startle responses in wild types ( $n = 7$ ) and *Fmr1* mutants ( $n = 7$ ) during the initial 60 ms period of the eyeblink responses. Note that this percentage was significantly increased during all sessions in *Fmr1* mutants. Middle and right panel show that peak amplitude and peak velocity of the startle responses of *Fmr1* mutants were significantly higher than those of wild types during all sessions.

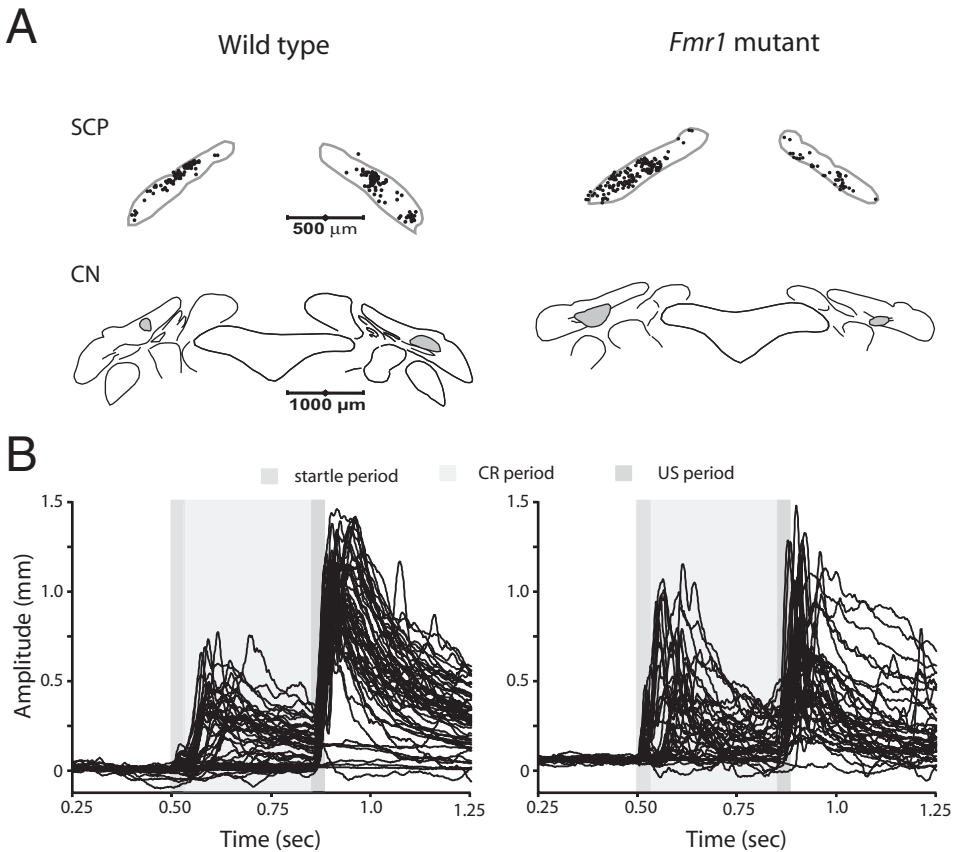


**Figure 5.7 Differences in eyeblink responses between *Fmr1* mutants and wild types are mainly due to cerebellar deficits.** A, confirmation of sites of cerebellar lesions. Top row depicts distribution of damaged fibers (silver staining) in the part of the superior cerebellar peduncle (SCP) that is known to carry the efferent fibers from the anterior interposed nuclei (Haroian et al., 1981). The bottom row shows the centers of the lesions in the cerebellar nuclei (CN). Note that they are situated in the anterior interposed nuclei. B, the recordings show that the differences between wild types and *Fmr1* mutants disappeared after the lesions except for the initial components of the responses (startle reflexes and short latency component amplitude).

nents (i.e. >150 ms after CS onset) of their conditioned responses are significantly reduced after the lesions, while the initial components of their conditioned responses are enhanced. The differences between all other components of the conditioned eyeblink responses disappeared after the lesions. These experiments show that the main differences in eyeblink conditioning parameters such as the changes in peak amplitude and peak velocity that we observed between unlesioned *Fmr1* mutants and their wild type littermates are largely due to a difference in cerebellar control.

## 5.5 Discussion

The present study shows that cerebellar abnormalities in fragile X syndrome can occur at at least three levels including the morphological level, cell physiological level and behavioral level. We found that the null-mutant for FMRP shows a unique phenotypical combination of elongated Purkinje cell spines, enhanced LTD at the parallel fibers that innervate these spines, and an impaired motor learning capability

which is controlled by cerebellar Purkinje cells. Therefore, this study does not only reveal to what extent cerebellar deficits can contribute to cognitive abnormalities in fragile X syndrome, but it also brings forward new clues about cerebellar function in general.

The abnormalities of dendritic spines that we observed in cerebellar Purkinje cells of *Fmr1* mutants mimic only partly those that have been described for pyramidal cells in the cerebral cortex<sup>14,36,37</sup>. They follow the same pattern in that the morphology of individual spines appear as immaturely shaped processes with elongated necks and heads. Why a lack of FMRP can lead to such abnormal spines remains to be elucidated. For pyramidal cells it has been suggested that FMRP negatively regulates the expression of microtubule associated protein MAP1b<sup>18</sup>, which indeed has been shown to affect synapse and spine morphology and which indeed has been shown to be upregulated in cells derived from fragile X patients<sup>38,39</sup>. Interestingly, altered expression of MAP1b in Purkinje cells also results in abnormally shaped dendritic processes<sup>40</sup>, supporting the possibility that a common mechanism is responsible for the aberrations in morphology of spines in fragile X syndrome. On the other hand Purkinje cells diverge from pyramidal cells in that we did not find any evidence in *Fmr1* mutants for an abnormal density of spines on their dendritic arbor neither with the use of light microscopic techniques nor following electron microscopy. Apparently, the density of spines in Purkinje cells is more tightly regulated by compensatory mechanisms than that in pyramidal cells. The spine density in Purkinje cells is largely subject to a well regulated process in which the climbing fibers and parallel fibers compete with each other for specific sites at the dendritic tree<sup>29,30</sup>. It is therefore attractive to hypothesize that the accelerated elimination of multiple climbing fiber inputs that we found in our electrophysiological recordings of *Fmr1* mutants reflects a mechanism so as to compensate for a slowdown in spine maturation. Such a view is supported by recent data obtained by Strata and colleagues who showed that at least two different mechanisms are responsible for spine density and spine pruning in Purkinje cells, i.e. one which is dependent on activity in the climbing fibers and one which is activity-independent<sup>41,42</sup>.

One of the major findings is that a lack of FMRP leads to enhanced parallel fiber LTD without affecting the basic electrical properties of Purkinje cells. Interestingly, this difference among *Fmr1* mutants and wild types, which has not been described for any other cerebellar mutant before, comes about 15 minutes after offset of conjunctive stimulation of the parallel fibers and climbing fibers or about 15 minutes after repetitive stimulation of parallel fibers alone. This period directly follows the critical time period during which the presence and expression of one or more rapidly turned-over protein(s) is/are required to induce LTD<sup>19</sup>. Thus, since FMRP can operate as a negative regulator of mRNA translation<sup>39,43</sup>, one may assume that FMRP probably normally inhibits the translation of at least one of the proteins that is required for the expression of parallel fiber LTD approximately 15 minutes after its induction. Similar time frames have been found for the impact of a lack of FMRP on the induction of LTD at the CA3 - CA1 synapse in the hippocampus<sup>18</sup>. Based on their recordings in hippocampal slices Bear and colleagues proposed a model in which they suggest that FMRP serves to limit expression of homosynaptic LTD by

inhibiting mGluR-dependent translation of local synaptic mRNAs involved in the stabilization of endocytosed AMPA receptors. Because parallel fiber LTD is also driven by activation of metabotropic glutamate receptors<sup>44</sup>, because parallel fiber LTD is ultimately also expressed as an endocytosis of AMPA-receptors<sup>45-47</sup>, and because the enhancement of parallel fiber LTD in *Fmr1* mutants also appears to be mainly homosynaptic, their hippocampal model may be remarkably applicable to cerebellar Purkinje cells.

Considering the common specificity of the electrophysiological effects in both the hippocampus and cerebellum in that a lack of FMRP causes enhanced homosynaptic LTD without affecting any basic electrophysiological property, one would expect that the specific behavioral consequence of such a unique defect is prominently present. Unfortunately, the hippocampal deficits that can be observed in *Fmr1* mutants subjected to spatial learning tests are partially controversial (see e.g.<sup>11,12,48</sup>). Here we show that when subjected to a classical associative eyeblink test, which allows us to detect deficits specific for cerebellar motor learning, that these mutants do have a robust phenotype. The *Fmr1* mutants showed significantly less conditioned eyeblink responses and they were unable to increase the peak amplitude and peak velocity of their conditioned responses during the training. In contrast, the latency to the peak amplitude of the conditioned responses was not affected in the mutant indicating that learning-dependent timing is not impaired by a lack of FMRP. In this respect the phenotype of LTD-enhanced *Fmr1* mutants diverges from that of LTD-deficient mutants. Transgenic mice in which parallel fiber LTD is selectively blocked by Purkinje cell specific expression of an inhibitory peptide against multiple isoforms of protein kinase C cannot adjust the timing of their conditioned responses to the moment of onset of the unconditioned stimulus<sup>24</sup>. On the other hand, these LTD-deficient mice show alike the *Fmr1* mutants a reduced percentage of conditioned eyeblink responses and they are also unable to increase the peak amplitude and peak velocity of their conditioned responses during the training. Thus, while the existence of parallel fiber LTD may be qualitatively necessary for the occurrence of learning dependent-timing of conditioned responses, the exact level of parallel fiber LTD may be quantitatively responsible for the amount of conditioned responses. Apparently, there is an optimal level for the expression of parallel fiber LTD in order to reach a maximum level of learned responses.

Due to the unique aberration of enhanced LTD in the *Fmr1* mutants and due to the unique combination of their deficits in classical conditioning we have been able to show for the first time the importance of an optimal instead of a maximum level of parallel fiber LTD for cerebellar motor learning and we have been able to demonstrate that cerebellar deficits can contribute to cognitive symptoms in fragile X syndrome. Over the past decade research on the potential roles of the cerebellum in cognitive processes has shown a remarkable advent. Investigations vary from transneuronal tracing studies showing robust reciprocal and topographic connections between the cerebral and cerebellar cortex via the pons and thalamus<sup>49,50</sup>, to clinical and neuropsychological studies showing cognitive dysfunctions following cerebellar lesions<sup>51</sup>, and imaging studies showing cerebellar activities correlated with cognitive activities<sup>52,53</sup>. Thus, although deficits in areas such as the cerebral cortex, amygdala

and hippocampus undoubtedly contribute substantially to the cognitive symptoms in fragile X patients, we propose based on the present data that cerebellar dysfunctions can contribute equally as well.

### Acknowledgements

We thank E. Dalm and J. v.d. Burg for their excellent technical assistance. The work in the group of C.I.D.Z. was supported by the Dutch Organization for Medical Sciences (NWO-PIONIER and ZON-MW), Life Sciences (NWO-ALW) and the European Community (EEC).

## 5.6 References

1. de Vries, B.B. et al. Screening and diagnosis for the fragile X syndrome among the mentally retarded: an epidemiological and psychological survey. Collaborative Fragile X Study Group. *Am J Hum Genet* 61, 660-7 (1997).
2. Turner, G., Webb, T., Wake, S. & Robinson, H. Prevalence of fragile X syndrome. *Am J Med Genet* 64, 196-7 (1996).
3. Hagerman, R.J. & Hagerman, P.J. The fragile X premutation: into the phenotypic fold. *Curr Opin Genet Dev* 12, 278-83 (2002).
4. Fu, Y.H. et al. Variation of the CGG repeat at the fragile X site results in genetic instability: resolution of the Sherman paradox. *Cell* 67, 1047-58 (1991).
5. Verkerk, A.J. et al. Identification of a gene (FMR-1) containing a CGG repeat coincident with a breakpoint cluster region exhibiting length variation in fragile X syndrome. *Cell* 65, 905-14 (1991).
6. Verheij, C. et al. Characterization and localization of the FMR-1 gene product associated with fragile X syndrome. *Nature* 363, 722-4 (1993).
7. Bakker, C.E. et al. Fmr1 knockout mice: A model to study fragile X mental retardation. *Cell* 78, 23-33 (1994).
8. Paradee, W. et al. Fragile X mouse: strain effects of knockout phenotype and evidence suggesting deficient amygdala function. *Neuroscience* 94, 185-92 (1999).
9. Chen, L. & Toth, M. Fragile X mice develop sensory hyperreactivity to auditory stimuli. *Neuroscience* 103, 1043-50 (2001).
10. Nielsen, D.M., Derber, W.J., McClellan, D.A. & Crnic, L.S. Alterations in the auditory startle response in Fmr1 targeted mutant mouse models of fragile X syndrome. *Brain Res* 927, 8-17 (2002).
11. D'Hooge, R. et al. Mildly impaired water maze performance in male Fmr1 knockout mice. *Neuroscience* 76, 367-76 (1997).
12. Dobkin, C. et al. Fmr1 knockout mouse has a distinctive strain-specific learning impairment. *Neuroscience* 100, 423-9 (2000).
13. Rudelli, R.D. et al. Adult fragile X syndrome. Clinico-neuropathologic findings. *Acta Neuropathol (Berl)* 67, 289-95 (1985).
14. Comery, T.A. et al. Abnormal dendritic spines in fragile X knockout mice: maturation and pruning deficits. *Proc Natl Acad Sci U S A* 94, 5401-4 (1997).
15. Irwin, S.A. et al. Abnormal dendritic spine characteristics in the temporal and visual cortices of patients with fragile-X syndrome: a quantitative examination. *Am J Med Genet*



98, 161-7 (2001).

16. Weiler, I.J. et al. Fragile X mental retardation protein is translated near synapses in response to neurotransmitter activation. *Proc Natl Acad Sci U S A* 94, 5395-400 (1997).

17. Li, Z. et al. The fragile X mental retardation protein inhibits translation via interacting with mRNA. *Nucleic Acids Res* 29, 2276-2283 (2001).

18. Huber, K.M., Gallagher, S.M., Warren, S.T. & Bear, M.F. Altered synaptic plasticity in a mouse model of fragile X mental retardation. *Proc Natl Acad Sci U S A* 99, 7746-50 (2002).

19. Karachot, L., Shirai, Y., Vigot, R., Yamamori, T. & Ito, M. Induction of long-term depression in cerebellar Purkinje cells requires a rapidly turned over protein. *J Neurophysiol* 86, 280-9 (2001).

20. Coesmans, M. et al. Mechanisms underlying cerebellar motor deficits due to mGluR1-autoantibodies. *Ann Neurol* 53, 325-36 (2003).

21. Hesslow, G. & Yeo, C. Cerebellum and learning: a complex problem. *Science* 280, 1817-9. (1998).

22. Ichikawa, R. et al. Distal extension of climbing fiber territory and multiple innervation caused by aberrant wiring to adjacent spiny branchlets in cerebellar Purkinje cells lacking glutamate receptor delta 2. *J Neurosci* 22, 8487-503 (2002).

23. Koekkoek, S.K.E., Den Ouden, W.L., Perry, G., Highstein, S.M. & De Zeeuw, C.I. Monitoring Kinetic and Frequency-Domain Properties of Eyelid Responses in Mice With Magnetic Distance Measurement Technique. *J Neurophysiol* 88, 2124-2133 (2002).

24. Koekkoek, S.K. et al. Cerebellar LTD and learning-dependent timing of conditioned eyelid responses. *Science* 301, 1736-9 (2003).

25. Van Pelt, J., Uylings, H.B., Verwer, R.W., Pentney, R.J. & Woldenberg, M.J. Tree asymmetry--a sensitive and practical measure for binary topological trees. *Bull Math Biol.* 54, 759-84 (1992).

26. Miyata, M., Okada, D., Hashimoto, K., Kano, M. & Ito, M. Corticotropin-releasing factor plays a permissive role in cerebellar long-term depression. *Neuron* 22, 763-75 (1999).

27. Hartell, N.A. Strong activation of parallel fibers produces localized calcium transients and a form of LTD that spreads to distant synapses. *Neuron* 16, 601-10 (1996).

28. Zucker, R.S. & Regehr, W.G. Short-term synaptic plasticity. *Annu. Rev. Physiol.* 64, 355-405 (2001).

29. Cesa, R., Morando, L. & Strata, P. Glutamate receptor delta2 subunit in activity-dependent heterologous synaptic competition. *J Neurosci* 23, 2363-70 (2003).

30. Kakizawa, S., Yamasaki, M., Watanabe, M. & Kano, M. Critical period for activity-dependent synapse elimination in developing cerebellum. *J Neurosci* 20, 4954-61 (2000).

31. Hashimoto, K. & Kano, M. Presynaptic origin of paired-pulse depression at climbing fibre-Purkinje cell synapses in the rat cerebellum. *J Physiol* 506 ( Pt 2), 391-405 (1998).
32. Kano, M. et al. Phospholipase cbeta4 is specifically involved in climbing fiber synapse elimination in the developing cerebellum. *Proc Natl Acad Sci U S A* 95, 15724-9 (1998).
33. De Zeeuw, C.I. et al. Expression of a protein kinase C inhibitor in Purkinje cells blocks cerebellar LTD and adaptation of the vestibulo-ocular reflex. *Neuron* 20, 495-508 (1998).
34. Whalen, P.J. & Kapp, B.S. Contributions of the amygdaloid central nucleus to the modulation of the nictitating membrane reflex in the rabbit. *Behav Neurosci* 105, 141-53 (1991).
35. Davis, M., Walker, D.L. & Myers, K.M. Role of the amygdala in fear extinction measured with potentiated startle. *Ann N Y Acad Sci* 985, 218-32 (2003).
36. Hinton, V.J., Brown, W.T., Wisniewski, K. & Rudelli, R.D. Analysis of neocortex in three males with the fragile X syndrome. *Am J Med Genet* 41, 289-94 (1991).
37. Irwin, S.A. et al. Dendritic spine and dendritic field characteristics of layer V pyramidal neurons in the visual cortex of fragile-X knockout mice. *Am J Med Genet* 111, 140-6 (2002).
38. Brown, V. et al. Microarray identification of FMRP-associated brain mRNAs and altered mRNA translational profiles in fragile X syndrome. *Cell* 107, 477-87 (2001).
39. Zhang, Y.Q. et al. *Drosophila* fragile X-related gene regulates the MAP1B homolog Futsch to control synaptic structure and function. *Cell* 107, 591-603 (2001).
40. Edelmann, W. et al. Neuronal abnormalities in microtubule-associated protein 1B mutant mice. *Proc Natl Acad Sci U S A* 93, 1270-5 (1996).
41. Bravin, M., Morando, L., Vercelli, A., Rossi, F. & Strata, P. Control of spine formation by electrical activity in the adult rat cerebellum. *Proc Natl Acad Sci U S A* 96, 1704-9 (1999).
42. Strata, P., Morando, L., Bravin, M. & Rossi, F. Dendritic spine density in Purkinje cells. *Trends Neurosci* 23, 198 (2000).
43. Laggerbauer, B., Ostareck, D., Keidel, E.M., Ostareck-Lederer, A. & Fischer, U. Evidence that fragile X mental retardation protein is a negative regulator of translation. *Hum Mol Genet* 10, 329-38 (2001).
44. Aiba, A. et al. Deficient cerebellar long-term depression and impaired motor learning in mGluR1 mutant mice. *Cell* 79, 377-88 (1994).
45. Xia, J., Chung, H.J., Wihler, C., Haganir, R.L. & Linden, D.J. Cerebellar long-term depression requires PKC-regulated interactions between GluR2/3 and PDZ domain-containing proteins. *Neuron* 28, 499-510 (2000).

46. Matsuda, S., Launey, T., Mikawa, S. & Hirai, H. Disruption of AMPA receptor GluR2 clusters following long-term depression induction in cerebellar Purkinje neurons. *Embo J* 19, 2765-74 (2000).
47. Linden, D.J. The expression of cerebellar LTD in culture is not associated with changes in AMPA-receptor kinetics, agonist affinity, or unitary conductance. *Proc Natl Acad Sci U S A* 98, 14066-71 (2001).
48. Van Dam, D. et al. Spatial learning, contextual fear conditioning and conditioned emotional response in *Fmr1* knockout mice. *Behav Brain Res* 117, 127-36 (2000).
49. Middleton, F.A. & Strick, P.L. Anatomical evidence for cerebellar and basal ganglia involvement in higher cognitive function. *Science* 266, 458-61 (1994).
50. Kelly, R.M. & Strick, P.L. Cerebellar loops with motor cortex and prefrontal cortex of a nonhuman primate. *J Neurosci* 23, 8432-44 (2003).
51. Leiner, H.C., Leiner, A.L. & Dow, R.S. Cognitive and language functions of the human cerebellum. *Trends Neurosci* 16, 444-7 (1993).
52. Kim, S.G., Ugurbil, K. & Strick, P.L. Activation of a cerebellar output nucleus during cognitive processing. *Science* 265, 949-51 (1994).
53. Vokaer, M. et al. The cerebellum may be directly involved in cognitive functions. *Neurology* 58, 967-70 (2002).
54. de Zeeuw, C.I., Holstege, J.C., Ruigrok, T.J. & Voogd, J. Ultrastructural study of the GABAergic, cerebellar, and mesodiencephalic innervation of the cat medial accessory olive: anterograde tracing combined with immunocytochemistry. *J Comp Neurol* 284, 12-35 (1989).
55. Llano, I., Marty, A., Armstrong, C.M. & Konnerth, A. Synaptic- and agonist-induced excitatory currents of Purkinje cells in rat cerebellar slices. *J Physiol* 434, 183-213 (1991).

## Chapter 6

Targeted mutation of *Cyln2* in the Williams syndrome critical region links CLIP-115 haploinsufficiency to neurodevelopmental abnormalities in mice

Casper C. Hoogenraad<sup>1,2</sup>, Bas Koekkoek<sup>2</sup>, Anna Akhmanova<sup>1</sup>, Harm Krugers<sup>3</sup>, Bjorn Dortland<sup>1</sup>, Marja Miedema<sup>1</sup>, Arjan van Alphen<sup>2</sup>, Werner M. Kistler<sup>2</sup>, Martine Jaegle<sup>1</sup>, Manoussos Koutsourakis<sup>1</sup>, Nadja Van Camp<sup>4</sup>, Marleen Verhoye<sup>4</sup>, Annemie van der Linden<sup>4</sup>, Irina Kaverina<sup>5</sup>, Frank Grosveld<sup>1</sup>, Chris I. De Zeeuw<sup>2</sup> & Niels Galjart<sup>1</sup>

Published online: 26 August 2002, doi:10.1038/ng954

Nature Genetics 32: 116-127, 2002

## 6.1 Abstract

Williams syndrome is a neurodevelopmental disorder caused by the hemizygous deletion of 1.6 Mb on human chromosome 7q11.23. This region comprises the gene *CYLN2*, encoding CLIP-115, a microtubule-binding protein of 115 kD. Using a gene-targeting approach, we provide evidence that mice with haploinsufficiency for *Cyln2* have features reminiscent of Williams syndrome, including mild growth deficiency, brain abnormalities, hippocampal dysfunction and particular deficits in motor coordination. Absence of CLIP-115 also leads to increased levels of CLIP-170 (a closely related cytoplasmic linker protein) and dynactin at the tips of growing microtubules. This protein redistribution may affect dynein motor regulation and, together with the loss of CLIP-115-specific functions, underlie neurological alterations in Williams syndrome.

## 6.2 Introduction

Williams (or Williams-Beuren) syndrome (OMIM 194050) is a rare neurodevelopmental disorder, with an incidence of 1 in 20,000. It is characterized by cardiovascular abnormalities (particularly supra-aortic stenosis, SVAS), transient juvenile hypercalcemia, abnormal weight gain and growth, and unusual facial features<sup>1</sup>. In addition, individuals with Williams syndrome generally have a unique neurological and behavioral profile<sup>2</sup>. Affected individuals have poor spatial cognition, but have notably intact language and musical abilities and relatively strong face-processing ability. Although they are not ataxic, individuals with Williams syndrome have coordination problems that are particularly obvious in walking up or down a staircase. Affected individuals are highly sensitive to certain classes of sounds, and have IQs in the mild to moderate range of mental retardation. Other characteristic behaviors include a friendly, outgoing personality and an apparent lack of fear.

Williams syndrome is caused by the hemizygous deletion of a region of approximately 1.6 Mb (the Williams syndrome critical region, or WSCR) of chromosome band 7q11.23 (ref. 3). The WSCR contains at least 17 genes, including those encoding syntaxin 1A (*STX1A*), elastin (*ELN*), LIM kinase 1 (*LIMK1*) and CLIP-115 (*CYLN2*). The region is bordered by repeats, leading to the hypothesis that Williams syndrome is caused by illegitimate homologous recombination at the repeats during meiosis. Affected individuals carrying minor deletions that span only part of the WSCR<sup>4</sup> have been identified, however. Study of these individuals and of affected individuals with point mutations has established that haploinsufficiency for *ELN* is linked to cardiovascular abnormalities in Williams syndrome, particularly SVAS<sup>5,6</sup>. It has also been suggested that insufficiency of LIM kinase 1 results in visuo-spatial cognition problems<sup>7</sup>, although more recent studies have not verified this hypothesis<sup>8</sup>. Therefore, although deficiency in *LIMK1* may contribute to part of the cognitive problems in Williams syndrome, it is now thought that other genes are responsible for most of the behavioral abnormalities associated with Williams syndrome. Deletion mapping in individuals with partial phenotypes and atypical deletions indicates that these genes are probably located in a region telomeric to *RFC2* that contains the *CYLN2*, *GTF2IRD1* and *GTF2I* loci<sup>3,4,8</sup>. We have cloned the cDNA encoding

CLIP-115, which is most abundantly expressed in dendrites and cell bodies of many neurons in the brain<sup>9</sup>. Both CLIP-115 and CLIP-170 belong to a group of proteins that specifically associate with the ends of growing microtubules<sup>10,11</sup>. These proteins are believed to have distinct roles in regulating microtubule dynamics and in establishing interactions between microtubule tips and various cellular structures, including cargoes destined for microtubule-based, minusend directed transport by dynein. In line with this view, both CLIPs interact with CLASPs, which are proteins involved in the regional stabilization of microtubules at the leading edge of motile fibroblasts<sup>12</sup>. Moreover, the ortholog of CLIP-170 in fission yeast has been shown to spatially organize microtubular dynamics<sup>13</sup>. In turn, CLIP-170 functions in the recruitment of dynactin, a protein complex that regulates dynein processivity, to the distal ends of microtubules<sup>14,15</sup>. CLIP-170 also regulates localization of LIS1, a protein implicated in brain development<sup>16</sup> and in several processes mediated by the dynein–dynactin pathway, to microtubule tips<sup>17</sup>. These data indicate that CLIP-170 has a role related to dynein and that this is mediated by the carboxy-terminal metal-binding motif of CLIP-170 that is not conserved in CLIP-115. The gene *CYLN2*, encoding CLIP-115, is located in the WSCR<sup>18,19</sup>. In mice, *Cyln2* is located at the telomeric end of chromosome 5 (ref. 18) in an area orthologous to human chromosome 7q11.23 (ref. 20). In both organisms, the gene is positioned between the *LIMK1* and *GTF2I* loci<sup>20,21</sup>. Here we describe the generation of an inducible *Cyln2*-knockout allele. Mice carrying a deletion of *Cyln2* showed mild growth deficiency and brain abnormalities, altered hippocampal functioning and specific deficits in motor coordination. These features partially mimic those of Williams syndrome and were observed in heterozygous *Cyln2*-knockout mice, indicating that haploinsufficiency for *CYLN2* is linked to neurodevelopmental features of Williams syndrome. Cell biological analysis revealed that absence of CLIP-115 did not significantly alter microtubule dynamics, but did enhance accumulation of CLIP-170 and dynactin at microtubule tips. This might affect the proper regulation of dynein motor activity. Together with the loss of functions specific to CLIP-115, the perturbation of CLIP-like protein distributions at microtubule tips might underlie neurodevelopmental problems in *Cyln2*-knockout mice and individuals with Williams syndrome.

## 6.3 Methods

### 6.3a - Generation of CLIP-T and CLIP-L mutant mice

We have previously described the characterization of mouse *Cyln2* from an AB1 embryonic stem (ES) cell DNA-derived cosmid library<sup>18</sup>. Based on these data, we used a 6.1-kb *XbaI*–*Sall* genomic subclone encompassing exon 3 with an *XbaI* site in intron 2 to target the 5' end of *Cyln2*. An 8-kb *NcoI*–*BamHI* fragment containing exons 15, 16 and 17 and a *HindIII* site downstream of the last exon was used to target the 3' end (Fig. 6.1a). We made the 5' end–targeting construct by inserting a neomycin-resistance gene, driven by a thymidine kinase promoter and flanked by *loxP* sequences, into the *XbaI* site in intron 2. The 3' end–targeting construct was made by inserting a puromycin-resistance gene, driven by the phosphon glycerate kinase (*Pgk*) promoter

and flanked by *loxP* sequences, together with a *lacZ* reporter sequence, in the HindIII site downstream of *Cyln2*. We constructed the *lacZ* reporter with a splice acceptor site at its 5' end, a 3' untranslated region (UTR) and polyadenylation signal at its 3' end, and sequences encoding a triple HA tag and nuclear localization signal (NLS) at the amino terminus of the *lacZ* protein. In both the 5'-end construct (called NEO) and the 3'-end construct (PURO-HA-NLS-*lacZ*), a negative-selection marker gene (thymidine kinase) was inserted in the polylinker of the vector.

E14 ES cells were electroporated first with a linearized 3' end-targeting construct and cultured in BRL-cell conditioned medium as described<sup>38</sup>. After selection with puromycin (0.7  $\mu\text{g ml}^{-1}$ ), colonies were isolated and expanded. We analyzed the karyotypes of puromycin-resistant ES cell lines targeted at the *Cyln2* locus, and electroporated one line with the correct number of chromosomes with the 5' end-targeting construct. After selection with G418 (200  $\mu\text{g ml}^{-1}$ ) for neomycin resistance, we identified homologous recombination at *Cyln2* by Southern-blot analysis. We carried out FISH, using the NEO and PURO-*lacZ* cassettes as probes, to find cell lines with both constructs targeted to the same allele (CLIP-T). We then electroporated ES cells with the correct karyotype with a construct containing the *Cre* recombinase gene, driven by a thymidine kinase promoter, in a vector backbone with a P<sub>gk</sub> hygromycin-resistance gene. After selection with hygromycin B (100  $\mu\text{g ml}^{-1}$ ), we detected deletion of the *Cyln2* region between the outermost *loxP* sites by Southern-blot analysis. We injected CLIP-T and CLIP-L ES cell lines with the correct karyotypes into C57Bl/6 blastocysts. Male chimeric mice were mated with female C57Bl/6 mice to transmit the modified *Cyln2* alleles to the germ line. We determined the genotypes of the CLIP-T and CLIP-L mice by either Southern-blot or PCR analysis using the probes and primer sets indicated in Fig 6.1a (primer sequences are available upon request).

### 6.3b - RNA and protein analyses

We prepared total RNA or protein from mouse brain as described<sup>9,23</sup> and performed northern- and western-blot analyses using standard protocols<sup>39</sup>. The *Cyln2*, *lacZ*, *Gapdh*, *Eif4h*, *Rfc2* and *Gtf2ird1* probes (the latter three obtained from IMAGE clones 1276725, 1396169 and 555547, respectively) were radioactively labeled using PCR or random prime methods. The antibodies against CLIP-115 (no. 2238), CLIP-115/170 (no. 2221) and CLIP-170 (no. 2360) used for western blotting have been described<sup>16,23</sup>.

### 6.3c - Histology and electron microscopy

Immunohistochemistry and electron microscopy on mouse brain sections were performed as published<sup>9</sup>. For X-gal staining, we fixed dissected brains for 30 min at room temperature in 2% paraformaldehyde, 0.2% glutaraldehyde in PBS buffer containing 2 mM MgCl<sub>2</sub>, 5 mM EGTA (pH 8.0) and 0.02% Nonidet P-40 (NP-40). We subsequently washed brains three times for 10 min each at room temperature in 0.02% NP-40 in PBS buffer and stained whole-mount brains and sections for 2 h (or overnight) at 37 °C in PBS buffer containing 1 mg ml<sup>-1</sup> X-gal, 5 mM K<sub>3</sub>Fe(CN)<sub>6</sub>, 5



mM  $K_4Fe(CN)_6$ , 2 mM  $MgCl_2$ , 0.01% SDS and 0.02% NP-40. For electron microscopy, two homozygous *Cyln2*-knockout, two heterozygous and two wildtype mice were transcardially perfused with 1% glutaraldehyde and 3% paraformaldehyde in 0.18 M cacodylate buffer. We dissected the brainstem, including the inferior olive, as well as the cerebellum and hippocampus and cut these brain regions on a Vibratome into sections 100  $\mu$ m thick. We subsequently osmicated, stained and blocked sections with 3% uranyl acetate and embedded sections in Araldite. We made pyramids of the various olivary subnuclei and cut ultrathin sections that were counterstained with 1% lead citrate and 2% uranyl acetate and examined under a Philips CM-100 electron microscope.

### **6.3d - Mouse strains, weights and calcium levels**

Generation of the *Cyln2*- knockout strains of mice was approved by the local animal experimental committee at the Erasmus University Rotterdam. Mice were housed at ambient temperature and subjected to a 12 h day:12 h night circadian cycle with constant access to food and water. When necessary, mice were allowed to accommodate to a new environment for an appropriate period of time before behavioral experiments were done. We sacrificed mice at different ages (P1, P14 and adult) and immediately analyzed body weights (including brain), total brain weight (including cerebellum, cerebrum, cerebrospinal fluid and brainstem) and calcium levels. Serum calcium concentrations were determined colorimetrically (600 nm, Arsenazo III) as described by the supplier (Sigma Diagnostics). For determination of the growth curve groups, we analyzed mice of different genotypes twice per week from two to ten weeks of age at fixed time points during the day.

### **6.3e - MRI analysis**

For the MRI analysis, we selected 5-month homozygous, heterozygous and wildtype littermates from the CLIP-L strain and age-matched CLIP-T mice. We anesthetized mice using 5% isoflurane induction and 1–1.5% isoflurane maintenance. Isoflurane was administered in a mixture of 30% oxygen and 70%  $NO_2$ . We firmly fixed the head of each mouse in a stereotactic device consisting of ear plugs and a tooth bar. During MRI, we kept the temperature of the mouse constant at  $37.0 \pm 0.5$  °C. Using Visual Basic code, we monitored the temperature with a rectal probe (PT100), which fed back to a temperature-controlled electrical heating pad (Uty Nelson). The MRI imaging was performed at 300 MHz on an SMIS MR microscope (MRRS) with a 7 T horizontal bore magnet and 8 cm aperture self-shielded gradients with a strength of  $0.1 \text{ T m}^{-1}$  (Oxford Instruments). We positioned the stereotactic apparatus in the center of a 30-mm wide RF bird-cage coil used for both transmitting and receiving. Scouting gradient-echo images in the three orthogonal directions were acquired to guide the reproducible positioning of the three-dimensional (3D) slab of the mouse head. We obtained high resolution coronal slices of the mouse brain using a 3D Fast Spin Echo sequence<sup>40–42</sup> with an echo-train length of four, reducing the imaging time by a factor of four. We acquired MR signals of a 3D volume of  $20 \times 20 \times 20$  mm<sup>3</sup> within a  $256 \times 128 \times 64$  matrix. The images were taken with a repetition time of

2,500 ms and a first echo time of 35 ms with an inter-echo delay of 25 ms (with echo times of 35, 60, 85 and 110 ms). The central line of the k-space was sampled at the first echo. We chose these parameters to obtain 3D images of the brain with optimal contrast between the different brain structures within an acceptable time period. The imaging procedure took about 85 min and allowed a short anesthesia period. We reconstructed the MR data to an image matrix of 256x256x256, containing 256 coronal slices of 78  $\mu\text{m}$  with in-plane resolution of 78x78  $\mu\text{m}^2$ . Volumes from different brain structures were estimated to find differences between CLIP-T, wildtype, *Cyln2*<sup>+/-</sup> and *Cyln2*<sup>-/-</sup> mice. We defined brain and ventricular structures on coronal MR images according to the Mouse Brain atlas and their positions in terms of antero-posterior distance to the interaural line (IA). To extract quantitative volumes of the total brain including the cerebellum (starting from IA -2.00 mm) from a set of images of the mouse obtained *in vivo*, we applied a semi-automatic 3D segmentation technique<sup>43</sup> on the 3D MRI data set using Visual C routines and Interactive Data Language (IDL, Research Systems). We used Surfdriver software to segment the volumes of the hippocampus (located from IA 2.86 mm to IA 0.72 mm), amygdala (located from IA 2.86 to 1.26 mm), corpus callosum (located from IA 1.50 mm to 3.00 mm) and the entire ventricular system. We later divided the entire ventricular system into the fourth ventricle, the aqueduct of Sylvius, the third ventricle and the lateral ventricles, according to the stereotactic atlas of Paxinos.

### 6.3f - Behavioral tests

We carried out all behavioral experiments in a doubleblind manner and analyzed wildtype and mutant mice for motor coordination as described<sup>30,44</sup>. We performed the elevated zero-maze test as previously described<sup>33,45</sup>, using a circular runway (46 cm in diameter, 5.5 cm wide and elevated by 40 cm) divided into two opposing open quadrants without walls and two opposing closed quadrants with walls 11 cm high. We placed male mice in the closed quadrant of the maze and allowed them to investigate for 5 min. We monitored the amount of time spent in the open quadrants with a stopwatch and counted the number of entries into open quadrants.

For the computer-assisted 24 h contextual fear-conditioning experiment<sup>46</sup>, we placed mice (5–6 months of age) in the conditioning chamber and administered a foot shock (2 s duration, 1.0 mA) after a 2-min baseline period. After 24 h, we placed the mice back into the same conditioning chamber for a 2-min contextual freezing test. In the cued fear-conditioning experiment<sup>46</sup>, we placed mice in the conditioning chamber, and after 2 min they received the cue (a tone of 10 s duration, 75 dB, 2.8 kHz). During the final 2 s, mice received a foot shock (1.0 mA). After 24 h, we placed mice in a different chamber and, after a 2-min baseline period, played the original training tone for 2 min. In both experiments, we scored freezing by computer, using a webcam at 5 Hz and customary written software (Matlab). In this manner, we could score freezing and activity frame by frame, similar to a previously published method<sup>46</sup>. In the open-field activity tests (50x50 cm), mice were tested for spontaneous locomotor activity. Mice always started from the same corner of the arena, and we recorded them for 5 min using a computerized video tracking system to measure walking distance, moving episodes and moving time at the horizontal and vertical planes

and entries of the mice in different imaginary parts of the field. The compensatory eye-movement test investigates the role of the vestibulocerebellum in controlling the gain and phase of the optokinetic reflex and the vestibulo-ocular reflex<sup>30</sup>. The mice received a head pedestal and an eyecoil under halothane anesthesia, and after recovery were subjected to visual and vestibular stimulation with the use of a drum and turntable at a wide variety of amplitudes (3–15°) and frequencies (0.1–1.6 Hz). We collected the eye movement data before and after visuovestibular training paradigms using Spike-2 (CED) and analyzed these data offline using Matlab programs. In the hanging wire test (to measure balance and grip strength), we placed mice on top of a wire cage lid taped around the edge and suspended 30 cm above the cage. The lid was shaken three times and then turned upside down, and the amount of time that each mouse held on to the lid was recorded, up to a maximum of 60 s. We assessed motor coordination and balance of mice by measuring the ability of the mice to cross a wooden beam 1 cm wide and 30 cm long placed horizontally above the bench surface. During training, we allowed mice to explore the beam for 5 min. During the test, we placed each mouse on one end of the beam and recorded the amount of time needed to walk across the beam, up to a maximum of 60 s. Four trials were carried out for each mouse. If a mouse fell off the beam, we scored the trial as 60 s. The accelerating rotorod test analyzes more complicated motor behaviors and motor learning. The rotorod consists of a smooth plastic roller (8 cm in diameter and 14 cm long) flanked by two large round plates (30 cm in diameter) to prevent mice from escaping. We placed each mouse on the roller for 10 s at a constant rotation (2 rpm) and then gradually increased the rotational speed to 12 rpm over the course of 2 min. We trained mice on day 1 using a stationary rotorod and then tested them over the next 5 d by carrying out three trials for each mouse every day, measuring the amount of time each mouse remained on the rotorod, up to a maximum of 60 s. The circadian running-wheel test measures the cage activity of mice over 24 h<sup>47</sup>. After an acclimatization period, we tested the circadian rhythms of wildtype (n = 4), *Cyln2*<sup>+/-</sup> (n = 4) and *Cyln2*<sup>-/-</sup> (n = 4) mice using a normal cage with a running wheel. All groups of mice had normal circadian rhythms (data not shown). We noted, however, that *Cyln2*<sup>-/-</sup> and *Cyln2*<sup>+/-</sup> mice showed strikingly poor coordination in the running wheel during the initial accommodation period. Although this behavior is not part of a standard test for movement and coordination, it was so notable that we recorded films of wildtype and *Cyln2*<sup>-/-</sup> mice and quantified their behavior. Whereas wildtype mice ran in the wheel with smooth coordination, *Cyln2*<sup>-/-</sup> mice had highly variable motions. This became obvious when interruptions of smooth running behavior were quantified for the four mice of each genotype during a period of 30 s. Wildtype mice averaged  $2.0 \pm 0.7$  interruptions per 30 s, whereas *Cyln2*- knockout mice averaged  $9.3 \pm 1.3$  interruptions per 30 s; the difference was statistically significant ( $P < 0.005$ ). Both *Cyln2*<sup>-/-</sup> and *Cyln2*<sup>+/-</sup> mice improved their running-wheel performance throughout the acclimatization period, which explains their normal circadian activity patterns afterward.

### 6.3g - Electrophysiological recordings

For electrophysiological measurements, we decapitated mice, quickly removed the brains and chilled them in carbogenated (95% O<sub>2</sub> and 5% CO<sub>2</sub>) artificial cerebrospi-

nal fluid (aCSF: 120 mM NaCl, 3.5 mM KCl, 1.3 mM MgSO<sub>4</sub>, 1.25 mM NaH<sub>2</sub>PO<sub>4</sub>, 2.5 mM CaCl<sub>2</sub>, 10 mM D-glucose, 25 mM NaHCO<sub>3</sub>). We prepared hippocampal slices (400 μm) from dissected brain with a tissue chopper and maintained these at room temperature in carbogenated aCSF. After an equilibration period of at least 1 h, we transferred one slice at a time to a recording chamber, which was continuously perfused with carbogenated aCSF (2–3 ml min<sup>-1</sup>) and kept at 30–32 °C. We fixed and submerged the slice between two nylon meshes and placed a bipolar stimulation electrode (delivering 150 μs pulses) in the Schaffer collateral–commissural fibers and low-resistance glass microelectrodes (2–5 MΩ, filled with aCSF) in the CA1 dendritic layer to record the field evoked post-synaptic potential (fEPSP). In each experiment, we first determined the maximal fEPSP amplitude by gradually increasing the stimulus intensity (using an interstimulus interval of 10 s) until the responses reached a saturating level. We fit the relationship between stimulus intensity and the evoked response to a sigmoidal function, and determined which stimulus intensity evoked a response that was ~50% of the maximal EPSP amplitude. In all experiments, we monitored baseline synaptic transmission for at least 10 min with stimuli delivered at an interval of 60 s. After this period, we administered theta-burst stimulation in a pattern consisting of two 30-ms bursts with four pulses at 100 Hz separated by 200 ms; the pattern was applied five times at intervals of 30 s. After theta-burst stimulation, we measured synaptic response for 40 min at 0.0166 Hz<sup>48</sup>.

### 6.3h - Cell biological analysis.

We have previously described GFP–CLIP-115 and GFP–CLIP-170 constructs, as well as methods for culturing and transfection of COS-1 cells<sup>23</sup>. To generate GFP–CLIP-170(–tail), we deleted the last 79 amino acids of rat brain–derived CLIP-170. The GFP–CLIP-115(+tail) construct contains the C-terminal 159 amino acids of CLIP-170 linked in-frame to CLIP-115. We obtained primary mouse fibroblasts either from the trunk region of E13.5 mouse embryos or from adult skin. Fibroblasts were grown for 3–6 passages before analysis. We carried out immunofluorescence studies<sup>12</sup> with the following primary and secondary antibodies and dilutions: rabbit antibody against CLIP-170 (antiserum no. 2360; 1:300), rabbit antibody against CLIP-115 (no. 2238; 1:300), rabbit antibody against CLIP-115/170 (no. 2221; 1:300), mouse antibody against p50<sup>dynamitin</sup>, mouse antibody against p150<sup>Glued</sup> and mouse antibody against EB1 (Transduction Laboratories, 1:100), rhodamine-labeled sheep antibody against mouse (Boehringer, 1:25), fluorescein isothiocyanate (FITC)–conjugated goat antibody against rabbit (Nordic Laboratories; 1:100), Alexa-594–conjugated goat antibody against rabbit (Molecular probes, 1:500) and Alexa-350–conjugated sheep antibody against mouse (Molecular probes, 1:250). We mounted slides using Vectashield mounting medium (Vector Laboratories) containing 4',6'-diamidino-2-phenylindolehydrochloride (DAPI) (Sigma) and acquired microscopic images as described<sup>12</sup>. To quantify the fluorescent signal on microtubule plus-ends, we exported images and analyzed pixel intensities using Image SXM, an extended version of the NIH Image public-domain software program. In Image SXM, we set identical threshold levels for each image and then calculated the surface of individual fluorescent plus-end signals in μm<sup>2</sup> per microtubule plus-end by manually selecting the

ends with the wand tool. For CLIP-170 fluorescent intensity, we analyzed ten images each from *Cyln2*-knockout and wildtype fibroblasts (>20 cells per genotype), and for dynactin signals we analyzed five images from the mixed cell cultures (>10 cells). We analyzed microtubule dynamic behavior by injection of Cy3-labeled tubulin into fibroblasts, as described previously<sup>49</sup>. Microtubule growth and shrinkage rates, as well as catastrophe and rescue events, were calculated by exporting movies of microtubules in living cells to Image SXM. Individual microtubules were followed frame by frame to record their behavior and generate life-history plots. The behavior of growing microtubule plus-ends was analyzed in live transfected cells as described previously<sup>12</sup>. Mouse fibroblasts (*Cyln2*-knockout and wildtype cells) were transfected with EB3-GFP, which is the best marker for visualization of growing microtubule ends in transfected cells (T. Stepanova, A.A., C.C.H., F.G. and N.G., manuscript in preparation).

### 6.3g - Statistical analysis.

We compared genotypes at fixed time points using either a two-tailed Student *t*-test (to compare data from two groups) or a one-way ANOVA (to compare data from more than two groups). In the latter case, if we obtained a significant difference, Dunnett's multiple comparison was used as a *post-hoc* test with wildtype littermates of CLIP-L mice as the reference group. We compared genotypes over time using a two-way repeated-measures ANOVA with a correction for differences in variance over time. Analysis of the interaction terms (genotype– time) failed to show significant differences in growth curves or rotorod behavior over time between the different genotypes. Thus, the shape of the curves shown in the figures is not significantly different between the genotypes. We analyzed data using Microsoft Excel, Graph- Pad Prism and SAS for Windows.

*Note: Supplementary information is available on the Nature Genetics website.*

## 6.4 Results

### 6.4a - An inducible *Cyln2*-knockout allele

To inactivate *Cyln2*, we introduced a neomycin-resistance gene surrounded by loxP sequences into intron 2, and a puromycinselection marker, surrounded by loxP sequences and followed by a modified  $\beta$ -galactosidase (*lacZ*) reporter gene, downstream of *Cyln2* (Fig. 6.1a). We introduced the resistance markers by two sequential rounds of homologous recombination (first round, puromycin cassette, 12% of picked clones targeted; second round, neomycin cassette, 15% targeted). Their integration was confirmed by a combination of Southern-blot, PCR and FISH analysis (Fig. 6.1b,c and data not shown). We named the doubly targeted *Cyln2* allele CLIP-T (Fig. 6.1a).

Subsequent Cre-mediated excision of the region between the outermost loxP sites in the CLIP-T allele generated a knocked-out *Cyln2* allele that we named CLIP-L (Fig.

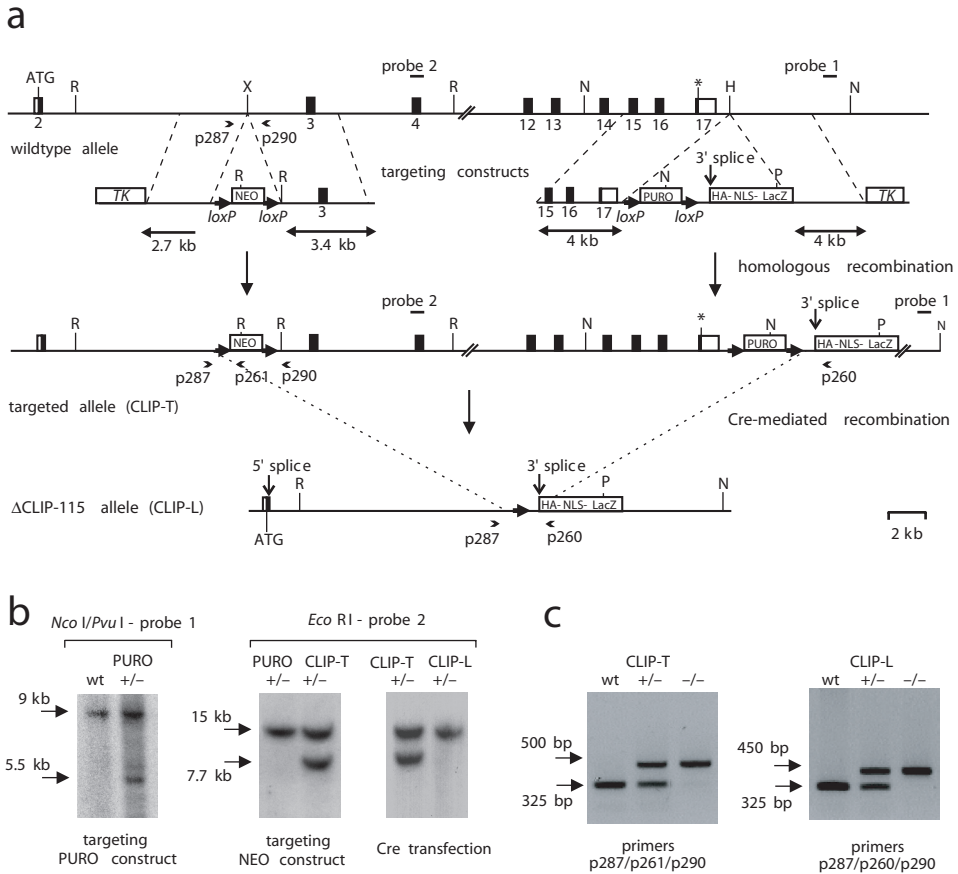


**Figure 6.1 Inducible targeting of the *Cyln2* gene.** a, The *Cyln2* locus and genotyping constructs. The top line represents *Cyln2*, with exons indicated by solid boxes (white boxes, 5' and 3' UTRs; black boxes, coding regions). Exon 2 contains the start codon (ATG) and exon 17 contains the stop codon (asterisk). The positions of Southern-blot probes 1 and 2 (horizontal lines) and PCR primers p287, p260, p261 and p290 (arrowheads) are indicated. Selected restriction enzyme sites are shown (R, *EcoRI*; H, *HindIII*; X, *XbaI*; N, *NcoI*; P, *PvuI*). The targeting constructs are shown below *Cyln2*. Homology with the *Cyln2* gene is indicated, as are the lengths of the homologous regions. The loxP sites are represented by arrows (not to scale). NEO, neomycin-resistance cassette; PURO, puromycin-resistance cassette; TK, thymidine kinase gene; HA-NLS-*lacZ*, HA- and NLS-tagged *lacZ* cassette, containing an engineered splice acceptor site (3' splice) and polyadenylation signal (not indicated). The doubly targeted *Cyln2* allele, CLIP-T (targeted), is shown below the targeting constructs. Cre-mediated recombination at the outermost loxP sites of the CLIP-T allele removes most of the *Cyln2* sequences and generates the CLIP-L (oxed) allele, which is represented by the bottom line. The splice acceptor site at the 5' end of the reporter *lacZ* cassette can be spliced onto *Cyln2* exon 2 sequences, generating a hybrid *Cyln2-lacZ* transcript. b, Southern-blot analysis of gene targeting and Cre-mediated recombination events. Left, Southern blot of DNA derived from wildtype (wt) and 3' PURO-targeted ES cells (PURO) and digested with *NcoI* and *PvuI*. The blot was hybridized with (external) probe 1, which detects fragments of 9 kb (wildtype allele) and 5.5 kb (PURO-targeted allele). One PURO-targeted clone with the correct karyotype was electroporated with the NEO targeting construct. Middle, blot with *EcoRI*-digested DNA from the original PURO-targeted ES cell clone and from a doubly targeted line (CLIP-T) probed with external probe 2, which detects fragments of 15 kb (PURO allele) and 7.7 kb (CLIP-T allele). One of the CLIP-T ES cell lines was electroporated with a Cre-recombinase construct to obtain the knocked-out *Cyln2* locus (CLIP-L). Cre-mediated recombination is identified (right) by the elimination of the 7.7-kb fragment. c, PCR analysis of wildtype, CLIP-T and CLIP-L alleles. Genomic tail DNA of wildtype, heterozygous and homozygous CLIP-T and CLIP-L mice was subjected to PCR with the indicated cocktails of primers, which yielded the expected fragments in the different genotypes (wildtype, p287–p290: 325 bp; CLIP-L, p287–p260: 450 bp; CLIP-T, p287–p261: 500 bp).



6.1a). In the CLIP-L allele, the *lacZ* reporter gene is located close to exon 2 of *Cyln2*. We engineered a splice acceptor site at the 5' end of the reporter cassette, which spliced onto *Cyln2* exon 2 sequences, generating a hybrid *Cyln2-lacZ* transcript. We obtained germline transmission with both the CLIP-T and CLIP-L alleles and crossed mice back to the C57Bl6 background. Northern-blot experiments on total RNA derived from the brains of these mice demonstrated that *Cyln2* mRNA was expressed from the CLIP-T allele but not from the CLIP-L allele, which expressed *lacZ* instead (Fig. 6.2a). Genes surrounding the *Cyln2* locus (*Wbscr1*, *Rfc2* and *Gtf2ird1*) were not affected by the targeting (data not shown). By western-blot analysis, we demonstrated that CLIP-115 was not produced in homozygous *Cyln2*-knockout mice (*Cyln2*<sup>-/-</sup>), but was produced in reduced amounts in heterozygous mice (*Cyln2*<sup>+/-</sup>) and in normal amounts in wildtype and CLIP-T mice (Fig. 6.2b). Reduction in the amount of CLIP-115 produced by CLIP-L mice did not lead to a significant up-regulation of CLIP-170 (Fig. 6.2b), indicating that there was no compensation by CLIP-170 for the absence of CLIP-115. We used the *lacZ* marker in CLIP-L mice as

**Figure 6.2 Expression of CLIP-115 in CLIP-L and CLIP-T mice.** a, Northern-blot analysis of total brain RNA from wildtype (wt), CLIP-T<sup>+/-</sup>, CLIP-T<sup>-/-</sup>, CLIP-L<sup>+/-</sup> and CLIP-L<sup>-/-</sup> mice. The blot was sequentially hybridized with *Cyln2* (top), *lacZ* (middle) and *Gapd* (bottom) probes. b, Western-blot analysis of brain proteins of wildtype (wt), CLIP-T<sup>+/-</sup>, CLIP-T<sup>-/-</sup>, CLIP-L<sup>+/-</sup> and CLIP-L<sup>-/-</sup> mice, separated by SDS-PAGE on 6% gels. Blots were incubated with antibodies against CLIP-115 (no. 2238), antibodies against CLIP-170 (no. 2360) and antibodies that recognize both CLIP-115 and CLIP-170 (no. 2221). Arrows indicate the position of CLIP-115 and arrowheads the position of CLIP-170. c, Whole-mount CLIP-L<sup>-/-</sup> mouse cerebellum expressing *lacZ*. The *lacZ* expression (corresponding to CLIP-115 expression) is distributed in sagittal bands. d-f, Brain sections of CLIP-L<sup>-/-</sup> mice expressing *lacZ*. Labeling in the hippocampus (Hi) is much more intense than in other areas, such as the cerebral cortex (Co) and amygdala (Ad). A high magnification view of the hippocampus (e) shows intense labeling of the pyramidal cells of the CA1 and CA3 areas and virtually no staining in the dentate gyrus (DG). The cerebellum (f) shows variable *lacZ* expression in the Purkinje cells (PC), consistent with the sagittal pattern in whole mounts. Arrows, Purkinje cells expressing *lacZ*; arrowhead, Purkinje cells not expressing *lacZ*. MO, molecular layer; GC, granular cell layer. g-j, Immunocytochemical staining of brain sections from wildtype (wt; g,i) and knockout (CLIP-L<sup>-/-</sup>; h,j) littermates with antibodies against CLIP-115 (antiserum no. 2238). The sagittal banding pattern of CLIP-115 in the cerebellum cannot be seen in the section in (i), which was chosen to demonstrate the abundant dendritic staining of Purkinje cells.

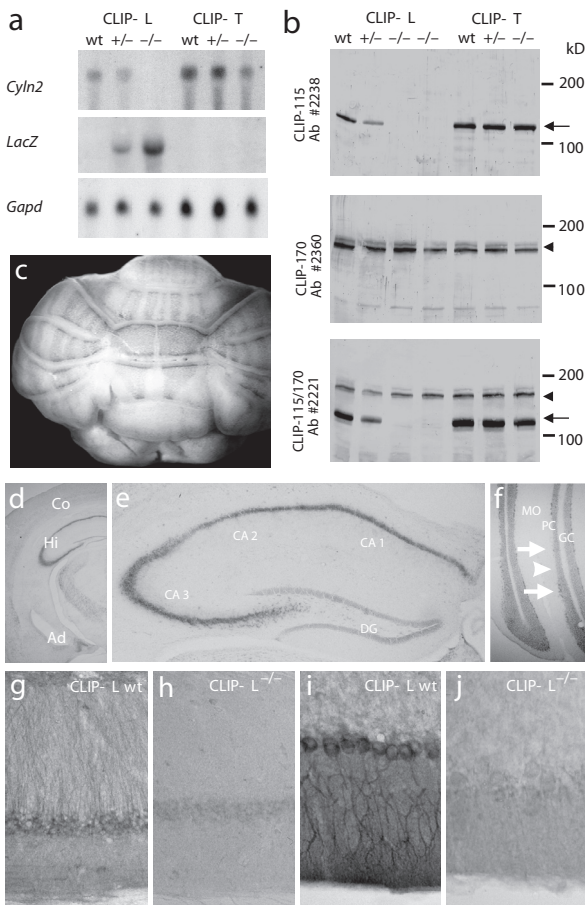


Figure 6.2a shows Northern blot analysis of total brain RNA from wildtype (wt), CLIP-T<sup>+/-</sup>, CLIP-T<sup>-/-</sup>, CLIP-L<sup>+/-</sup> and CLIP-L<sup>-/-</sup> mice. The blot was sequentially hybridized with *Cyln2* (top), *lacZ* (middle) and *Gapd* (bottom) probes. Figure 6.2b shows Western blot analysis of brain proteins of wildtype (wt), CLIP-T<sup>+/-</sup>, CLIP-T<sup>-/-</sup>, CLIP-L<sup>+/-</sup> and CLIP-L<sup>-/-</sup> mice, separated by SDS-PAGE on 6% gels. Blots were incubated with antibodies against CLIP-115 (no. 2238), antibodies against CLIP-170 (no. 2360) and antibodies that recognize both CLIP-115 and CLIP-170 (no. 2221). Arrows indicate the position of CLIP-115 and arrowheads the position of CLIP-170. Figure 6.2c shows a whole-mount CLIP-L<sup>-/-</sup> mouse cerebellum expressing *lacZ*. The *lacZ* expression (corresponding to CLIP-115 expression) is distributed in sagittal bands. Figure 6.2d-f shows brain sections of CLIP-L<sup>-/-</sup> mice expressing *lacZ*. Labeling in the hippocampus (Hi) is much more intense than in other areas, such as the cerebral cortex (Co) and amygdala (Ad). A high magnification view of the hippocampus (e) shows intense labeling of the pyramidal cells of the CA1 and CA3 areas and virtually no staining in the dentate gyrus (DG). The cerebellum (f) shows variable *lacZ* expression in the Purkinje cells (PC), consistent with the sagittal pattern in whole mounts. Arrows, Purkinje cells expressing *lacZ*; arrowhead, Purkinje cells not expressing *lacZ*. MO, molecular layer; GC, granular cell layer. Figure 6.2g-j shows immunocytochemical staining of brain sections from wildtype (wt; g,i) and knockout (CLIP-L<sup>-/-</sup>; h,j) littermates with antibodies against CLIP-115 (antiserum no. 2238). The sagittal banding pattern of CLIP-115 in the cerebellum cannot be seen in the section in (i), which was chosen to demonstrate the abundant dendritic staining of Purkinje cells.



an indicator of *Cyln2* gene activity, either on whole-brain mounts or on 40- $\mu$ m sections of the brain, to identify regional variations in expression levels of CLIP-115. The *lacZ* gene was expressed abundantly in the CA areas of the hippocampus and more moderately in a number of other brain regions, including the amygdala, cerebral cortex and cerebellum (Fig. 6.2c–f). In the hippocampus, the pyramidal cells of the CA1 and CA3 areas were densely labeled, whereas the dentate gyrus was virtually devoid of labeling (Fig. 6.2d,e). In the cerebellum, *lacZ* was expressed in bands, resembling the topographical organization of the olivocerebellar system<sup>22</sup> (Fig. 6.2c,f). Within the cerebellar cortex, *lacZ* was expressed most prominently in the hemispheres and paravermis and relatively weakly in the vestibulocerebellum (data not shown). With longer periods of *lacZ* staining, many other areas of the brain expressed the marker (albeit with comparatively less intensity), and the sagittal pattern of expression in the cerebellum, though still present, became less obvious (data not shown). The *lacZ* staining patterns were consistent with those seen on immunocytochemical analysis in which sections were incubated with antibodies against CLIP-115 (antiserum no. 2238; ref. 23; Fig. 6.2g–j). Electron microscopic analysis of the inferior olive in the *Cyln2*<sup>-/-</sup> mice revealed that the absence of CLIP-115 did not affect the ultrastructure, distribution or density of dendritic lamellar bodies. These data indicate that CLIP-115 is not involved in the transport of dendritic lamellar bodies<sup>9</sup>, as we had originally suggested.

#### **6.4b - Growth deficits and brain abnormalities in *Cyln2*-knockout mice**

Both the CLIP-L and CLIP-T strains of mice were viable and fertile, and offspring derived from heterozygous crosses were born in a normal mendelian ratio (data not shown). Newborn (P1) and adult *Cyln2*-knockout mice had blood calcium levels and total brain weights (including cerebrospinal fluid) comparable to those of wildtype littermates and control CLIP-T mice (Table 1). Calcium levels in postnatal day 14 (P14) wildtype, *Cyln2*<sup>+/-</sup> and *Cyln2*<sup>-/-</sup> mice were also comparable (data not shown). Body weights of adult female *Cyln2*-knockout mice were significantly lower than those of control mice, and those of adult male *Cyln2*-knockout mice were also lower, although this difference was not statistically significant (Table 1 and Fig. 6.3a). The lower body weight in female *Cyln2*-knockout mice was paralleled by shorter body and bone lengths (Fig. 6.3b), suggesting that these mice experienced a general growth deficit. Because growth deficiency in infancy is characteristic of Williams syndrome<sup>1,24</sup>, we examined the growth curves of CLIP-L and CLIP-T mice from two to ten weeks of age (Fig. 6.3c,d). A significant growth retardation was apparent in male and female *Cyln2*<sup>-/-</sup> mice as compared to wildtype littermates and CLIP-T mice. Weights of *Cyln2*<sup>+/-</sup> mice were intermediate between those of wildtype mice and *Cyln2*<sup>-/-</sup> homozygotes. Taken together, these data indicate that haploinsufficiency of *Cyln2* causes a mild growth retardation during the first weeks of postnatal development, an effect that persists in adult female mice. X-ray analysis revealed no obvious craniofacial irregularities in *Cyln2*-knockout mice, and investigation of brain sections stained with hematoxylin and eosin did not show gross abnormalities in brain morphology (data not shown). To investigate whether the mice had subtle macroscopic abnormalities, we carried out high resolution magnetic resonance im-

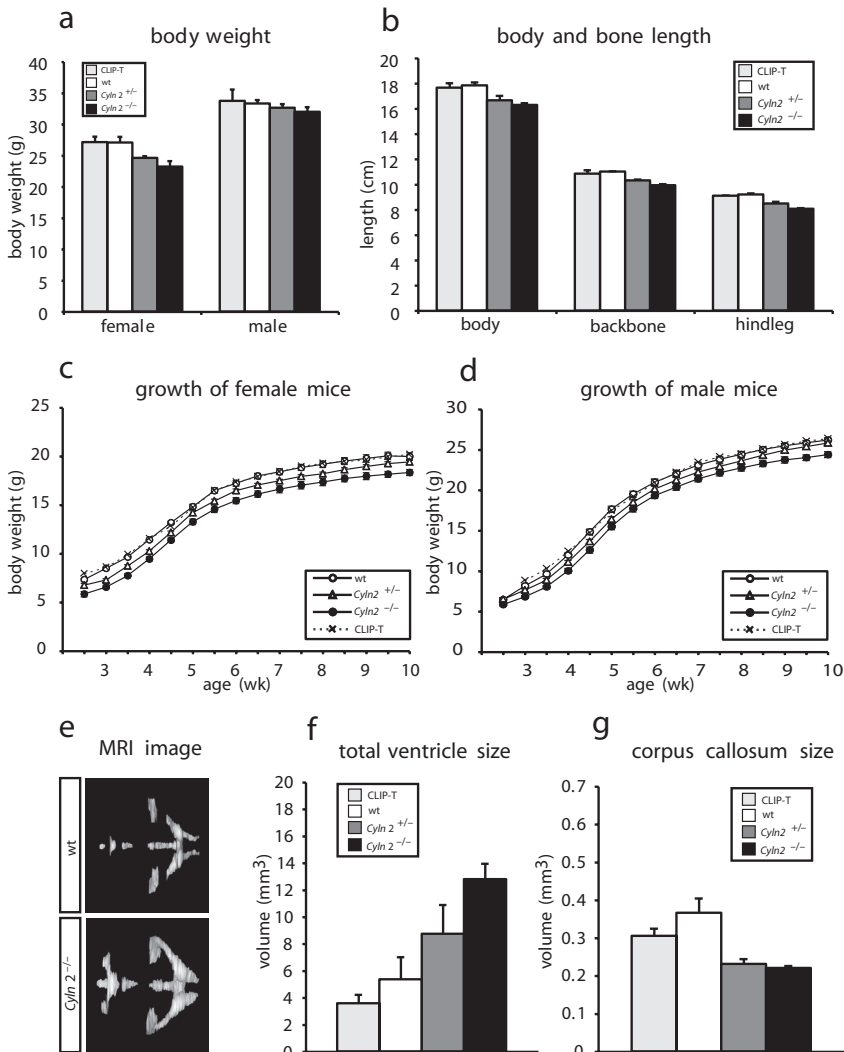


**Figure 6.3 Growth deficiency and brain abnormalities in *Cyn2*-knockout mice.** a, Body weights of adult mice (mean  $\pm$  s.e.m.). Wildtype littermates from the CLIP-L strain (wt; 7 female, 7 male), CLIP-T (11 female, 7 male), CLIP-L<sup>+/-</sup> (*Cyn2*<sup>+/-</sup>; 34 female, 17 male) and CLIP-L<sup>-/-</sup> (*Cyn2*<sup>-/-</sup>; 5 female, 7 male) mice 6.5 months of age were weighed. Heterozygous and homozygous female CLIP-L mice have a lower body weight (9% and 15%, respectively) than their wild-type littermates ( $P < 0.05$ ). CLIP-T mice do not differ significantly from wildtype CLIP-L mice. The body weights of heterozygous and homozygous male CLIP-L mice are not significantly different from those of wildtype littermates, although a trend towards reduced body weight is detected. b, Body and bone length of female wildtype (wt; n = 5), CLIP-L<sup>+/-</sup> (*Cyn2*<sup>+/-</sup>; n = 5), CLIP-L<sup>-/-</sup> (*Cyn2*<sup>-/-</sup>; n = 5) and CLIP-T (n = 5) mice. The body and bone length of 6 month female mice was determined by X-ray analysis. Lengths of total body, backbone and bones in left hind leg were statistically shorter ( $P < 0.05$ ) by 11% in homozygous CLIP-L mice and 7% in heterozygous CLIP-L mice relative to wildtype mice. CLIP-T mice did not differ significantly from wildtype mice of the CLIP-L strain. c, Growth curves of wildtype (wt; n = 15), CLIP-T (n = 24), CLIP-L<sup>+/-</sup> (*Cyn2*<sup>+/-</sup>; n = 40) and CLIP-L<sup>-/-</sup> (*Cyn2*<sup>-/-</sup>; n = 12) female mice. Body weights of the mice were measured twice per week starting at two weeks. Depending on their age, heterozygous and homozygous CLIP-L female mice were 5–14% and 10–22%, respectively, lighter than their wildtype littermates and the CLIP-T mice. Pairwise comparisons showed that the differences in body weight between the genotypes were statistically significant ( $P < 0.005$ ), except between wildtype mice of the CLIP-L strain and mice of the CLIP-T strain. d, Growth curves of wildtype (wt; n = 20), CLIP-T (n = 17), CLIP-L<sup>+/-</sup> (*Cyn2*<sup>+/-</sup>; n = 31) and CLIP-L<sup>-/-</sup> (*Cyn2*<sup>-/-</sup>; n = 23) male mice. Body weights were measured as described above. Depending on their age, heterozygous and homozygous CLIP-L male mice are 2–8% and 7–17%, respectively, lighter than their wildtype littermates and the CLIP-T mice. Pairwise comparisons demonstrated that differences in body weight among the different genotypes were statistically significant ( $P < 0.01$ ), except between wildtype mice of the CLIP-L strain and mice of the CLIP-T strain and between wildtype and heterozygous CLIP-L mice. e, 3D surface rendering of the segmented ventricles in the brain of a wildtype (wt) and *Cyn2*<sup>-/-</sup> mouse. The 3D reconstruction is viewed from above with the anterior at the right. All major ventricles appear enlarged. f, Ventricle size of adult wildtype (wt; n = 4), CLIP-L<sup>+/-</sup> (*Cyn2*<sup>+/-</sup>; n = 4), CLIP-L<sup>-/-</sup> (*Cyn2*<sup>-/-</sup>; n = 4) and CLIP-T mice (n = 4) as determined by high resolution MRI. Ventricle volumes (mean  $\pm$  s.e.m.) of homozygous knockout CLIP-L mice were enlarged compared with wildtype mice ( $P < 0.05$ ). The ventricular volume of heterozygous CLIP-L mice (or CLIP-T mice) was not significantly different from that of wildtype littermates. g, Size of the corpus callosum in wildtype (wt; n = 5), CLIP-L<sup>+/-</sup> (*Cyn2*<sup>+/-</sup>; n = 4), CLIP-L<sup>-/-</sup> (*Cyn2*<sup>-/-</sup>; n = 6) and CLIP-T mice (n = 3). Corpus callosum volumes of the homozygous and heterozygous knockout mice were significantly smaller than those of wildtype mice ( $P < 0.01$ ). Sizes of the corpus callosum in wildtype mice of the CLIP-L and CLIP-T strains did not differ significantly from each other.

aging (MRI) analysis, which allows accurate surface and volume calculations of brain structures. Volumes of the cerebellum, cerebrum, hippocampus and amygdala did not differ significantly between *Cyln2*-knockout and wildtype mice (data not shown). Notably, the average brainventricle volume of *Cyln2*-knockout mice was significantly larger than that of wildtype littermates, and the average corpus callosum volume was significantly smaller (Fig. 6.3e–g). Thus, a reduction in CLIP-115 levels in mice caused mild brain abnormalities.

### 6.4c - Behavioral and physiological analyses of CLIP-L and CLIP-T mouse strains

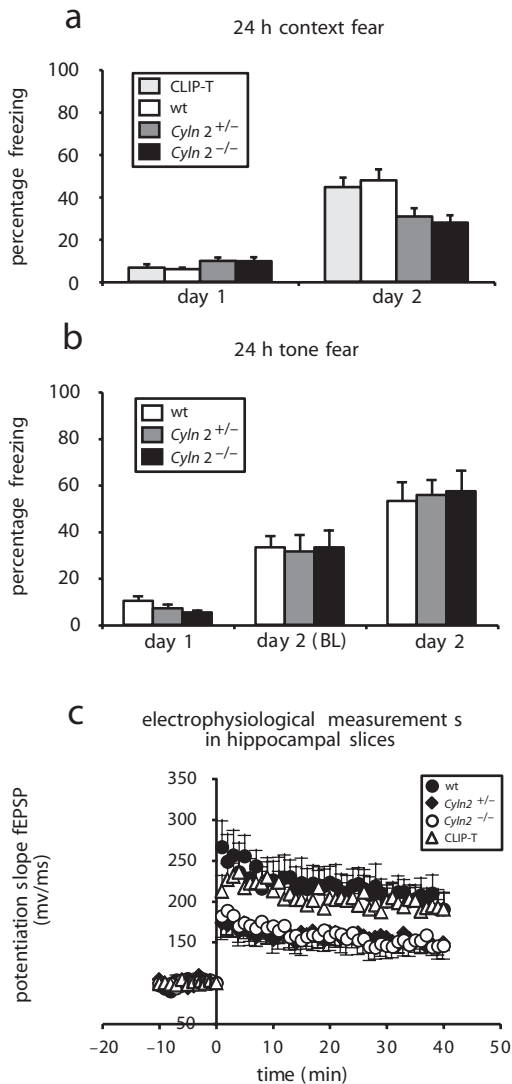
The prominent distribution of CLIP-115 in the hippocampus, amygdala and cerebellum of mice raises the possibility that behavioral functions controlled by these brain regions may be disturbed in *Cyln2*-knockout mice. We assessed this by subjecting the mice to a number of behavioral tests. We investigated the functioning of hippocampus and amygdala with the elevated zero-maze assay and contextual and cued fear-conditioning paradigms. The elevated zero-maze test revealed no differences among *Cyln2*-knockout, CLIP-T and wildtype mice (data not shown), indicating that amygdala functioning was not measurably affected by the deletion of *Cyln2*. In the contextual fear-conditioning experiment, mice were placed in a test cage, subjected to a foot shock and then removed and placed back in the test cage 24 hours later. The amount of time the mice spent ‘freezing’ while in the test cage on each occasion was measured. Wildtype and CLIP-T mice showed a significant increase in the average

**Table 1 • Body weights, brain weights and calcium levels in *cyln2*-knockout and control mice**

Sex/age	Genotype	Sample size (n)	Body weight (g)	Brain weight <sup>a</sup> (mg)	Calcium level (mg/dl serum)
Male					
P1	CLIP-T	11	1.37 ± 0.02	79.0 ± 1.8	9.4 ± 0.7
	wt	11	1.39 ± 0.03	83.7 ± 2.7	9.0 ± 0.5
	CLIP-L <sup>+/-</sup>	19	1.42 ± 0.04	83.2 ± 2.3	9.1 ± 0.4
	CLIP-L <sup>-/-</sup>	4	1.48 ± 0.1	90.1 ± 9.5	9.0 ± 1.6
Adult	CLIP-T	7 (7) <sup>b</sup>	33.7 ± 2.14	ND <sup>c</sup>	ND
	wt	13 (7) <sup>b</sup>	33.3 ± 0.63	ND <sup>c</sup>	9.9 ± 0.2
	CLIP-L <sup>+/-</sup>	11 (17) <sup>b</sup>	32.6 ± 0.65	ND <sup>c</sup>	9.6 ± 0.2
	CLIP-L <sup>-/-</sup>	10 (7) <sup>b</sup>	32.0 ± 0.81	ND <sup>c</sup>	9.5 ± 0.2
Female					
P1	wt	15	1.33 ± 0.02	75.9 ± 1.4	9.8 ± 0.4
	CLIP-L <sup>+/-</sup>	7	1.38 ± 0.07	81.0 ± 2.8	9.5 ± 1.2
	CLIP-L <sup>-/-</sup>	14	1.34 ± 0.04	76.8 ± 2.3	9.5 ± 0.7
	CLIP-T	12	1.44 ± 0.05	85.6 ± 3.2	9.2 ± 0.5
Adult	wt	19 (11) <sup>b</sup>	27.40 ± 0.84	476.0 ± 5.9	ND
	CLIP-L <sup>+/-</sup>	8 (7) <sup>b</sup>	27.07 ± 0.94	476.3 ± 8.7	10.2 ± 0.2
	CLIP-L <sup>-/-</sup>	13 (34) <sup>b</sup>	24.61 ± 0.30 <sup>d</sup>	ND	10.0 ± 0.2
		14 (5) <sup>b</sup>	23.20 ± 0.95 <sup>d</sup>	481.1 ± 6.8	10.1 ± 0.2

Data are expressed as mean ± s.e.m. ND, not determined. <sup>a</sup>Includes cerebrum, cerebellum and brain stem. <sup>b</sup>The number of adult mice used for body weight determination differs from that used for the other analyses and is indicated between brackets. <sup>c</sup>Mice were reserved for MRI analysis. <sup>d</sup>Values are significantly different from wild type ( $P < 0.05$ ), as determined by one-way ANOVA.

**Figure 6.4 Hippocampal deficits in *Cyln2*-knockout mice.** a, 24 h contextual fearconditioning test in CLIP-T (n = 10), wildtype (wt; n = 17), *Cyln2*<sup>+/-</sup> (n = 19) and *Cyln2*<sup>-/-</sup> (n = 16) mice. Percentage freezing time (mean ± s.e.m.) is shown at day 1 (baseline activity before foot shock) and day 2 (24 h after foot shock). There is no significant difference in freezing behavior among groups of mice during the baseline period. At 24 h after the foot shock, all mice freeze significantly more than on day 1 (P < 0.05), yet both heterozygous and homozygous CLIP-L mice exhibit a significant deficit in freezing relative to wildtype mice (P < 0.05). Wildtype mice from the CLIP-L strain and mice from the CLIP-T strain show no significant difference in freezing time. b, 24 h cued fear-conditioning test in wildtype (wt; n = 7), *Cyln2*<sup>+/-</sup> (n = 11) and *Cyln2*<sup>-/-</sup> (n = 11) mice. Percentage freezing time (mean ± s.e.m.) is shown at day 1 (before foot shock and tone) and at day 2 before (baseline, BL) and after tone. There is no significant difference in the percentage freezing time among different genotypes at any time point measured. c, Hippocampal long-term potentiation induced by theta-burst stimulation. Hippocampal slices from CLIP-T mice (n = 10) and wildtype (wt; n = 7), *Cyln2*<sup>+/-</sup> (n = 6) and *Cyln2*<sup>-/-</sup> (n = 8) mice were stimulated at 0.0166 Hz while fEPSPs were recorded from CA1 dendritic fields. After 10 min of baseline, slices were stimulated using a theta-burst stimulation paradigm followed by 40 min of 0.0166 Hz recording. Synaptic plasticity in the hippocampal CA1 area is lower in heterozygous and homozygous knockout mice than in wildtype mice (P < 0.05). Wildtype mice from the CLIP-L strain and mice from the CLIP-T strain show no significant differences from one another.



amount of time spent freezing when they were placed back in the test cage 24 hours after foot shock (Fig. 6.4a). Both the *Cyln2*<sup>+/-</sup> and *Cyln2*<sup>-/-</sup> mutants also showed an increase in average freezing time, but this increase was significantly smaller than that observed in control mice (Fig. 6.4a). In the cued fear-conditioning test, mice were placed in a conditioning chamber, where they received a cue followed by a foot shock. They were then removed, and after 24 hours were placed in a different chamber where they received the same cue but no foot shock. The amount of time the mice spent freezing was measured on each occasion. Mutant and control mice behaved similarly in this test, showing increased freezing time in response to the cue when placed in a different environment (Fig. 6.4b). Because lesions in the hippocampus affect contextual fear conditioning, whereas lesions in the amygdala affect both contextual and cued fear conditioning<sup>25-27</sup>, the data from the zero-maze and fear-conditioning tests suggest that absence of CLIP-115 affects hippocampal de-

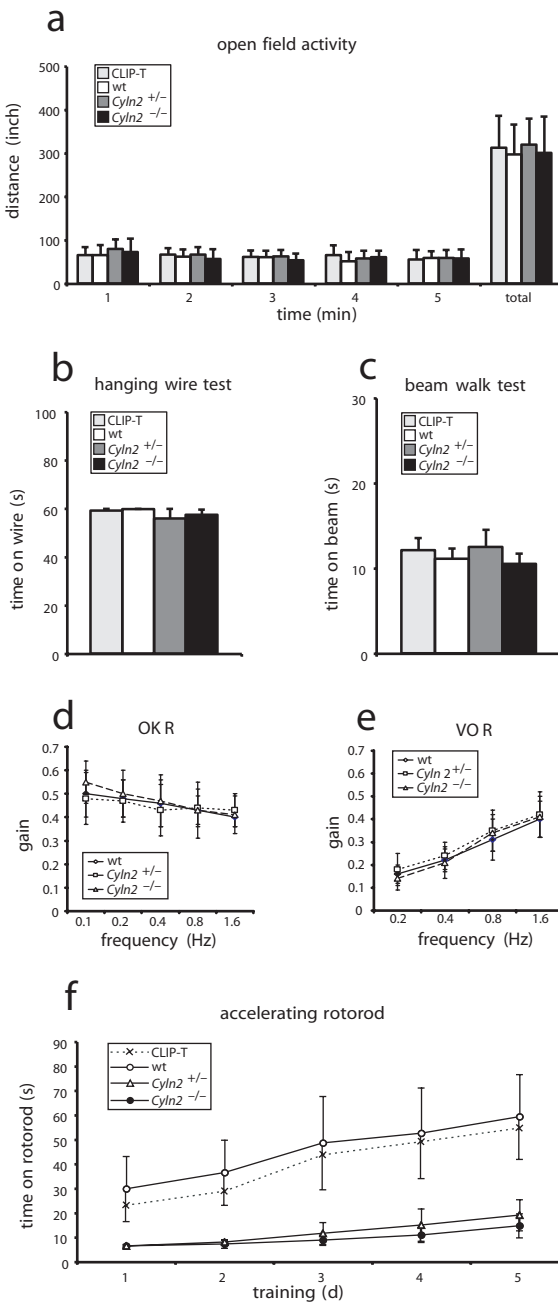


**Figure 6.5 Motor coordination in *Cyln2*-knockout mice.** a, Spontaneous locomotion. Movements of CLIP-T (n = 13), wildtype (wt; n = 11), CLIP-L <sup>+/-</sup> (*Cyln2*<sup>+/-</sup>; n = 24) and CLIP-L <sup>-/-</sup> (*Cyln2*<sup>-/-</sup>; n = 13) mice were monitored during 1-min intervals (mean ± s.e.m.) in an open-field activity test. No differences among mouse lines were observed. b, Hanging wire test. To measure balance and grip strength of CLIP-T (n = 7), wildtype (wt; n = 7), CLIP-L <sup>+/-</sup> (*Cyln2*<sup>+/-</sup>; n = 10) and CLIP-L <sup>-/-</sup> (*Cyln2*<sup>-/-</sup>; n = 8) mice, a hanging wire test was carried out. Time on the wire was recorded up to a maximum of 60 s. No differences among mouse lines were observed. c, Beamwalk test. CLIP-T (n = 7), wildtype (wt; n = 7), CLIP-L <sup>+/-</sup> (*Cyln2*<sup>+/-</sup>; n = 10) and CLIP-L <sup>-/-</sup> (*Cyln2*<sup>-/-</sup>; n = 8) mice were tested for basic motor coordination and balance by measuring their ability to cross a wooden beam. The time required to cross the beam was equivalent between the groups of mice. d,e, Compensatory eye movements. The compensatory eye movements of wildtype (wt; n = 4), CLIP-L <sup>+/-</sup> (*Cyln2*<sup>+/-</sup>; n = 2) and CLIP-L <sup>-/-</sup> (*Cyln2*<sup>-/-</sup>; n = 4) mice were tested during visual or vestibular stimulation at frequencies varying from 0.1 to 1.6 Hz. At a peak velocity of 8°s<sup>-1</sup>, the average gain of the optokinetic reflex ranged from 0.40 to 0.50 in the wildtype mice, from 0.43 to 0.48 in the homozygous knockout mice, and from 0.41 to 0.55 in the heterozygous mice. At an amplitude of 10°, the average gain of the vestibulo-ocular reflex ranged from 0.16 to 0.40 in the wildtype mice, from 0.18 to 0.42 in the homozygous knockout mice and from 0.14 to 0.41 in the heterozygotes. Thus, the gain values of the various strains did not differ for any stimulus paradigm tested. f, Accelerating rotarod test. To measure more complicated motor behaviors and a form of motor learning, CLIP-T (n = 7), wildtype (wt; n = 7), CLIP-L <sup>+/-</sup> (*Cyln2*<sup>+/-</sup>; n = 10) and CLIP-L <sup>-/-</sup> (*Cyln2*<sup>-/-</sup>; n = 8) mice were subjected to the rotarod test, in which they were tested for their ability to stay on the rotarod. A repeated-measures ANOVA, including all four genotypes, showed a significant block effect for genotype (P < 0.05). Pairwise comparisons showed that both the heterozygous and homozygous CLIP-L mice had a significant performance deficit, relative to wildtype mice of the CLIP-L strain and mice of the CLIP-T strain (P < 0.05). Whereas the latter strains improved their performance during the training period (P < 0.05), both the heterozygous and homozygous CLIP-L mice did not significantly increase performance levels.

pendent memory processes. We therefore examined hippocampal synaptic plasticity in *Cyln2*<sup>+/-</sup> and *Cyln2*<sup>-/-</sup> mice by studying long-term potentiation, a prominent cellular model of learning and memory formation. In support of our behavioral data, we found that synaptic plasticity in the hippocampal CA1 area was significantly lower in both *Cyln2*<sup>+/-</sup> and *Cyln2*<sup>-/-</sup> mice than in wildtype and CLIP-T mice (Fig. 6.4c). Taken together, these behavioral and electrophysiological data strongly suggest that hippocampal synaptic function is affected in *Cyln2*-knockout mice.

In a second series of behavioral tests, we examined motor behavior in control and mutant mice. In the open-field activity test, the *Cyln2*-knockout mice performed similarly to control mice (Figure 6.5a), indicating that spontaneous locomotor activity was not affected by reduced CLIP-115 levels. Because the expression of CLIP-115 in the cerebellum was variable, we subjected *Cyln2*-knockout mice to more subtle tests of motor coordination, each addressing a specific cerebellar function controlled by a particular cerebellar area. These investigations included recordings of compensatory eye movements to investigate the vestibulocerebellum, the hanging wire and beam-walk tests to investigate the cerebellar vermis, and coordination tests on the accelerating rotorod to investigate the cerebellar hemispheres and paravermis<sup>28-31</sup>. The cerebellar vermis, which controls proximal musculature involved in balance, was functionally intact, as the *Cyln2*-knockout mice demonstrated normal performance on the hanging wire test (Figure 6.5b) and the horizontal and vertical beam-walk tests (Fig. 6.5c and data not shown).

The vestibulocerebellum was also not impaired in *Cyln2*-knockout mice, because the gain and phase values of both the optokinetic and vestibulo-ocular reflex were normal, and the adaptation of the vestibulo-ocular reflex was also adequate (Fig. 6.5d,e and data not shown). Both *Cyln2*<sup>+/-</sup> and *Cyln2*<sup>-/-</sup> mice remained on the accelerating rotorod for significantly shorter periods than did control mice (Fig. 6.5f). Consistent with this, *Cyln2*-knockout mice showed poor initial coordination on a running wheel, resulting in highly erratic motions and occasional ejection from the wheel (see Web Movies online). Taken together, these results suggest that the CLIP-L mutant mice were not ataxic, but that their motor coordination was impaired when the function of the cerebellar hemispheres and paravermis was challenged.

#### **6.4d - Cell biological analysis of CLIP-115 deficiency**

To analyze the effect of CLIP-115 deficiency on microtubule dynamics and protein distribution at microtubule tips, we derived embryonic and adult primary cultured fibroblasts from *Cyln2*- knockout mice and wildtype littermates and from the CLIP-T strain. We chose fibroblasts instead of cultured hippocampal neurons for our analysis because it is difficult to analyze individual microtubules in the narrow dendritic and axonal compartments, and we have shown that both CLIP-170 and CLIP-115 are expressed in cultured fibroblasts<sup>12</sup>. Injection of Cy3-labeled tubulin into fibroblasts and measurement of microtubule dynamic events by fluorescence microscopy in living cells showed no significant differences between knockout cells and wildtype fibroblasts in the rates of microtubule growth and shrinkage or in the frequencies of catastrophe (transition from a growing microtubule to a shrinking one) and rescue (transition from a shrinking microtubule to a growing one; data not shown). Transfection of adult and embryonic fibroblasts with green fluorescent protein-tagged EB3-GFP, a marker that specifically associates with the ends of growing microtubules in living cells (T. Stepanova, A.A., C.C.H., F.G. and N.G., unpublished data), revealed similar microtubule growth rates in knockout cells ( $0.51 \pm 0.10 \mu\text{m s}^{-1}$ , 159 microtubule plus-ends measured, derived from 17 cells in 3 independent experiments) and wildtype fibroblasts ( $0.47 \pm 0.10 \mu\text{m s}^{-1}$ , 133 microtubule plus-ends



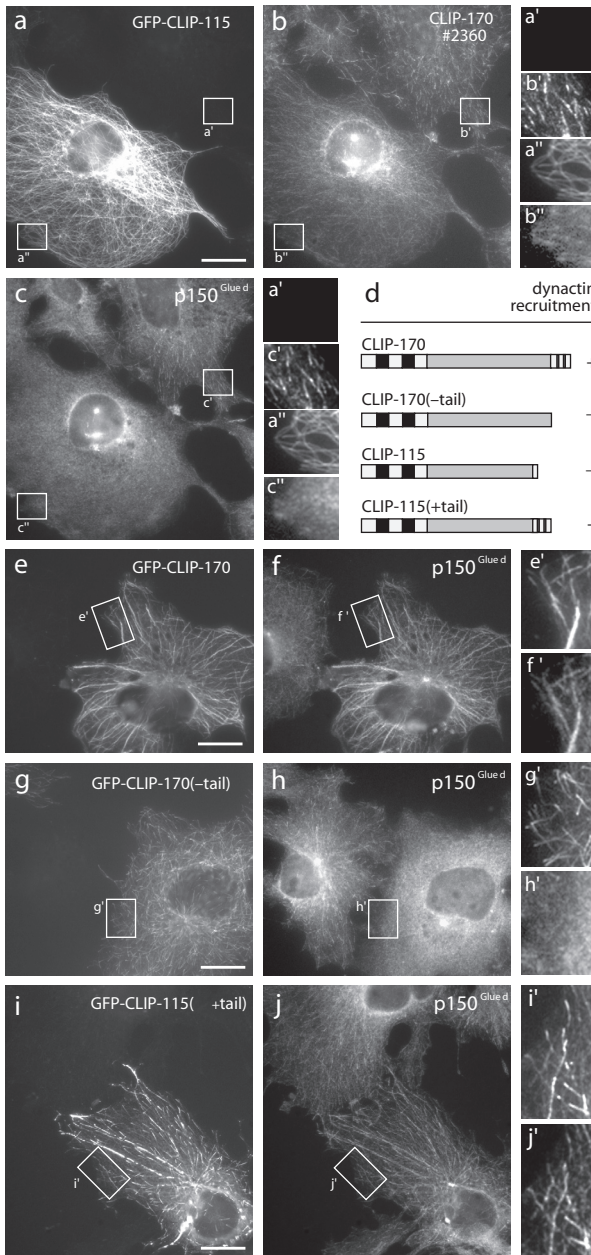


**Figure 6.6 Competition between CLIP-115 and CLIP-170 at microtubule plus-ends.** a–c, COS-1 cells were transfected with GFP–CLIP-115 (GFP signal in a) and cells were stained with antibodies against CLIP-170 (no. 2360; b) and an antibody against p150<sup>Glued</sup> (c). Both endogenous proteins are displaced from microtubule tips by GFP–CLIP-115. d, Summary of endogenous dynactin recruitment to (+) or displacement from (–) microtubule tips by the different overexpression constructs as demonstrated by staining with an antibody against p150<sup>Glued</sup>. e–j, COS-1 cells were transfected with GFP–CLIP-170 (e,f), GFP–CLIP-170(–tail) (g,h) or GFP–CLIP-115(+tail) (i,j). GFP signals are shown in e, g and i. Cells were stained for endogenous dynactin (f,h,j). In all panels, insets are enlarged to better show the presence or absence of microtubule plus-end staining. Bar, 10  $\mu$ m in all panels.

measured, derived from 14 cells in 3 independent experiments). Thus, absence of CLIP-115 did not significantly affect microtubule growth rates, as measured by two independent methods, or overall microtubule dynamic events, as measured by Cy3–tubulin injection in living cells. Furthermore, stabilized microtubule arrays formed normally in cells at the edge of a wounded monolayer in *Cyln2*-knockout fibroblasts, suggesting that CLASP function was not measurably compromised in these cells. We have previously shown that CLIP-115 tagged with green fluorescent protein (GFP–CLIP-115) and CLIP-170 tagged with hemagglutinin (HA–CLIP-170) are detected at the same microtubule distal ends<sup>23</sup>. Because these proteins have highly similar microtubule-binding domains, we tested the possibility that CLIPs actually compete for binding sites at growing microtubule distal ends. Expression of GFP–CLIP-115 in COS-1 cells displaced endogenous CLIP-170 from microtubule tips (Fig. 6.6a,b), supporting the hypothesis of competition. The dynactin component p150<sup>Glued</sup> was also displaced in these cells (Fig. 6.6c), consistent with the notion that CLIP-170 and the dynein–dynactin motor system work in concert at microtubule plus-ends<sup>14,15</sup>. In line with these observations, overexpression of GFP–CLIP-170 recruited p150<sup>Glued</sup> to distal microtubule

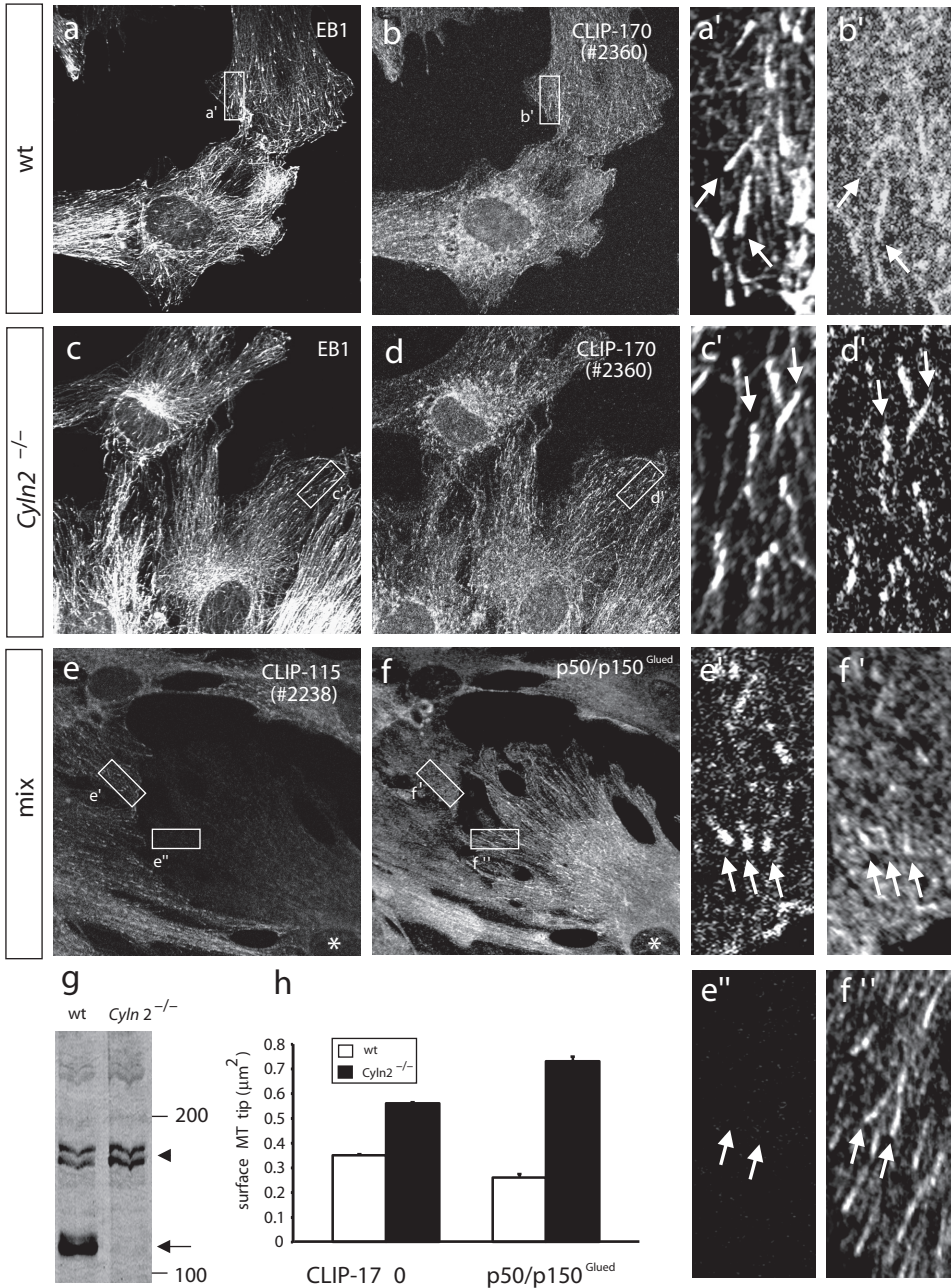


segments (Fig. 6.6e,f). Overexpression of a mutant GFP–CLIP-170 (named GFP–CLIP-170(-tail)) in which the last 79 amino acids were removed resulted in removal of dynactin from the microtubule plus-ends as a result of dislocation of endogenous CLIP-170 by mutant GFP–CLIP-170 (Fig. 6.6g,h). Thus, overexpressed GFP–CLIP-170(-tail) behaved like GFP–CLIP-115 in its effect on p150<sup>Glued</sup>, supporting the hypothesis that the C-terminal metal-binding motif of CLIP-170 is important in the interaction with dynactin<sup>14,15</sup>. By contrast, when the final 159 amino acids of the C-terminal domain of CLIP-170 were transferred to the end of GFP–CLIP-115 (GFP–CLIP-115(+tail)), this fusion protein recruited the dynactin complex to plusends (Fig. 6.6i, j). These results indicate that the last 159 amino acids of CLIP-170 were sufficient to confer to CLIP-115 the capacity to relocalize dynactin.

Notably, we detected greater CLIP-170 staining at microtubule tips in *Cyln2*-knockout fibroblasts than in wildtype cells (Fig. 6.7b,d). The average CLIP-170 staining per microtubule tip was 1.6 times greater in knockout than in wildtype cells (Fig 6.7h), but varied considerably between individual microtubule ends. In contrast, the distribution of EB1, a specific marker of growing microtubule plus-ends with no similarity to the CLIPs, was similar in wildtype and knockout cells (Fig 6.7a,c). The localization of the dynactin complex, as measured with antibodies against p150<sup>Glued</sup> and p50 (dynamitin), was markedly different in knockout and wildtype cells. Average dynactin staining per microtubule tip in *Cyln2*-knockout cells was 2.8 times greater than in wildtype fibroblasts (Fig 6.7e,f,h). The higher level of dynactin at microtubule tips was not due to different cell culture conditions, because the differential staining pattern was clearly visible in experiments where *Cyln2*-knockout fibroblasts were mixed with wildtype cells (Fig 6.7e,f). Similar observations were made in embryonic and adult *Cyln2*-knockout fibroblasts (data not shown). The greater staining at microtubule tips was not due to greater total levels of CLIP-170 or dynactin in knockout fibroblasts, as demonstrated by western blotting (Fig 6.7i and data not shown). To our knowledge, this is the first documentation of differences in protein distribution at microtubule distal ends in cells with endogenous levels of protein (that is, without overexpression).

## 5.5 Discussion

Although the deletion region common in Williams syndrome has been characterized in detail<sup>3,4</sup> and a firm linkage between mutations in *ELN* and cardiovascular abnormalities has been established<sup>5,6</sup>, the genes that, when mutated, contribute to neurodevelopmental aspects of Williams syndrome have not been clearly defined. The neurological symptoms and behavioral profile of individuals affected with Williams syndrome are very similar between individuals, and finding the genes associated with this phenotype is of considerable interest, as they might reveal molecular mechanisms underlying basic neuronal functioning. Here, we show that a reduced level of CLIP-115 in mice results in a mild growth deficit, brain abnormalities and specific behavioral and neurophysiological deficits. As discussed below, defects in *Cyln2*-knockout mice resemble deficiencies in individuals with Williams syndrome. As in Williams syndrome, these deficits are apparent in heterozygous knockout mice. Tak-



en together, our data strongly suggest that haploinsufficiency for *CYLN2* in humans underlies some of the developmental, neurological and behavioral abnormalities observed in Williams syndrome. This conclusion is supported by studies of rare individuals with small deletions in the WSCR<sup>3,4,8</sup>. Differences in genetic background are known to cause significant variations in behavior and brain physiology<sup>32,33</sup>. This complicated the interpretation of behavioral and electrophysiological results in our mouse gene-targeting studies, in which the genetic background surrounding the targeted allele (129sv-derived) is different from that surrounding the wildtype allele (C57B16-derived). Because the gene number and order of the WSCR in humans is conserved in mice<sup>20</sup>, a mutation impairing the function of any gene in the 129sv-derived genomic region surrounding the *Cyln2* locus might theoretically give rise to a Williams syndrome-like phenotype in the CLIP-L mice. To avoid misinterpretations, we generated an inducible, rather than a conventional, *Cyln2*-knockout allele. This strategy has allowed us to use as controls not only wildtype littermates of the CLIP-L mice, but also mice of the CLIP-T strain, in which *Cyln2* is expressed but the genomic region surrounding the *Cyln2* locus is 129sv-derived as in the CLIP-L strain. Thus, the phenotypes we observe are not due to genetic background differences in the region surrounding the *Cyln2* locus, but can be directly attributed to the absence of CLIP-115. Although CLIP-115 is not essential for life, the growth deficiency in *Cyln2*<sup>+/-</sup> and *Cyln2*<sup>-/-</sup> mice indicates that this protein may be necessary for proper mouse development. A postnatal growth deficiency has been documented in individuals affected with Williams syndrome<sup>1,24</sup>. The MRI data from *Cyln2*-knockout mice indicate that a reduction in CLIP-115 levels also affects the morphology of the adult mouse brain. Whether this is due to aberrant development, absence of CLIP-115 in the adult brain or both remains to be investigated. It is noteworthy that the volume of cerebrospinal fluid in individuals with Williams syndrome increases with age relative to controls<sup>34</sup>. This result correlates with the enlarged ventricle size detected in adult *Cyln2*-knockout mice. MRI studies have also documented a smaller total brain volume in individuals with Williams syndrome relative to controls, with white matter affected more than gray matter<sup>34</sup>. We did not find evidence for smaller brains in adult *Cyln2*-knockout mice, either by MRI or by weighing the brains. It is remarkable, however, that the corpus callosum (which represents one of the main white-matter tracts of the brain) is smaller in homozygous *Cyln2*-knockout mice than in wildtype mice. A recent report documents the same phenotype in individuals with Williams syndrome<sup>35</sup>. Together, these data suggest that the deficiency of CLIP-115 underlies a considerable proportion of the neurodevelopmental problems associated with Williams syndrome. Tests of behavioral and electrophysiological performance indicated that functions controlled by the hippocampus are disturbed in CLIP-L mice. These results correlate with behavioral data on individuals with Williams syndrome, who score poorly on spatial cognition tests<sup>36</sup>. In addition, both *Cyln2*-knockout mice and individuals with Williams syndrome have difficulties executing specific motor tasks, although neither group is ataxic. Thus, in the behavioral models tested, we find a correlation between the dysfunctions of *Cyln2*-knockout mice and individuals with Williams syndrome. Furthermore, there is a good correlation between impaired behavior in mice and the level of expression of CLIP-115 in the specific brain re-

gion that controls this behavior. Studies using crosses between CLIP-T mice and tissue-specific Cre-recombinase transgenes should allow a more detailed analysis of the developmental, acute and spatial consequences of CLIP-115 deficiency in mice. Immunocytochemistry studies on mouse brain sections using CLIP-170-specific antibodies revealed that in many areas of the brain, including the CA areas of the hippocampus, CLIP-115 and CLIP-170 were co-expressed (C.C.H., A.A., C.I.D.Z., F.G. and N.G., manuscript in preparation). To explain the brain phenotype of the *Cyln2*-knockout mice, one must therefore consider that CLIP-170 may partially compensate for the absence of CLIP-115. This would help explain, for example, why CLASP localization and microtubule dynamics are not disrupted in *Cyln2*-knockout cells. On the other hand, our data from cultured fibroblasts indicate that deletion of *Cyln2* actually results in an accumulation of CLIP-170 and dynactin at microtubule tips. Thus, CLIP-115 normally competes with CLIP-170 and dynactin for binding sites at the distal ends of growing microtubules. Dynactin distribution at microtubule tips may be influenced both by direct competition with CLIP-115 (it has CLIP-like microtubule-binding domains) and by indirect effects on CLIP-170 (refs 14, 15). Our data indicate that the cytoplasmic concentration of CLIP-170 in normal cells is in excess of the total amount of available plus-end binding sites, such that when CLIP-115 is absent, there is sufficient cytoplasmic CLIP-170 to occupy more binding sites. It has been proposed that the microtubule-tip localization of CLIP-170 and dynactin enables dynein-bound cargo to attach to microtubules and be transported to the minus-ends<sup>15</sup>. We have recently shown that CLIP-170 interacts with LIS1 through its metal-binding C-terminal domain<sup>16</sup>. Mutations in the gene LIS1 give rise to lissencephaly, a severe brain disorder<sup>17</sup>, and detailed analysis of the LIS1 protein has shown that it is essential for nuclear migration and, like dynactin, modulates dynein function<sup>37</sup>. Our data suggest that, although direct interactions of CLIP-115 with CLIP-170, LIS1 or dynactin have not been documented, the actions of these proteins might still be compromised in *Cyln2*-knockout cells. It will therefore be of interest to consider dynein motor perturbations, in addition to a loss of CLIP-115-specific functions, when further investigating disturbed molecular processes in *Cyln2*-knockout mice and individuals with Williams syndrome.

#### Acknowledgments

We would like to thank G. van Cappellen for his help with the quantification of the fluorescence data and live imaging analysis, M. Rutteman for x-gal staining experiments and A. Langeveld for FISH experiments. This research was supported by the Netherlands Organization for Scientific Research (NWO) and the Royal Dutch Academy of Sciences (KNAW).



## 5.6 references

1. Morris, C.A., Demsey, S.A., Leonard, C.O., Dilts, C. & Blackburn, B.L. Natural history of Williams syndrome: physical characteristics. *J. Pediatr.* 113, 318–326 (1988).
2. Bellugi, U., Lichtenberger, L., Mills, D., Galaburda, A. & Korenberg, J.R. Bridging cognition, the brain and molecular genetics: evidence from Williams syndrome. *Trends Neurosci.* 22, 197–207 (1999).
3. Francke, U. Williams-Beuren syndrome: genes and mechanisms. *Hum. Mol. Genet.* 8, 1947–1954 (1999).
4. Osborne, L.R. Williams-Beuren syndrome: unraveling the mysteries of a microdeletion disorder. *Mol. Genet. Metab.* 67, 1–10 (1999).
5. Tassabehji, M. et al. Elastin: genomic structure and point mutations in patients with supravalvular aortic stenosis. *Hum. Mol. Genet.* 6, 1029–1036 (1997).
6. Olson, T.M. et al. A 30 kb deletion within the elastin gene results in familial supravalvular aortic stenosis. *Hum. Mol. Genet.* 4, 1677–1679 (1995).
7. Frangiskakis, J.M. et al. LIM-kinase1 hemizyosity implicated in impaired visuospatial constructive cognition. *Cell* 86, 59–69 (1996).
8. Tassabehji, M. et al. Williams syndrome: use of chromosomal microdeletions as a tool to dissect cognitive and physical phenotypes. *Am. J. Hum. Genet.* 64, 118–125 (1999).
9. De Zeeuw, C.I. et al. CLIP-115, a novel brain-specific cytoplasmic linker protein, mediates the localization of dendritic lamellar bodies. *Neuron* 19, 1187–1199 (1997).
10. Schuyler, S.C. & Pellman, D. Microtubule “plus-end-tracking proteins”: the end is just the beginning. *Cell* 105, 421–424 (2001).
11. Perez, F., Diamantopoulos, G.S., Stalder, R. & Kreis, T.E. CLIP-170 highlights growing microtubule ends in vivo. *Cell* 96, 517–527 (1999).
12. Akhmanova, A. et al. Clasps are CLIP-115 and -170 associating proteins involved in the regional regulation of microtubule dynamics in motile fibroblasts. *Cell* 104, 923–935 (2001).
13. Brunner, D. & Nurse, P. CLIP170-like tip1p spatially organizes microtubular dynamics in fission yeast. *Cell* 102, 695–704 (2000).
14. Valetti, C. et al. Role of dynactin in endocytic traffic: effects of dynamitin overexpression and colocalization with CLIP-170. *Mol. Biol. Cell* 10, 4107–4120 (1999).
15. Vaughan, K.T., Tynan, S.H., Faulkner, N.E., Echeverri, C.J. & Vallee, R.B. Colocalization of cytoplasmic dynein with dynactin and CLIP-170 at microtubule distal ends. *J. Cell Sci.* 112, 1437–1447 (1999).

16. Reiner, O. et al. Isolation of a Miller-Dieker lissencephaly gene containing G protein  $\beta$ -subunit-like repeats. *Nature* 364, 717–721 (1993).
17. Coquelle, F.M. et al. LIS1, CLIP-170's key to the dynein/dynactin pathway. *Mol. Cell. Biol.* 22, 3089–3102 (2002).
18. Hoogenraad, C.C. et al. The murine *CYLN2* gene: genomic organization, chromosome localization, and comparison to the human gene that is located within the 7q11.23 Williams syndrome critical region. *Genomics* 53, 348–358 (1998).
19. Osborne, L.R. et al. Identification of genes from a 500-kb region at 7q11.23 that is commonly deleted in Williams syndrome patients. *Genomics* 36, 328–336 (1996).
20. Valero, M.C., de Luis, O., Cruces, J. & Perez Jurado, L.A. Fine-scale comparative mapping of the human 7q11.23 region and the orthologous region on mouse chromosome 5G: the low-copy repeats that flank the Williams-Beuren syndrome deletion arose at breakpoint sites of an evolutionary inversion(s). *Genomics* 69, 1–13 (2000).
21. Peoples, R. et al. A physical map, including a BAC/PAC clone contig, of the Williams-Beuren syndrome–deletion region at 7q11.23. *Am. J. Hum. Genet.* 66, 47–68 (2000).
22. Voogd, J. & Glickstein, M. The anatomy of the cerebellum. *Trends Neurosci.* 21, 370–375 (1998).
23. Hoogenraad, C.C., Akhmanova, A., Grosveld, F., De Zeeuw, C.I. & Galjart, N. Functional analysis of CLIP-115 and its binding to microtubules. *J. Cell Sci.* 113, 2285–2297 (2000).
24. Pankau, R., Partsch, C.J., Gosch, A., Oppermann, H.C. & Wessel, A. Statural growth in Williams-Beuren syndrome. *Eur. J. Pediatr.* 151, 751–755 (1992).
25. Bourchuladze, R. et al. Deficient long-term memory in mice with a targeted mutation of the cAMP-responsive element-binding protein. *Cell* 79, 59–68 (1994).
26. Kim, J.J. & Fanselow, M.S. Modality-specific retrograde amnesia of fear. *Science* 256, 675–677 (1992).
27. Phillips, R.G. & LeDoux, J.E. Differential contribution of amygdala and hippocampus to cued and contextual fear conditioning. *Behav. Neurosci.* 106, 274–285 (1992).
28. Armstrong, D.M. Supraspinal contributions to the initiation and control of locomotion in the cat. *Prog. Neurobiol.* 26, 273–361 (1986).
29. Bloedel, J.R. & Courville, J. *Handbook of Physiology Vol. II: Motor Control. A Review of Cerebellar Afferent Systems* 735–830 (Williams & Wilkins, Baltimore, 1981).
30. De Zeeuw, C.I. et al. Expression of a protein kinase C inhibitor in Purkinje cells blocks cerebellar LTD and adaptation of the vestibulo-ocular reflex. *Neuron* 20, 495–508 (1998).
31. De Zeeuw, C.I. et al. Microcircuitry and function of the inferior olive. *Trends Neurosci.* 144

- 21, 391–400 (1998).
32. Silva, A.J. et al. Mutant mice and neuroscience: recommendations concerning genetic background. Banbury Conference on genetic background in mice. *Neuron* 19, 755–759 (1997).
33. Tarantino, L.M., Gould, T.J., Druhan, J.P. & Bucan, M. Behavior and mutagenesis screens: the importance of baseline analysis of inbred strains. *Mamm. Genome* 11, 555–564 (2000).
34. Reiss, A.L. et al. IV. Neuroanatomy of Williams syndrome: a high-resolution MRI study. *J. Cogn. Neurosci.* 12, 65–73 (2000).
35. Schmitt, J.E., Eliez, S., Warsofsky, I.S., Bellugi, U. & Reiss, A.L. Corpus callosum morphology of Williams syndrome: relation to genetics and behavior. *Dev. Med Child Neurol.* 43, 155–159 (2001).
36. Bellugi, U., Lichtenberger, L., Jones, W., Lai, Z. & St George, M.I. The neurocognitive profile of Williams syndrome: a complex pattern of strengths and weaknesses. *J. Cogn. Neurosci.* 12, 7–29 (2000).
37. Vallee, R.B., Tai, C. & Faulkner, N.E. LIS1: cellular function of a disease-causing gene. *Trends Cell Biol.* 11, 155–160 (2001).
38. Jaegle, M. et al. The POU factor Oct-6 and Schwann cell differentiation. *Science* 273, 507–510 (1996).
39. Sambrook, J., Fritsch, E.F. & Maniatis, T. *Molecular Cloning: A Laboratory Manual* 2nd edn (Cold Spring Harbor Laboratory Press, Cold Spring Harbor, New York, 1989).
40. Kooy, R.F. et al. Neuroanatomy of the fragile X knockout mouse brain studied using in vivo high resolution magnetic resonance imaging. *Eur. J. Hum. Genet.* 7, 526–532 (1999).
41. Fransen, E. et al. L1 knockout mice show dilated ventricles, vermis hypoplasia and impaired exploration patterns. *Hum. Mol. Genet.* 7, 999–1009 (1998).
42. Yuan, C., Schmiedl, U.P., Weinberger, E., Krueck, W.R. & Rand, S.D. Threedimensional fast spin-echo imaging: pulse sequence and in vivo image evaluation. *J. Magn. Reson. Imaging* 3, 894–899 (1993).
43. Sijbers, J. et al. Watershed-based segmentation of 3D MR data for volume quantization. *Magn. Reson. Imaging* 15, 679–688 (1997).
44. Storm, D.R., Hansel, C., Hacker, B., Parent, A. & Linden, D.J. Impaired cerebellar long-term potentiation in type I adenylyl cyclase mutant mice. *Neuron* 20, 1199–1210 (1998).
45. Anagnostaras, S.G., Josselyn, S.A., Frankland, P.W. & Silva, A.J. Computer-assisted behavioral assessment of Pavlovian fear conditioning in mice. *Learn. Mem.* 7, 58–72 (2000).



46. van der Horst, G.T. et al. Mammalian Cry1 and Cry2 are essential for maintenance of circadian rhythms. *Nature* 398, 627–630 (1999).
47. Heisler, L.K. et al. Elevated anxiety and antidepressant-like responses in serotonin 5-HT1A receptor mutant mice. *Proc. Natl Acad. Sci. USA* 95, 15049–15054 (1998).
48. Krugers, H.J. et al. Altered synaptic plasticity in hippocampal CA1 area of apolipoprotein E deficient mice. *Neuroreport* 8, 2505–2510 (1997).
49. Kaverina, I., Krylyshkina, O. & Small, J.V. Microtubule targeting of substrate contacts promotes their relaxation and dissociation. *J. Cell Biol.* 146, 1033–1044 (1999)

# Chapter 7

General discussion

In this thesis we have investigated molecular mechanisms underlying associative motor learning. We described particular how molecular mechanisms such as long term depression can influence associative learning. This has been demonstrated for classical conditioning of the eyelid reflex and aspects of conditioned fear but also for adaptation of the vestibulo-ocular reflex. Adaptation of the VOR can be classified as associative motor learning although there is an important difference. The VOR is almost constantly occurring; therefore it is constantly adapting to best fit the conditions at that instance. Adaptation of the VOR is actually an online process, while classical conditioning of the eyeblink and fear responses are more processed offline.

We have presented a new recording technique which allowed us to accurately measure eyelid position over time in mice. Accurate recording of position signals enabled us to reliably calculate derivative signals such as eyelid velocity and acceleration. These signals together provide eyelid response profiles. These profiles of conditioned and unconditioned eyelid responses in mice were measured, documented and compared with results from a variety of other animal models. With the use of MDMT recordings and the use of LTD impaired L7-PKCi and LTD enhanced FMR1 mutants we were able to investigate cellular mechanisms underlying eyelid motor performance and to dissect at least some of the molecular components of the cerebellar network that are responsible for the control of eyeblink conditioning. Since MDMT allowed us to investigate the kinetics continuously over time, we were also able to investigate specific cerebellar conditioning hypotheses in which timing mechanisms play a dominant role (Mauk et al. 2000; Mauk and Ruiz 1992; Medina et al. 2000; Medina et al. 2000; Ohyama et al. 2002; Perrett et al. 1993).

### **7.1 Technical considerations**

In the process of developing, fine tuning, validating and finally using the MDMT system an extensive body of data (i.e. about half a million blinks obtained from >500 mice) has been gathered under largely varying conditions and protocols. In this process it became increasingly clear that simply minimizing the scale of the setup used in larger animals and consequently applying this setup and procedures to mice is not appropriate. Although such a system is able to produce data that initially seem to be consistent with data collected on larger systems. However, it quickly becomes obvious that a few strange phenomena occur. After analysis, one has to conclude that data acquired in such a way do not resemble data obtained in larger animals, indicating that either mice are completely different from other species tested or the measurement system needs serious reconsideration. Despite this a number of studies using these copied setups have been used in mice to assess functions of genes and proteins on associative learning and have been published in high impact journals (Aiba et al. 1994; Bao et al. 1998; Bao et al. 1998; Chen et al. 1995; Chen et al. 1996; Chen et al. 1999; Chen et al. 1999; Kim et al. 1997; Kishimoto et al. 1997; Kishimoto et al. 2001; Miyata et al. 2001; Qiao et al. 1998; Shibuki et al. 1996; Weiss et al. 2002). The authors are making all sorts of claims, but as we will argue below, these are based on behavioral data that are probably not correct. These studies all made use of an EMG recording method. As discussed in chapter 2, this is a reliable method for larger

species, but our experience is that the mouse, and especially the muscle controlling the eyelid closure is simply too small to permanently implant EMG electrodes in a reliable way. Simultaneous EMG and video recordings demonstrated that EMG electrodes were not always reflecting eyelid movement, probably due to displacement of the electrodes after some period of blinking. Since comparisons of measurements are usually made over consecutive days, the possibility that electrodes shifted between measurement times needs to be excluded. Since it is impossible to detect whether EMG electrodes have shifted when they are the only recording method in use, as is the case with the studies mentioned above, the results are at least very susceptible to error. Even when the electrodes are in the proper place they are still sensitive to the activity of large muscles surrounding the musculus orbicularis oculi (MOO), due to the relative large size of the electrode tips compared to the MOO.

Additionally, all of the studies mentioned above made use of a tone CS that, when presented as described in the various methods sections, has proven to be inaudible to mice. These all made use of a 1 kHz pure tone of around 80 dB sound pressure level, while mice have a hearing sensitivity threshold of at least 90 dB at frequencies below 2 kHz (Koay et al., 2002). So if they hear anything at all at these low frequencies, their perception may be disturbed by various noisy signals at the edge of threshold, or by side effects in the ultrasonic frequency range due to physical characteristics of the setup (i.e. high frequency reflections, vibration of speaker cones, etc). This lack of a precise CS will burden dramatically the mouse's perception of the moment of CS onset and may therefore robustly influence various aspects of conditioning. Although some of the conclusions made in the studies mentioned above are compatible with the ones presented in this thesis, many are not and most of those conflicting results deal with parameters reflecting conditioned response timing. These differences can perfectly be explained by the reasons mentioned above. Other conflicting results deal with response counts. This difference can be explained by the fact that not only the measurement system was copied from the ones used for larger animals, also the analysis methods were copied. For rabbits, it became customary to exclude any CR that contains a startle response. As a consequence of an excluded trial the number of samples is reduced, since the protocol is fixed. Rabbits do not make many auditory startle responses so this is acceptable, but mice easily do. This difference is important in that, when mice are used, simply excluding all responses that contain an auditory startle response can considerably lower the sample size. The percentage of responses is calculated by the number of positive trials divided by the number of valid trials. Since the number of samples/ session typically used to describe conditioned responsiveness is not very large, this startle exclusion may lead to erroneous percentage estimates. Especially dangerous is the situation where the mutant shows an increased or reduced tendency for making startles compared to the wild type (e.g. the FMR1 mutant). Based on the velocity and acceleration profiles MDMT allows us to dissect the auditory startle response from the CR (see chapter 2 and 4). Therefore we decided not to exclude trials simply because they contained a startle response. CR related measurements, such as velocity and peak latency, were made in a time window starting after the period in which startle responses are displayed (i.e. effects of startles are visible from 8-50 ms, analysis started > 75 ms).

In the last five years a lot of effort has been spent in trying to reduce the number of auditory startle responses during eyelid conditioning in mice. At the time the experiments presented in this thesis were done, the percentage of startle responses in wild types usually did not exceed 20 percent. We recently found that the best effect on startle reduction can be obtained by the introduction of a tone CS that gradually increases (in 30 ms) in amplitude. This effect can be due to either a reduction of high frequency side effects (i.e. ultrasonic clicks) of suddenly presenting a loud sound using a normal loud speaker or perhaps some sort of pre-pulse inhibition effect of the gradient CS on the startle response (for review on pre-pulse inhibition see Frost et al. 2003). Interestingly, this reduction in the startle responses was not observed in the short latency responses, which indicates that indeed different mechanisms underly the two early blink components (see figure 7.3).

## **7.2 Cellular mechanisms and molecular components underlying classical conditioning**

### ***7.2a - Long term depression and PKC***

L7-PKCi transgenic mice selectively express a protein kinase C inhibitor in cerebellar Purkinje cells. Since PKC is required for the induction of long term depression of the parallel fiber to Purkinje cell synapse, this main cellular candidate mechanism for cerebellum dependent motor learning is blocked. The finding that LTD indeed was blocked in cultured cells has now been supported by additional findings. The blockage of LTD has been demonstrated in vivo. In an elegant neuro-imaging study; (Gao et al. 2003) has demonstrated that anaesthetized wild type mice do, but L7-PKCi mutant mice do not show an optical response induced by conjunctive stimulation of parallel and climbing fibers. Besides the blockage of LTD in cerebellar Purkinje cells it has been demonstrated that these mice have no other impairments. It has also been shown that the simple spike and complex spike-firing properties (such as mean firing rate, interspike interval, and spike count variability), oscillations, and climbing fiber pause in the L7-PKCi mutants were indistinguishable from those in their wild-type littermates. PKC could be involved in phenomena like dendritic excitability changes (Farley and Auerbach, 1986), which have been correlated to learning procedures such as classical conditioning. (Schreurs et al. 1998). Blockade of PKC could then disturb learning through blockade of these phenomena rather than LTD. We cannot exclude this possibility but since evidence of the involvement of PKC in such processes is scarce and restricted to models such as the Hermisenda we think it is unlikely. Nevertheless, experiments in mice such as e.g. P-cell specific AMPA receptor subunit mutants are needed to properly assess this possibility. Finally, we found that multiple climbing fiber innervation does not occur in cerebellar slices obtained from 3- to 6-month-old mutants (Goossens et al. 2001). As a consequence the impaired motor learning as observed in older adult L7-PKCI mutants cannot be attributable either to a disturbance in the baseline simple spike and complex spike activities of their Purkinje cells or to a persistent multiple climbing fiber innervation.

Furthermore, the impaired adaptation of the vestibulo-ocular reflex (VOR) seemed to be the only deficit in oculomotor performance. Normal values for other oculomotor behavior were recorded. This led to the suggestion that LTD dependent learning might not be the only form of plasticity available to the animal but reflect a relatively fast adaptive system that acts in concert with slower learning mechanisms (see chapter 3). Indeed, it has been demonstrated now that, slow implementation of adaptive changes to the VOR remains possible even without cerebellar LTD (van Alphen and De Zeeuw 2002).

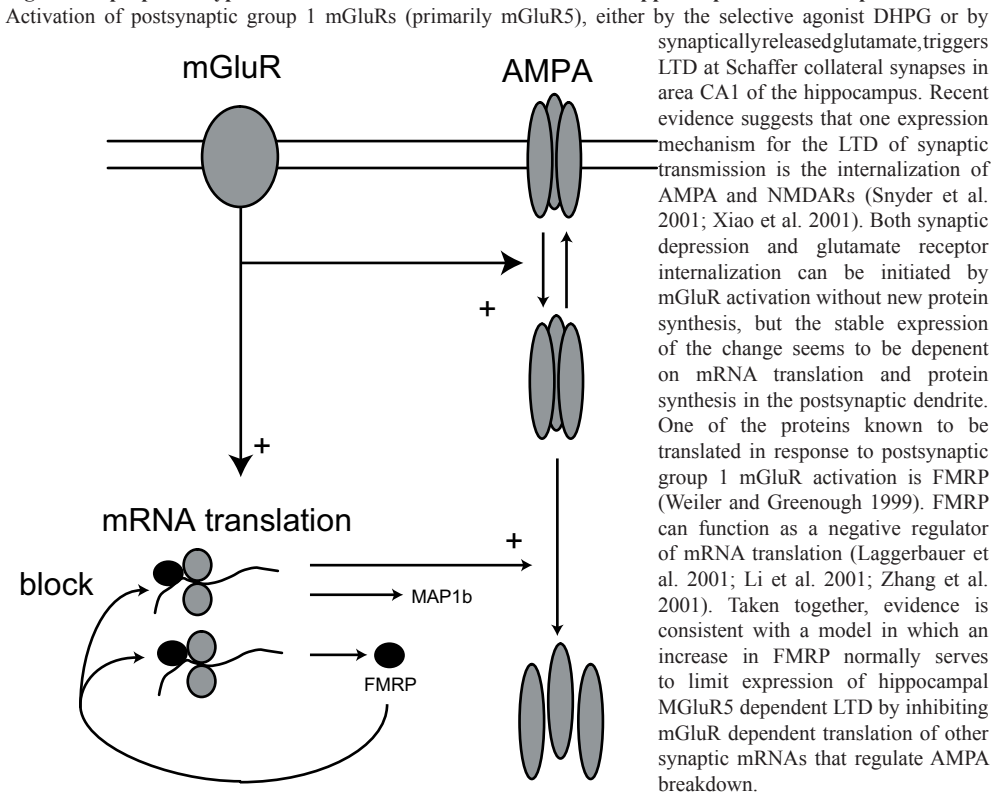
With respect to the role of LTD in classical eyeblink conditioning our study presented in chapter 4 provides evidence that LTD also contributes to the temporal shaping of conditioned responses. Although not all components of eyelid conditioning in mice are under cerebellar control, the data demonstrate that mice without parallel fiber LTD show cerebellum-dependent conditioned responses, but these lack any form of temporal adaptive capacity. Thus, mice without functional cerebellar LTD are able to learn new responses during classical conditioning tasks, but are not able to adaptively time these responses so as to make them truly effective. This evidence indicates that learning-dependent timing is probably mediated by PKC-dependent parallel fiber LTD. During the learning of well-timed movements, the efficacy of a specific set of parallel fiber–Purkinje cell synapses may be diminished by LTD induction so that, ultimately, different ISIs trigger different time rings of different sets of granule cells and Purkinje cells (Kistler and De Zeeuw 2003; Mauk and Donegan 1997), which in turn may lead to the induction of long-term potentiation or to an increase in the intrinsic excitability of the cerebellar nuclei target neurons (Aizenman et al. 2000; Aizenman and Linden 2000). This mechanism is comparable to that proposed for adaptation of the VOR (chapter 3) in which timing properties are related to input specificity of Purkinje cells. Indeed, blockage of LTD impairs the level of VOR adaptation after a few hours of visuovestibular training in a frequency-specific fashion, whereas the adaptation becomes non–frequency-specific when mechanisms other than LTD can come into play (van Alphen and De Zeeuw 2002). Thus, it may be a general concept for cerebellar motor learning that LTD does not only control the amplitude of trained movements but also their timing by means of an input specific mechanism (see also figure 7.3).

### **7.2b - Long term depression and FMRP**

The *Fmr1* mutants showed significantly less conditioned eyeblink responses and they were unable to increase the peak amplitude and peak velocity of their conditioned responses during the training. In contrast, the latency to the peak amplitude of the conditioned responses was not affected in the mutant indicating that learning-dependent timing is not impaired by a lack of FMRP.

Thus, while the existence of parallel fiber LTD may be qualitatively necessary for the occurrence of learning dependent-timing of conditioned responses, the exact level of parallel fiber LTD may be quantitatively responsible for the amount of conditioned responses. Apparently, there is an optimal level for the expression of parallel fiber LTD in order to reach a maximum level of learned responses. These results agree with the model proposed by Bear and colleagues (figure 7.1), in which they

**Figure 7.1 proposed hypothetical model of how FMRP enhances hippocampal mGluR5 dependent LTD.**



suggest that FMRP serves to limit expression of homosynaptic LTD by inhibiting mGluR-dependent translation of local synaptic mRNAs involved in the stabilization of endocytosed AMPA receptors (Huber et al. 2002). Because in the cerebellum parallel fiber LTD is also driven by activation of metabotropic glutamate receptors (Aiba et al. 1994), because parallel fiber LTD is ultimately also expressed as an endocytosis of AMPA-receptors (Linden 2001), and because the enhancement of parallel fiber LTD in *Fmr1* mutants also appears to be mainly homosynaptic, their hippocampal model may be remarkably applicable to cerebellar Purkinje cells. The net effect of this model would be an increase of LTD due to lack of FMRP. Indeed, it has now been demonstrated that this is the case for both hippocampal mGluR5 dependent LTD (Huber et al. 2002) and cerebellar LTD of the parallel fiber to Purkinje cell synapse (chapter 5).

### 7.2c - long term potentiation, clip-115 and conditioned fear

The prominent distribution of CLIP-115 in the hippocampus and cerebellum of mice raises the possibility that behavioral functions controlled by these brain regions may be disturbed in *Cyln2*-knockout mice. We assessed this by subjecting the mice to a number of behavioral tests. We investigated the functioning of hippocampus and amygdala with contextual and cued fear-conditioning paradigms. *Cyln2*-knockout mice showed increased fear after both contextual and cued fear conditioning paradigms. However, on the contextual fear paradigm *Cyln2*-knockout mice displayed



significantly less fear compared to wild types.

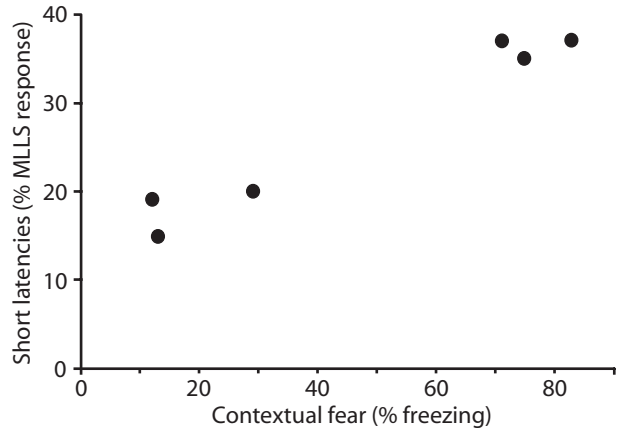
Because lesions in the hippocampus affect contextual fear conditioning, whereas lesions in the amygdala affect both contextual and cued fear conditioning (Phillips and LeDoux 1992), the data from the fear conditioning tests suggest that absence of CLIP-115 affects hippocampal dependent memory processes. Interestingly, we additionally demonstrated that hippocampal synaptic long term potentiation is affected in *Cyln2*-knockout mice. Although these findings are suggestive of the involvement of CLIP-115 in hippocampal memory processes, the underlying mechanisms remain unclear. Microtubules and (associated proteins) are believed to generate scaffolds so as to regulate the localization and density of neurotransmitter receptors at postsynaptic membrane specializations (Kneussel and Betz 2000). Alternatively, it is possible that CLIP-115 is required to regulate microtubule dynamics. In neurons these dynamics may play a role in important processes, such as growth cone motility, synaptic plasticity or morphological adaptation of dendritic spines (van Rossum and Hanisch 1999). It has been suggested that dendrites display sprouting of new spines, and that this phenomenon is correlated with synaptic plasticity (Toni, 1999; Engert, 1999). CLIP-115 could very well have a role in such a structural remodeling of synapses and the formation of new synaptic contacts. This thesis provides additional evidence that LTP in the hippocampal CA1 region is necessary for generating the contextual cue needed in the contextual fear conditioning procedure. The strong relation between amygdalar LTP and cued fear conditioning, together with the normal behavior of *Cyln2*-knockout mice on the cued fear conditioning led us to believe that, despite the heavy expression of CLIP-115 in the amygdalar region, this did not result in loss of amygdalar synaptic plasticity. This can be explained by the fact that most of the expression is actually in the medial amygdala, thereby leaving the basolateral and central nuclei of the amygdala, which mediate fear conditioning, intact.

### **7.3 Possible origins of the remnant CR's after anterior interposed lesions**

As described extensively in the introduction classical conditioning of the eyelid responses is largely dependent on the cerebellum (Lavond et al. 1985; McCormick et al. 1981; Yeo 1991). Lesions of the interposed nuclei, and more specifically the anterior interposed nuclei disrupt the expression of classically conditioned eyelid responses and prevent learning of new responses (Clark et al. 1984; Lavond 2002; Lavond et al. 1985). However, as demonstrated in both chapter 4 and chapter 5, well-trained mice show a considerable number of conditioned responses after the anterior interposed nuclei were lesioned. The explanation may simply be that the lesions were too small and did not sufficiently damage the interposed nuclei to disrupt conditioning. Although we cannot exclude this possibility we do think that it is unlikely for two reasons. First, Lavond and colleagues have demonstrated that very small lesions, merely the size of the canula used to make them in the interposed nuclei were sufficient to robustly disrupt all conditioning (Clark et al. 1984; Lavond et al. 1985). Some of the lesions we made encompassed the whole lateral anterior

interposed nuclei bilaterally. Second, other lesions in the direct vicinity, but missing the lateral anterior interposed nuclei showed no apparent effect on classical conditioning response behavior. This led us to believe these responses were not cerebellar in origin. The fact that Lurcher mice, natural mutants that have virtually no Purkinje cells and only a degenerated version of deep cerebellar nuclei (making their deficit equal to a complete cerebellar lesion), show an ability to rapidly acquire and retain similar looking conditioned responses (unpublished data), strengthen this idea.

**Figure 7.2 Stress sensitive mice make more short latency responses.** the percentage of short-latency responses of 6 mice (L7-PKCi mice in this case), which were subjected to a contextual fear conditioning task and 1 month later subjected to an eyeblink conditioning task, is plotted. The remarkable correlation between the amount of freezing and the percentage of short latency responses displayed on day 2 of training suggests that fear related processes are inducing or controlling the occurrence of short-latency eyeblinks during classical conditioning tasks in mice.



The responses that remained after lesioning the deep cerebellar nuclei all had similar shapes. They were reduced in both percentage and amplitude, but the most robust effect was the fact that all remnant responses showed a fixed, relatively short onset-latency and peak-latency (see figs 4.3 and 5.7). These remnant responses are remarkably similar to the so-called short-latency responses, which usually occur during classical eyelid conditioning in the mouse (see chapter 2,4 and 5 as well as Aiba et al. 1994). These short-latency responses are established rapidly (sometimes within the first block of training), seem to have some correlation with US strength and appear to be exerted by the whole facial musculature rather than just the eyelids (see chapter 2). The responses seem to be a result of association between the CS and the US, because they occur minimally in randomly unpaired trials. This finding stands in contrast to the auditory startle responses; although the startle responses usually increase in percentage and amplitude between the first and the second day of training, this is more likely due to context specific fear increases (see figure 7.3). In short, mice probably recognize the cage as being the place where they are likely to receive some small shocks on the eyelid or airpuffs on the eyeball and therefore have an increased level of anxiety which induces enhanced startle behavior. The short-latency response shows an onset latency of around 70 ms and peaks 50-75 ms later, while the startle response occur at 10-30 ms. Using response profiles the short latency response is easily separated from the auditory startle response. In normal wild-type mice these responses are largest in amplitude on day 2 after which they reduce to minimal levels on day 4 (measured with EMG electrodes in snout musculature, see figure 2.4). The responses are subject to some degree of variability, i.e. wild types that are littermates show different amounts of short-latency responses with different amplitudes. Figure 7.2 shows the result of 6 mice (L7-PKCi mice in

this case) which were subjected to a contextual fear conditioning task and 1 month later subjected to an eyeblink conditioning task.

The remarkable correlation between the amount of freezing and the percentage of short latency reponses displayed on day 2 of training suggests that fear related processes are inducing or controlling the occurrence of short-latency eyeblinks during classical conditioning tasks in mice (see figure 7.3).

It is not hard to see the similarities between fear and classical conditioning. Since the US used in classical eyelid conditioning experiments can be seen as a mild version of the US used in fear conditioning experiments, it has already been recognized that eyelid conditioning is essentially a form of defence conditioning (as is fear conditioning) that is extended over trials to the point at which the initially expressed diffuse responses are gradually shaped into a precise adaptive response (Medina et al. 2002). If the US in classical conditioning is aversive enough for mice, but not for larger animals, to induce cued-fear conditioning in association with the tone CS, the mouse specific short-latency response could be explained as a facial expression of this induced fear. This also explains why they remain in cerebellar nuclei lesioned animals, since the cerebellum probably has nothing to do with them. True evidence for this explanation remains to be demonstrated as well as possible mechanisms of how exactly CS-US based plasticity in the amygdala could result in the characteristic short-latency responses (see figure 7.3).

Naive situation (paired trial)

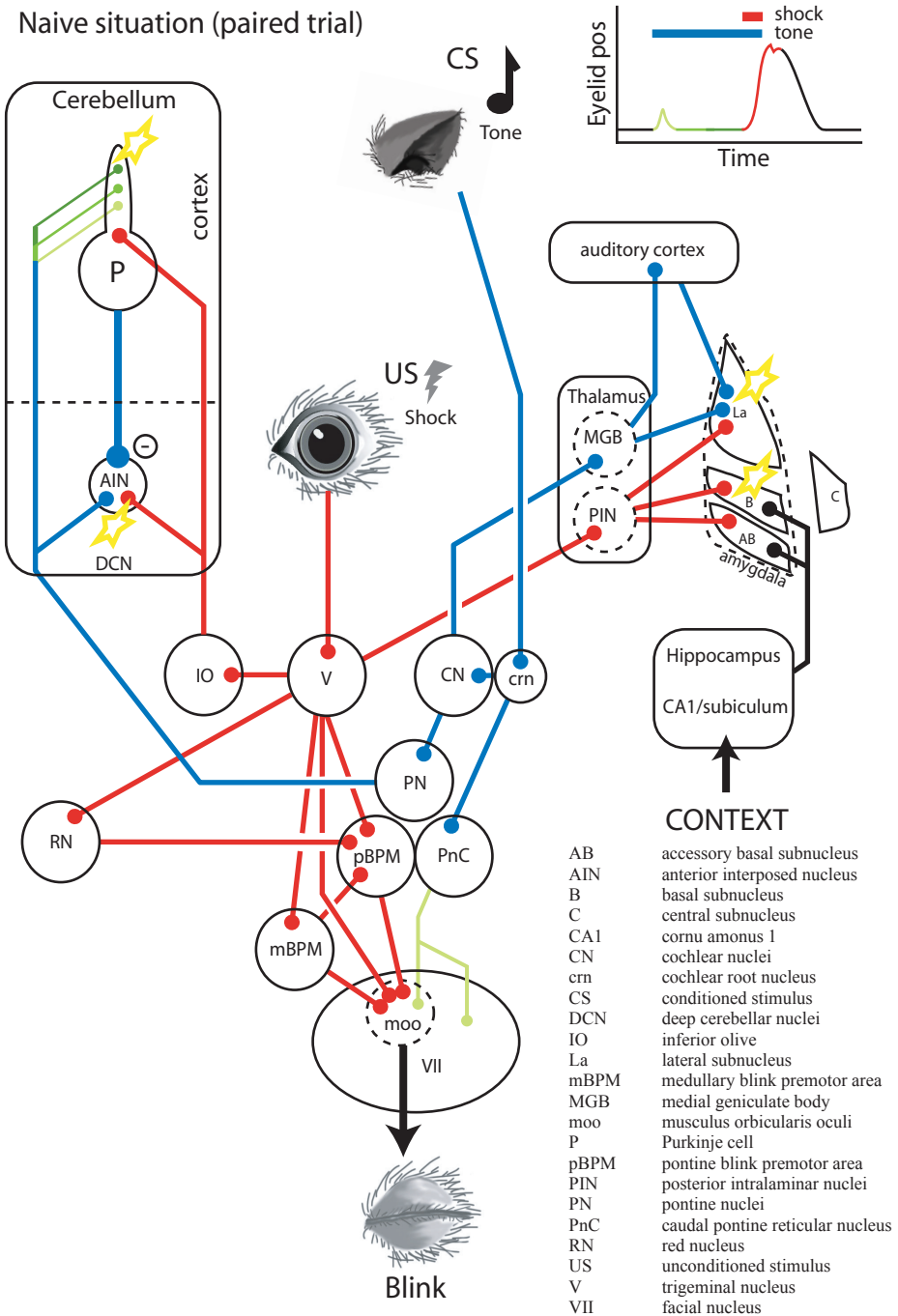


**Figure 7.3a Proposed components of the mouse conditioned eyelink reponse I; Naive situation.** Relevant transport of information about the CS (blue) and US (red) is depicted. Plasticity can occur at sites of convergence (yellow stars). Connectivity in the cerebellar cortex is responsible for time coding (shades of green) the CS information, making this structure suitable for processing temporal properties of the CR. Next to the convergence sites in the cerebellum, a convergence in the amygdala exists. Plasticity can, therefore, lead to CS-US pairing related fear responses. Plasticity can also occur in relation to contextual stimuli (black), resulting in enhanced states of fear when the subject is reexposed to the experimental surroundings. The only behavioral response in naive mice as a consequence of the CS is usually a small auditory startle response (light green).

Trained situation (CS-only trial)

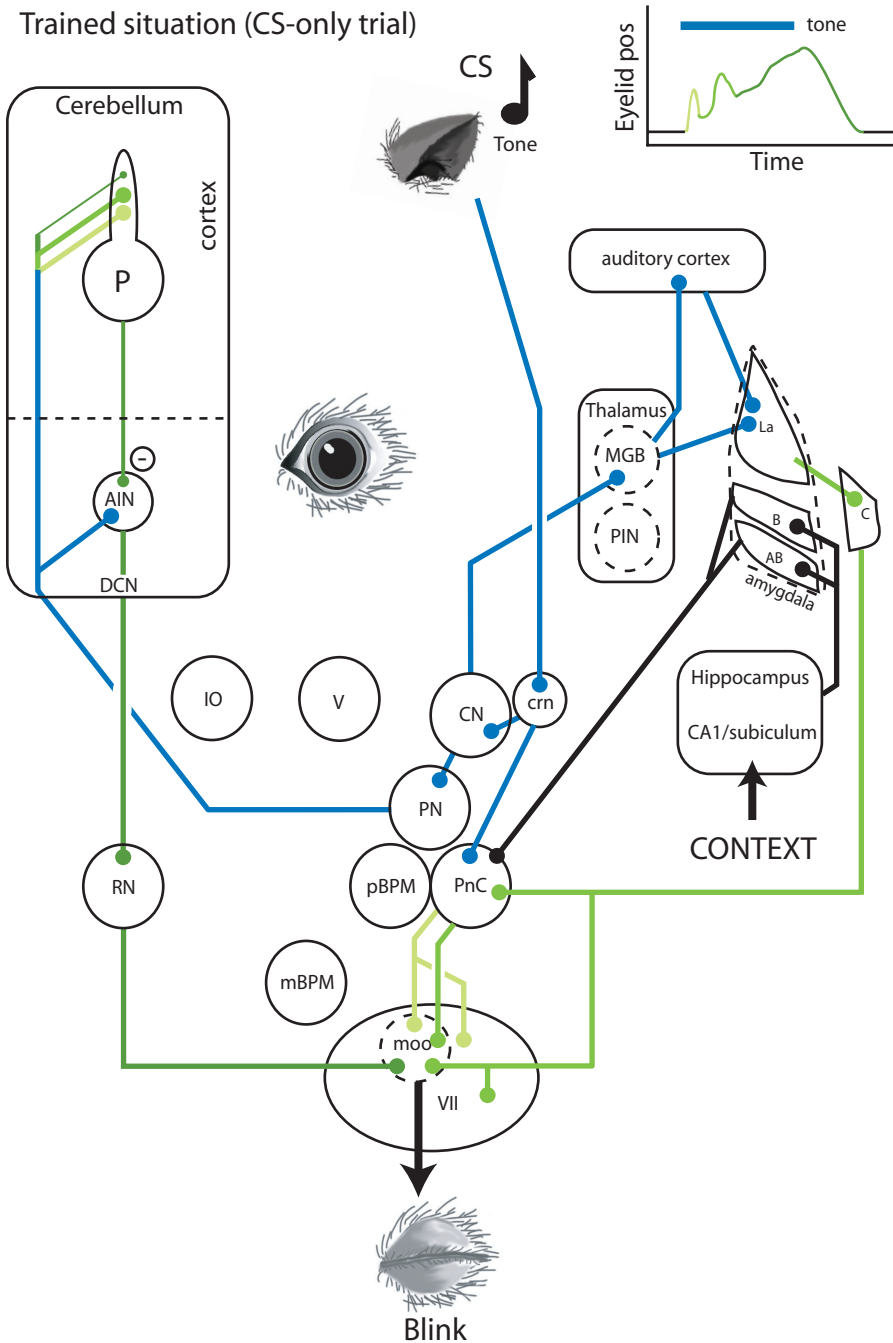


**Figure 7.3b Proposed components of the mouse conditioned eyeblink response II; Trained situation.** When the subject is trained, the initially neutral CS now induces a conditioned response. In mice three individual components can be dissected: 1) a slightly enhanced non-discreet auditory startle response (light green) due to re-exposure to a potentially harmful environment (fear potentiated startle, black); 2) A non-discreet short latency component, probably as a result from CS-US pairing related plasticity in the lateral subnucleus of the amygdala via either direct projections to VII or PnC (medium green); 3) An adaptively timed longer latency component, which is a discreet eyeblink and peaks at the moment the US would arrive. This component is cerebellar of origin, and the timing properties are dependent on cerebellar LTD (dark green).

## 7.4 references

- Aiba, A., M. Kano, C. Chen, M. E. Stanton, G. D. Fox, K. Herrup, T. A. Zwingman and S. Tonegawa (1994). "Deficient cerebellar long-term depression and impaired motor learning in mGluR1 mutant mice." *Cell* 79(2): 377-88.
- Aizenman, C. D., E. J. Huang, P. B. Manis and D. J. Linden (2000). "Use-dependent changes in synaptic strength at the Purkinje cell to deep nuclear synapse." *Prog Brain Res* 124: 257-73.
- Aizenman, C. D. and D. J. Linden (2000). "Rapid, synaptically driven increases in the intrinsic excitability of cerebellar deep nuclear neurons." *Nat Neurosci* 3(2): 109-11.
- Bao, S., L. Chen, X. Qiao, B. Knusel and R. F. Thompson (1998). "Impaired eye-blink conditioning in waggler, a mutant mouse with cerebellar BDNF deficiency." *Learn Mem* 5(4-5): 355-64.
- Bao, S., L. Chen and R. F. Thompson (1998). "Classical eyeblink conditioning in two strains of mice: conditioned responses, sensitization, and spontaneous eyeblinks." *Behav Neurosci* 112(3): 714-8.
- Chen, C., M. Kano, A. Abeliovich, L. Chen, S. Bao, J. J. Kim, K. Hashimoto, R. F. Thompson and S. Tonegawa (1995). "Impaired motor coordination correlates with persistent multiple climbing fiber innervation in PKC gamma mutant mice." *Cell* 83(7): 1233-42.
- Chen, L., S. Bao, J. M. Lockard, J. K. Kim and R. F. Thompson (1996). "Impaired classical eyeblink conditioning in cerebellar-lesioned and Purkinje cell degeneration (pcd) mutant mice." *J Neurosci* 16(8): 2829-38.
- Chen, L., S. Bao, X. Qiao and R. F. Thompson (1999). "Impaired cerebellar synapse maturation in waggler, a mutant mouse with a disrupted neuronal calcium channel gamma subunit." *Proc Natl Acad Sci U S A* 96(21): 12132-7.
- Chen, L., S. Bao and R. F. Thompson (1999). "Bilateral lesions of the interpositus nucleus completely prevent eyeblink conditioning in Purkinje cell-degeneration mutant mice." *Behav Neurosci* 113(1): 204-10.
- Clark, G. A., D. A. McCormick, D. G. Lavond and R. F. Thompson (1984). "Effects of lesions of cerebellar nuclei on conditioned behavioral and hippocampal neuronal responses." *Brain Res* 291(1): 125-36.
- Engert, F. and T. Bonhoeffer (1999). "Dendritic spine changes associated with hippocampal long-term synaptic plasticity." *Nature* 399(6731): 66-70.
- Farley J. and Auerbach S. (1986). "Protein kinase C activation induces conductance changes in Hermissenda photoreceptors like those seen in associative learning." *Nature* 319(6050): 220-223
- Frost, W. N., L. M. Tian, T. A. Hoppe, D. L. Mongeluzi and J. Wang (2003). "A cellular



mechanism for prepulse inhibition.” *Neuron* 40(5): 991-1001.

Gao, W., R. L. Dunbar, G. Chen, K. C. Reinert, J. Oberdick and T. J. Ebner (2003). “Optical imaging of long-term depression in the mouse cerebellar cortex in vivo.” *J Neurosci* 23(5): 1859-66.

Goossens, J., H. Daniel, A. Rancillac, J. van der Steen, J. Oberdick, F. Crepel, C. I. De Zeeuw and M. A. Frens (2001). “Expression of protein kinase C inhibitor blocks cerebellar long-term depression without affecting Purkinje cell excitability in alert mice.” *J Neurosci* 21(15): 5813-23.

Huber, K. M., S. M. Gallagher, S. T. Warren and M. F. Bear (2002). “Altered synaptic plasticity in a mouse model of fragile X mental retardation.” *Proc Natl Acad Sci U S A* 99(11): 7746-50.

Kim, J. J., J. C. Shih, K. Chen, L. Chen, S. Bao, S. Maren, S. G. Anagnostaras, M. S. Fanselow, E. De Maeyer, I. Seif and R. F. Thompson (1997). “Selective enhancement of emotional, but not motor, learning in monoamine oxidase A-deficient mice.” *Proc Natl Acad Sci U S A* 94(11): 5929-33.

Kishimoto, Y., S. Kawahara, Y. Kirino, H. Kadotani, Y. Nakamura, M. Ikeda and T. Yoshioka (1997). “Conditioned eyeblink response is impaired in mutant mice lacking NMDA receptor subunit NR2A.” *Neuroreport* 8(17): 3717-21.

Kishimoto, Y., S. Kawahara, M. Suzuki, H. Mori, M. Mishina and Y. Kirino (2001). “Classical eyeblink conditioning in glutamate receptor subunit delta 2 mutant mice is impaired in the delay paradigm but not in the trace paradigm.” *Eur J Neurosci* 13(6): 1249-53.

Kistler, W. M. and C. I. De Zeeuw (2003). “Time windows and reverberating loops: a reverse-engineering approach to cerebellar function.” *Cerebellum* 2: 44.

Kneussel, M. and H. Betz (2000). “Clustering of inhibitory neurotransmitter receptors at developing postsynaptic sites: the membrane activation model.” *Trends Neurosci* 23(9): 429-35.

Koay, G., R. Heffner and H. Heffner (2002). “Behavioral audiograms of homozygous med(J) mutant mice with sodium channel deficiency and unaffected controls.” *Hear Res* 171(1-2): 111-118.

Laggerbauer, B., D. Ostareck, E. M. Keidel, A. Ostareck-Lederer and U. Fischer (2001). “Evidence that fragile X mental retardation protein is a negative regulator of translation.” *Hum Mol Genet* 10(4): 329-38.

Lavond, D. G. (2002). “Role of the nuclei in eyeblink conditioning.” *Ann N Y Acad Sci* 978: 93-105.

Lavond, D. G., T. L. Hembree and R. F. Thompson (1985). “Effect of kainic acid lesions of the cerebellar interpositus nucleus on eyelid conditioning in the rabbit.” *Brain Res* 326(1): 179-82.

Li, Z., Y. Zhang, L. Ku, K. D. Wilkinson, S. T. Warren and Y. Feng (2001). "The fragile X mental retardation protein inhibits translation via interacting with mRNA." *Nucleic Acids Res* 29(11): 2276-83.

Linden, D. J. (2001). "The expression of cerebellar LTD in culture is not associated with changes in AMPA-receptor kinetics, agonist affinity, or unitary conductance." *Proc Natl Acad Sci U S A* 98(24): 14066-71.

Mauk, M. D. and N. H. Donegan (1997). "A model of Pavlovian eyelid conditioning based on the synaptic organization of the cerebellum." *Learn Mem* 4(1): 130-58.

Mauk, M. D., J. F. Medina, W. L. Nores and T. Ohyama (2000). "Cerebellar function: coordination, learning or timing?" *Curr Biol* 10(14): R522-5.

Mauk, M. D. and B. P. Ruiz (1992). "Learning-dependent timing of Pavlovian eyelid responses: differential conditioning using multiple interstimulus intervals." *Behav Neurosci* 106(4): 666-81.

McCormick, D. A., D. G. Lavond, G. A. Clark, R. E. Kettner, C. E. Rising and R. F. Thompson (1981). "The engram found? Role of the cerebellum in classical conditioning of nictitating membrane and eyelid responses." *Bulletin of the Psychonomic Society* 18: 103-105.

Medina, J. F., J. Christopher Repa, M. D. Mauk and J. E. LeDoux (2002). "Parallels between cerebellum- and amygdala-dependent conditioning." *Nat Rev Neurosci* 3(2): 122-31.

Medina, J. F., K. S. Garcia, W. L. Nores, N. M. Taylor and M. D. Mauk (2000). "Timing mechanisms in the cerebellum: testing predictions of a large-scale computer simulation." *J Neurosci* 20(14): 5516-25.

Medina, J. F., W. L. Nores, T. Ohyama and M. D. Mauk (2000). "Mechanisms of cerebellar learning suggested by eyelid conditioning." *Curr Opin Neurobiol* 10(6): 717-24.

Miyata, M., H. T. Kim, K. Hashimoto, T. K. Lee, S. Y. Cho, H. Jiang, Y. Wu, K. Jun, D. Wu, M. Kano and H. S. Shin (2001). "Deficient long-term synaptic depression in the rostral cerebellum correlated with impaired motor learning in phospholipase C beta4 mutant mice." *Eur J Neurosci* 13(10): 1945-54.

Ohyama, T., J. F. Medina, W. L. Nores and M. D. Mauk (2002). "Trying to understand the cerebellum well enough to build one." *Ann N Y Acad Sci* 978: 425-38.

Perrett, S. P., B. P. Ruiz and M. D. Mauk (1993). "Cerebellar cortex lesions disrupt learning-dependent timing of conditioned eyelid responses." *J Neurosci* 13(4): 1708-18.

Phillips, R. G. and J. E. LeDoux (1992). "Differential contribution of amygdala and hippocampus to cued and contextual fear conditioning." *Behav Neurosci* 106(2): 274-85.

Schreurs, B. G., Gusev, P. A., Tomsic, D., Alkon, D. L., and Shi, T. (1998). "Intracellular correlates of acquisition and long-term memory of classical conditioning in Purkinje cell dendrites in slices of rabbit cerebellar lobule HVI." *J Neurosci* 18, 5498-5507.

- Qiao, X., L. Chen, H. Gao, S. Bao, F. Hefti, R. F. Thompson and B. Knusel (1998). "Cerebellar brain-derived neurotrophic factor-TrkB defect associated with impairment of eyeblink conditioning in Stargazer mutant mice." *J Neurosci* 18(17): 6990-9.
- Shibuki, K., H. Gomi, L. Chen, S. Bao, J. J. Kim, H. Wakatsuki, T. Fujisaki, K. Fujimoto, A. Katoh, T. Ikeda, C. Chen, R. F. Thompson and S. Itohara (1996). "Deficient cerebellar long-term depression, impaired eyeblink conditioning, and normal motor coordination in GFAP mutant mice." *Neuron* 16(3): 587-99.
- Toni, N., P. A. Buchs, I. Nikonenko, C. R. Bron and D. Muller (1999). "LTP promotes formation of multiple spine synapses between a single axon terminal and a dendrite." *Nature* 402(6760): 421-5.
- Snyder, E. M., B. D. Philpot, K. M. Huber, X. Dong, J. R. Fallon and M. F. Bear (2001). "Internalization of ionotropic glutamate receptors in response to mGluR activation." *Nat Neurosci* 4(11): 1079-85.
- van Alphen, A. M. and C. I. De Zeeuw (2002). "Cerebellar LTD facilitates but is not essential for long-term adaptation of the vestibulo-ocular reflex." *Eur J Neurosci* 16: 486-490.
- van Rossum, D. and U. K. Hanisch (1999). "Cytoskeletal dynamics in dendritic spines: direct modulation by glutamate receptors?" *Trends Neurosci* 22(7): 290-5.
- Weiler, I. J. and W. T. Greenough (1999). "Synaptic synthesis of the Fragile X protein: possible involvement in synapse maturation and elimination." *Am J Med Genet* 83(4): 248-52.
- Weiss, C., P. N. Venkatasubramanian, A. S. Aguado, J. M. Power, B. C. Tom, L. Li, K. S. Chen, J. F. Disterhoft and A. M. Wyrwicz (2002). "Impaired eyeblink conditioning and decreased hippocampal volume in PDAPP V717F mice." *Neurobiol Dis* 11(3): 425-33.
- Xiao, M. Y., Q. Zhou and R. A. Nicoll (2001). "Metabotropic glutamate receptor activation causes a rapid redistribution of AMPA receptors." *Neuropharmacology* 41(6): 664-71.
- Yeo, C. H. (1991). "Cerebellum and classical conditioning of motor responses." *Ann N Y Acad Sci* 627: 292-304.
- Zhang, Y. Q., A. M. Bailey, H. J. Matthies, R. B. Renden, M. A. Smith, S. D. Speese, G. M. Rubin and K. Broadie (2001). "Drosophila fragile X-related gene regulates the MAP1B homolog Futsch to control synaptic structure and function." *Cell* 107(5): 591-603.



## Summary

This thesis primarily attempts to solve some long standing issues regarding classical eyelid conditioning. More specifically, what is the specific role of cerebellar LTD in classical eyeblink conditioning, and how does the answer change the view on cerebellar functioning on associative motor learning. The approach used in this thesis is a combination of the above mentioned genetic approach with classical conditioning experiments. The genetic techniques are by far best possible in mice because of their fast breeding and the availability of genetically well characterized inbred strains. Often gene function is tested by creating transgenic or knockout mice. In transgenic mice, artificial DNA is introduced in the genome of a mouse, which will lead to expression of the transgene in the adult animal. In knockout mice a targeted gene is completely deleted from the genome. The protein that was coded by this gene will no longer be expressed.

To be able to study the effect of genetic lesions on classical conditioning we needed a system that could reliably measure the performance of a mouse on such a learning task. Some studies using mice in eyeblink conditioning tasks already existed. All these studies used electromyographic (EMG) recordings of the MOO muscle to assess responsiveness on the training paradigm. Attempts to repeat this procedure led to the realization that to obtain reliable EMG recordings of the MOO muscle in a mouse over a number of consecutive days is close to impossible, simply because of the small size of a mouse eyelid. We therefore developed a new system that could reliably measure eyelid position over time in mice. Since it makes use of magnetism we called it the magnetic distance measurement technique (MDMT). Chapter 2 describes the developmental process and validation of the technique. The basic principle is to generate a local magnetic field that moves with the animal and that is picked up by either a field-sensitive chip or coil. With the use of MDMT, but not with the use of EMG, we were able to measure mean latency, peak amplitude, velocity, and acceleration of unconditioned eyelid responses, which equaled  $7.9 \pm 0.2$  ms,  $1.2 \pm 0.02$  mm,  $28.5 \pm 1$  mm/s, and  $637 \pm 22$  mm/s<sup>2</sup>, respectively (means  $\pm$  SD). During conditioning, the mice reached an average of 78% of conditioned responses over four training sessions, while animals that were subjected to randomly paired conditioned and unconditioned stimuli showed no significant increases. The mean latency of the conditioned responses decreased from  $222 \pm 40$  ms in session 2 to  $127 \pm 6$  ms in session 4, while their mean peak latency increased from  $321 \pm 45$  to  $416 \pm 67$  ms. The mean peak amplitudes, peak velocities, and peak acceleration of these responses increased from  $0.62 \pm 0.02$  to  $0.77 \pm 0.02$  mm, from  $3.9 \pm 0.3$  to  $7.7 \pm 0.5$  mm/s, and from  $81 \pm 7$  to  $139 \pm 10$  mm/s<sup>2</sup>, respectively. Power spectra of acceleration records illustrated that both the unconditioned and conditioned responses of mice had oscillatory properties with a dominant peak frequency close to 25 Hz that was not dependent on training session, interstimulus interval, or response size. These data show that MDMT can be used to measure the kinetics and frequency domain properties of conditioned eyelid responses in mice and that these properties follow the dynamic characteristics of other mammals.

Previous studies using various knockout mice (mGluR1, GluR $\delta$ 2, glial fibrillary

acidic protein) have supported the claim that LTD was underlying several forms of motor learning; however, this work has suffered from the limitations that the knockout technique lacks anatomical specificity and that functional compensation can occur via similar gene family members. To overcome these limitations, a transgenic mouse (called L7-PKCi) has been produced in which the pseudosubstrate PKC inhibitor, PKC [19-31], was selectively expressed in Purkinje cells under the control of the *pcp-2(L7)* gene promoter. The creation of this mouse, the effect of the transgene on LTD, normal motor behavior and VOR adaptation is described in Chapter 3. Cultured Purkinje cells prepared from heterozygous or homozygous L7-PKCi embryos showed a complete blockade of LTD induction. In addition, the compensatory eye movements of L7-PKCi mice were recorded during vestibular and visual stimulation. Whereas the absolute gain, phase and latency values of the vestibulo-ocular reflex and optokinetic reflex of the L7-PKCi mice were normal, their ability to adapt their vestibulo-ocular reflex gain during visuovestibular training was absent. These data strongly support the hypothesis that activation of PKC in the Purkinje cell is necessary for cerebellar LTD induction, and that cerebellar LTD is required for a particular form of motor learning, adaptation of the vestibulo-ocular reflex. To demonstrate what the lack of cerebellar LTD means for the performance of L7-PKCi mouse on classical eyelid conditioning. We subjected the L7-PKCi mice to classical conditioning procedures using MDMT. In chapter 4 we showed that protein kinase C-dependent long-term depression in Purkinje cells is necessary for learning-dependent timing of Pavlovian conditioned eyeblink responses.

Absence of functional FMRP has been shown to cause the cognitive disorder fragile X syndrome. Recently, it was demonstrated that abnormalities in the cerebral cortex and hippocampus may contribute to the cognitive deficits of fragile X syndrome. So far the potential roles of cerebellar deficits have not been investigated. In chapter 5 we demonstrated that Purkinje cells of *Fmr1* null-mutants show elongated spines and enhanced LTD induction at the parallel fiber synapses that innervate these spines. In addition, they show impaired cerebellar delay eyeblink conditioning in that the percentage of conditioned responses, peak amplitude and peak velocity are reduced, while the latencies to peak amplitude and peak velocity of their conditioned responses as well as the kinetics of their unconditioned responses are normal. Lesions of the cerebellar nuclei of trained fragile X mice show that apart from their initial enhanced startle reflex all major components of their eyeblink responses are controlled by the cerebellum. Due to the unique aberration in cellular cerebellar plasticity and due to the unique combination of deficits in classical conditioning parameters these data suggest that an optimal instead of a maximum level of parallel fiber LTD is essential for cerebellar motor learning and that cerebellar deficits can contribute to cognitive symptoms in fragile X patients.

Our studies in mice using MDMT for classical eyelid conditioning indicated that only part of the behavior could be explained by the standard classical eyeblink conditioning circuitry. This realization led us to investigate and take into account the processes and phenomenon of classical conditioning of the fear response. Large similarities between the two procedures i.e. both the stimulus presentations and behavioral measures are actually easy to recognize. We therefore created a fear conditioning



---

setup and subjected a variety of mice to this test. Chapter 6 describes how using a gene-targeting approach, we provided evidence that mice with haploinsufficiency for *Cyln2* have featured reminiscent of Williams syndrome, including mild growth deficiency, brain abnormalities, hippocampal dysfunction and particular deficits in motor coordination. Dysfunction of hippocampal dependent learning was tested both electrophysiologically and in the performance on contextual fear conditioning vs cued-fear conditioning. It is demonstrated that next to impaired hippocampal LTP indeed specifically the hippocampal dependent aspects of fear conditioning, but not those of the amygdala were disturbed in the CLIP-115 Ko mice.

In Chapter 7 the implications of the results from this thesis were discussed. In addition, interesting findings we observed over the past 5 years concerning eyeblink conditioning in Mice were reported. Important differences between mice and other animal models with regard to the eyeblink conditioning task were discussed as well as possible effects of fear related processes on the eyeblink performance of mice.



## Nederlandse samenvatting

Begin 1900 deed Pavlov fysiologisch onderzoek naar de functie van speeksel bij de vertering van voedsel. Hij gebruikte daarvoor honden. Om de speekselproductie bij de honden op gang te krijgen gaf hij ze voedsel. Het viel hem echter op dat naarmate hij langer met een bepaalde hond bezig was, deze hond al begon te kwijlen voordat hij het voedsel liet zien, nog later kwijlde de hond zelfs al voordat hij de kamer betrad. Het feit dat een natuurlijke reflex zoals kwijlen kennelijk kon worden veranderd door een leerproces vond hij zo interessant dat hij zijn onderzoeksrichting wijzigde en zich volledig oriënteerde op dit fenomeen. In een karakteristiek experiment hield hij een hond voedsel voor. De aanblik van voedsel zorgde ervoor dat het dier begon te kwijlen. Deze reflex noemde hij de ongeconditioneerde respons (OR), en het voedsel de ongeconditioneerde stimulus (OS). Nu luidde Pavlov steeds een bel voordat het voedsel aangereikt werd. Aanvankelijk had de bel totaal geen effect, maar na voldoende herhaling bleek dat de speekselproductie al op gang kwam bij het geluid van de bel. De bel was nu een geconditioneerde stimulus (CS) en de vroegtijdige speekselproductie de geconditioneerde respons (CR). Uiteindelijk was er geen voedsel meer nodig om de speekselreflex te activeren. De honden waren nu geconditioneerd.

Deze vorm van associatief leren wordt klassieke conditionering genoemd. In de loop van de jaren is dit veelvuldig toegepast om te onderzoeken hoe het leerproces dat hieraan ten grondslag ligt precies werkt. Sinds de jaren zestig wordt er veel gebruik gemaakt van conditionering van de oogknipper (eyeblink) reflex. Als CS word er meestal een toon gebruikt en als OS een luchtpufje op de oogbol of een klein stroomstootje rondom het oog. De hersenstructuur die essentieel is gebleken voor het leerproces, en dus het ontstaan van de geconditioneerde respons, is het cerebellum (de kleine hersenen). De meeste wetenschappers zijn het er over eens dat de verbindingen tussen neuronen (de synapsen) voor een belangrijk deel verantwoordelijk zijn voor informatieopslag in het brein. Veranderingen in de informatie-overdracht door deze synapsen als gevolg van biochemische processen noemt men wel synaptische plasticiteit. Een heel duidelijke vorm van synaptische plasticiteit blijkt te bestaan in het cerebellum. Deze vorm noemt men long term depression (LTD). LTD vindt plaats in de dendritische uitlopers van Purkinje-cellen. Elke Purkinje-cel heeft synaptische contacten met honderdduizenden korrelcellen. Ook maken dezelfde Purkinje-cellen elk contact met het axon van een enkel neuron in de oliva inferior, een celgroep in de hersenstam. In het kort komt het er, volgens de meest gangbare hypothese, op neer dat de projectie vanuit de oliva inferior de OS doorgeeft en dat de CS vertaald wordt door een klein deel van de projecties vanuit de korrelcellen. Elke korrelcel activeert de Purkinje-cel een heel klein beetje, maar stimulatie vanuit de oliva inferior zorgt voor een massale activatie van de Purkinje-cel. De synaptische contacten met korrelcellen, die actief zijn op het moment dat de activiteit vanuit de oliva inferior arriveert zouden volgens de LTD-hypothese dan verzwakt worden zodat, als dit een aantal keren gebeurt, de Purkinje-cel niet meer geactiveerd word door de desbetreffende korrelcellen. De CS remt dan de activiteit van de Purkinje-cel. De Purkinje-cel zelf heeft ook een remmende invloed op de activiteit in de dieper

gelegen cerebellaire kernen. Remming van de Purkinje-cel-activiteit zou dan een verhoging van de activiteit in deze kernen tot gevolg hebben en zodoende de basis leggen voor een geconditioneerde respons (zie figuur 1.4, 1.5 en 1.6).

In dit proefschrift wordt een poging gedaan een antwoord te geven op reeds lang bestaande vraagstukken omtrent klassieke conditionering van de oogknipperreflex (eye blink conditioning, EBC). Het belangrijkste vraagstuk hiervan is wel in hoeverre LTD daadwerkelijk van invloed is op het leerproces dat ten grondslag ligt aan EBC, en hoe het antwoord op deze vraag onze kijk verandert op hoe het cerebellum functioneert en bijdraagt aan associatief motorisch leren. Om deze vragen het beste te kunnen beantwoorden moesten we gebruik maken van genetisch gemanipuleerde muizen. De muis is de enige hogere diersoort is waarbij de genetische gereedschapskist in zijn volle omvang met behoorlijke kans van slagen kan worden gebruikt. Dit hield wel in dat er een experimentele opstelling ontwikkeld diende te worden waarin muizen geëvalueerd konden worden op hun EBC-prestaties. Er waren op dat moment al enige studies gepubliceerd waarin EBC-experimenten op muizen werden beschreven. Al deze studies maakten gebruik van dezelfde methode. Het meten van de eyeblink gebeurde met behulp van minuscule electrodes in de spier die verantwoordelijk is voor het sluiten van de oogleden. Met deze elektroden kon dan een eyeblink worden opgewekt door een klein stroomstootje te geven, juist genoeg om het ooglid te laten sluiten. Met twee andere elektroden kon een electromyogram (EMG) gemaakt worden, oftewel een elektrische weergave van de spieractiviteit. Deze techniek is eigenlijk een kopie van een techniek die reeds lang gebruikt werd bij grotere dieren. Onze pogingen om met behulp van deze EMG-techniek betrouwbare resultaten in muizen te verkrijgen hebben ons uiteindelijk doen realiseren dat deze techniek voor muizen niet geschikt is. Dit komt vooral doordat een muis, en met name het ooglid van een muis, te klein is om een dergelijke techniek betrouwbaar toe te passen. Het is daarom dat we een geheel nieuwe methode hebben ontwikkeld om de eyeblink te meten. Het resultaat is een methode die op basis van magnetisme real time de positie van het ooglid van een muis kan meten, terwijl het dier vrij kan rondlopen in een kooi.

De ontwikkeling en het valideren van deze techniek wordt beschreven in hoofdstuk 2. Het basisprincipe is dat een lokaal magnetisch veldje wordt opgewekt op de muis zelf. Dit magnetisch veldje verandert door of beweegt mee met beweging van het ooglid. Een magnetisch gevoelige sensor (een chip of spoel) die eveneens op de muis geplaatst is registreert deze beweging en dit wordt vervolgens vertaald naar ooglidpositie (magnetic distance measurement technique, MDMT). Verder wordt in dit hoofdstuk aangetoond dat voor deze toepassing de MDMT methode daadwerkelijk beter is dan de EMG techniek, met name in de weergave van temporele aspecten van de ooglidbeweging.

De bovengenoemde eerdere studies, waarbij gebruik werd gemaakt van genetisch gemanipuleerde muizen, toonden aan dat cerebellaire LTD betrokken was bij verscheidene vormen van motorisch leren. Maar al deze studies hadden te kampen met het probleem dat de genetische laesie geen anatomische specificiteit bevatte, oftewel: het genetische defect was aanwezig in elke cel van deze muizen. Om dit probleem te-

gen te gaan hebben we een muis ontwikkeld waarbij LTD geblokkeerd is, maar enkel in de Purkinje-cellen van het cerebellum. De ontwikkeling van deze muis, de blokkade van LTD en het effect van deze manipulatie op zowel het normale motorische gedrag als op adaptatie van de vestibulo-oculaire reflex is beschreven in hoofdstuk 3. In dit hoofdstuk wordt gedemonstreerd dat LTD compleet geblokkeerd is in cultu- res van Purkinje-cellen verkregen uit homo- en heterozygote muizenembryos. Ook wordt aangetoond dat alle gemeten parameters met betrekking tot de compensatoire oogbewegingen normaal waren, maar het vermogen deze bewegingen aan te passen tijdens visuo-vestibulaire training was verstoord. Hoofdstuk 4 beschrijft vervolgens met gebruik van bovenstaande muizen hoe een verstoorde LTD de prestaties gedu- rende de EBC-test beïnvloedt. Hieruit blijkt dat met name de temporele aspecten van de geconditioneerde eyeblink verstoord zijn. Zonder cerebellaire LTD leert de muis dus nog wel zijn ooglid te sluiten op basis van de CS, maar de sluiting is in tijd niet meer aangepast aan het moment van de OS; deze komt te vroeg.

Naast een muismodel waarin LTD geblokkeerd is hebben we ook een muismodel gebruikt waarin cerebellaire LTD versterkt aanwezig is. Dit muizenmodel was te- vens een model voor Fragile X syndroom. In hoofdstuk 5 is beschreven dat deze muizen cerebellaire afwijkingen in morfologie vertonen, dat cerebellaire LTD is ver- sterkt en dat deze muizen minder goed leren in de EBC-test. In tegenstelling tot de muizen waar LTD verlaagd was zijn het bij deze muizen niet zozeer de temporele aspecten die verstoord zijn maar meer het aantal, de hoogte en de snelheid van de eyeblink. Verder vertoonden deze muizen een verhoogd schrik-effect op de CS toon. Dit uitte zich in een zeer snelle partiële knipperbeweging direct na de start van de toon. Normaliter is deze schrikreactie op een sterk geluid een maat voor de algemene angsttoestand. Denk bijvoorbeeld aan het feit dat je veel harder schrikt van een be- paald geluid wanneer je naar een spannende film kijkt dan wanneer je gewoon koffie aan het drinken bent. De observatie dat Fragile-X-muizen angstiger lijken te zijn dan controle-muizen is niet nieuw, maar wel van groot belang voor de interpretatie van resultaten van de EBC-test. Het angstsysteem heeft een sterke invloed op het systeem dat de ooglidmotoriek bestuurt. Aangezichtsspieren zorgen voor bepaalde karakteristieke gelaatsuitdrukkingen, ook bij muizen is dit het geval. Een bange muis knijpt bijvoorbeeld de oogleden wat samen. Dit betekent dat de gevolgen van angst direct van invloed kunnen zijn op de EBC-meting. Wanneer bijvoorbeeld de gene- tische manipulatie zelf verschillen in angstreacties veroorzaakt kan dit leiden tot verschillen in EBC-prestaties tussen de gemuteerde en de controle-muizen, die niets met het cerebellum te maken hebben.

Daarom hebben we bij getrainde Fragile-X- en controle-dieren kleine laesies ge- maakt in de cerebellaire kernen, precies in het gebiedje dat de enige uitvoerende signalen vanuit het cerebellum doorgeeft naar de hersenstam. Het bleek dat er na deze laesies geen verschil meer bestond tussen de 2 groepen. Het verschil dat vóór de laesie nog aanwezig was werd dus inderdaad veroorzaakt door het effect van de genetische laesie in het cerebellum.

Interessant en van groot belang was de observatie dat in tegenstelling tot wat er be- schreven is in de literatuur (met name bij modellen in grotere diersoorten), een laesie van de cerebellaire uitvoerbanen niet leidt tot een volledig verdwijnen van de gecon-

ditioneerde eyeblink. Het restant van de eyeblink is niet meer temporeel gerelateerd aan de OS maar meer aan de start van de CS, maar is wel degelijk anders dan de snelle schrik-eyeblink. Omdat wij vermoedden dat ook deze resterende eyeblinks gestuurd werden vanuit het angststelsel (mede door angstconditionerings-processen) hebben wij, om dit beter te kunnen bestuderen, een angstconditionerings-opstelling gemaakt.

Er zijn twee vormen van angstconditionering, contextuele en cued angstconditionering. Bij de eerste vorm wordt een associatie aangeleerd tussen een angstwekkende stimulus en de omgeving (context) waarin deze stimulus kan optreden. Bij de tweede vorm wordt een associatie aangeleerd tussen een specifieke CS (cue) zoals een toon en een angstwekkende stimulus. De CR is bij beide vormen gelijk, namelijk een angstreactie opgewekt door de blootstelling aan de context of de cue. Deze uit zich bij muizen door een versterkte schrikreactie en door zogenaamd freezing gedrag: het dier blijft gedurende korte periodes doodstil zitten. Bij de meeste angstconditionerings-methoden wordt de angstreactie gekwantificeerd door het percentage freezing-tijd over enkele minuten te berekenen.

Hoofdstuk 6 beschrijft de ontwikkeling van een muismodel voor onderzoek naar het Williams-syndroom met als voor dit proefschrift belangrijkste effect dat de normale functie van de hippocampus verstoord was. Dit is zowel electrofysiologisch (verstoorde long term potentiation of LTP) als wel gedragsmatig (verstoerde contextuele angstconditionering) aangetoond. Bij contextuele angstconditionering is de hippocampus essentieel omdat in deze structuur de context-herkenning plaatsvindt. De cued angstconditionering was bij deze muizen niet verstoord. Interessant is dat juist in de delen van de amygdala die verondersteld worden betrokken te zijn bij cued angstconditionering de genetische afwijking niet tot expressie komt.

In het laatste hoofdstuk worden naast een integratie van de hierboven beschreven bevindingen ook belangrijke verschillen besproken tussen onze bevindingen omtrent EBC bij muizen en die van andere laboratoria. Ook verschillen tussen muizen en andere diersystemen komen aan de orde. Het komt er in het kort op neer dat doordat muizen zo klein zijn, de stimulatiemethoden op dit moment waarschijnlijk nog niet verfijnd genoeg zijn om klassieke eyeblink-conditionering te induceren, zonder dat de muis deze stimuli als zo vervelend ervaart dat er geen angstconditionering optreedt. Dat is niet een groot probleem zolang de onderzoeker zich dit maar realiseert, en de meetmethode goed genoeg is om de twee componenten van elkaar te kunnen scheiden.



## Dankwoord

Mijn naam staat op de kaft, maar dit proefschrift is zeker niet enkel mijn verdienste. Het is dankzij de hulp, in vele vormen en van vele mensen, dat het boekje waarvan u nu het dankwoord aan het lezen bent, daadwerkelijk in uw handen terecht is gekomen. Als het enkel aan mij had gelegen was ik nu waarschijnlijk nog steeds hard bezig vooral niet aan mijn promotie te denken. Het is de jongste van het hele rijtje mensen dat hieronder volgt, nu slechts 3 maanden oud, die er daadwerkelijk in geslaagd is mij tot het schrijven van dit proefschrift aan te zetten. Door jouw komst werd het voor mij echt tijd verder te gaan naar het volgende hoofdstuk in mijn leven en daarbij hoorde ook deze afronding van een lang maar leuk en uiteindelijk ook vruchtbaar traject. Seppe, bedankt! Dan vervolgens degene die mij al enige tijd aanspoorde tot deze promotie, overigens zonder al teveel succes; Chris, onze eerste ontmoeting was een ontzettende ommekeer in mijn leven en toekomstperspectief. Het ene moment wilde ik mijn afstudeeronderzoek gaan doen op de afdeling Hematologie om daarna zo snel mogelijk arts te worden. Een half uurtje later ging ik, riant betaald, een half jaar neurowetenschapper spelen op het lab van Jerry Simpson, New York University, midden in Manhattan. Na deze ultra-gave ervaring was ik verkocht en had ik besloten dat deze tak van wetenschap helemaal mijn ding was. Ik heb hier tot op de dag van vandaag nog geen spijt van gehad. Toendertijd nog zonder geld (Frank Grosveld, bedankt !!) en met weinig ruimte, met jouw bevologenheid, je vertrouwen in mij en Arjan, de enorme creativiteit van Hans en een aftandse slangenpomp hebben we de muizen oogbewegingen techniek opgezet. Daarbij moet vermeld worden dat Arjan en ik er ongeveer een jaar over gedaan hebben om het succes van jouw eerste pilot-experiment (weliswaar zonder data, en wij hebben het nooit gezien, maar dit terzijde) te herhalen. Ondanks het grote succes van de laatste tijd, de enorme berg geld die je nu steeds binnen haalt en alles wat je hebt bereikt, ben je geen steek veranderd, en dat is in mijn ogen een compliment. Eigenlijk is het nog steeds net zoals in dat oude kamertje van je, volgepropt met ons en de papers van Romeo. Nog steeds word je laaiend enthousiast (lees: rode wangen, glimmend voorhoofd) over een of ander klein onderwerp wat je interesseert, heb je niet zoveel benul of interesse (is mij nooit echt duidelijk geworden) over ons technisch gewouwel en heb je altijd tijd om echt te luisteren naar zaken die helemaal niets met het werk te maken hebben. Chris, bedankt voor de niet aflatende steun en vooral het vertrouwen; ik hoop dat onze samenwerking nog lang niet is afgelopen.

Verder al genoemd, maar nog niet genoeg is Hans. Hans, je moest eens weten wat ik wel allemaal niet van jou geleerd heb. De “Hans” in mij was door de studie geneeskunde volledig verdwenen, maar kwam, geïnspireerd door jouw gave om in maximal twee seconden elk probleem weg te hansen (zien is pas geloven dus er volgt geen verdere uitleg), gelukkig gauw weer boven drijven. Al zal ik jouw hansvermogen nooit kunnen evenaren, enorm bedankt hiervoor evenals voor het plezier door met je samen te werken.

Arjan, de anti-hans, maar daarom niet minder effectief. Eerst weten waarom je iets doet voordat je het doet werkt ook goed, daarvan ben jij het bewijs. Het probleem met deze aanpak voor mij is dat je dan juist wel moet begrijpen waar je mee bezig

bent. Altijd in staat om in mooie bewoordingen precies uit te leggen wat er mis was en wat er zou moeten gebeuren om het op te lossen. Gelukkig voor de Hansen onder ons, hield het daar ook wel eens bij op en moest er uiteindelijk alsnog onverklaarbaar gehandsd worden om datgene wat Arjan bedoelde voor elkaar te krijgen. De samenwerking was altijd erg goed en plezierig. We hebben zelfs een behoorlijke tijd samengewoond, gelukkig (“no offense”, maar dat hoeft ik jou niet te vertellen!) onder andere omstandigheden dan dat de buurtbewoners dachten. In no-time had ik een haast encyclopedische kennis van Star-Trek, was ik op dinsdag steeds mijn emmer kwijt, at ik regelmatig een vreemd, oranje soort beton en vond ik op dinsdag vaak mijn emmer weer terug, naast de bank?! Je was altijd weer bereid om op elk moment een “worst-case scenario” te schetsen, meestal vele malen erger dan het ergste wat in mijn voorstellingsvermogen mogelijk was. Zonder jouw, voor zo’n grote jongen toch relatief grote, ‘voorzichtigheid’ was ik waarschijnlijk wel in genante positie opgegeten door hyena’s of ander soort kwalijk spul. Goed, kortom teveel om op te noemen, bedankt voor de leuke tijd. De uitslag van ons onderzoek naar het effect van een aantal niet nader genoemde middelen op wetenschappelijke creativiteit zal waarschijnlijk nog lang op zich laten wachten.

Jerry, thank you for the enormously inspiring time you let me spend in your lab. Your views on how to collect data and what to do with it are still by far the best I ever encountered. Whenever possible (which is the biggest problem with Jerry’s view), I still try to implement a lot of the things I saw and learned in your lab. Besides making photographs and figures for you, it also was a lot of fun to work with you. Please keep visiting the lab in Rotterdam, despite all the time you take up by making the baddest jokes possible, you are very helpful. Discussing old and new problems with you, and your gift to immediately point your finger to the one little problem there is with the setup or data makes your visits not only a lot of fun, but also very fruitful.

Michiel, een verhaal apart. Gedurende mijn studietijd zelf al een bron van inspiratie voor mij. Vooral door steeds weer in te zien hoe mijn kijk op bepaalde zaken dan toch in ieder geval positiever was dan die van jou. Je bent een uiterst kleurrijk persoon, die als je het al niet onmiddellijk zegt in ieder geval laat zien dat iets je niet zint (ook hier geldt: zien is pas geloven), dat is mooi want anders had jouw gebruiks aanwijzing al helemaal niet in de boekenkast gepast. We hebben veel lol gehad. En zoals enkele stapels foto’s mij net weer hebben laten zien, vaak ook om redelijk bizarre zaken, hopelijk blijft dat zo. We kunnen er trots op zijn dat we, behalve de laatste paar weken (i.v.m. onze haast gelijktijdige promotie) haast nooit over wetenschap geouwehoerd hebben. Je hebt in samenwerking met een aantal andere aparte mensen, via de ggKOTZ, mijn studietijd in ieder geval zeer memorabel gemaakt. Verder was je ook nooit te beroerd om mee te doen aan het experiment over het effect van een aantal niet nader genoemde middelen op wetenschappelijke creativiteit. Al vermoed ik dat het jou toch meer ging om het meedoen, ook bij jou was de dinsdag toch meestal de beste dag. Ik vind het dan ook niet meer dan passend dat we ons promotiefeest samen geven.

Na Michiel moet ik toch ook even Menno noemen. Je bent maar relatief kort op de afdeling geweest maar je hebt veel invloed gehad. B.A. Baracus hangt nog steeds aan de deur. Ik weet zeker dat vele bezoekers dan wel nieuwe personeelsleden zich

verbaasd hebben over deze niet te missen poster. Nog slechts weinigen begrijpen waarom. Menno bedankt voor deze poster.

Bjorn, bedankt voor het vele werk. Door jou interesse in de wetenschappelijke vraagstukken achter de experimenten worden alle experimenten vanzelf blind uitgevoerd. Dit is een groot voordeel, Veel plezier met het lezen van de introductie van dit proefschrift en verzin maar vast een paar experimenten. Robert, door jouw koppigheid hebben we uiteindelijk toegegeven, sommige zaken zijn dan ook daadwerkelijk een stuk beter nu. Hiervoor bedankt en veel plezier straks bij Jerry, het gaat een top-tijd worden daar.

Tom, niet alleen een wandelende neuro-anatomisch naslagwerk, maar een echte tovenaer. Met een electrode als toverstokje heb je telkens weer exact het juiste gebiedje weten te raken. Alle laesies bij elkaar waarschijnlijk niet meer dan een kubieke milimeter. Bedankt hiervoor.

Niels, oligo dan maar; Moshe, bedankt voor alle hulp!

Leon, Wilmar en Hester, bedankt voor het vele werk, en geduld bij mijn onvermogen sommige dingen fatsoenlijk uit te leggen. Het resultaat staat in dit proefschrift. Hester, met name jouw werk heeft hoofdstuk 4 naar grote hoogte doen stijgen. Veel plezier met je co-schappen nog en hopelijk gaat het lukken met die agico constructie. Casper, je was al een hot-shot toen je binnenkwam, nu schitter je op MIT hopelijk kom je gauw weer terug. Bedankt voor hoofdstuk 6.

Nog een verhaal apart. Edith, het is erg maar ik kan niet eens iets fatsoenlijks verzinnen. Bedankt, voor het altijd aanwezig zijn wanneer het nodig is, het regelen, het eten, het drinken, de dingen, en buiten dat ben je ook altijd al op de hoogte, zodat erover praten een stuk makkelijker word. Altijd geïnteresseerd en enthousiast. Bedankt, bedankt.

Erika, Mandy en Elize, zonder jullie was al het histologie en lab-werk gewoonweg mislukt. Niet alleen het lab-werk ook het hele gedoe met die muizen was op een ramp uitgelopen als Mandy het niet had bijgehouden. Daarnaast zijn jullie, naast Cees ook de reden voor de 300 kilo zand die we hebben moeten droogkoken in jullie stoof. Bedankt!

Eddie, Bedankt voor het maken van de (weliswaar enige) redelijk fatsoenlijke foto op het fotobord. Verder bedankt voor het meestal zeer snelle foto- en scan werk, het vaak wat langzamere computerwerk en ondersteuning en de maar niet aflatende stroom onbegrijpelijke uitspraken.

Cees, sorry nog voor de demonstratie dat de Pavlov methode bij honden dus niet altijd goed werkt. Buiten dat, enorm veel bedankt voor al de borrels. Ik hoop echt dat ze in de nieuwe situatie gewoon doorgaan. Nu heb ik gelukkig wel wat meer tijd om ook daadwerkelijk weer langs te komen. Ook bedankt voor wat waarschijnlijk de meest bizarre ervaringen uit mijn leven zullen blijken te zijn.

Ondertussen heb ik al een niet nader te noemen middel achter de kiezen en mijn creativiteit is duidelijk afgenomen. Mochten er in dit lijstje dan nog mensen ontbreken dan ligt dat hieraan. Voor iedereen die ik vergeten ben. Bedankt

Tot slot mijn ouders; Ma, ontzettend bedankt voor de niet aflatende steun, in vele vormen. Het is slechts een klein zinnetje maar je weet hoe goed ik het bedoel. Pa, zonder jou was dit proefschrift gewoon niet mogelijk geweest. Niet zozeer vanwege

je steun door de jaren heen maar vooral vanwege het feit dat jij diegene bent geweest die door het uitvinden en maken van het prototype MDMT meetsysteem er voor gezorgd heeft dat wij deze methode daadwerkelijk konden toepassen. Ook ben jij er denk ik verantwoordelijk voor, door mij door de jaren heen altijd maar zelf dingen te laten knutselen, prutsen, solderen en verknoeien, dat de “Hans” al in mij aanwezig was voordat ik met de studie geneeskunde begon. Ook jij ontzettend bedankt.

Dan rest mij enkel nog Veerle, door jou heb ik dan toch helemaal mezelf gevonden, ongelooflijk bedankt voor alles, er zijn niet genoeg woorden voor. De toekomst met ons Seppeke en hopelijk nog meerdere kinderen beloofd veel goeds. Nu heb ik voorlopig weer meer tijd voor ons. Bedankt.

# Curriculum Vitae

Sebastiaan Karel Emile Koekkoek

Geboren: 22 oktober 1970 te Eindhoven

- 1984-1990 HAVO & VWO; Gemeentelijke Scholengemeenschap Woensel in Eindhoven
- 1990 start studie geneeskunde; Erasmus Universiteit Rotterdam
- 1994-1995 research assistant (7mnd); department of Physiology & Biophysics; New York University; New York.
- 1995 tijdelijke aanstelling wetenschappelijk assistent afdeling cel biologie aan deze universiteit.
- 1996 Doctoraal geneeskunde; Erasmus Universiteit Rotterdam. Aansluitend start als AIO; afdeling anatomie (tegenwoordig Neurowetenschappen) aan deze universiteit.
- 2000 werkbezoek (6wkn) Vestibular research Lab; Department of Otolaryngology; Washington University; St Louis.
- 2001 werkbezoek (6wkn) Department of neurosurgery; University of Minnesota; Minneapolis.





## List of Publications

**Koekkoek, S. K.**, W. Yamaguchi, W. De Graaf, B. R. Dortland, T. J. H. Ruigrok, K. E. Bakker, B. Oostra, S. Itoharu, S. Kakizawa, C. I. De Zeeuw and M. Ito (2004). "Enhanced LTD at enlarged Purkinje cell spines causes motor learning deficits in fragile X syndrome." submitted.

**Koekkoek, S. K.**, H. C. Hulscher, B. R. Dortland, R. A. Hensbroek, Y. Elgersma, T. J. Ruigrok and C. I. De Zeeuw (2003). "Cerebellar LTD and learning-dependent timing of conditioned eyelid responses." *Science* 301(5640): 1736-9.

Hoogenraad, C. C., **S. Koekkoek**, A. Akhmanova, H. Krugers, B. Dortland, M. Miedema, A. van Alphen, W. M. Kistler, M. Jaegle, M. Koutsourakis, N. Van Camp, M. Verhoye, A. van der Linden, I. Kaverina, F. Grosveld, C. I. De Zeeuw and N. Galjart (2002). "Targeted mutation of *Cyln2* in the Williams syndrome critical region links CLIP-115 haploinsufficiency to neurodevelopmental abnormalities in mice." *Nat Genet* 32(1): 116-27.

Kistler, W. M., M. T. De Jeu, Y. Elgersma, R. S. Van Der Giessen, R. Hensbroek, C. Luo, **S. K. Koekkoek**, C. C. Hoogenraad, F. P. Hamers, M. Gueldenagel, G. Sohl, K. Willecke and C. I. De Zeeuw (2002). "Analysis of *Cx36* knockout does not support tenet that olivary gap junctions are required for complex spike synchronization and normal motor performance." *Ann N Y Acad Sci* 978: 391-404.

**Koekkoek, S. K.**, W. L. Den Ouden, G. Perry, S. M. Highstein and C. I. De Zeeuw (2002). "Monitoring kinetic and frequency-domain properties of eyelid responses in mice with magnetic distance measurement technique." *J Neurophysiol* 88(4): 2124-33.

Sun, J. C., A. M. Van Alphen, M. Wagenaar, P. Huygen, C. C. Hoogenraad, T. Hasson, **S. K. Koekkoek**, B. A. Bohne and C. I. De Zeeuw (2001). "Hereditary familial vestibular degenerative diseases." *Ann N Y Acad Sci* 942: 493-6.

Sun, J. C., A. M. van Alphen, M. Wagenaar, P. Huygen, C. C. Hoogenraad, T. Hasson, **S. K. Koekkoek**, B. A. Bohne and C. I. De Zeeuw (2001). "Origin of vestibular dysfunction in Usher syndrome type 1B." *Neurobiol Dis* 8(1): 69-77.

De Zeeuw, C. I., C. Hansel, F. Bian, **S. K. Koekkoek**, A. M. van Alphen, D. J. Linden and J. Oberdick (1998). "Expression of a protein kinase C inhibitor in Purkinje cells blocks cerebellar LTD and adaptation of the vestibulo-ocular reflex." *Neuron* 20(3): 495-508.

De Zeeuw, C. I., J. I. Simpson, C. C. Hoogenraad, N. Galjart, **S. K. Koekkoek** and T. J. Ruigrok (1998). "Microcircuitry and function of the inferior olive." *Trends Neurosci* 21(9): 391-400.

de Zeeuw, C. I., A. M. van Alphen, **S. K. Koekkoek**, E. Buharin, M. P. Coesmans, M. M. Morpurgo and J. van den Burg (1998). "Recording eye movements in mice: a new approach to investigate the molecular basis of cerebellar control of motor learning and motor timing." *Otolaryngol Head Neck Surg* 119(3): 193-203.

Fransen, E., R. D'Hooge, G. Van Camp, M. Verhoye, J. Sijbers, E. Reyniers, P. Soriano, H. Kamiguchi, R. Willemsen, **S. K. Koekkoek**, C. I. De Zeeuw, P. P. De Deyn, A. Van der Linden, V. Lemmon, R. F. Kooy and P. J. Willems (1998). "L1 knockout mice show dilated ventricles, vermis hypoplasia and impaired exploration patterns." *Hum Mol Genet* 7(6): 999-1009.

Toonen, M., H. van Dijken, J. C. Holstege, T. J. Ruigrok, **S. K. Koekkoek**, R. K. Hawkins, T. M. Teune, J. vd Burg and C. I. De Zeeuw (1998). "Light microscopic and ultrastructural investigation of the dopaminergic innervation of the ventrolateral outgrowth of the rat inferior olive." *Brain Res* 802(1-2): 267-73.

De Zeeuw, C. I. and **S. K. Koekkoek** (1997). "Signal processing in the C2 module of the flocculus and its role in head movement control." *Prog Brain Res* 114: 299-320.

De Zeeuw, C. I., **S. K. Koekkoek**, D. R. Wylie and J. I. Simpson (1997). "Association between dendritic lamellar bodies and complex spike synchrony in the olivocerebellar system." *J Neurophysiol* 77(4): 1747-58.

**Koekkoek, S. K.**, A. M. v Alphen, J. vd Burg, F. Grosveld, N. Galjart and C. I. De Zeeuw (1997). "Gain adaptation and phase dynamics of compensatory eye movements in mice." *Genes Funct* 1(3): 175-90.

**Koekkoek, S. K.** and T. J. Ruigrok (1995). "Lack of a bilateral projection of individual spinal neurons to the lateral reticular nucleus in the rat: a retrograde, non-fluorescent, double labeling study." *Neurosci Lett* 200(1): 13-6.